Thèse de doctorat

Pour obtenir le grade de Docteur de

l'UNIVERSITE POLYTECHNIQUE HAUTS-DE-FRANCE

et de l'INSA HAUTS-DE-FRANCE

Spécialité: Automatique

Présentée et soutenue par
Amine DEHAK

22 Juin 2022, à Valenciennes

École doctorale :
Polytechnique Hauts-de-France (ED PHF n°635)

Unité de recherche :
Laboratoire d'Automatique, de Mécanique et d'Informatique Industrielles et Humaines (LAMIH - UMR CNRS 8201)

Approches polytopiques quasi-LPV pour les systèmes descripteurs non linéaires : modélisation à complexité réduite, commande et application aux robots manipulateurs

JURY

Présidente de jury

- SIGUERDIDJANE, Houria. Professeur, CentralSupélec Gif-Sur-Yvette.

Rapporteurs

- CHEVREL, Philippe. Professeur, Institut Mines-Telecom Atlantique Nantes.
- EL HAJJAJI, Ahmed. Professeur, Université de Picardie Jules Verne.

Examinateurs

- SEDDIKI, Lynda. Maître de Conférences, Université Paris 8 Vincennes-Saint-Denis.

Co-directeurs

- VERMEIREN, Laurent. Professeur, Université Polytechnique Hauts-de-France.
- DAMBRINE, Michel. Professeur, Université Polytechnique Hauts-de-France.

Co-encadrants

- NGUYEN, Anh-Tu. Maître de Conférences, INSA Hauts-de-France.
- DEQUIDT, Antoine. Maître de Conférences, INSA Hauts-de-France.

Membre invité

- ALLOUCHE, Benyamine. Ingénieur R&D, IRT Jules Verne.

PhD Thesis

Submitted for the degree of Doctor of Philosophy from

UNIVERSITE POLYTECHNIQUE HAUTS-DE-FRANCE

and INSA HAUTS-DE-FRANCE

Subject : Automatic

Presented and defended by.

Amine DEHAK

June 22th 2022, Valenciennes

Doctoral school:

Doctoral School Polytechnique Hauts-de-France (ED PHF n°635)

Research unit:

Laboratory of Industrial and Human Automation control Mechanical engineering and Computer science (LAMIH – UMR CNRS 8201)

Polytopic Quasi-LPV Approaches for Nonlinear Descriptor Systems: Reduced-Complexity Modeling, Control Design and Application to Robot Manipulators

JURY

President of jury

- SIGUERDIDJANE, Houria. Professor, CentralSupélec Gif-Sur-Yvette.

Reviewers

- CHEVREL, Philippe. Professor, Institut Mines-Telecom Atlantique Nantes.
- EL HAJJAJI, Ahmed. Professor, University of Picardie Jules Verne.

Examiners

- SEDDIKI, Lynda. Associate Professor, Université Paris 8 Vincennes-Saint-Denis.

Co-directors :

- VERMEIREN, Laurent. Professor, Polytechnic University Hauts-de-France.
- DAMBRINE, Michel. Professor, Polytechnic University Hauts-de-France.

Co-supervisors :

- NGUYEN, Anh-Tu. Associate Professor, INSA Hauts-de-France.
- DEQUIDT, Antoine. Associate Professor, INSA Hauts-de-France.

Invited members

- ALLOUCHE, Benyamine. Ingénieur R&D, IRT Jules Verne.

Declaration of Authorship

I, Amine Dehak, declare that this thesis titled, "Polytopic Quasi-LPV Approaches for Nonlinear Descriptor Systems: Reduced-Complexity Modeling, Control Design and Application to Robot Manipulators" and the work presented in it are my own. I confirm that:

- This work was done wholly or mainly while in candidature for a research degree at this University.
- Where any part of this thesis has previously been submitted for a degree or any other qualification at this University or any other institution, this has been clearly stated.
- Where I have consulted the published work of others, this is always clearly attributed.
- Where I have quoted from the work of others, the source is always given. With the exception of such quotations, this thesis is entirely my own work.
- I have acknowledged all main sources of help.
- Where the thesis is based on work done by myself jointly with others, I have made clear exactly what was done by others and what I have contributed myself.

Signed: 

Date: 22/06/2022

Ce(tte) œuvre est mise à disposition selon les termes de la Licence Creative Commons Attribution - Pas d'Utilisation Commerciale - Partage dans les Mêmes Conditions 4.0 International.

"*Acquire knowledge and teach it to people. Learn along with it dignity, serenity, and be humble to those from whom you learned knowledge, and be humble to those you teach knowledge to. Do not be tyrannical scholars for your knowledge will not be based on your ignorance.*"

Umar Ibn Al-Khattab

Abstract

Descriptor systems provide a natural and flexible framework to represent and analyze a large class of engineering applications. Motivated by this fact, this PhD project investigates new quasi-LPV approaches for modeling and control design of descriptor systems with a large number of nonlinearities. The main goal is to derive polytopic quasi-LPV models and the corresponding control design procedures with a numerical reduced-complexity for real-time implementation while paying a special attention on the design conservatism. Although the focused application is related to the control issues of robotic manipulators, with their generic features, the proposed control tools can be also applied to a large class of engineering systems. This manuscript is composed of three main technical parts.

For the first part, we introduce the key proprieties and assumptions related to the considered class of nonlinear descriptor systems. We further study the admissibility analysis and the stabilization of nonlinear descriptor systems using Takagi-Sugeno (TS) fuzzy modeling with the well-known sector nonlinearity approach. Based on the initial TS models of nonlinear systems, a complexity-reduction method is proposed to reduce the number of vertices from 2^r to $r+1$ where r is the number of premise variables. Numerical results are provided to illustrate the design conservatism of this method.

For the second part, we develop a new approach to derive an equivalent polytopic representation for a given nonlinear system within a compact set. Although all powerful tools of TS fuzzy framework can be directly applied to the proposed approach, the model complexity only grows *proportionally* with the number of premise variables, rather than *exponentially* when compared to the conventional TS fuzzy modeling. Moreover, for the same predefined set of premise variables, the vertices of the proposed polytopic models can admit an *infinite* number of representations. This non-uniqueness feature allows introducing specific slack variables at the modeling step, which are useful to reduce the control design conservatism. Using the proposed modeling and the descriptor redundancy approach, reduced-complexity admissibility analysis and control design conditions for singular nonlinear systems are derived in terms of linear matrix inequalities (LMIs). Both numerical and physically motivated examples are given to demonstrate the interests of the new control approach with respect to existing TS fuzzy model-based control results.

For the third part, using the polytopic quasi-LPV approach proposed in the second part, we develop a new tracking control method for nonlinear descriptor systems with a special focus on manipulator robot applications. The robot systems under algebraic constraints and unmeasured premise variables are transformed into uncertain descriptor polytopic quasi-LPV models for control design. Exploiting the specific structures of robot models, we propose a nonlinear output feedback control scheme for dynamic trajectory tracking, including three key control components: i) feedforward control to account for known disturbances, ii) disturbance-estimation-based control to compensate unknown uncertainties/disturbances, iii) feedback control to guarantee the closed-loop predefined specifications. The control design procedure is recast as a convex optimization under strict LMI constraints, which is a major contribution for output feedback tracking control of nonlinear uncertain descriptor systems. Comparative studies with respect to state-of-the-art tracking control approaches are performed with two manipulators of different natures to demonstrate both theoretical and practical interests of the new approach.

Keywords: Nonlinear descriptor systems, quasi-LPV control framework, complexity reduction, nonlinear tracking control, Lyapunov methods, linear matrix inequality.

Résumé

Les systèmes de descripteurs fournissent un cadre naturel et flexible pour représenter et analyser une large classe d'applications en ingénierie. Motivé par ce fait, ce projet de doctorat étudie de nouvelles approches quasi-LPV pour la modélisation et la conception de commande des systèmes descripteurs avec un grand nombre de non-linéarités. L'objectif principal est de dériver des modèles quasi-LPV polytopiques et le design de commande correspondant avec une complexité numérique réduite pour une mise en œuvre en temps réel tout en portant une attention particulière au conservatisme du design. Bien que l'application ciblée soit liée aux problématiques de commande des robots manipulateurs, avec leurs caractéristiques génériques, les outils de commande proposés peuvent également être appliqués à une large classe de systèmes physiques. Ce manuscrit est composé de trois grandes parties techniques.

Dans une première partie, nous introduisons les principales propriétés et hypothèses liées à la classe de systèmes de descripteurs non linéaires. Nous étudions plus avant l'analyse de l'admissibilité et la stabilisation de systèmes de descripteurs non linéaires à l'aide de la modélisation floue Takagi-Sugeno (TS) avec l'approche des secteurs non-linéaires. Basé sur ces modèles TS, une méthode de réduction de la complexité est proposée pour réduire le nombre de sommets de 2^r à $r+1$ où r est le nombre de variables de prémisse. Des résultats numériques sont fournis pour illustrer le conservatisme du design pour cette méthode.

Pour la deuxième partie, nous développons une nouvelle approche pour dériver une représentation polytopique équivalente pour un système non linéaire donné dans un ensemble compact. Bien que tous les outils puissants du cadre TS flou peuvent être directement appliqués à l'approche proposée, la complexité du modèle ne croît que proportionnellement avec le nombre de variables de prémisse, plutôt que de façon exponentielle contrairement à la modélisation TS. De plus, la forme polytopique obtenue peut admettre un nombre infini de représentations. Cette propriété permet d'introduire des variables d'écart spécifiques à l'étape de modélisation servant à réduire le conservatisme du design. En utilisant la modélisation proposée, des conditions d'analyse d'admissibilité et de stabilisation pour la classe des systèmes considérés sont dérivées sous formes LMI. Des exemples à la fois numériques et motivés physiquement sont donnés pour démontrer l'intérêt de la nouvelle approche de commande par rapport aux résultats existants des approches de commande TS floues basés sur un modèle.

Pour la troisième partie, en utilisant l'approche quasi-LPV polytopique proposée dans la deuxième partie, une nouvelle méthode de commande de suivi pour les systèmes descripteurs non linéaires avec un accent particulier sur l'applications aux robots manipulateurs est proposée. Les systèmes robotiques sous contraintes algébriques et variables de prémisse non mesurés sont transformées en modèles descripteurs incertains quasi-LPV polytopiques pour le design de la commande. Nous proposons une commande par retour d'état basée sur un observateur étendu pour le suivi de trajectoire, comprenant trois composants de commande clés, à savoir une action anticipatrice, une action corrective de tendance basée sur l'observateur de perturbation et un retour d'état reconstruit. La synthèse est refondue comme une optimisation convexe sous des contraintes LMI strictes, ce qui est une contribution majeure pour le suivi des trajectoires à base de retour d'état reconstruit pour cette classe de systèmes descripteurs. Une comparaison aux approches de commande de suivi de trajectoire dans l'état d'art sont effectuées avec deux manipulateurs de différents natures pour démontrer les intérêts à la fois théoriques et pratiques de la nouvelle approche.

Mots clés : Systèmes descripteurs, quasi-LPV, réduction de la complexité, commande de suivi non linéaire, état reconstruit.

Acknowledgements

As I begin to write this section, in which I intend to give my thanks and gratitude to all those who contributed to the completion of this thesis, I recall the words of the father of Algebra: "That fondness for science, ... that affability and condescension which God shows to the learned, that promptitude with which he protects and supports them in the elucidation of obscurities and in the removal of difficulties, has encouraged me to compose a short work on calculating by al-jabr and al-muqabala, confining it to what is easiest and most useful in arithmetic." While the presented work in this manuscript pales in comparison, I nevertheless feel the same sense of gratitude and thus I first and foremost wish to give my thanks to God.

I also address my sincere and deep gratitude to Laurent Vermeiren and Michel Dambrine, for giving me the chance to discover the world of research. I find it personally the most important element in this thesis experience. I also thank them for their constructive criticism and patience which have allowed me to improve my work markedly and their exceptional human qualities which without a doubt made the thesis period a real pleasure. I additionally give my thanks to Michel for inspiring me to always be vigilant and to trust but verify and Laurent for showing me the ropes at the IUT and for giving me the opportunity to pursue an ATER post.

I also wish to thank Antoine Dequidt for his exceptional work ethics and dedication, for sharing his vast expertise with me and for always welcoming my questions and engaging in discussions despite having a busy schedule. I will always remember him conducting my doctorat interview over the phone and then welcoming me the first day at LAMIH with the same enthusiasm and energy.

The dictionary defines superlative as: of the highest kind, quality, or order, surpassing all others. Exceptional. I define it as Anh-Tu Nguyen. As a researcher, as a mentor, and as a supervisor he is of the highest quality, and order. Exceptional. I have learned from him so many lessons about discipline, hardwork, the importance of a well written paper and the complex nature of a researcher's life. I will always be grateful for the time he took to listen to my ideas and give me confidence to further develop my qualities as a scientific researcher.

There are no words that can express the gratitude i feel toward the sacrifice my parents endured. Their unconditional love and their continuous support is what drives me to persist and overcome the hardships so far for home. I can never repay them and can only hope I will always live up to their expectations and make them proud. I am also grateful to my extended family for their support and prayers. I dedicate this work to my loving parents, my brother, my two aunts and the rest of my very large family.

I give my thanks to the few friends that managed to remain so even after knowing me a bit longer!

A final word of thanks to the Polytechnic University of Hauts-de-France, to all my fellow colleagues at IUT and at the LAMIH, for those who smile and exchange pleasantries, as well as those who are too busy to be bothered by a random human interaction. I thank you all for being part of this journey.

Contents

Declaration of Authorship i

Abstract iii

Résumé iv

Acknowledgements v

General Introduction 1

I Takagi-Sugeno Fuzzy Modeling via Sector Nonlinearity 5
- I.1 Introduction . . . 6
- I.2 Sector Nonlinearity Approach Applied to a Class of Nonlinear Systems . . . 7
- I.3 A Brief Overview of LMI Problems Formulation . . . 10
  - I.3.1 Classes of LMI Problems . . . 10
    - a) Feasibility Problem . . . 11
    - b) Generalized Eigenvalues Problem . . . 11
    - c) Constrained Optimization Problem . . . 11
  - I.3.2 Useful Lemmas and Properties . . . 11
- I.4 Control Design for Descriptor TS Fuzzy Systems . . . 12
  - I.4.1 Admissibility of Descriptor TS Fuzzy Models . . . 13
  - I.4.2 Stabilization of Descriptor TS Fuzzy Models . . . 15
- I.5 Robustness and Model Complexity of Descriptor TS Fuzzy Systems . . . 18
  - I.5.1 Robust Stabilization for Descriptor TS Fuzzy Systems . . . 19
  - I.5.2 Reduced Complexity Modeling for TS Fuzzy Approach . . . 20
- I.6 Conclusions . . . 28

II A New Polytopic Quasi-LPV Framework for Nonlinear Systems 29
- II.1 Introduction . . . 30
- II.2 Polytopic Quasi-LPV Representation . . . 31
  - II.2.1 Classical Polytopic Quasi-LPV Representation . . . 31
  - II.2.2 Novel Polytopic Quasi-LPV Representation . . . 32
- II.3 Reduced-Complexity Quadratic Control Design of Descriptor Systems . . . 36
  - II.3.1 Descriptor-Redundancy Based Control Design . . . 36
  - II.3.2 Control Design without Descriptor-Redundancy Approach . . . 39
  - II.3.3 Numerical Examples . . . 40
- II.4 Nonquadratic Control of Descriptor Systems Using Reduced-Complexity Polytopic Representation . . . 45
  - II.4.1 Descriptor-Redundancy Based Control Design . . . 46
  - II.4.2 Control Design without Descriptor-Redundancy Approach . . . 50
  - II.4.3 Numerical Examples . . . 51
- II.5 Conclusions . . . 53

III Robust Trajectory Tracking for Uncertain Descriptor Systems **54**
III.1 Introduction . . . 55
III.2 Uncertain Polytopic Quasi-LPV Modeling for Nonlinear Descriptor Systems . . . 55
III.2.1 Uncertain Quasi-LPV Modeling . . . 56
III.2.2 Robust Stabilization of Uncertain Descriptor Systems . . . 58
III.2.3 Control Design Based on System Redundancy . . . 59
III.3 Trajectory Tracking for Serial Manipulators . . . 65
III.3.1 Uncertain Robot Manipulator Dynamics . . . 66
III.3.2 $\mathcal{H}_\infty$-Performance Trajectory Tracking Control . . . 67
III.3.3 Application of $\mathcal{H}_\infty$ Control to a 3DoF Serial Manipulator . . . 70
a) Square Trajectory Tracking . . . 72
b) Circular Trajectory Tracking . . . 73
III.4 The Case of Unmeasured Scheduling Variables . . . 76
III.5 Conclusions . . . 77

IV Disturbance-Observer Based Tracking Control for Robot Manipulators **78**
IV.1 Introduction . . . 79
IV.2 Robot Modeling . . . 80
IV.2.1 Mathematical Model of Robot Manipulators . . . 80
IV.2.2 Tracking Control Goal and Robot Model Transformation . . . 83
IV.3 Observer-Based Tracking Control Problem Formulation . . . 84
IV.3.1 Feedforward Control . . . 85
IV.3.2 Disturbance-Observer-Based Control . . . 86
IV.3.3 Feedback Control . . . 87
IV.4 Convex Design for Observer-Based Output Feedback Tracking Control . . . 88
IV.5 Illustrations and Performance Evaluation . . . 92
IV.5.1 A Serial Manipulator Example . . . 93
a) Square Trajectory Tracking . . . 95
b) Circular Trajectory Tracking . . . 98
IV.5.2 A Parallel Manipulator Example . . . 102
a) Simulation Results and Comparative Study . . . 105
IV.6 Discussions on Control Performance with respect to Unknown Disturbances . . . 109
IV.7 Conclusions . . . 113

Conclusions and Perspectives **113**

Résumé Étendu en Français **117**

Bibliography **134**

List of Tables

I.1 Mechanical Constants of the 2-DoF Manipulator Robot. 17
I.2 Numerical Complexity for a 2-DoF serial robot. 25
I.3 Scheduling Variables of the 3-DoF Manipulator Robot. 26
I.4 Mechanical Constants of the 3-DoF Manipulator Robot. 27
I.5 Computational burden for 3-DoF serial robot. 27

II.1 Complexity Characteristics Numbers of Different Control Results. 40
II.2 Numerical Complexity of Different Control Results. 44
II.3 Numerical Complexity of Different Control Results. 45
II.4 Numerical Complexity of Six quasi-LPV Control Results. 52

III.1 Linear trajectory tracking performance 73
III.2 Circular trajectory tracking performance 74
III.3 Functions sets of nonlinearity considered for $f(\cdot)$ 77

IV.1 Linear trajectory tracking performance. 97
IV.2 Circular trajectory tracking performance 101
IV.3 Parallel robot parameters. 103
IV.4 Expressions of parallel robot nonlinearities. 104
IV.5 Spiral trajectory tracking performance 107
IV.6 Square trajectory tracking performance 112
IV.7 Non-linéarités du robot manipulateur 3ddl. 127

List of Abbreviations

TS	**T**akagi-**S**ugeno
LPV	**L**inear **P**arameter **V**arying
LMI	**L**inear **M**atrix **I**nequality
SDP	**S**emi **D**efinite **P**rogramming
PDC	**P**arallel **D**istribution **C**ompensation
DoF	**D**egrees (of) **F**reedom
SMC	**S**liding **M**ode **C**ontrol
EID	**E**qual **I**nput **D**isturbance
DO	**D**isturbance **O**bserver
DOB	**D**isturbance **O**bserver **B**ased
RMS	**R**oot **M**ean **S**quare
MAV	**M**aximal **A**bsolute **V**alue
CTC	**C**omputed **T**orque **C**ontrol
PID	**P**roportional **I**ntegral **D**erivative

List of Symbols

$\mathcal{I}_n$	set of natural numbers $\{1, 2, \ldots, n\}$	
$\mathcal{I}_{n\setminus m}$	set of natural numbers $\{m+1, m+2, \ldots, n\}$	
z_i	i-th premise component	
z	premises vector	
$\mathbb{R}^{m\times n}$	set of $m \times n$ matrices with real elements	
$\mathbb{S}^n$	set of $n \times n$ symmetric matrices with real elements	
I	identity matrix of appropriate dimensions	
$X^\top$	the transpose of X	
X^{-1}	the inverse of X	
$\det(X)$	the determinant of X	
$\mathrm{diag}(X_1, X_2, \ldots, X_n)$	n-block diagonal matrix composed of the matrices X_i for $i \in \mathcal{I}_n$	
$\mathrm{rank}(X)$	rank of matrix X	
$\mathrm{He}[X]$	designs $X + X^\top$	
$X \succ Y$	$X - Y$ is a symmetric positive definite matrix	
$X \prec Y$	$Y - X$ respectively negative definite matrix	
$\star$	stands for matrix blocks that can be deduced by symmetry	
$\bullet$	stands for matrix blocks that are omitted	
θ	active angular position	rad
$\dot{\theta}$	active angular velocity	rad.s^{-1}
$\ddot{\theta}$	active acceleration	rad.s^{-2}
q	passive angular position	rad
$\dot{q}$	passive angular velocity	rad.s^{-1}
$\ddot{q}$	passive angular acceleration	rad.s^{-2}
λ	internal forces	N.m

Dedicated to my loving family and friends. In loving memory of my late grandfather Loghlimi Dehak and late uncle Mohammed El Alaoui whom recent departures left a huge place in my heart.

General Introduction

The research presented in this thesis focuses on evaluating the viability of the Takagi-Sugeno (TS) modeling approach for both the control and observer design of highly nonlinear complex robotic systems. The aim is to develop new theoretical tools to reduce the numerical complexity and design conservatism for both feasibility and practical implementation of model-based controller/observer. We consider a class of nonlinear descriptor systems covering a large number of engineering applications including robot manipulators under algebraic constraints.

Robot manipulators are widely used in different applications, be it in the industry such as welding automation and assembly lines, in medicine such as robotic surgery and exoskeletons, or for entertainment. The dynamic modeling of a robot manipulator defines the relationship between joint position, angular velocity, and angular acceleration to the torque necessary to achieve desired position, velocity, and acceleration. Applying Lagrangian formulation, a systematic approach in developing a dynamic model, results in a differential equation governing the motion of the system with algebraic equations that represents the different mechanical constraints within the system. These differential-algebraic forms also known as generalized state-space systems or singular systems provide a natural framework to represent and analyze a large number of engineering applications. However, they require more involved techniques when compared to the classical state-space systems since not only stability but also regularity and admissibility have to be addressed. Stability property of descriptor systems has been classically studied based on the system index or the coordinates reduction techniques. Nonetheless, such methods require extensive algebraic manipulations, which can be unsuitable for a large class of engineering problems. To avoid this drawback, Lyapunov methods directly based on descriptor system formulation have been proposed. Despite significant advances in numerical analysis and simulation, the problem of stability analysis and control for general descriptor systems remains challenging, especially for systems with a large number of nonlinearities.

Given that the dynamics of an engineering system can be represented by a mathematical model, its state variables have some physical meaning and thus always have limited amplitudes. Since bounded nonlinearities in a region of the state space can be fitted inside "boxes", many nonlinear systems can be embedded into time-varying polytopic linear ones. As a result, model-based control and observer approaches such as *linear parameter varying* (LPV) control and Takagi-Sugeno (TS) via sector nonlinearity offer a superior solution to non-model-based approaches for the precise and robust control of nonlinear systems via linear matrix inequality (LMI) formulation and convex optimization. Specifically TS paradigm has become one of the most popular techniques for nonlinear control systems, even more so in recent years where a vast amount of literature on TS-based control has been generated and successfully applied to various engineering applications. From a theoretical viewpoint, it is possible to derive asymptotically necessary and sufficient stability conditions for TS systems. Nevertheless, in practice these stability conditions are conceptual rather than implementable since the computational burden swiftly increases such that most numerical solvers crash. This leads to another challenge of TS approaches in deriving less conservative sufficient conditions for stability analysis of nonlinear systems with a reasonable numerical burden. To reduce the design conservatism, various Lyapunov functions have been effectively exploited for TS systems.

Recent contributions in the field focus on introducing new LMI conditions to improve feasibility and reduce the conservatism by introducing nonquadratic Lyapunov functions [Lee, Park, and

Joo, 2012; Guerra and Vermeiren, 2004; Mozelli, Palhares, and Avellar, 2009; Nguyen, Guerra, and Campos, 2019], multiple-sum relaxation approaches [Sala and Ariño, 2007; Coutinho et al., 2020]. However, an underlying problem with the TS fuzzy modeling approach is the number of local linear submodels used to build the state model as it exponentially increases in function of the number of the premise variables. For example, if the TS fuzzy model is based on p nonlinear terms then the number of fuzzy rules is 2^p. The complexity introduced by this increase can render the application of TS fuzzy approach limited to systems with a small number of nonlinearities. To overcome this major limitation, several approaches have been proposed to reduce the numerical complexity of TS systems. For example, singular value decomposition was proposed to reduce the number of rules, leading to approximate TS Fuzzy models. Disregarding a certain number of system nonlinearities into system uncertainties to reduce the number of vertices of TS models has also been explored. Alternatively, data-based methods have been proposed for dimensionality reduction of the premise variables, *e.g.*, principal component analysis, deep neural network. However, given that these modeling methods can only deal with nonlinear systems in the sense of approximation, it can turn out to be unsuitable for fast dynamical systems. In particular, data-driven approaches fundamentally rely on experimental data obtained from typical trajectories of the premise variables, which require not only additional optimization steps but also extensive simulations to collect data. Additionally, due to the "data-based" feature, the stability analysis and control performance obtained with the resulting TS models highly depend on the collected data.

New approaches for exact convex representations of nonlinear systems aiming at reducing both numerical complexity and conservatism of controller/observer design with respect to practical implementation and feasibility are developed in this thesis. LMI conditions for admissibility analysis and stabilization of nonlinear singular systems are developed using the proposed exact polytopic representations. Several numerical example with different degrees of numerical complexity will be presented to illustrate the effectiveness of the proposed approaches. We additionally target the problem of high precision trajectory tracking of robot manipulators with the presence of structural uncertainties and external disturbances. This dissertation is composed of 4 chapters.

Chapter I: Takagi-Sugeno Fuzzy Modeling via Sector Nonlinearity

In this chapter we present the class of nonlinear singular systems considered and how to derive an exact convex representation using TS modeling approach via sector nonlinearity. We also prove LMI conditions for the analysis of admissibility and stabilization with a reminder of the fundamental elements of LMI formulation and robustness with respect to structural uncertainties. We close the chapter by introducing an initial attempt at complexity reduction of the TS model exploiting linear dependencies between its local sub-models while maintaining an exact convex representations. We finally draw conclusions on the trade-off nature of the relation between complexity reduction and design conservatism of the proposed approach.

Chapter II: A New Polytopic Quasi-LPV Framework for Nonlinear Systems

We introduce in this chapter a novel and systematic quasi-LPV polytopic model representation of nonlinear systems where the number of vertices grows *proportionally* with respect to the number of premises contrary to the exponential growth related to TS-based approaches. Additionally, the vertices of the proposed polytopic models can admit an *infinite* number of representations for the same predefined set of premise variables. This *non-uniqueness* feature allows introducing some specific slack variables at the modeling step to reduce the control design conservatism. Based on the proposed polytopic representation and Lyapunov stability theory, we derive reduced-complexity admissibility analysis and design conditions, expressed in terms of linear matrix inequalities, for the considered class of descriptor systems. In particular, a new nonlinear control law is proposed for regular descriptor systems to avoid using the extended redundancy form, which may yield numerically complex and conservative results due to the imposed special control structure. Both numerical and physically motivated examples

are given to demonstrate the interests of the new control approach with respect to existing TS fuzzy model-based control results.

Chapter III: Robust Trajectory Tracking Control for Uncertain Descriptor Systems The main focus of this chapter is to extend the proposed polytopic model representation to uncertain singular systems and introduce a new treatment of the structural uncertainties where due to the unique additional properties of the polytopic approach, the parametric uncertainties can be modeled into the polytopic form. A new feedback control is proposed which ensures the stability of the resulting uncertain polytopic model. A comparison of the proposed approach to the classical treatment of uncertainties on two different examples of uncertain singular systems is provided and shows that our approach is less conservative in finding a stabilizing feedback control. Additionally, we target in this chapter the problem of high precision trajectory tracking control for serial manipulators with full measurement of the states and where the presence of parametric uncertainties and unknown disturbances is considerate.

Chapter IV: Disturbance-Observer Based Tracking Control for Robot Manipulators In this final chapter, we consider robot manipulators under algebraic constraints with the presence of uncertainties, external disturbances and unmeasured premises. We propose a disturbance-observer based design exploiting the structure and intrinsic properties of the system to provide an effective solution to the problem of unmeasured premises while maintaining a peak trajectory tracking performance. The viability of the disturbance rejection scheme for model reduction with respect to tracking performance and state estimation is evaluated, and a conclusion on the optimal choice for the mixed disturbance observer and model-based control designs is provided.

Contributions

- The main contribution of this thesis boils down to the novel polytopic model representation and its potential for model-based design techniques, especially for highly nonlinear systems where the need for cost effective nonlinear observers and robust controllers arises.
- A new control input is proposed for regular descriptor systems with a significant reduction in design conservatism and complexity with respect to redundancy-based control design.
- An alternative treatment of structural uncertainties is made available thanks to the additional properties of the proposed polytopic model representation.
- The disturbance-observer approach is exploited to deal with unmeasured premises for robot manipulators and offer an active joints formulation for a seamless treatment of both serial and parallel robots alike.

Personal Publications

Revues

1. A. Dehak, A.-T. Nguyen, A. Dequidt, L. Vermeiren, M. Dambrine (2022). "Reduced-complexity LMI conditions for admissibility analysis and control design of singular nonlinear systems". IEEE Transactions Fuzzy Systems. **(in revision)**
2. A. Dehak, A.-T. Nguyen, A. Dequidt, L. Vermeiren, M. Dambrine (2022). "Takagi-Sugeno fuzzy disturbance-observer-based output tracking control for robot manipulators: Design and experiments". IEEE Transactions on Control Systems Technology. **(in preparation)**

Conferences

1. A. Dehak, A.-T. Nguyen, A. Dequidt, L. Vermeiren, M. Dambrine (2019). "Disturbance-observer based tracking control of industrial SCARA robot manipulators". 45th Annual Conference of the IEEE Industrial Electronics, Lisbon, Portugal, October.

2. A. Dehak, A.-T. Nguyen, A. Dequidt, L. Vermeiren, M. Dambrine (2020). "Reduced-complexity affine representation for Takagi-Sugeno fuzzy systems". 21st IFAC World Congress, Berlin, Germany, July.

3. A. Dehak, A.-T. Nguyen, A. Dequidt, L. Vermeiren, M. Dambrine (2020). "Stability Analysis of TS Systems via Reduced-Complexity Affine Representation". Rencontres Francophones sur la Logique Floue et ses Applications (Sète, France), pp. 109-114, Cépaduès Editions, I.S.B.N. : 9782364938663.

Chapter I

Takagi-Sugeno Fuzzy Modeling via Sector Nonlinearity

"Persistence in scientific research leads to what I call instinct for truth."

Louis Pasteur

Contents

I.1 Introduction 6
I.2 Sector Nonlinearity Approach Applied to a Class of Nonlinear Systems 7
I.3 A Brief Overview of LMI Problems Formulation 10
I.3.1 Classes of LMI Problems 10
I.3.2 Useful Lemmas and Properties 11
I.4 Control Design for Descriptor TS Fuzzy Systems 12
I.4.1 Admissibility of Descriptor TS Fuzzy Models 13
I.4.2 Stabilization of Descriptor TS Fuzzy Models 15
I.5 Robustness and Model Complexity of Descriptor TS Fuzzy Systems 18
I.5.1 Robust Stabilization for Descriptor TS Fuzzy Systems 19
I.5.2 Reduced Complexity Modeling for TS Fuzzy Approach 20
I.6 Conclusions 28

I.1 Introduction

The theory of fuzzy sets was announced by Lotfi Zadeh in the sixties [Zadeh, 1965], and constitutes a powerful tool for the representation of ambiguous classes of physical objects. This approach stems from man's ability to decide and act in an intelligent way based on observation skills and natural tendency to categorize and classify objects and experiences. In the field of automation, it was introduced as a tool allowing for an expert to methodically implement his knowledge and expertise for controlling complex, or difficult to model, physical systems. The first paper on fuzzy control was published in 1975 by [Mamdani and Assilian, 1975] laying the foundation and principles for applying the fuzzy logic to control design. The successful application of the fuzzy control on the Sendai metro in Japan rendered the approach famous, and sparked the interest of many researchers for which the relative contributions in this field continues to grow to this day. One of the historical advantages of this approach is that it does not require a mathematical model for the control design making the approach appealing when dealing with physical systems that are either difficult to model or yield complex mathematical models [Takagi and Sugeno, 1985]. However the heuristic nature of the approach is less appealing when dealing with applications for which a certain guarantee of robustness and proof of stability of the control design are crucial. To break ties with the heuristic nature of the fuzzy control approach, [Tanaka and Sugeno, 1992] proposed an alternative model-based approach while retaining the same philosophy of the fuzzy logic design. The resulting approach bared great similarity in its mathematical formulation to Linear Parameter Varying models (LPV) [Sala, Guerra, and Babuška, 2005], allowing the use of basic theoretical tools of automatic control as Lyapunov theory and LMI formulation (Linear Matrix Inequalities).

Over the past decades, Takagi-Sugeno (TS) models have been widely used for the representation of nonlinear systems. Characterized by a set of If-Then fuzzy rules with consequent parts being local linear representations, the TS fuzzy modeling approach can represent a nonlinear system by a convex combination of linear models [Tanaka, Ikeda, and Wang, 1998; Sala and Ariño, 2009]. The transition from the nonlinear model to the TS representation can be carried out by linearization around several operating points [Johansen, Shorten, and Murray-Smith, 2000] or the use of the nonlinear sector approach [Ohtake, Tanaka, and Wang, 2003]. Proven to constitute a class of universal approximators [Tanaka and Wang, 2004], the fuzzy model approach provides a powerful solution for development of function approximation, system identification as well as systematic techniques to stability analysis and controller design. In fact, for sufficiently smooth nonlinear systems, an equivalent representation can be obtained semiglobally using the sector nonlinearity based TS fuzzy modeling approach.

The study of the stability or stabilization of TS models is generally based on the choice of a candidate Lyapunov function. By imposing a dissipative behavior on this function, we often end up with conditions of stability in the form of linear matrix inequalities [Tanaka and Wang, 2004]. Once these conditions are established, convex optimization algorithms are used to solve the semi-definite problem thus formulated [Gahinet et al., 1995; Boyd et al., 1994].

The aim of this chapter is to provide a short overview of the different results for continuous TS models based on sector nonlinearity approach. First, a description of the TS approach as well as the procedure for modeling a class of nonlinear systems is given. In the second part, we review the main results in stability, stabilization, and robustness relevant to the work presented in the remainder of this manuscript. Subsequently, we discuss the main drawback for all exact modeling polytopic approaches including the TS fuzzy approach, that is, the modeling complexity which grows exponentially with the number of scheduling variables. We discuss the suggested solutions in the literature and offer an initial proposal to systematically reduce the complexity of TS fuzzy models.

I.2 Sector Nonlinearity Approach Applied to a Class of Nonlinear Systems

A nonlinear system is a system for which the variation of the output is not proportional to the variation of the input. The vast majority of existing physical systems are inherently nonlinear in nature. These dynamical systems are described mathematically by a set of nonlinear differential or algebraic equations, describing changes over time in the state variables of the physical system. As nonlinear dynamical equations are generally difficult to solve, it follows that some aspects of their behavior can appear to be unpredictable, counter-intuitive, or even chaotic, contrasting with the much simpler linear systems.

The generic representation of a nonlinear dynamical system can be expressed as the following set of equations

$$\begin{cases} f(\dot{x}(t), x(t), u(t)) = 0 & \text{(I.1a)} \\ y(t) = g(x(t), u(t)) & \text{(I.1b)} \end{cases}$$

where $x(t) \in \mathbb{R}^{n_x}$ is the vector of internal variables, $u(t) \in \mathbb{R}^m$ the control input vector, $y(t) \in \mathbb{R}^{n_y}$ the measured output vector, and f, g are nonlinear functions with values, respectively, in $\mathbb{R}^{n_x}$ and $\mathbb{R}^{n_y}$. A useful class of nonlinear dynamical system can be described in the following descriptor representation

$$\begin{cases} E(z)\dot{x}(t) = A(z)x(t) + B(z)u(t) & \text{(I.2a)} \\ y(t) = C(z)x(t) + D(z)u(t) & \text{(I.2b)} \end{cases}$$

where $z(t) \in \mathbb{R}^r$ is the premise vector, also known as the vector of scheduling variables which will be assumed depends continuously on the vector $x(t)$ or other time-varying parameters and remains in a compact set $\mathscr{D}_z$ of the form

$$\mathscr{D}_z = \left\{ z \in \mathbb{R}^r : z_i^0 \leq z_i \leq z_i^1,\ i = 1, 2, \ldots, r \right\}, \tag{I.3}$$

in which z_i denotes the i-th entry of vector z, and z_i^0, z_i^1 are some given bounds. The expression (I.2a) represents the differential equation and (I.2b) is the output equation. The matrices $E(z)$, $A(z) \in \mathbb{R}^{n_x \times n_x}$, $B(z) \in \mathbb{R}^{m \times n_x}$, $C(z) \in \mathbb{R}^{n_y \times n_x}$, and $D(z) \in \mathbb{R}^{ny \times m}$ depend affinely on z. The sector nonlinearity approach [Tanaka and Wang, 2004; Ohtake, Tanaka, and Wang, 2003] is based on a convex polytopic transformation of the nonlinear terms z_i of the model. This method

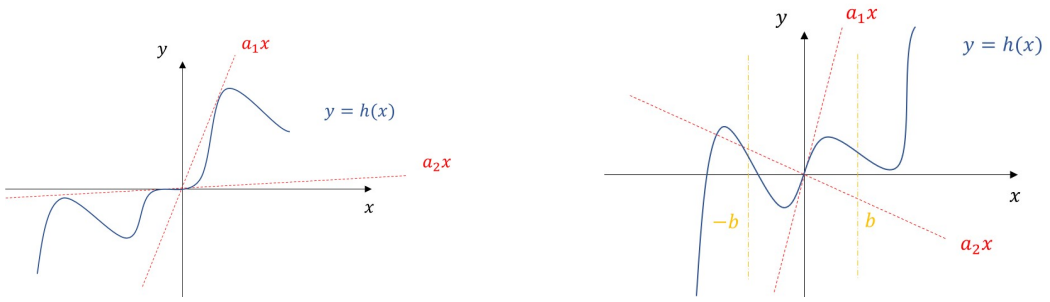

(a) Global (b) Local

FIGURE I.1: Nonlinear Sector

allows to build a TS model describing, at least locally, the exact dynamics of a nonlinear system. In fact, given that, for any physical system, the internal variables are bounded then one can always find, for each nonlinear term appearing in the system dynamics, a sector containing it; thus making it possible to represent locally the nonlinear term as a convex combination of the two values taken at the sector borders as shown in Figure I.1

Using the sector nonlinearity approach [Taniguchi et al., 2001], the state-dependent terms z_p can be *convexly* rewritten for $z \in \mathscr{D}_z$ as

$$z_p = \omega_p^0(z_p) z_p^0 + \omega_p^1(z_p) z_p^1, \quad p \in \mathcal{I}_r, \tag{I.4a}$$

$$\omega_p^0(z_p) = \frac{z_p^1 - z_p}{z_p^1 - z_p^0}, \quad \omega_p^1(z_p) = 1 - \omega_p^0(z), \tag{I.4b}$$

The nonlinear system (I.2a)-(I.2b) is then represented by the $n_r = 2^r$ If-Then fuzzy rules:

$\mathcal{R}_i$: ***If*** (z_1 is $\Omega_1^{i_1}$) ***and*** (z_2 is $\Omega_2^{i_2}$) ... ***and*** (z_r is $\Omega_r^{i_r}$)

Then

$$\begin{cases} E_i \dot{x}(t) = A_i x(t) + B_i u(t) & \text{(I.5a)} \\ y(t) = C_i x(t) + D_i u(t) & \text{(I.5b)} \end{cases}$$

where, for $p \in \mathcal{I}_r$, the index i_p is in $\{0, 1\}$ and $\Omega_p^{i_p}$ is a fuzzy set admitting $\omega_p^{i_p}$ as membership function such that $\omega_p^{i_p}(z_p) \in [0, 1]$ determines the membership level of the premise $z_p(t)$ in the fuzzy set $\Omega_p^{i_p}$ with $A_i \in \mathbb{R}^{n_x \times n_x}$, $B_i \in \mathbb{R}^{n_x \times m}$, $C_i \in \mathbb{R}^{n_y \times n_x}$, and $D_i \in \mathbb{R}^{n_y \times m}$. The interpretation of the fuzzy rules $\mathcal{R}_i$ dictates that the operator « ***And*** » is considered as a product operator. As such, we define for each local sub-model (I.5a-I.5b) a membership level to the global model using normalized membership functions (MFs) defined from (I.4b) as such

$$\mu_i(z) = \prod_{p=1}^{r} \omega_p^{i_p}(z_p), \tag{I.6}$$

with $i = 1 + i_1 + i_2 \times 2 + \cdots + i_r \times 2^{r-1}$ in $\mathcal{I}_{n_r}$. As a result, the nonlinear system (I.2a-I.2b) can be equivalently rewritten on the polytopic form

$$\sum_{i=1}^{n_r} \mu_i(z) E_i \dot{x}(t) = \sum_{i=1}^{n_r} \mu_i(z)(A_i x(t) + B_i u(t)), \tag{I.7}$$

with, for $X \in \{E, A, B\}$ and $i \in \mathcal{I}_{n_r}$, $X_i = X(\xi^i)$ for the unique vector $\xi^i \in \mathscr{D}_z$ such that $\mu_i(\xi^i) = 1$. Note that the MFs verify the convex sum property

$$0 \leq \mu_i(z) \leq 1, \quad \forall i \in \mathcal{I}_{n_r}, \quad \sum_{i=1}^{n_r} \mu_i(z) = 1, \quad \forall z \in \mathscr{D}_z. \tag{I.8}$$

Remark I.1. The TS representation via sector nonlinearity approach is not unique. In fact, the algebraic manipulations on the nonlinear model lead to different premise vectors which completely change the vertices of the obtained polytopic form (I.7).

Remark I.2. There exist other TS fuzzy modeling approaches such as, for instance, linearizing the system around a given number of operating points, and then subsequently, interconnecting the different first-order approximations through nonlinear functions [Ma, Sun, and He, 1998; Johansen, Shorten, and Murray-Smith, 2000] or using a data-driven modeling approach [Takagi and Sugeno, 1985]. That being said, the main advantage of using the sector nonlinearity approach for obtaining the TS fuzzy model resides in the ability to *exactly* represent the nonlinear system as a convex polytopic form. However, the total number of rules is related exponentially to the number of nonlinear terms, $n_r = 2^r$ (I.7). This can be a drawback when modeling complex nonlinear systems where an important number of rules can lead to numerically intractable problems.

Example I.1 (Illustrative Nonlinear Descriptor System)
We consider the following nonlinear dynamical system taken from [Bouarar, Guelton, and Manamanni, 2010]:

$$\begin{aligned} \dot{x}_1 + \dot{x}_2 &= \cos(x_2)^2 x_2 - \frac{x_2}{1+x_1^2} + (1 + \frac{1}{1+x_1^2})u \\ -\dot{x}_1 + \cos(x_2)^2 \dot{x}_2 &= -1.5x_1 + (b\ \frac{2+x_1^2}{1+x_1^2}\mathrm{sinc}(x_2) - 3)x_2 + (a\cos(x_2)^2 - 2)u \\ y &= x \end{aligned} \tag{I.9}$$

with $x = \begin{bmatrix} x_1 & x_2 \end{bmatrix}^\top$ is the state vector, u is the control input, y is the measured output, and a, b are some constant parameters. System (I.9) can be written in the nonlinear descriptor form (I.2a)–(I.2b) with the following state-dependent matrices:

$$\begin{aligned} &E(z) = \begin{bmatrix} 1 & 1 \\ -1 & z_1 \end{bmatrix}, \quad A(z) = \begin{bmatrix} 0 & z_1 - z_2 \\ -1.5 & -3 + bz_3 \end{bmatrix}, \quad B(z) = \begin{bmatrix} z_2 \\ az_1 - 2 \end{bmatrix}, \\ &C(z) = I, \quad D(z) = 0, \end{aligned} \tag{I.10}$$

where the scheduling vector is defined as $z = \begin{bmatrix} z_1 & z_2 & z_3 \end{bmatrix}^\top$ with

$$z_1 = \cos^2(x_2), \qquad z_2 = \frac{1}{1+x_1^2}, \qquad z_3 = \frac{2+x_1^2}{1+x_1^2}\ \mathrm{sinc}(x_2).$$

Note that for $x_1 \in \mathbb{R}$ and $x_2 \in [-\pi, \pi]$, we have $z \in \mathscr{D}_z$ with

$$\mathscr{D}_z = \{z \in \mathbb{R}^3 : 0 \le z_i \le 1,\ i \in \mathcal{I}_2,\ \ 0 \le z_3 \le 2\}.$$

Moreover, matrix $E(z)$ in (I.10) is invertible, with

$$E(z)^{-1} = \frac{1}{\cos(x_2)^2 + 1} \begin{bmatrix} \cos(x_2)^2 & -1 \\ 1 & 1 \end{bmatrix}, \quad \forall z \in \mathscr{D}_z.$$

Using the sector nonlinearity approach [Taniguchi et al., 2001], the scheduling variables z_p for $p \in \mathcal{I}_3$ can be *convexly* rewritten for $z \in \mathscr{D}_z$ as in (I.4) with

$$\begin{aligned} \omega_1^0 &= 1 - \cos^2(x_2), & \omega_1^1 &= 1 - \omega_1^0, \\ \omega_2^0 &= \frac{x_1^2}{1+x_1^2}, & \omega_2^1 &= 1 - \omega_2^0, \\ \omega_3^0 &= \frac{2(1+x_1^2) - (x_1^2+2)\mathrm{sinc}(x_2)}{2(1+x_1^2)}, & \omega_3^1 &= 1 - \omega_3^0. \end{aligned}$$

Sorting all the possible combinations, the normalized MFs are obtained according to (I.6) with

$$\begin{aligned} &\mu_1 = \omega_1^0\omega_2^0\omega_3^0, \quad \mu_2 = \omega_1^0\omega_2^0\omega_3^1, \quad \mu_3 = \omega_1^0\omega_2^1\omega_3^0, \quad \mu_4 = \omega_1^0\omega_2^1\omega_3^1, \\ &\mu_5 = \omega_1^1\omega_2^0\omega_3^0, \quad \mu_6 = \omega_1^1\omega_2^0\omega_3^1, \quad \mu_7 = \omega_1^1\omega_2^1\omega_3^0, \quad \mu_8 = \omega_1^1\omega_2^1\omega_3^1. \end{aligned}$$

The nonlinear descriptor system (I.10) can then be represented *exactly* by the descriptor TS fuzzy model (I.7) with $2^3 = 8$ vertices. For illustrations, the system matrices and the corresponding MFs of two vertices of the descriptor TS fuzzy model (I.7) are given by

$$E_1 = \begin{bmatrix} 1 & 1 \\ -1 & 0 \end{bmatrix}, \qquad A_1 = \begin{bmatrix} 0 & 0 \\ -1.5 & -3 \end{bmatrix}, \qquad B_1 = \begin{bmatrix} 0 \\ -2 \end{bmatrix}, E_8 = \begin{bmatrix} 1 & 1 \\ -1 & 1 \end{bmatrix}, \qquad A_8 = \begin{bmatrix} 0 & 0 \\ -1.5 & -3+2b \end{bmatrix},$$

$$\mu_1(z) = \frac{(1-\cos^2(x_2))x_1^2(2(1+x_1^2)-(x_1^2+2)\text{sinc}(x_2))}{2(1+x_1^2)^2}, \quad \mu_8(z) = \frac{\cos^2(x_2)(x_1^2+2)\text{sinc}(x_2)}{2(1+x_1^2)^2}.$$

Remark I.3. The previous example is a regular descriptor system as the differential matrix $E(z)$ is invertible on $\mathscr{D}_z$. A standard state-space representation can be obtained by pre-multiplying all the terms by the inverse of $e(z)$ ($A^\star(z) = E^{-1}(z)A(z)$, $B^\star(z) = E^{-1}(z)A(z)$) . Using the sector nonlinearity approach on the obtained form leads to a polytopic representation with $2^6 = 64$ vertices which make the control design more complex from a numerical perspective. For these reasons, it is interesting to note that the descriptor TS representation (I.7) yields a reduced number of rules and further reduces the conservatism design [Tanaka and Wang, 2004; Taniguchi et al., 2001; Guelton, Delprat, and Guerra, 2008; Guerra and Vermeiren, 2004].

Note that the case of state-space representation is recovered when $E(z) = I$. In the remainder of this manuscript, we will focus on the general case where $E(z)$ is nonlinear and possibly singular as it does not affect the polytopic modeling form, while paying special attention to the regular cases when the need arises.

I.3 A Brief Overview of LMI Problems Formulation

The main advantage of a polytopic representation for nonlinear systems comes from the systematization of the direct Lyapunov method [Tanaka and Sugeno, 1992] for control design. The objective is to find a candidate Lyapunov function in order to express the conditions of stability in the form of linear matrix inequalities (LMIs). The resolution of LMIs can be done via convex optimization techniques. In this section, we introduce some basic notions necessary for the logical continuation of this manuscript. For more details on the use of LMIs in the field of control, the reader may refer to [Boyd et al., 1994; Scherer and Weiland, 2000].

Definition I.1 *A function $f : \mathbb{R}^n \to \mathbb{R}$ is convex if and only if $\forall (x, y) \in \mathbb{R}^n$ and $\forall \beta \in [0, 1]$:*

$$f(\beta x + (1-\beta)y) \leq \beta f(x) + (1-\beta)f(y) \tag{I.11}$$

Definition I.2 *A linear matrix inequality $M(x)$ is an expression of the form*

$$M(x) \triangleq M_0 + \sum_{i=1}^{m} x_i M_i \prec 0 \tag{I.12}$$

where $x \in \mathbb{R}^m$ is a vector containing the decision variables x_i and $M_i \in \mathbb{R}^{n\times n}$ are known symmetric matrices ($\forall i \in \mathcal{I}_m \cup \{0\}$, $M_i = M_i^\top$).

The LMI as defined in (I.12) is considered strictly negative definite and is negative semi-definite if $M(x) \preceq 0$. Alternatively, the LMI can be strictly positive definite (resp. positive semi-definite) if $M(x) \succ 0$ (resp. $M(x) \succeq 0$).

I.3.1 Classes of LMI Problems

In semi-definite programming (SDP), one seeks to minimize a linear objective function subject to the constraint that an affine combination of symmetric matrices is positive semi-definite (resp. negative semi-definite), in other words, subject to a LMI constraint. Such a constraint is nonlinear but convex, so semi-definite programming is in fact a subfield of convex optimization [Vandenberghe and Boyd, 1996]. For control applications, we are mainly concerned with three types of SDP:

a) Feasibility Problem

Considering the LMI constraint in (I.12), the LMI problem is said to be feasible if there exist a vector $x \in \mathbb{R}^m$ such that the constraint (I.12) holds for m given matrices $M_i = M_i^\top$.

b) Generalized Eigenvalues Problem

The LMI formulation for the generalized eigenvalue problem consists in finding a solution $x \in \mathbb{R}^m$ that minimizes a real scalar α such that some LMI constraints hold. The equivalent mathematical expression is given as such:

$$\begin{aligned} \min \quad & \alpha \\ \text{s. t.} \quad & M(x) \prec \alpha N(x) \\ & N(x) \succ 0 \\ & C(x) \prec 0 \end{aligned} \tag{I.13}$$

where $M(x)$, $N(x)$, and $C(x)$ are affine combinations of symmetric matrices.

c) Constrained Optimization Problem

The problem considered here is minimizing a linear function of the variable $x \in \mathbb{R}^m$ defined by the problem data vector $c \in \mathbb{R}^m$ and subject to a matrix inequality $M(x)$:

$$\begin{aligned} \min \quad & c^\top x \\ \text{s. t.} \quad & M(x) \succ 0 \end{aligned} \tag{I.14}$$

I.3.2 Useful Lemmas and Properties

At this point, some useful lemmas are presented. They are used to transform a nonlinear optimization problem into a SDP under LMI constraints as well as obtain relaxed control design conditions.

Lemma I.1 (Congruence Transformation) [Boyd et al., 1994]
Consider $\mathcal{R} \in \mathbb{S}^n$ and $\mathcal{Q} \in \mathbb{R}^{n \times n}$, with $\text{rank}(Q) = n$. The matrix inequality $\mathcal{R} \prec 0$ is satisfied if and only if $\mathcal{Q}^\top \mathcal{R} \mathcal{Q} \prec 0$ or, equivalently, $\mathcal{Q} \mathcal{R} \mathcal{Q}^\top \prec 0$.

A congruence transformation preserves the definiteness of a matrix by ensuring that $\mathcal{R} \prec 0$ and $\mathcal{Q}^\top \mathcal{R} \mathcal{Q} \prec 0$ are equivalent. A congruence transformation is related, but not equivalent, to a similarity transformation $\mathcal{T}^{-1} \mathcal{R} \mathcal{T}$, which preserves not only the definiteness, but also the eigenvalues of a matrix. The case of $\mathcal{R} \succ 0$ is equivalent to $-\mathcal{R} \prec 0$. A congruence transformation is equivalent to a similarity transformation in the special case when $\mathcal{Q}$ is an orthogonal matrix, that is $\mathcal{Q}^\top = \mathcal{Q}^{-1}$.

Lemma I.2 (Shur Complement) [Boyd et al., 1994]
Consider $\mathcal{R} \in \mathbb{S}^n$, $\mathcal{Q} \in \mathbb{S}^m$, and $\mathcal{S} \in \mathbb{R}^{m \times n}$. The following statements are equivalent:

$$\begin{bmatrix} \mathcal{R} & \mathcal{S}^\top \\ \mathcal{S} & \mathcal{Q} \end{bmatrix} \prec 0 \tag{I.15}$$

$$\begin{cases} \mathcal{R} \prec 0 \\ \mathcal{Q} - \mathcal{S} \mathcal{R}^{-1} \mathcal{S}^\top \prec 0 \end{cases} \tag{I.16}$$

$$\begin{cases} \mathcal{Q} \prec 0 \\ \mathcal{R} - \mathcal{S}^\top \mathcal{Q}^{-1} \mathcal{S} \prec 0 \end{cases} \tag{I.17}$$

The Schur complement is an instrumental tool in manipulating nonlinear inequalities, often used to transform apparent bilinear matrix inequalities (BMIs) into equivalent LMIs, it is the base for many other LMI properties and lemmas.

Lemma I.3 (Square Completion) [Xie and Souza Carlos, 1992]
Consider $\mathcal{R} \in \mathbb{R}^{m\times n}$ and $\mathcal{Q} \in \mathbb{R}^{m\times n}$, then the following LMI holds for any invertible matrix $\mathcal{S} \in \mathbb{S}^m$.

$$\mathcal{R}^\top\mathcal{Q} + \mathcal{Q}^\top\mathcal{R} \preceq \mathcal{R}^\top\mathcal{S}\mathcal{R} + \mathcal{Q}^\top\mathcal{S}^{-1}\mathcal{Q} \tag{I.18}$$

This result allows to obtain a bound on the non-quadratic expression $\mathcal{R}^\top\mathcal{Q} + \mathcal{Q}^\top\mathcal{R}$ which combined with the Schur complement lemma can lead to LMI conditions. Although being generally more conservative and constraining compared to the initial problem, these last conditions remain convex and thus can be solved as a SDP.

Many controller and observer design problems can be reformulated in the MFs-dependent inequality of the form

$$\Upsilon(z) = \sum_{i,j\in\mathcal{I}_{n_r}} w_i(z)w_j(z)\Upsilon_{ij} \prec 0, \quad \forall z \in \mathscr{D}_z, \tag{I.19}$$

where $w(z) = \Big[w_1(z), w_2(z), \ldots, w_{n_r}(z)\Big] \in \Omega$, and Ω is a set of sufficiently smooth functions satisfying the convex sum properties, *i.e.*, $0 \leq w_i(z) \leq 1$, $\sum_{i=1}^{n_r} w_i(z) = 1$. The matrices Υ_{ij} are linearly dependent on the decision variables. The following relaxation result allows to convert (I.19) into a finite set of LMI constraints.

Lemma I.4 (Double Sum Relaxation) [Tuan et al., 2001]
Let Υ_{ij} be symmetric matrices of appropriate dimensions where $i, j \in \mathcal{I}_{n_r}$. Then, inequality (I.19) holds if for all $i, j \in \mathcal{I}_{n_r}$

$$\begin{aligned} &\Upsilon_{ii} \prec 0, \\ &\frac{2}{r-1}\Upsilon_{ii} + \Upsilon_{ij} + \Upsilon_{ji} \prec 0, \quad i \neq j. \end{aligned} \tag{I.20}$$

Note that other relaxation results with different degrees of complexity or conservatism can be found in [Tuan et al., 2001; Sala and Ariño, 2007].

Lemma I.5 (Extended Form Relaxation) [Peaucelle et al., 2000]
Let $\mathscr{A}$, $\mathscr{R}$, $\mathscr{L}$, $\mathscr{P}$ and $\mathscr{Q}$ be matrices of proper dimensions. The following statements are equivalent:

i) $\mathscr{P}^\top\mathscr{A}^\top + \mathscr{A}\mathscr{P} + \mathscr{Q} \prec 0,$

ii) $\exists \mathscr{R}, \mathscr{L} : \begin{bmatrix} \mathscr{L}^\top\mathscr{A}^\top + \mathscr{A}\mathscr{L} + \mathscr{Q} & \star \\ \mathscr{P} - \mathscr{L} + \mathscr{R}^\top\mathscr{A}^\top & -\mathscr{R} - \mathscr{R}^\top \end{bmatrix} \prec 0.$

Via the introduction of slack variables, Lemma I.5 offers an extra flexibility to reduce the number of sums involved in MFs-dependent inequalities in case of nonquadratic control designs, thus reducing the complexity and conservatism. However, it comes at the price of an increased computational burden as the LMI doubles in size.

I.4 Control Design for Descriptor TS Fuzzy Systems

For a singular descriptor system ($\text{rank}(E(z)) < n_x$), the notion of stability is linked to a more complex notion, admissibility [Regaieg et al., 2019]. In the linear and autonomous case ($u(t) = 0$), the descriptor system characterized by the couple (E, A) is considered admissible if it is

- *regular*: $\det(sE - A) \neq 0$, $\forall s \in \mathbb{C}$,

- *impulse-free*: $\deg(\det(sE - A)) = \operatorname{rank}(E)$, and
- *stable*: $sE - A$ is Hurwitz.

This definition of admissibility is difficult to extend for nonlinear descriptor systems as the established definitions of both *regularity* and *non-impulsiveness* are not as easily defined for the nonlinear case. In order to construct an appropriate definition of admissibility for nonlinear descriptor systems we will first limit our interest to a class of descriptor systems and then examine its index-one property [Yang et al., 2013].

I.4.1 Admissibility of Descriptor TS Fuzzy Models

We consider the following class of nonlinear differential-algebraic systems:

$$E_1(z)\dot{x}_d(t) = A_{11}(z)x_d(t) + A_{12}(z)x_a(t) + B_1(z)u(t), \tag{I.21a}$$
$$0 = A_{21}(z)x_d(t) + A_{22}(z)x_a(t) + B_2(z)u(t), \tag{I.21b}$$

where $x_d(t) \in \mathbb{R}^q$ is the differential state vector, $x_a(t) \in \mathbb{R}^s$ is the vector of algebraic variables, and $u(t) \in \mathbb{R}^m$ is the control input. The vector of premise variables $z(t) \in \mathbb{R}^r$ continuously depend on the system state such that $z(t) \in \mathscr{D}_z$. The matrices $E_1(z)$, $A_{11}(z) \in \mathbb{R}^{q\times q}$, $A_{12}(z) \in \mathbb{R}^{q\times s}$, $A_{21}(z) \in \mathbb{R}^{s\times q}$, $A_{22}(z) \in \mathbb{R}^{s\times s}$, $B_1(z) \in \mathbb{R}^{q\times m}$, and $B_2(z) \in \mathbb{R}^{s\times m}$ *affinely* depend on $z(t)$. Moreover, we consider the case where $E_1(z)$ is regular for all $z \in \mathscr{D}_z$.

Various engineering systems can be represented in the form (I.21), *e.g.*, constrained robot systems [Krishnan and Mcclamroch, 1994], chemical processes [Kumar and Daoutidis, 2020], etc. Moreover, if $x = x_d$ and $x_a \in \emptyset$, then system (I.21) becomes regular, which has been widely studied in the literature [Lewis, Dawson, and Abdallah, 2003; Taniguchi et al., 2001; Tanaka and Wang, 2004; Bouarar, Guelton, and Manamanni, 2010].

For compactness, system (I.21) can be rewritten in the singular form

$$E(z)\dot{x}(t) = A(z)x(t) + B(z)u(t), \tag{I.22}$$

where $x = \begin{bmatrix} x_d^\top & x_a^\top \end{bmatrix}^\top \in \mathbb{R}^n$, with $n = q + s$, $E(z) = \operatorname{diag}(E_1(z), 0)$ and

$$A(z) = \begin{bmatrix} A_{11}(z) & A_{12}(z) \\ A_{21}(z) & A_{22}(z) \end{bmatrix}, \quad B(z) = \begin{bmatrix} B_1(z) \\ B_2(z) \end{bmatrix}.$$

The following definition is important to analyze the regular and impulse-free properties of system (I.21).

Definition I.3 [Yang et al., 2013] The unforced singular system (I.21), *i.e.*, $u = 0$, is of index-one if there exists a unique solution $x_a = f(x_d)$ in some neighborhood of the equilibrium $x(0) = 0$ satisfying $f(0) = 0$ and

$$A_{21}(z)x_d(t) + A_{22}(z)f(x_d(t)) = 0. \tag{I.23}$$

We consider the following assumption for system (I.21).

Assumption 1. The premise variables depend only on x_d, *i.e.*, $z(x) = g(x_d)$, where $g : \mathbb{R}^q \to \mathbb{R}^r$ is a differentiable function with respect to x_d.

Note that under Assumption 1, the unforced system (I.21) is of index-one if $\det(A_{22}(z)) \neq 0$, for all $z(t) \in \mathscr{D}_z$. Moreover, in this case the unique solution of equation (I.23) is given by

$$x_a = f(x_d) = -A_{22}(z)^{-1}A_{21}(z)x_d. \tag{I.24}$$

It is also clear from (I.24) that if $x_d \to 0$, then $x_a \to 0$. The following definition is useful for the admissibility analysis of system (I.21).

Definition I.4 *The unforced singular system* (I.21), i.e., $u = 0$, *is admissible if it is of index-one and its solution* $x = 0$ *is asymptotically stable.*

For analysis, the compact form (I.21) can be rewritten in the extended form

$$\bar{E}_o \dot{x}_e(t) = \sum_{i=1}^{n_r} \mu_i(z)(\bar{A}_i x_e(t) + \bar{B}_i u(t)), \tag{I.25}$$

where

$$x_e = \begin{bmatrix} x_d \\ \dot{x}_d \\ x_a \end{bmatrix}, \quad \bar{E}_o = \begin{bmatrix} I & 0 & 0 \\ 0 & 0 & 0 \\ 0 & 0 & 0 \end{bmatrix}, \quad \bar{A}(z) = \begin{bmatrix} 0 & I & 0 \\ A_{11}(z) & -E_1(z) & A_{12}(z) \\ A_{21}(z) & 0 & A_{22}(z) \end{bmatrix}, \quad \bar{B}(z) = \begin{bmatrix} 0 \\ B_1(z) \\ B_2(z) \end{bmatrix}.$$

Theorem I.1 *If there exist a positive definite matrix* $P_{11} \in \mathbb{S}^q$ *and matrices* $P_{21} \in \mathbb{R}^{(q+s)\times q}$, $P_{22} \in \mathbb{R}^{(q+s)\times(q+s)}$ *such that*

$$\bar{A}_i^\top P + P^\top \bar{A}_i \prec 0 \tag{I.26}$$

where

$$P = \begin{bmatrix} P_{11} & 0 \\ P_{21} & P_{22} \end{bmatrix}, \qquad \sum_{i=1}^{n_r} \mu_i(z)\bar{A}_i = \bar{A}(z)$$

for all $i \in \mathcal{I}_{n_r}$, *then the singular system* (I.21) *with* $u = 0$ *and under Assumption 1 is admissible.*

Proof:
Consider the following Lyapunov candidate function:

$$\mathcal{V}(x_e) = x_e^\top \bar{E}_o^\top P x_e$$

Since $P = \begin{bmatrix} P_{11} & 0 \\ P_{21} & P_{22} \end{bmatrix}$ *with* $P_{11} \succ 0$, *the condition* $\mathcal{V}(x_e) \geq 0$ *for all* $x_e \neq 0$ *is satisfied as* $\bar{E}_o^\top P = P^\top \bar{E}_o \succeq 0$ *is verified. On the other hand, we have*

$$\begin{aligned} \dot{\mathcal{V}}(x_e) &= \dot{x}_e^\top \bar{E}_o^\top P x_e + x_e^\top P^\top \bar{E}_o \dot{x}_e \\ &= x_e^\top (\bar{A}^\top(z)P + P^\top \bar{A}(z)) x_e \\ &= x_e^\top \sum_{i=1}^{n_r} \mu_i(z)(\bar{A}_i^\top P + P^\top \bar{A}_i) x_e \end{aligned}$$

According to the convex sum property of the MFs $\mu_i(z)$, *if condition* (I.26) *holds then we have* $\dot{\mathcal{V}}(x_e) = \dot{x}_d^\top P_{11} x_d + x_d^\top P_{11} \dot{x}_d < 0$ *as such the solution* $x = 0$ *is asymptotically stable. Moreover, according to* (I.25) *we have*

$$\bar{A}^\top(z)P + P^\top \bar{A}(z) = \begin{bmatrix} \bullet & \bullet \\ \bullet & \bar{A}_{22}^\top(z)P_{22} + P_{22}^\top \bar{A}_{22}(z) \end{bmatrix} \prec 0$$

where "$\bullet$*" denotes matrix terms irrelevant to the theoretical developments and*

$$\bar{A}_{22}(z) = \begin{bmatrix} -E(z) & A_{12}(z) \\ 0 & A_{22}(z) \end{bmatrix} \in \mathbb{R}^{n\times n}.$$

It follows that $\det(A_{22}(z)) \neq 0$ *for all* $z \in \mathscr{D}_z$ *which implies that system* (I.21) *is admissible.*

Remark I.4. For the regular case, *i.e.*, $\operatorname{rank}(E(z)) = n_x$, we have $x_a(t) \in \emptyset$ with $q = n_x$ and $s = 0$. The issue of admissibility is reduced to that of stability with similar conditions to (I.26). As for the special case of $E(z) = I$, similar conditions for stability analysis can be obtained with the following substitutions $\bar{A}(z) = A_{11}(z)$ and $P = P_{11}$.

I.4.2 Stabilization of Descriptor TS Fuzzy Models

The problem of stabilization consists in finding a control law $u(t)$ for system (I.25) satisfying closed-loop performances. For TS models, the most widely used control law is the parallel distributed compensation (PDC) scheme by [Wang, Tanaka, and Griffin, 1996; Tanaka, Ikeda, and Wang, 1998]. Since then, several variants have been proposed depending on the class of TS models considered. For example, there is the modified PDC for TS model descriptor (non-PDC) [Taniguchi, Tanaka, and Wang, 2000], the proportional PDC by [Lin and Er, 2001], and the compensation and division control scheme for fuzzy models by [Guerra and Vermeiren, 2001].

Similarly to stability analysis, the notion of stabilization for descriptor systems is linked to that of stabilization. Considering the following PDC control law

$$u(t) = \bar{F}(z)x_e(t), \quad \bar{F}(z) = \begin{bmatrix} F(z) & 0 \end{bmatrix}, \quad F(z) = \sum_{i=1}^{n_r} \mu_i(z)F_i \tag{I.27}$$

with $F_i \in \mathbb{R}^{m\times q}$. The closed-loop form of system (I.25) with the PDC control (I.27) is given by

$$\bar{E}_o\dot{x}_e(t) = \bar{A}_c(z)x_e(t) \tag{I.28}$$

with

$$\bar{A}_c(z) = \bar{A}(z) + \bar{B}(z)\bar{F}(z) = \begin{bmatrix} 0 & I & 0 \\ A_{11}(z) + B_1(z)F(z) & -E(z) & A_{12}(z) \\ A_{21}(z) + B_2(z)F(z) & 0 & A_{22}(z) \end{bmatrix}. \tag{I.29}$$

Theorem I.2 *If there exist a positive definite matrix* $P_{11} \in \mathbb{S}^q$, *matrices* $P_{21} \in \mathbb{R}^{(q+s)\times q}$, $P_{22} \in \mathbb{R}^{(q+s)\times(q+s)}$, *and* $M_j \in \mathbb{R}^{m\times q}$ *such that for all* $i, j \in \mathcal{I}_{n_r}$

$$\begin{aligned} &\Upsilon_{ii} \prec 0, \\ &\frac{2}{r-1}\Upsilon_{ii} + \Upsilon_{ij} + \Upsilon_{ji} \prec 0, \quad i \neq j, \end{aligned} \tag{I.30}$$

with

$$\Upsilon_{ij} = \bar{A}_iP + P^\top\bar{A}_i^\top + \bar{B}_i\bar{M}_j + \bar{M}_j^\top\bar{B}_i^\top,$$

$$P = \begin{bmatrix} P_{11} & 0 \\ P_{21} & P_{22} \end{bmatrix}, \quad \bar{M}_j = \begin{bmatrix} M_j & 0 \end{bmatrix},$$

then the solution $x = 0$ *of the closed-loop system* (I.28) *is asymptotically stable and the singular system* (I.25) *under Assumption 1 is admissible with the following PDC control law*

$$u(t) = \sum_{j=1}^{n_r} \mu_j(z)F_jx_d(t), \quad F_j = M_jP_{11}^{-1}. \tag{I.31}$$

Proof:
Applying the dual sum relaxation Lemma I.4, the conditions (I.30) imply the following result

$$\Upsilon(z) = \sum_{i=1}^{n_r}\sum_{j=1}^{n_r} \mu_i(z)\mu_j(z)\Upsilon_{ij} \prec 0. \tag{I.32}$$

On the other hand, we have $\bar{M}(z) = \bar{F}(z)P$ *and*

$$\Upsilon(z) = \mathrm{He}\left((\bar{A}(z) + \bar{B}(z)\bar{F}(z))P\right) \prec 0 \tag{I.33}$$

which implies that $\det(P) \neq 0$ *and thus* P *is invertible. Using the congruence transformation Lemma I.1 with* $\mathcal{R} = \mathrm{He}\left(\bar{A}(z)P + \bar{B}(z)\bar{F}(z)P\right)$ *and* $\mathcal{Q} = P^{-\top}$*, the result in (I.33) is equivalent to*

$$\mathrm{He}\left(P^{-\top}\bar{A}(z) + P^{-\top}\bar{B}(z)\bar{F}(z)\right) \prec 0. \tag{I.34}$$

Considering the following Lyapunov candidate function

$$\mathcal{V}(x_e) = x_e^\top \bar{E}_o^\top P^{-1} x_e,$$

since $P = \begin{bmatrix} P_{11} & 0 \\ P_{21} & P_{22} \end{bmatrix}$ *with* $P_{11} \succ 0$*, the condition* $\mathcal{V}(x_e) \geq 0$ *for all* $x_e \neq 0$ *is satisfied as* $\bar{E}_o^\top P^{-1} = P^{-\top}\bar{E}_o \succeq 0$ *is verified. On the other hand, we have*

$$\begin{aligned} \dot{\mathcal{V}}(x_e) &= \dot{x}_e^\top \bar{E}_o^\top P^{-1} x_e + x_e^\top P^{-\top}\bar{E}_o \dot{x}_e \\ &= x_e^\top \mathrm{He}\left(P^{-\top}\bar{A}(z) + P^{-\top}\bar{B}(z)\bar{F}(z)\right)x_e < 0. \end{aligned}$$

According to (I.34), we have $\dot{\mathcal{V}}(x_e) = \dot{x}_d^\top P_{11}^{-1} x_d + x_d^\top P_{11}^{-1}\dot{x}_d < 0$ *as such the solution* $x = 0$ *is asymptotically stable. Moreover, according to (I.28) and (I.34) we have*

$$\bar{A}_c(z)P + P^\top \bar{A}_c^\top(z) = \begin{bmatrix} \bullet & \bullet \\ \bullet & \bar{A}_{22}(z)P_{22} + P_{22}^\top \bar{A}_{22}^\top(z) \end{bmatrix} \prec 0,$$

where "$\bullet$*" denotes matrix terms irrelevant to the theoretical developments and*

$$\bar{A}_{22}(z) = \begin{bmatrix} -E(z) & A_{12}(z) \\ 0 & A_{22}(z) \end{bmatrix} \in \mathbb{R}^{n\times n}.$$

It follows that $\det(A_{22}(z)) \neq 0$ *for* $z \in \mathscr{D}_z$ *and thus system (I.25) under Assumption 1 is admissibilizable with the PDC control law (I.32).*

Remark I.5. Similarly to the case of admissibility, the stabilization for the regular case, *i.e*, $\mathrm{rank}(E(z)) = n_x$, renders the Assumption 1 trivial while maintaining the same LMI conditions as Theorem I.2. As for the special case where $E(z) = I$, similar conditions for a stabilizing PDC control design can be obtained with the following substitutions $\bar{A}_i = A_i$, $P = P_{11}$, $\bar{M}_j = M_j$, $\bar{F}_j = F_j$, and $u(t) = \sum_{j=1}^{n_r} \mu_j(z)F_j x(t)$.

Example I.2 (2-DoF Serial Robot Manipulator)
The dynamics of a general n-DoF serial manipulator can be expressed as [Spong and Vidyasagar, 2008]

$$M(\theta)\ddot{\theta}(t) + N(\theta,\dot{\theta})\dot{\theta}(t) + G(\theta) = \Gamma(t), \tag{I.35}$$

where $\theta(t) \in \mathbb{R}^n$ is the vector of generalized coordinates in joint space, $\Gamma(t) \in \mathbb{R}^n$ is the vector of generalized control forces, $M(\theta) \in \mathbb{R}^{n\times n}$ is the inertia matrix, $N(\theta, \dot{\theta}) \in \mathbb{R}^{n\times n}$ is the Coriolis/centripetal matrix plus the viscous friction coefficients of the joints, and $G(\theta) \in \mathbb{R}^n$ represents the gravity matrix. Note that the dynamics (I.35) can account for many types of robot manipulators. Since the vector field $G(\theta)$ is smooth and $G(0) = 0$, we can then parameterize $G(\theta) = H(\theta)\theta(t)$.

Let us denote $x(t) = \begin{bmatrix}\theta^\top(t) & \dot{\theta}^\top(t)\end{bmatrix}^\top$ and $u(t) = \Gamma(t)$. The manipulator dynamics (I.35) can be rewritten into the descriptor form (I.25) with

$$\bar{E}_o = \begin{bmatrix} I & 0 \\ 0 & 0 \end{bmatrix}, \quad \bar{A}(z) = \begin{bmatrix} 0 & I \\ A_{11}(z) & -E(z) \end{bmatrix}, \quad \bar{B} = \begin{bmatrix} 0 \\ I \end{bmatrix},$$

$$A_{11}(z) = \begin{bmatrix} 0 & I \\ -H(\theta) & -N(\theta, \dot{\theta}) \end{bmatrix}, \quad E(z) = \begin{bmatrix} I & 0 \\ 0 & M(\theta) \end{bmatrix}.$$

Given that the matrix $E(z)$ is regular then assumption 1 holds with $x_a(t) \in \emptyset$. For illustration, we consider the following case of $n = 2$ degrees of freedom as shown in Fig. I.3. The characteristic matrices of the robot manipulator are then given by

$$M(\theta) = \begin{bmatrix} c_1 + 2c_2\cos\theta_2 & c_3 + c_2\cos\theta_2 \\ c_3 + c_2\cos\theta_2 & c_3 \end{bmatrix}, \quad N(\theta, \dot{\theta}) = \begin{bmatrix} 2c_2\dot{\theta}_2\sin\theta_2 - f_{v1} & c_2\dot{\theta}_2\sin\theta_2 \\ -c_2\dot{\theta}_1\sin\theta_2 & 0 - f_{v2} \end{bmatrix},$$

$$H(\theta) = \begin{bmatrix} -c_4\,\mathrm{sinc}\,\theta_1 - c_5\,\mathrm{sinc}\,\theta_{12} & -c_5\,\mathrm{sinc}\,\theta_{12} \\ -c_5\,\mathrm{sinc}\,\theta_{12} & -c_5\,\mathrm{sinc}\,\theta_{12} \end{bmatrix},$$

where $\theta_{12} = \theta_1 + \theta_2$, $c_1 = m_1 r_1^2 + I_1 + m_2 L_1^2 + m_2 r_2^2 + I_2$, $c_2 = m_2 L_1 r_2$, $c_3 = m_2 r_2^2 + I_2$, $c_4 = m_1 g r_1 + m_2 g L_1$, $c_5 = m_2 g r_2$. The TS fuzzy representation is then given by

$$\bar{E}_o\dot{x}(t) = \sum_{i=1}^{n_r} \mu_i(z)\bar{A}_i(z)x(t) + \bar{B}u(t) \tag{I.36}$$

where the five premise variables of this 2-DoF robot are defined as follows:

$$z_1 = \cos\theta_2,\ z_2 = -c_4\,\mathrm{sinc}\,\theta_1 - c_5\,\mathrm{sinc}\,\theta_{12},\ z_3 = -c_5\,\mathrm{sinc}\,\theta_{12},\ z_4 = c_2\dot{q}_2\sin\theta_2,\ z_5 = -c_2\dot{q}_1\sin\theta_2.$$

Applying Theorem I.2, we design a stabilizing control law for the 2-DoF serial robot manip-

TABLE I.1: Mechanical Constants of the 2-DoF Manipulator Robot.

Symbol	Description	Nominal value
g	Gravitational constant	9.81 [m/s^2]
L_1	Length of arm link 1	0.5 [m]
L_2	Length of arm link 2	0.5 [m]
I_1	Inertia of arm link 1	0.3125 [kg.m^2]
I_2	Inertia of arm link 2	0.1875 [kg.m^2]
m_1	Mass of arm link 1	15 [kg]
r_1	Distance to gravity center 1	0.25 [m]
m_2	Mass of arm link 2	9 [kg]
r_2	Distance to gravity center 2	0.25 [m]

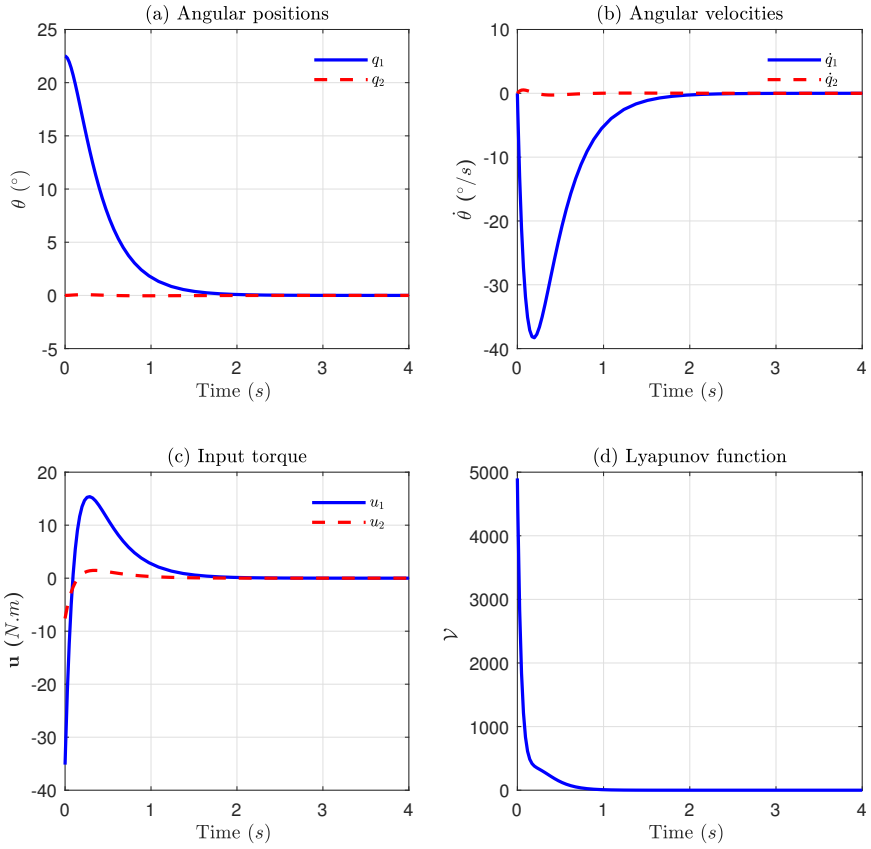

FIGURE I.2: Stabilization of 2-DoF Serial Robot Manipulator

ulator. Figure I.2 depicts the results of simulation on a high fidelity Simscape SimMechanics model with the viscous friction coefficients set to $f_{v1} = f_{v2} = 0$ rendering the system unstable in open loop. Given the dynamics of the system, a decay rate of $\alpha = 1$ was adopted to improve the convergence rate of the state variables [Lendek et al., 2011]. An initial point has been set at $x_0 = \begin{bmatrix} 22.5 & 0 & 0 & 0 \end{bmatrix}^\top$. Figure I.2 presents the trajectories of: (a) the angular position $\theta(t)$ in degrees, (b) the angular velocities $\dot{\theta}(t)$ in degrees per second, (c) the input torque in Newton per meter, and (d) the Lyapunov candidate function. We can see that all of the state variables converge towards the equilibrium state according to the decay rate. Table I.1 provides the value for the mechanical constants of the 2-DoF robot.

The issue of stabilization can further be complicated by the presence of either imperfections within the mathematical model or unforeseen disturbances that can impact the dynamics of the system. This may lead to a degradation of the desired performance and even destabilize the system. An effective solution for this problem is to design robust controller that can guarantee the desired performance level and the stability of the system in the presence of such uncertainties.

I.5 Robustness and Model Complexity of Descriptor TS Fuzzy Systems

Modeling a physical system is a crucial phase for model-based control design approaches. Due to uncertainties, the mathematical model may not reflect closely the real physical behavior of the system. However, by characterizing these uncertainties, it is possible to embed the nominal

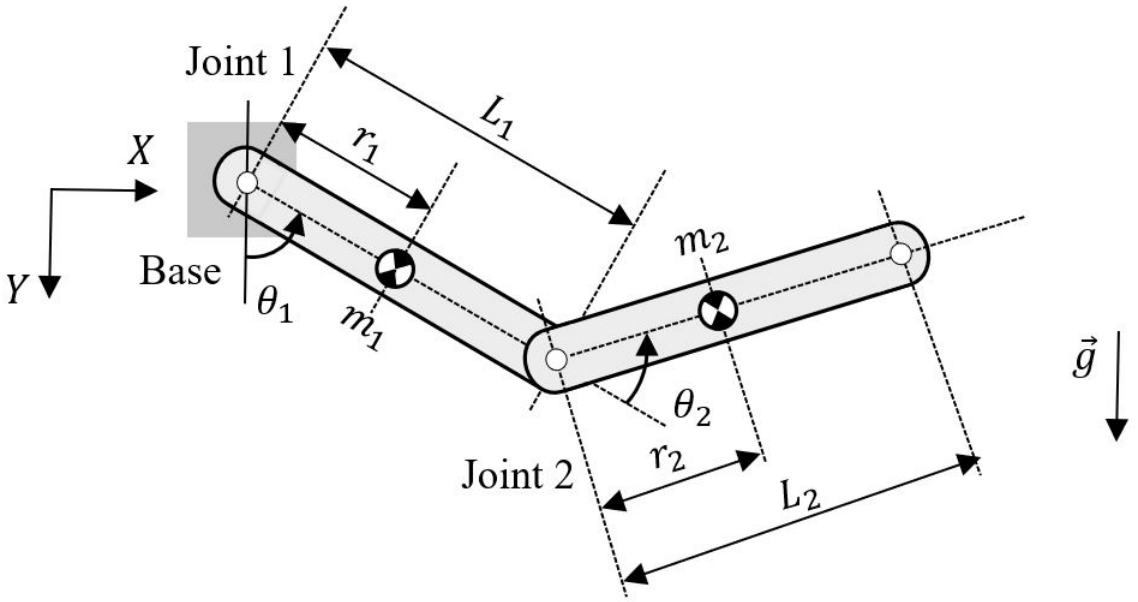

FIGURE I.3: Schematic of the 2-DoF robot manipulator in the vertical plane.

model in a larger class of systems that would include the "exact" model of the physical system. Designing a controller for a class of uncertain systems is generally more difficult but the designed controller has the benefit of being robust. There are many sources of uncertainties, but they are generally classified into two categories [Yedavalli, 2014; Sira-Ramírez et al., 2017]

- **Non-structural uncertainties**, also known as non-parametric uncertainties. They represent external dynamics, for example: measurement noise, input disturbances, etc. In general, their dynamics are unknown. However, they remain bounded in norm.
- **Structural uncertainties**, also known as modeling or parametric uncertainties. They are generally due to approximation errors and/or necessary simplifications in order to obtain a reduced complexity model that best reflects the dynamic behavior of the physical system.

In this part, only the robustness of TS controllers in relation to structural uncertainties is presented.

I.5.1 Robust Stabilization for Descriptor TS Fuzzy Systems

Considering the following uncertain descriptor system:

$$E(z)\dot{x}(t) = \big(A(z) + \Delta A(z)\big)x(t) + \big(B(z) + \Delta B(z)\big)u(t) \tag{I.37}$$

with $E(z) = \text{diag}(E_1(z), 0)$, $\text{rank}(E_1(z)) = q$, $\Delta A(z) = H_a \Delta_a(z) W_a$, $\Delta B(z) = H_b \Delta_b(z) W_b$, $\Delta_a(z)\Delta_a^\top(z) \leq I$, and $\Delta_b(z)\Delta_b^\top(z) \leq I$. Considering Assumption 1 for the descriptor system (I.37), we define the following extended form

$$\bar{E}_o \dot{x}_e(t) = \big(\bar{A}(z) + \Delta\bar{A}(z)\big)x_e(t) + \big(\bar{B}(z) + \Delta\bar{B}(z)\big)u(t) \tag{I.38}$$

where $x_e(t)$, $\bar{E}_o$, $\bar{A}(z)$, and $\bar{B}(z)$ are as defined in (I.25) while $\Delta\bar{A}(z) = \bar{H}_a \Delta_a(z) \bar{W}_a$, $\Delta\bar{B}(z) = \bar{H}_b \Delta_b(z) W_b$ with

$$\bar{H}_a = \begin{bmatrix} 0 \\ H_a \end{bmatrix}, \qquad \bar{H}_b = \begin{bmatrix} 0 \\ H_b \end{bmatrix}, \qquad \bar{W}_a = \begin{bmatrix} W_a & 0 \end{bmatrix}. \tag{I.39}$$

Applying the PDC control law (I.27) to system (I.38) under Assumption 1 yields a closed-loop system similar to (I.28) with

$$\bar{A}_c(z) = \bar{A}(z) + \Delta\bar{A}(z) + \Big(\bar{B}(z) + \Delta\bar{B}(z)\Big)\bar{F}(z) \tag{I.40}$$

Theorem I.3 *If there exist a positive definite matrix $P_{11} \in \mathbb{S}^q$, matrices $P_{21} \in \mathbb{R}^{s\times 2q}$, $P_{22} \in \mathbb{R}^{s\times s}$, $F_j \in \mathbb{R}^{m\times q}$, and scalars $\epsilon_a > 0$, $\epsilon_b > 0$ such that, for all $i, j \in \mathcal{I}_{n_r}$,*

$$\begin{aligned} &\Upsilon_{ii} \prec 0, \\ &\frac{2}{r-1}\Upsilon_{ii} + \Upsilon_{ij} + \Upsilon_{ji} \prec 0, \quad i \neq j. \end{aligned} \tag{I.41}$$

with

$$\Upsilon_{ij} = \begin{bmatrix} \bar{A}_i P + P^\top \bar{A}_i^\top + \bar{B}_i\bar{M}_j + \bar{M}_j^\top \bar{B}_i^\top + \epsilon_a \bar{H}_a\bar{H}_a^\top + \epsilon_b \bar{H}_b\bar{H}_b^\top & \star & \star \\ \bar{W}_a P & -\epsilon_a I & \star \\ W_b\bar{M}_j & 0 & -\epsilon_b I \end{bmatrix},$$

$$P = \begin{bmatrix} P_{11} & 0 \\ P_{21} & P_{22} \end{bmatrix}, \qquad \bar{M}_j = \bar{F}_j P, \qquad \bar{F}_j = \begin{bmatrix} F_j & 0 \end{bmatrix},$$

then the solution $x = 0$ of the closed-loop system (I.38) is asymptotically stable and the uncertain descriptor system (I.37) under Assumption 1 is robustly admissibilizable with the following PDC control law

$$u(t) = \sum_{j=1}^{n_r} \mu_j(z)\bar{F}_j x_e(t), \quad F_j = M_j P_{11}^{-1} \tag{I.42}$$

Proof:
Applying Lemma I.4 to the conditions in (I.41) yields the following result

$$\Upsilon(z) = \begin{bmatrix} \mathrm{He}\left(\bar{A}(z)P + \bar{B}(z)\bar{M}(z)\right) + \epsilon_a \bar{H}_a\bar{H}_a^\top + \epsilon_b \bar{H}_b\bar{H}_b^\top & \star & \star \\ \bar{W}_a P & -\epsilon_a I & \star \\ W_b\bar{M}(z) & 0 & -\epsilon_b I \end{bmatrix} \prec 0 \tag{I.43}$$

It follows from both Lemmas I.3 and I.5 that

$$\mathrm{He}\Big((\bar{A}(z) + \Delta\bar{A})P + (\bar{B}(z) + \Delta\bar{B})\bar{M}(z)\Big) \prec 0 \tag{I.44}$$

Taking the Lyapunov candidate function $\mathcal{V}(x_e) = x_e^\top \bar{E}_o^\top P^{-1} x_e$, the remainder of the proof is similar to that of Theorem I.2.

Remark I.6. Considering some scheduling variables as parametric uncertainties may lead to another uncertain TS polytopic representation with a smaller number of vertices n_r. This allows reducing the numerical complexity of the LMI constraints [Nguyen et al., 2019]. However, considering the size of the conditions (I.41) and the presence of positive definite terms ($\epsilon_a \bar{H}_a\bar{H}_a^\top \succeq 0, \epsilon_b \bar{H}_b\bar{H}_b^\top \succeq 0$) in the diagonal blocks of the LMI, it can dramatically increase the conservatism in finding feasible solutions to the design conditions.

I.5.2 Reduced Complexity Modeling for TS Fuzzy Approach

Recent contributions in the field of TS fuzzy systems focus on introducing new LMI conditions to improve feasibility and reduce the conservatism, for example via the introduction of nonquadratic

Lyapunov functions [Lee, Park, and Joo, 2012; Guerra and Vermeiren, 2004; Mozelli, Palhares, and Avellar, 2009; Nguyen, Guerra, and Campos, 2019] and the development of multiple-sum relaxation approaches [Sala and Ariño, 2007; Coutinho et al., 2020]. However, an underlying problem with the TS fuzzy modeling approach is the number of local linear submodels that is needed to build the whole model as it increases exponentially in function of the number of the premise variables. As written above, using the sector nonlinearity approach, a TS fuzzy model based on r nonlinear terms has $n_r = 2^r$ number of fuzzy rules. The complexity introduced by this exponential growth can render the application of TS fuzzy approach limited to systems with a small number of nonlinearities.

In this regard, we propose a reduced complexity model with $r + 1$ fuzzy rules obtained directly from an initial TS fuzzy model derived from the sector nonlinearity approach. It relies on existing linear relations between the different matrix vertices of the TS model. Consider the descriptor TS fuzzy model (I.7). The different vertices X_i with X in $\{E, A, B\}$ satisfy

$$X_i = X(z_1^{i_1},\ z_2^{i_2},\ \dots\ ,\ z_r^{i_r}) \tag{I.45}$$

with $i_k \in \{0,\ 1\}$ such that $i = 1 + i_1 + i_2 \times 2 + \cdots + i_r \times 2^{r-1}$ (that is, $i_r \dots i_2 i_1$ is the binary representation of the integer $i - 1$ using r bits).

As $X(z)$ is assumed affine in z, it can be expressed as

$$X(z) = \hat{X}_0 + \sum_{p=1}^{r} z_p \hat{X}_p \tag{I.46}$$

for some given matrices $\hat{X}_k$. In other words, all the matrices X_i belong to the linear subspace spanned by the $r+1$ matrices $\hat{X}_p$. We will show now that they are also in the subspace generated by the set of matrices $\mathcal{S}_r := \{X_j : j \in \mathcal{J}_r\}$ with $\mathcal{J}_r := \{2^p - 1 : p \in \mathcal{I}_r\} \cup \{2\}$.

As $\mathcal{I}_2 = \mathcal{J}_1$, this obviously holds for $r = 1$. So, let us proceed by induction on r: assume that for some integer $p \in \mathcal{I}_{r-1}$, the matrices X_i for all i in $\mathcal{I}_{2^p}$ belong to the subspace $\mathrm{span}(\mathcal{S}_p)$. Then, as $\mathcal{J}_p \subset \mathcal{J}_{p+1}$, they also belong to $\mathrm{span}(\mathcal{S}_{p+1})$. Now, let j be an arbitrary integer in $\mathcal{I}_{2^{p+1}} \setminus \mathcal{I}_{2^p}$, and let $i = j - 2^p$. Then $i \in \mathcal{I}_{2^p}$, and according to (I.45), we have

$$\begin{aligned} X_i &= X(z_1^{i_1}, z_2^{i_2}, \dots, z_p^{i_p}, z_{p+1}^0, z_{p+2}^0, \dots, z_r^0) \\ X_j &= X(z_1^{i_1}, z_2^{i_2}, \dots, z_p^{i_p}, z_{p+1}^1, z_{p+2}^0, \dots, z_r^0) \end{aligned}$$

So that, from (I.46),

$$X_j - X_i = (z_{r_0+1}^1 - z_{p+1}^0)\hat{X}_{p+1}$$

As a particular case, for $i = 2^p - 1$, we get

$$(z_{p+1}^1 - z_{p+1}^0)\hat{X}_{p+1} = X_{2^{p+1}-1} - X_{2^p-1},$$

so that

$$X_j = X_{2^{p+1}-1} - X_{2^p-1} + X_i,$$

which shows that X_j is in the subspace $\mathrm{span}(\mathcal{S}_{p+1})$. So, by mathematical induction, any matrix X_i for $i \in \mathcal{I}_{2^r}$ can be expressed as a combination of matrices X_j for $i \in \mathcal{J}_r$ and

$$X_i = X_{2^p-1} - X_{2^{p-1}-1} + X_{i-2^{p-1}}, \quad \forall p, i : 2 \le p \le r,\ 1 + 2^{p-1} \le i \le 2^p \tag{I.47}$$

Note that from the previous recurrence relation, it may be shown that X_i is in fact an affine combination of matrices X_j in $\mathcal{S}_r$, that is the sum of the coefficients is always equal to 1, and also that these coefficients belong to $\{0,\ 1,\ -1\}$. This may be easily checked for $r = 3$, for which

the relations between the matrices are:
$X_1, X_2, X_3, X_4 = X_3 - X_1 + X_2, X_5 = X_7 - X_3 + X_1, X_6 = X_7 - X_3 + X_2, X_7, X_8 = X_7 + X_2 - X_1.$

Exploiting further the recurrence relation (I.47), it is possible to characterize more precisely the coefficients of the linear combinations. For $j \in \mathcal{J}_r$, denote $I_j^+(r)$, respectively $I_j^-(r)$, the set of indexes $i \in \mathcal{I}_{2^r}$ such that the component of X_i with respect to X_j is $+1$, respectively -1.

Using (I.47), we have $I_1^+(p+1) = \{i + \epsilon 2^p : i \in I_1^+(p),\ \epsilon \in \{0,1\}\}$ for $p \geq 2$. Initializing this relation with $I_1^+(2) = \{1\}$ yields $I_1^+(r) = \{1 + \epsilon_1 2^2 + \epsilon_2 2^3 + \cdots + \epsilon_{r-2} 2^{r-1} : \epsilon_i \in \{0,1\},\ \forall i \in \mathcal{I}_{r-1}\}$, or equivalently $I_1^+(r) = \{1 + 4k : 0 \leq k \leq 2^{r-2} - 1\}$, for $r \geq 2$.

Similarly, $I_1^-(r) = \{4 + 4k : 0 \leq k \leq 2^{r-2} - 1\}$, $I_2^+(r) = \{2 + 2k : 0 \leq k \leq 2^{r-1} - 1\}$, $I_2^-(r) = \emptyset$.

For the integers j of the form $2^p - 1$ (with $p \geq 2$), there are several cases :

- If $\ell < p$, then $I_j^+(\ell) = I_j^-(\ell) = \emptyset$.
- $I_j^+(p) = \{i : 1 + 2^{p-1} \leq i \leq 2^p\}$, $I_j^-(k) = \emptyset$.
- $I_j^+(p+1) = I_j^+(p)$, $I_j^-(p+1) = \{i : 1 + 2^p \leq i \leq 2^{p-1} + 2^p\}$.
- for $\ell \geq p + 2$, we have the relations $I_j^+(\ell + 1) = \{i + \epsilon 2^\ell : i \in I_j^+(\ell), \epsilon \in \{0,1\}\}$, and $I_j^-(\ell + 1) = \{i + \epsilon 2^\ell : i \in I_j^-(\ell), \epsilon \in \{0,1\}\}$, which yield
  $I_j^+(r) = \{i + 2^{p+1}k : 1 + 2^{p-1} \leq i \leq 2^p, 0 \leq k \leq 2^{r-p-1} - 1\}$, and
  $I_j^-(r) = \{i + 2^{p+1}k : 1 + 2^p \leq i \leq 2^{p-1} + 2^p, 0 \leq k \leq 2^{r-p-1} - 1\}$ for $2 \leq p \leq r - 1$.

This allows us to state the following result.

Lemma I.6 [Dehak et al., 2020]
Consider the descriptor TS model (I.7) characterized by the vertices E_i, A_i, B_i and the membership functions μ_i for $i \in \mathcal{I}_{2^r}$. Then, for $r \geq 2$, an equivalent representation is given by

$$\sum_{j \in \mathcal{J}_r} \tilde{\omega}_j(z) E_j \dot{x}(t) = \sum_{j \in \mathcal{J}_r} \tilde{\omega}_j(z)(A_j x(t) + B_j u(t)), \tag{I.48}$$

where the weights $\tilde{\omega}_j(z)$ are defined as

$$\begin{aligned} &\tilde{\omega}_1 = \sum_{j=1}^{2^{r-2}} \mu_{4j-3} - \sum_{j=1}^{2^{r-2}} \mu_{4j}, \quad \tilde{\omega}_2 = \sum_{j=1}^{2^{r-1}} \mu_{2j}, \quad \tilde{\omega}_{2^r-1} = \sum_{j=1+2^{r-1}}^{2^r} \mu_j \\ &\tilde{\omega}_{2^k-1} = \sum_{j=1}^{2^{r-k-1}} \left(\sum_{i=1+2^{k-1}}^{2^k} \mu_{i+(j-1)2^{k+1}} - \sum_{i=2^k+1}^{2^{k-1}+2^k} \mu_{i+(j-1)2^{k+1}} \right), \quad \forall k \in \mathcal{I}_{r-1} \setminus \{1\}. \end{aligned} \tag{I.49}$$

Furthermore, we have that

$$-1 \leq \tilde{\omega}_j(z) \leq 1,\ \forall j \in \mathcal{J}_r, \text{ and } \sum_{j \in \mathcal{J}_r} \tilde{\omega}_j(z) = 1. \tag{I.50}$$

Proof:
It remains to prove only the last point. For this, let us remark that the obtained decomposition does not depend on a particular choice of the initial vertices. That is, any affine function $A(z)$ for which the sector nonlinearity approach gives the decomposition

$$A(z) = \sum_{i \in \mathcal{I}_{2^r}} \mu_i(z) A_i$$

can also be rewritten as

$$A(z) = \sum_{j \in \mathcal{J}_r} \tilde{\omega}_j A_j$$

Taking $A(z) = I$ *leads to* $A_i = I$ *for all* $i \in \mathcal{I}_{2^r}$*, and so* $\sum_{i \in \mathcal{I}_{2^r}} \mu_i(z) = \sum_{j \in \mathcal{J}_r} \tilde{\omega}_j = 1$.

As the scalar functions $\tilde{\omega}_j(z)$ are not nonnegative, model (I.48) cannot be directly exploited in order to obtain LMI stability conditions as previously done. A new model transformation is needed for that.

Theorem I.4 [Dehak et al., 2020]
Associated with the model (I.48), let us define matrices

$$\tilde{X}_i = rX_i - \sum_{p=1}^{r-1} X_{2^p-1}, \tag{I.51}$$

where X denotes any matrix in $\{E, A, B\}$, and functions $\tilde{\mu}_2 = \frac{\tilde{\omega}_2}{r}$, $\tilde{\mu}_{2^r-1} = \frac{\tilde{\omega}_{2^r-1}}{r}$, $\tilde{\mu}_{2^p-1} = \frac{1+\tilde{\omega}_{2^p-1}}{r}$, for all $p \in \mathcal{I}_{r-1}$. Then, an equivalent convex polytopic representation of (I.48) is given by

$$\sum_{j \in \mathcal{J}_r} \tilde{\mu}_j(z) \tilde{E}_j \dot{x}(t) = \sum_{j \in \mathcal{J}_r} \tilde{\mu}_j(z)(\tilde{A}_j x(t) + \tilde{B}_j u(t)). \tag{I.52}$$

Proof:
By a direct substitution, for $X \in \{E, A, B\}$, $z \in \mathscr{D}_z$, *it comes*

$$\begin{aligned}
\sum_{j \in \mathcal{J}_r} \tilde{\mu}_j(z) \tilde{X}_j &= \sum_{j \in \mathcal{J}_r} \tilde{\omega}_j(z) \left(X_j - \frac{1}{r} \sum_{p=1}^{r-1} X_{2^p-1} \right) + \sum_{k=1}^{r-1} \frac{1}{r} \left(rX_{2^k-1} - \sum_{p=1}^{r-1} X_{2^p-1} \right) \\
&= \sum_{j \in \mathcal{J}_r} \tilde{\omega}_j(z) X_j + \sum_{p=1}^{r-1} X_{2^p-1} \left(-\frac{1}{r} \sum_{j \in \mathcal{J}_r} \tilde{\omega}_j(z) + 1 - \frac{r-1}{r} \right) \\
&= \sum_{j \in \mathcal{J}_r} \tilde{\omega}_j(z) X_j
\end{aligned}$$

as $\sum_{j \in \mathcal{J}_r} \tilde{\omega}_j(z) = 1$ *for* $z \in \mathscr{D}_z$. *Similarly,* $\sum_{j \in \mathcal{J}_r} \tilde{\mu}_j(z) = \frac{1}{r} \tilde{\omega}_j(z) + \sum_{k=1}^{r-1} \frac{1}{r} = \frac{1}{r} + \frac{r-1}{r} = 1$, *and all the weights* $\tilde{\mu}_j$ *are nonnegative.*

Being a convex polytopic representation of system(I.2a), both admissibility and stabilization conditions stated in Th. I.1 and Th. I.2 can be adapted to the representation (I.52). Two real-world examples are given in this section to show the interest of the proposed approach. Both examples are concerned with the stability study of the $n-$DoF robot manipulators introduced in Example I.2.

Example I.3 (Comparative Study Case)
We first consider the case $n = 2$ and compare the computational burden of both Theorems I.1 and I.2 for both the TS fuzzy model (I.7) with 32 vertices and the reduced representation (I.52) with 6 vertices. Table I.2 presents a comparison between the number $\mathcal{N}_{var}$ of scalar decision variables and the number $\mathcal{N}_{row}$ of LMI constraints for both modeling approaches. We observe a decrease in the computational burden for the proposed approach (I.52) compared to the standard TS fuzzy approach (I.7).

Varying both the mass of the second arm link ($m_2 \in [1, 7]$) and the viscous friction coefficient ($f_{v1} = 0.5 f_{v2} \in [0, 50]$), we evaluate the feasibility of LMI conditions given in Theorems I.1 and I.2 for both the standard TS fuzzy model (I.7) and the reduced model (I.52). Feasibility

regions of admissibility conditions in Theorem I.1 and Theorem I.2 are shown, respectively, in Figures I.4a and I.4b. As can be seen, the reduced-complexity model may induce extra conservatism compared to the classical sector nonlinearity modeling approach. To relax the

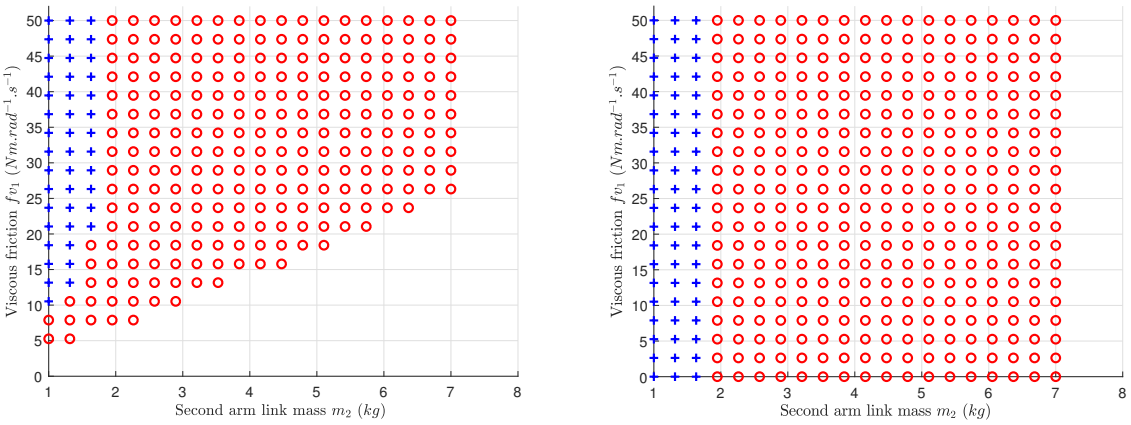

(a) Admissibility region Theorem I.1

(b) Stabilization region Theorem I.2

FIGURE I.4: Feasibility regions for 2-DoF serial robot: Standard TS fuzzy model (I.7) "+,∘", Reduced model (I.52) "+".

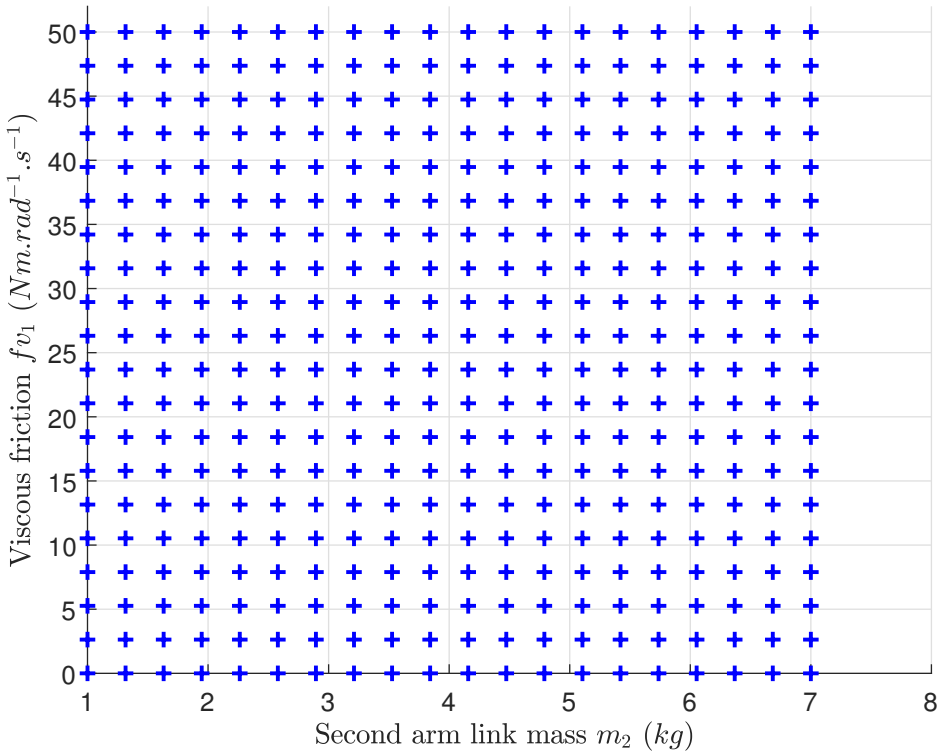

FIGURE I.5: Stabilization region of 2-Dof serial robot manipulator using extended PDC control (I.53) and reduced complexity TS fuzzy model (I.52).

conservatism of the stabilization conditions, we consider an extended PDC control given by the following expression:

$$u(t) = \sum_{j \in \mathcal{J}} \mu_j(z) K_j x_e(t), \tag{I.53}$$

where $K_j \in \mathbb{R}^{m\times 2n_x}$. Contrary to the standard PDC control (I.27), the extended form (I.53) utilizes the full extended state vector and thus requires the measurement of the derivative state [Cardim et al., 2007]. Figure I.5 depicts the feasibility region for the extended PDC applied to the reduced complexity TS fuzzy model (I.52) and shows that despite a significant reduction of complexity, this control approach lead to the same feasibility domain as the standard TS fuzzy approach thanks to the additional degrees of freedom stemming from the control gains of the extended PDC control (I.53). The extended control law is compatible for mechanical systems using accelerometers as sensors. Alternatively, an output dynamical control law can be used based on the design of an observer providing an estimation of the derivative states.

TABLE I.2: Numerical Complexity for a 2-DoF serial robot.

Problem	$\mathcal{N}_{var}$	$\mathcal{N}_{row}$
Analysis-TS	42	260
Analysis-Reduced	78	60
Design-TS	298	260
Design-Reduced	142	60

Example I.4 (3-DoF Serial Robot Manipulator)
For this example, we consider a 3-DoF serial manipulator depicted in Figure I.6, whose dynamics (I.35) can be rewritten in the nonlinear descriptor form (I.25) with $\theta(t) = \begin{bmatrix}\theta_1(t) & \theta_2(t) & \theta_3(t)\end{bmatrix}^\top$, $x(t) = \begin{bmatrix}\theta^\top(t) & \dot\theta^\top(t)\end{bmatrix}^\top \in \mathbb{R}^6$ and

$$\begin{aligned}\bar E_o &= \begin{bmatrix} I_6 & 0\\ 0 & 0\end{bmatrix}, \quad \bar A(z) = \begin{bmatrix} 0 & I\\ A_{11}(z) & -E(z)\end{bmatrix}, \quad \bar B(z) = \begin{bmatrix}0\\ I\end{bmatrix},\\ A_{11}(z) &= \begin{bmatrix} 0 & I\\ -H(z) & -N(z)\end{bmatrix}, \quad E(z) = \begin{bmatrix} I & 0\\ 0 & M(z)\end{bmatrix}.\end{aligned} \tag{I.54}$$

The state-dependent matrices $M(z)$, $N(z)$ and $Y(z)$ in (I.54) are given by

$$N(z) = \begin{bmatrix} n_{11} & n_{12} & n_{13}\\ n_{21} & n_{22} & n_{23}\\ n_{31} & n_{32} & n_{33}\end{bmatrix}, \quad M(z) = \begin{bmatrix} m_{11} & m_{12} & m_{13}\\ \star & 2c_6z_2 + c_8 & c_6z_2 + c_9\\ \star & \star & c_9\end{bmatrix},$$

$$H(z) = \begin{bmatrix} c_1z_{10} + c_2z_{11} + c_3z_{12} & c_2z_{11} + c_3z_{12} & c_3z_{12}\\ \star & c_2z_{11} + c_3z_{12} & c_3z_{12}\\ \star & \star & c_3z_{12}\end{bmatrix},$$

with

$$\begin{aligned}
&m_{11} = 2(c_4z_1 + c_6z_2 + c_5z_3 + c_7), && m_{12} = c_4z_1 + 2c_6z_2 + c_5z_3 + c_8, && m_{13} = c_6z_2 + c_5z_3 + c_9,\\
&n_{11} = c_5(z_6 - z_9) + c_6(z_7 - z_8), && n_{12} = -c_4z_4 + c_6(z_7 - z_8) - c_5z_9, && n_{13} = -c_6z_8 - c_5z_9,\\
&n_{21} = c_4z_5 + c_5z_6 + c_6(z_7 - z_8), && n_{22} = c_6(z_7 - z_8), && n_{23} = -c_6z_8,\\
&n_{31} = c_5z_6 + c_6z_7, && n_{32} = c_6z_7, && n_{33} = 0,\\
&c_1 = g(L_1m_2 + L_1m_3 + m_1r_1), && c_2 = g(L_2m_3 + m_2r_2), && c_3 = gm_3r_3,\\
&c_4 = L_1(L_2m_3 + m_2r_2), && c_5 = L_1m_3r_3, && c_6 = L_2m_3r_3,\\
&c_7 = (m_2 + m_3)L_1^2 + L_2^2m_3 + \sum_{i=1}^{3} I_i, && c_8 = L_2^2m_3 + I_2 + I_3, && c_9 = I_3.
\end{aligned}$$

The expressions of the scheduling variables z_i, for $i \in \mathcal{I}_{12}$, are given in Table I.3, whereas the values of the constant parameters c_i, for $i \in \mathcal{I}_9$, are given in Table I.4.

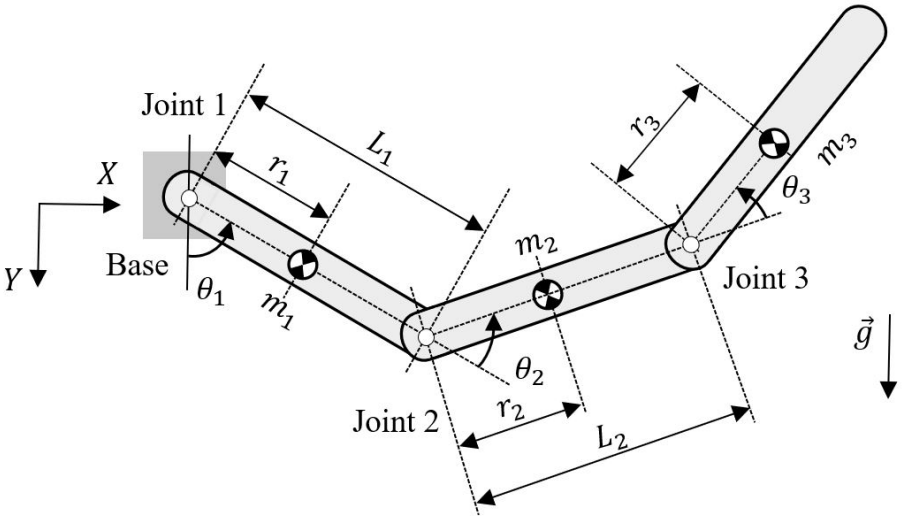

FIGURE I.6: Schematic of the 3-DoF robot manipulator in the vertical plane.

TABLE I.3: Scheduling Variables of the 3-DoF Manipulator Robot.

Scheduling variable	Expression
z_1	$\cos(\theta_2)$
z_2	$\cos(\theta_3)$
z_3	$\cos(\theta_2 + \theta_3)$
z_4	$2\dot{\theta}_1 + \dot{\theta}_2 \sin(\theta_2)$
z_5	$\dot{\theta}_1 \sin(\theta_2)$
z_6	$\dot{\theta}_1 \sin(\theta_2 + \theta_3)$
z_7	$(\dot{\theta}_1 + \dot{\theta}_2) \sin(\theta_3)$
z_8	$(\dot{\theta}_1 + \dot{\theta}_2 + \dot{\theta}_3) \sin(\theta_3)$
z_9	$(\dot{\theta}_1 + \dot{\theta}_2 + \dot{\theta}_3) \sin(\theta_2 + \theta_3)$
z_{10}	$\mathrm{sinc}(\theta_1)$
z_{11}	$\mathrm{sinc}(\theta_1 + \theta_2)$
z_{12}	$\mathrm{sinc}(\theta_1 + \theta_2 + \theta_3)$

For this example with a high number of scheduling variables ($r = 12$), the standard TS fuzzy modeling approach (I.7) yields $2^{12} = 4096$ vertices, which is computationally complex for the control design and especially real-time implementation. The reduced complexity model (I.52) leads to only $12+2 = 14$ vertices, allowing for a feasible control solution. A comparison between the numbers of scalar decision variables and of constraints in the LMI conditions, as well as the number of vertices for both modeling approaches given in Table I.5 shows a significant decrease in the computational burden for the proposed approach compared to the standard TS fuzzy approach.

To evaluate the conservatism of the approach for this example, we let vary two system parameters and evaluate the feasibility of LMI conditions of stabilization Theorem I.2 for the reduced complexity model (I.52) using the extended PDC control (I.53). The two chosen parameters are the mass of the third arm link ($a = m_3$) varying between 1 and 15 kg and the viscous friction

TABLE I.4: Mechanical Constants of the 3-DoF Manipulator Robot.

Symbol	Description	Nominal value
g	Gravitational constant	9.81 [m/s^2]
L_1	Length of arm link 1	1 [m]
L_2	Length of arm link 2	0.9 [m]
L_3	Length of arm link 3	0.8 [m]
I_1	Inertia of arm link 1	2 [kg.m^2]
I_2	Inertia of arm link 2	1.9 [kg.m^2]
I_3	Inertia of arm link 3	1.3 [kg.m^2]
m_1	Mass of arm link 1	5 [kg]
r_1	Distance to gravity center 1	0.5 [m]
m_2	Mass of arm link 2	4.9 [kg]
r_2	Distance to gravity center 2	0.489 [m]
m_3	Mass of arm link 3	4.2 [kg]
r_3	Distance to gravity center 3	0.4 [m]

TABLE I.5: Computational burden for 3-DoF serial robot.

Problem	$\mathcal{N}_{var}$	$\mathcal{N}_{row}$	Nb. Vertices
Design-TS	49158	147549	4096
Design-Reduced	174	441	14

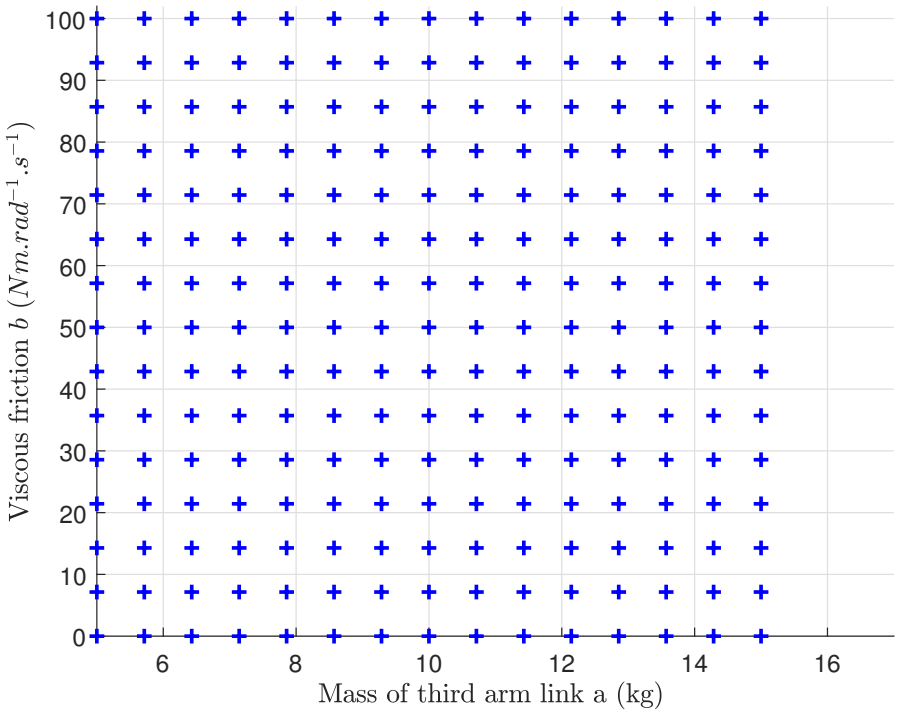

FIGURE I.7: Stabilization region of 3-Dof serial robot manipulator using extended PDC control (I.53) and reduced complexity TS fuzzy model (I.52)

coefficient ($b = f_v$) in the range [0, 100] SI. Figure I.7 depicts the results of the feasibility test and shows that the system has been successfully rendered admissible for the whole testing

region.

Remark I.7. Note that the previous result is based on the use of the extended PDC control (I.53) which requires the measurement of the derivative states and can be useful for the control of mechanical systems using accelerometers as sensors. However, this solution is costly as it requires the use of an advanced type of sensors and does not solve the underlying conservatism problem for the proposed reduced complexity models.

I.6 Conclusions

In this chapter we have introduced the TS fuzzy representation for a class of nonlinear systems. Sufficient conditions for admissibility or stabilization have been formulated using Lyapunov's theory of stability and LMI framework. For the sake of brevity, only quadratic Lyapunov functions were used for obtaining the LMIs constraints. Several lemmas useful for expressing nonlinear constraints as convex ones or relaxing LMIs constraints have been presented. The design of control laws that are robust with respect to structural uncertainties has been given for systems under TS fuzzy representation.

The underlying problem of numerical complexity for TS fuzzy models has been examined and has proven to impede the control design of complex robotics systems. The use of structural uncertainties as a mean to reduce the number of rules was presented alongside its restrictions and feasibility conservatism. Finally, we proposed a reduced complexity representation for TS fuzzy systems and concluded on its potential usefulness for highly nonlinear systems given the reduced numerical complexity of the design as well as its limitations from a practical point of view given the conservatism of the control design conditions.

The prime focus of the next chapter will be striking a compromise between the numerical complexity and the conservatism of control design conditions via the introduction of a novel polytopic modeling approach.

Chapter II

A New Polytopic Quasi-LPV Framework for Nonlinear Systems

"Creativity is not just 'something' that happens in some people's head – it is a process."

Ibn Rushd

Contents

II.1 Introduction 30
II.2 Polytopic Quasi-LPV Representation 31
II.2.1 Classical Polytopic Quasi-LPV Representation 31
II.2.2 Novel Polytopic Quasi-LPV Representation 32
II.3 Reduced-Complexity Quadratic Control Design of Descriptor Systems 36
II.3.1 Descriptor-Redundancy Based Control Design 36
II.3.2 Control Design without Descriptor-Redundancy Approach 39
II.3.3 Numerical Examples 40
II.4 Nonquadratic Control of Descriptor Systems Using Reduced-Complexity Polytopic Representation 45
II.4.1 Descriptor-Redundancy Based Control Design 46
II.4.2 Control Design without Descriptor-Redundancy Approach 50
II.4.3 Numerical Examples 51
II.5 Conclusions 53

II.1 Introduction

For existing polytopic LPV approaches, the numerical complexity of stability analysis, observation and control design conditions *exponentially* grows with respect to the number of scheduling variables [Rizvi et al., 2016]. This limits the applicability of such approaches to systems with only few nonlinearities or time-varying parameters [Hoffmann and Werner, 2015]. To overcome this major drawback, data-based methods have been proposed for reducing the number of scheduling variables in polytopic LPV models, such as, for instance, principal component analysis (PCA) [Kwiatkowski and Werner, 2008], kernel PCA [Rizvi et al., 2016], deep neural network [Koelewijn and Tóth, 2020]. However, these methods suffer some major drawbacks. First, we can only deal with nonlinear systems in the sense of approximation, which could be unsuitable for fast dynamical nonlinear systems. Second, such parameter-reduction methods fundamentally rely on experimental data obtained from typical scheduling trajectories, which require not only additional optimization steps but also extensive simulations to collect data. Third, due to the "data-based" feature, the control performance obtained with the resulting LPV models highly depends on the collected data.

From a theoretical viewpoint, it is possible to derive necessary and sufficient stability conditions for quasi-LPV systems [Sala and Ariño, 2007]. Nevertheless, in practice these stability conditions are conceptual rather than implementable since the computational burden swiftly increases such that most numerical solvers crash [Nguyen et al., 2019]. This leads to another challenge of LPV approaches in deriving less conservative sufficient conditions for stability analysis of nonlinear systems with reasonable numerical burden. Then, to reduce the design conservatism, various poly-quadratic Lyapunov functions has been effectively exploited in the literature for LPV systems [Briat, 2014; Nguyen, Chevrel, and Claveau, 2018; Mohammadpour and Scherer, 2012]. In contrast to quadratic stability, exploiting the information on the scheduling variables and their rates of variation plays a key role for poly-quadratic stability of LPV systems [Wu et al., 1996; Apkarian, Gahinet, and Becker, 1995; Sato, 2011; Nguyen, Chevrel, and Claveau, 2018]. However, within quasi-LPV framework the scheduling variables depend on the state vector. Then, the information on the time-derivative of scheduling variables is generally not available for control design of system (I.21). This implies much more numerical and theoretical challenges when using poly-quadratic Lyapunov functions, also called nonquadratic or multiple Lyapunov functions [Tanaka, Ohtake, and Wang, 2007; Mozelli, Palhares, and Avellar, 2009; Márquez et al., 2016], for stability analysis and control design of continuous-time quasi-LPV systems. Most of existing control results are formulated using *local* analysis settings with different degrees of conservativeness [Nguyen et al., 2019]. Note that within local polytopic quasi-LPV control framework, it is still not possible to *theoretically* demonstrate that nonquadratic results include those derived from quadratic Lyapunov functions.

This chapter presents a solution to two main drawbacks of polytopic quasi-LPV paradigm: i) numerical complexity of the design conditions, especially for systems (I.21) with a large number of scheduling variables; ii) design conservatism of the resulting polytopic representation. Specifically, the main contributions are summarized as follows

- We propose a new *equivalent* polytopic representation of a nonlinear system described by (I.21). The model complexity grows *proportionally* with the number of scheduling variables, rather than *exponentially* when compared to existing approaches. Moreover, for the same predefined scheduling variables, the vertices of the proposed polytopic model can admit an *infinite* number of representations. This *non-uniqueness* feature allows introducing slack variables at the modeling step, which is useful to further reduce the control design conservatism.

- Using the proposed modeling approach, two LMI-based procedures are provided for nonquadratic control design of system (I.21). The first control design exploits the classical descriptor-redundancy approach [Fridman and Shaked, 2002; Tanaka, Ohtake, and Wang, 2007; Bouali, Yagoubi, and Chevrel, 2008], requiring a special control structure when defining the extended redundancy form. This may yield conservative results as similarly discussed in [Guerra, Estrada-Manzo, and Lendek, 2015; Nguyen et al., 2021b] for quasi-LPV descriptor observer design. With a new nonlinear control law, the second design allows avoiding the extended redundancy form for regular descriptor systems, leading to less conservative results. We prove with theoretical arguments and numerical illustrations that the proposed nonquadratic control results precisely include those derived from quadratic Lyapunov functions.

II.2 Polytopic Quasi-LPV Representation

In this section, we consider again the class of systems (I.21) that we rewrite on the following form

$$E(z)\dot{x}(t) = A(z)x(t) + B(z)u(t), \tag{II.1}$$

where $x(t) = \begin{bmatrix} x_d^T(t) & x_a^T(t) \end{bmatrix}^T \in \mathbb{R}^{n_x}$ (with $n_x = q + s$), $E(z) = \text{diag}\,(E_1(z), 0)$, $A(z) = \begin{bmatrix} A_{11}(z) & A_{12}(z) \\ A_{21}(z) & A_{22}(z) \end{bmatrix}$, $B(z) = \begin{bmatrix} B_1(z) \\ B_2(z) \end{bmatrix}$. It is recalled that all the system matrices are affine functions of the premise vector z belonging to the bounded set $\mathscr{D}_z$ defined in (I.3), page 7, and $E_1(z)$ is an invertible matrix for all $z \in \mathscr{D}_z$.

For this class of systems, we introduce a new polytopic quasi-LPV representation with a significantly reduced complexity compared to classical ones [Taniguchi et al., 2001; Hoffmann and Werner, 2015]. Moreover, the proposed representation allows introducing some extra flexibility in the model that is useful for the control design.

II.2.1 Classical Polytopic Quasi-LPV Representation

Considering that $E(z)$, $A(z)$ and $B(z)$ depend affinely on $z(x)$, these matrices can be decomposed in the form

$$X(z) = \bar{X}_0 + \sum_{p=1}^{r} z_p \bar{X}_p, \quad X \in \{E, A, B\}, \tag{II.2}$$

with $\bar{E}_p$, $\bar{A}_p \in \mathbb{R}^{n\times n}$, $\bar{B}_p \in \mathbb{R}^{m\times n}$ for $p \in \mathcal{I}_r \cup \{0\}$. Using the sector nonlinearity approach [Taniguchi et al., 2001], the state-dependent term z_p can be expressed as a convex combination of its bounds

$$z_p = \omega_p^0(z_p) z_p^0 + \omega_p^1(z_p) z_p^1, \tag{II.3a}$$

$$\text{with} \qquad \omega_p^0(z_p) = \frac{z_p^1 - z_p}{z_p^1 - z_p^0}, \quad \omega_p^1(z_p) = 1 - \omega_p^0(z_p), \tag{II.3b}$$

We then define the following products, called membership functions (MFs)

$$\mu_i(z) = \prod_{p=1}^{r} \omega_p^{i_p}(z_p), \tag{II.4}$$

with $i = 1 + i_1 + i_2 \times 2 + \cdots + i_r \times 2^{r-1}$, $i_p \in \{0, 1\}$ (that is, $i_r i_{r-1} \ldots i_1$ is the binary representation of the integer number $i-1$). As a result, the quasi-LPV descriptor system (II.1) can be *equivalently*

rewritten in the polytopic form

$$\sum_{i=1}^{n_r} \mu_i(z)\hat{E}_i\dot{x}(t) = \sum_{i=1}^{n_r} \mu_i(z)(\hat{A}_i x(t) + \hat{B}_i u(t)), \tag{II.5}$$

with $n_r = 2^r$, $\hat{X}_i = X(z)|_{\mu_i=1}$, for $X \in \{E, A, B\}$ and $i \in \mathcal{I}_q$. Note that the MFs verify the convex sum property, *i.e.*, $0 \leq \mu_i(z) \leq 1$ and $\sum_{i=1}^{n_r} \mu_i(z) = 1$, for $z \in \mathscr{D}_z$.

Model (II.5) allows for an exact polytopic representation of the quasi-LPV system (I.21) in the compact set $\mathscr{D}_z$. The MFs precisely capture the nonlinearities involved in system (I.21). However, it is important to note that the numerical complexity of model (II.5) grows exponentially with the number of scheduling variables, *i.e.*, $n_r = 2^r$. To avoid this major drawback for quasi-LPV control, we propose hereafter a novel reduced-complexity polytopic representation.

II.2.2 Novel Polytopic Quasi-LPV Representation

We reconsider the decomposition (II.3). Then, it follows from (II.2) and (II.3a) that

$$\begin{aligned} X(z) &= \bar{X}_0 + \sum_{p=1}^{r} \left(\omega_p^1(z_p)z_p^1 + \omega_p^0(z_p)z_p^0\right)\bar{X}_p \\ &= \sum_{p=1}^{r} \left(\frac{\omega_p^1(z_p)}{r}(\bar{X}_0 + rz_p^1\bar{X}_p) + \frac{\omega_p^0(z_p)}{r}(\bar{X}_0 + rz_p^0\bar{X}_p)\right) \\ &= \sum_{i=1}^{2r} w_i(z)X_i, \end{aligned} \tag{II.6}$$

with $X \in \{E, A, B\}$ and for $p \in \mathcal{I}_r$

$$\begin{aligned} w_{2p-1}(z) &= \frac{1}{r}\omega_p^1(z_p), & w_{2p}(z) &= \frac{1}{r}\omega_p^0(z_p), \\ X_{2p-1} &= \bar{X}_0 + rz_p^1\bar{X}_p, & X_{2p} &= \bar{X}_0 + rz_p^0\bar{X}_p. \end{aligned} \tag{II.7}$$

Applying the matrix decomposition (II.6), the quasi-LPV descriptor system (II.1) can be equivalently represented in the following polytopic form

$$\sum_{i=1}^{2r} w_i(z)E_i\dot{x}(t) = \sum_{i=1}^{2r} w_i(z)\left(A_i x(t) + B_i u(t)\right). \tag{II.8}$$

The new nonlinear weights $w_i(z)$, for $i \in \mathcal{I}_{2r}$, satisfy the following properties

$$\sum_{i=1}^{2r} w_i(z) = 1, \quad 0 \leq w_i(z) \leq 1, \tag{II.9a}$$

$$w_{2p-1}(z) + w_{2p}(z) = \frac{1}{r}, \quad \forall p \in \mathcal{I}_r. \tag{II.9b}$$

We will denote Ω the set of the nonlinear weights $w : z \mapsto \left[w_1(z), w_2(z), \ldots, w_{2r}(z)\right]$ satisfying (II.9).

The vertex X_i can be directly derived from $X(z)$, for $X \in \{E, A, B\}$ and $i \in \mathcal{I}_{2r}$. To this end, we define the vectors $\zeta^1, \ldots, \zeta^r$ forming the canonical basis of $\mathbb{R}^r$ as

$$\zeta^i = [0, \ldots, 0, \overbrace{1}^{i\text{th}}, 0, \ldots, 0]^\top, \quad i \in \mathcal{I}_r.$$

Then, the vertices X_i of system (II.8) are directly obtained from $X(z)$ as

$$X_i = \begin{cases} X(r \times z_p^1 \times \zeta^p) & \text{if } i = 2p-1, \\ X(r \times z_p^0 \times \zeta^p) & \text{if } i = 2p, \quad p \in \mathcal{I}_r. \end{cases} \tag{II.10}$$

With the new polytopic representation (II.8), the MFs $w_i(z)$, for $i \in \mathcal{I}_{2r}$, defined in (II.7), directly come from (II.3b), *i.e.*, a combination product as in (II.4) is no longer required. Then, model (II.8) has $2r$ vertices, which can significantly reduce the numerical complexity compared to the classical polytopic representation (II.5) with 2^r vertices [Taniguchi et al., 2001; Tanaka and Wang, 2004]. This feature is particularly interesting when dealing with nonlinear systems with a large number r of scheduling variables.

Another interesting feature of the proposed representation (II.8) consists in the non-uniqueness of the vertices X_i, with $X \in \{E, A, B\}$, for *a priori* predefined MFs $w_i(z)$, for $i \in \mathcal{I}_{2r}$. Indeed, let $\{T_p\}_{1 \leq p \leq r}$ be a family of matrices with the same dimensions as X and $T = \frac{1}{r}\sum_{p=1}^{r} T_p$. For $p \in \mathcal{I}_r$, we define

$$X_{2p-1}^* = X_{2p-1} + T_p - T, \quad X_{2p}^* = X_{2p} + T_p - T. \tag{II.11}$$

Then, it follows from (II.9) and (II.11) that

$$\begin{aligned} \sum_{i=1}^{2r} w_i(z) X_i^* &= \sum_{p=1}^{r} \left[w_{2p-1}(z)(X_{2p-1} + T_p) + w_{2p}(z)(X_{2p} + T_p) \right] - T \\ &= \sum_{i=1}^{2r} w_i(z) X_i + \sum_{p=1}^{r} (w_{2p-1} + w_{2p}) T_p - T \\ &= \sum_{i=1}^{2r} w_i(z) X_i. \end{aligned}$$

Hence, matrix $X(z)$ admits an *infinite* number of representations of the form (II.6) with the same MFs $w(z) \in \Omega$. We will further show that this non-uniqueness feature of the proposed polytopic representation (II.8) offers a flexibility to introduce slack variables into LMI-based stabilization conditions, which allows reducing their conservatism, see Example II.7.

Example II.5 (Illustrative Example)
To further examine the proprieties of the proposed modeling approach, we consider the following unforced singular descriptor system

$$\begin{bmatrix} 1 & 0 \\ 0 & 0 \end{bmatrix} \begin{bmatrix} \dot{\theta}(t) \\ \dot{v}(t) \end{bmatrix} = \begin{bmatrix} -1 & \cos(\theta) + 5\sin(\theta) \\ a\sin(\theta) & b \end{bmatrix} \begin{bmatrix} \theta(t) \\ v(t) \end{bmatrix} \tag{II.12}$$

where a and b are some known parameters. The number of scheduling variables is $r = 2$ and the premises vector is defined as $z = \begin{bmatrix} \cos(\theta) & \sin(\theta) \end{bmatrix}^\top$. The system matrix is

$$A(z) = \begin{bmatrix} -1 & z_1 + 5z_2 \\ az_2 & b \end{bmatrix} \tag{II.13}$$

and $\mathscr{D}_z = [-1, 1] \times [-1, 1]$. Accordingly, there are $2^r = 4$ vertices for the polytopic TS representation (II.5) given by

$$\hat{A}_1 = \begin{bmatrix} -1 & -6 \\ -a & b \end{bmatrix}, \qquad \hat{A}_2 = \begin{bmatrix} -1 & 4 \\ a & b \end{bmatrix},$$

$$\hat{A}_3 = \begin{bmatrix} -1 & -4 \\ -a & b \end{bmatrix}, \qquad \hat{A}_4 = \begin{bmatrix} -1 & 6 \\ a & b \end{bmatrix}.$$

On the other hand, the proposed modeling approach (II.8) yields the following $2 \times r = 4$ vertices

$$A_1 = \begin{bmatrix} -1 & -2 \\ 0 & b \end{bmatrix}, \qquad A_2 = \begin{bmatrix} -1 & 2 \\ 0 & b \end{bmatrix},$$
$$A_3 = \begin{bmatrix} -1 & -10 \\ -2a & b \end{bmatrix}, \qquad A_4 = \begin{bmatrix} -1 & 10 \\ 2a & b \end{bmatrix}.$$

As shown in (II.10), the lower and upper bounds z_p^0 and z_p^1 are multiplied by r when constructing the vertices of model (II.8). This may lead to a modeling overbounding [Kwiatkowski and Werner, 2008], which can be a source of conservatism with respect to the design conditions for the proposed polytopic approach. To illustrate this phenomena, let us focus on the decomposition of the scheduling variables obtained for different methods.

For the TS representation, the vertices are defined as

$$\begin{bmatrix} z_1 \\ z_2 \end{bmatrix} = h_1(z) \begin{bmatrix} z_1^0 \\ z_2^0 \end{bmatrix} + h_2(z) \begin{bmatrix} z_1^0 \\ z_2^1 \end{bmatrix} + h_3(z) \begin{bmatrix} z_1^1 \\ z_2^0 \end{bmatrix} + h_4(z) \begin{bmatrix} z_1^1 \\ z_2^1 \end{bmatrix}$$
$$= h_1(z)\hat{V}_1 + h_2(z)\hat{V}_2 + h_3(z)\hat{V}_3 + h_4(z)\hat{V}_4. \tag{II.14}$$

Similarly, for the proposed representation, it comes that

$$\begin{bmatrix} z_1 \\ z_2 \end{bmatrix} = w_1(z) \begin{bmatrix} rz_1^0 \\ 0 \end{bmatrix} + w_2(z) \begin{bmatrix} rz_1^1 \\ 0 \end{bmatrix} + w_3(z) \begin{bmatrix} 0 \\ rz_2^0 \end{bmatrix} + w_4(z) \begin{bmatrix} 0 \\ rz_2^1 \end{bmatrix}$$
$$= w_1(z)V_1 + w_2(z)V_2 + w_3(z)V_3 + w_4(z)V_4. \tag{II.15}$$

Given that the control design conditions for nearly all polytopic models are applied to the set of linear systems constituting the polytopic representation, which are derived from the direct knowledge of the bounds on the scheduling variables, then the presence of an overbounding can impact the conservatism of the design conditions since it directly affects the entrees of the matrices in each linear system of the polytopic set. In Figure (II.1) are drawn the set of premise variables and the polytopes computed from the TS methodology (II.5), the modified TS approach [Dehak et al., 2020] presented in the previous section and the formula (II.6) with and without the use of *slack variables*. As can be seen on that figure both the vertices of the TS representation (II.5) and of the proposed model (II.8) present an overbounding as their vertices are not included in the set of premise variables. Evidently, the resulting overbounding in case of TS fuzzy modeling is much smaller.

Let us now examine the effect of the *slack variables* on the overbounding issue. To that end, consider the following shift on the vertices of the polytope for the proposed modeling approach

$$\begin{bmatrix} z_1 \\ z_2 \end{bmatrix} = w_1(z) \begin{bmatrix} rz_1^0 + 1 \\ 1 \end{bmatrix} + w_2(z) \begin{bmatrix} rz_1^1 + 1 \\ 1 \end{bmatrix} + w_3(z) \begin{bmatrix} -1 \\ rz_2^0 - 1 \end{bmatrix} + w_4(z) \begin{bmatrix} -1 \\ rz_2^1 - 1 \end{bmatrix}$$
$$= w_1(z)V_1^* + w_2(z)V_2^* + w_3(z)V_3^* + w_4(z)V_4^* \tag{II.16}$$

Figure (II.1) shows that the shifted vertices V_1^* and V_4^* coincide with the vertex $\hat{V}_1$ of the polytope for the TS approach. This shows that the *slack variables* can further reduce the number of vertices. However, while the resulting polytope due to the proposed shifting changed form into a triangle shape, it still contains the polytope for the TS approach delimited by the vertices

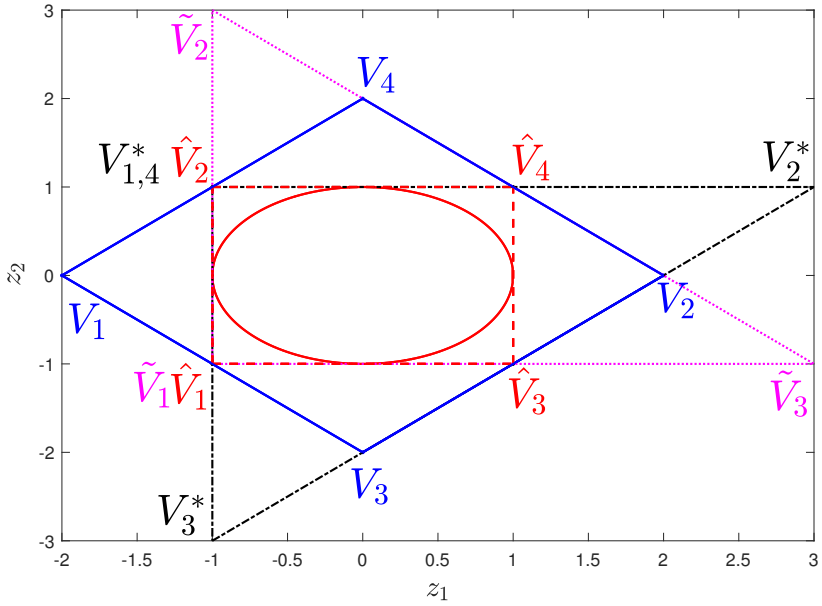

FIGURE II.1: Set of premise variables —— and polytopes with associated vertices for Ex. II.5 with TS modeling - - -; with the proposed modeling (no shifting) ——; with the proposed modeling (with shifting) —·-; with the reduced TS approach [Dehak et al., 2020] ·····.

$\hat{V}_i$. In fact, the overbounding caused by the proposed approach will always be greater than for the TS approach. The reduced TS approach in [Dehak et al., 2020] yields $r+1$ vertices selected from 2^r vertices of the original TS model, however the resulting polytopic expression is an affine combination needing some transformations in order to obtain a convex sum. The resulting polytope with the vertices $\tilde{V}_i$ is then similar to II.16. However, this approach does not offer the same possibility of defining *slack variables* and also depends on the TS model.

Remark II.8. Once a choice is selected for the scheduling variables and the reduced set $\mathcal{J}$, the polytope obtained from [Dehak et al., 2020] is of fixed vertices as it is not possible for that approach to provide any *slack variables* to shift the vertices contrary to the representation proposed in this manuscript. In fact, if we consider the following values for shifting the vertices in (II.16)

$$\begin{aligned}\begin{bmatrix} z_1 \\ z_2 \end{bmatrix} &= w_1(z)\begin{bmatrix} rz_1^0+1 \\ -1 \end{bmatrix} + w_2(z)\begin{bmatrix} rz_1^1+1 \\ -1 \end{bmatrix} + w_3(z)\begin{bmatrix} -1 \\ rz_2^0+1 \end{bmatrix} + w_4(z)\begin{bmatrix} -1 \\ rz_2^1+1 \end{bmatrix} \\ &= w_1(z)V_1^{**} + w_2(z)V_2^{**} + w_3(z)V_3^{**} + w_4(z)V_4^{**} \end{aligned} \tag{II.17}$$

then, not only the expression (II.17) is strictly equivalent to the previous expressions, but we also have $V_1^{**} = V_3^{**} = \tilde{V}_1$, $V_2^{**} = \tilde{V}_3$ and $V_4^{**} = \tilde{V}_2$. The resulting polytope delimited by the shifted vertices V_i^{**} in (II.17) is identical to the polytope delimited by the vertices $\tilde{V}_i$ achieved with [Dehak et al., 2020].

For any given matrix $X(z)$ that depends affinely on the premise vector $z(t)$, the constant entries of $X(z)$ retain the same values across the vertices of the polytopic representation. This holds true for all polytopic representations including the TS model (II.5) and the proposed approach (II.8). However, thanks to the property (II.9b), model (II.8) offers a degree of flexibility by introducing *slack variables* that affect the entries of the vertices according to the expression (II.11). Furthermore, as will be shown subsequently, they can be introduced as decision variables in the LMI stabilizability conditions allowing to reduce the design conservatism of the

proposed polytopic approach. In some cases, it can even outperform the TS modeling approach (see Example II.8).

II.3 Reduced-Complexity Quadratic Control Design of Descriptor Systems

This section first presents the quadratic control design for system (II.1) using the proposed model (II.8). Then, a special attention is paid to the control design of regular systems, *i.e.*, there is no algebraic equation (I.21b), which has been widely treated in TS fuzzy control framework.

II.3.1 Descriptor-Redundancy Based Control Design

We consider the nonlinear singular system (II.1) in its extended form. Applying the reduced-complexity modeling in (II.8) gives the equivalent representation

$$\bar{E}_o \dot{x}_e(t) = \sum_{i=1}^{2r} w_i(z)(\bar{A}_i x_e(t) + \bar{B}_i u(t)). \tag{II.18}$$

For the stabilization of system (II.18), we consider the control law

$$u(t) = \sum_{i=1}^{2r} w_i(z)\bar{K}_i x_e(t) \doteq \bar{K}(z) x_e(t), \tag{II.19}$$

where the feedback gains $\bar{K}_i = \begin{bmatrix} K_i & 0 \end{bmatrix}$, with $K_i \in \mathbb{R}^{m\times q}$, $i \in \mathcal{I}_{2r}$, are to be determined such that the closed-loop system (I.25) is admissible. The following theorem provides LMI conditions to tune the parameters of the controller (II.19).

Theorem II.5 *Consider system (II.1) with Assumption 1. If there exist a positive definite matrix $V \in \mathbb{S}^{q\times q}$, symmetric matrices T_j, $S_j \in \mathbb{S}^{2(n+q)\times 2(n+q)}$, and matrices L_j, $R_j \in \mathbb{R}^{(n+q)\times(n+q)}$, $F_j \in \mathbb{R}^{m\times q}$, $W_{ij} \in \mathbb{R}^{n\times q}$, $Z_{ij} \in \mathbb{R}^{n\times n}$, for $i,j \in \mathcal{I}_{2r}$, such that*

$$\begin{aligned} &\bar{\Xi}_{ii} \prec 0, \quad i \in \mathcal{I}_{2r}, \\ &\frac{2}{2r-1}\bar{\Xi}_{ii} + \bar{\Xi}_{ij} + \bar{\Xi}_{ji} \prec 0, \quad i,j \in \mathcal{I}_{2r},\ i \neq j, \end{aligned} \tag{II.20}$$

with $T_{2p} = T_{2p-1}$, $S_{2p} = S_{2p-1}$, for all $p \in \mathcal{I}_r$, and

$$\bar{\Xi}_{ij} = \bar{\Psi}_{ij} + T_i + S_j - \frac{1}{r}(T+S), \quad S = \sum_{p=1}^{r} S_{2p}, \quad T = \sum_{p=1}^{r} T_{2p},$$

$$\bar{\Psi}_{ij} = \mathrm{He}\begin{bmatrix} \bar{A}_i L_j + \bar{B}_i \bar{F}_j & \bar{A}_i R_j \\ \mathcal{P}_{ij} - L_j & -R_j \end{bmatrix}, \quad \bar{F}_j = \begin{bmatrix} F_j & 0 \end{bmatrix}, \ \mathcal{P}_{ij} = \begin{bmatrix} V & 0 \\ W_{ij} & Z_{ij} \end{bmatrix}.$$

Then, the closed-loop system (II.1)-(II.19) is admissible for the feedback gains given by

$$K_i = F_i V^{-1}, \quad i \in \mathcal{I}_{2r}. \tag{II.21}$$

Proof:
For brevity, we introduce the following notations

$$\bar{\Xi}(z) = \sum_{i,j\in\mathcal{I}_{2r}} w_i(z)w_j(z)\bar{\Xi}_{ij}, \quad \bar{\Psi}(z) = \sum_{i,j\in\mathcal{I}_{2r}} w_i(z)w_j(z)\bar{\Psi}_{ij}, \quad L(z) = \sum_{j=1}^{2r} w_j(z)L_j,$$
$$\mathcal{P}(z) = \begin{bmatrix} V & 0 \\ W(z) & Z(z) \end{bmatrix} = \sum_{i,j\in\mathcal{I}_{2r}} w_i(z)w_j(z)\mathcal{P}_{ij}, \quad R(z) = \sum_{j=1}^{2r} w_j(z)R_j,$$
$$\bar{F}(z) = \begin{bmatrix} F(z) & 0 \end{bmatrix}, \quad F(z) = \sum_{j=1}^{2r} w_j(z)F_j.$$

It follows from the definition of $\bar{\Psi}_{ij}$ *that*

$$\bar{\Psi}(z) = \mathrm{He}\begin{bmatrix} \bar{A}(z)L(z) + \bar{B}(z)\bar{F}(z) & \bar{A}(z)R(z) \\ \mathcal{P}(z) - L(z) & -R(z) \end{bmatrix}. \tag{II.22}$$

Moreover, from property (II.9)*, we have*

$$\begin{aligned} \sum_{i,j\in\mathcal{I}_{2r}} w_i(z)w_j(z)(T_i + S_j) &= \sum_{i=1}^{2r} w_i(z)T_i + \sum_{j=1}^{2r} w_j(z)S_j \\ &= \sum_{k=1}^{r}(w_{2k-1}(z)T_{2k} + w_{2k}(z)T_{2k}) + \sum_{\ell=1}^{r}(w_{2\ell-1}(z)S_{2\ell} + w_{2\ell}(z)S_{2\ell}) \\ &= \frac{1}{r}\sum_{p=1}^{r}(T_{2p} + S_{2p}) = \frac{1}{r}(T + S). \end{aligned} \tag{II.23}$$

Then, it follows from (II.22)–(II.23) *that* $\bar{\Xi}(z) = \bar{\Psi}(z)$*. By Lemma I.4, LMI conditions* (II.20) *imply that* $\bar{\Xi}(z) \prec 0$*, or equivalently*

$$\bar{\Psi}(z) \prec 0. \tag{II.24}$$

Applying Lemma I.4 to inequality (II.24) *with* $\mathscr{A} = \bar{A}(z)$, $\mathscr{R} = R(z)$, $\mathscr{L} = L(z)$, $\mathscr{P} = \mathcal{P}(z)$ *and* $\mathscr{Q} = \bar{B}(z)\bar{F}(z)$*, we obtain*

$$\mathrm{He}\left[\bar{A}(z)\mathcal{P}(z) + \bar{B}(z)\bar{F}(z)\right] \prec 0. \tag{II.25}$$

Note that

$$\mathrm{He}\left[\bar{A}(z)\mathcal{P}(z) + \bar{B}(z)\bar{F}(z)\right] = \begin{bmatrix} \bullet & \bullet \\ \bullet & -\mathrm{He}[\bar{A}_{22}(z)Z(z)] \end{bmatrix} \tag{II.26}$$

where "$\bullet$*" denotes some matrix terms and* $\bar{A}_{22}(z) = \begin{bmatrix} -E_1(z) & A_{12}(z) \\ 0 & A_{22}(z) \end{bmatrix}$*. It follows from* (II.25) *and* (II.26) *that*

$$\bar{A}_{22}(z)Z(z) + Z(z)^\top \bar{A}_{22}(z)^\top \succ 0, \tag{II.27}$$

which ensures that $\det(\bar{A}_{22}(z)Z(z)) \neq 0$*, thus* $\det(Z(z)) \neq 0$*, for all* $z \in \mathscr{D}_z$*. Combining with the fact that* $V \succ 0$*, it follows that* $\mathcal{P}(z)$ *is invertible on* $\mathscr{D}_z$ *with*

$$\mathcal{P}(z)^{-1} = \begin{bmatrix} V^{-1} & 0 \\ -Z^{-1}(z)W(z)V^{-1} & Z^{-1}(z) \end{bmatrix}. \tag{II.28}$$

Note from (II.28) *that*

$$\bar{E}^\top \mathcal{P}^{-1}(z) = \mathcal{P}^{-1}(z)\bar{E} = \text{diag}(V^{-1}, 0) \succeq 0. \tag{II.29}$$

From (II.21) *and* (II.28)*, it follows that*

$$\bar{K}(z) = \bar{F}(z)\mathcal{P}(z)^{-1}. \tag{II.30}$$

Pre- and post-multiplying (II.25) *with* $\mathcal{P}(z)^{-\top}$ *and* $\mathcal{P}(z)^{-1}$ *while considering expression* (II.30)*, it follows that*

$$\text{He}\left[\mathcal{P}(z)^{-\top}(\bar{A}(z) + \bar{B}(z)\bar{K}(z))\right] \prec 0. \tag{II.31}$$

We consider the Lyapunov function candidate

$$\mathcal{V}(z, x_e) = x_e^\top \bar{E}^\top \mathcal{P}(z)^{-1} x_e. \tag{II.32}$$

It follows from (II.29) *and* (II.32) *that* $\mathcal{V}(z, x_e) = x_d^\top V^{-1} x_d > 0$*, for all* $x_e \neq 0$*. The time derivative of* $\mathcal{V}(z, x_e)$ *along the solutions of system* (II.1) *is given by*

$$\dot{\mathcal{V}}(z, x_e) = \text{He}\left[x_e^\top \mathcal{P}(z)^{-\top}(\bar{A}(z) + \bar{B}(z)\bar{K}(z))x_e\right]. \tag{II.33}$$

It is clear from (II.31) *and* (II.33) *that* $\dot{\mathcal{V}}(z, x_e) < 0$*,* $\forall x_e \neq 0$*. Hence, the solution* $x_e = 0$ *of system* (II.1) *is asymptotically stable. Moreover, according to the result* (II.27) *we have* $\det(\bar{A}_{22}(z)) \neq 0$ *with* $\bar{A}_{22}(z) = \left[\begin{smallmatrix} -E_1(z) & A_{12}(z) \\ 0 & A_{22}(z) \end{smallmatrix}\right]$*. This latter ensures that* $\det(A_{22}(z)) \neq 0$*. Hence, the nonlinear singular system* (I.25) *under Assumption 1 is of index-one. This concludes the proof.*

The following corollary provides LMI-based design conditions without using slack variables T_i and S_i, for $\forall i \in \mathcal{I}_{2r}$, specifically offered by the proposed polytopic model (II.8).

Corollary 1. *Consider system* (I.25) *with Assumption 1. If there exist a positive definite matrix* $V \in \mathbb{S}^{q\times q}$*, and matrices* $L_j \in \mathbb{R}^{(n+q)\times(n+q)}$*,* $R_j \in \mathbb{R}^{(n+q)\times(n+q)}$*,* $F_j \in \mathbb{R}^{m\times q}$*,* $W_{ij} \in \mathbb{R}^{(n+q)\times q}$*,* $Z_{ij} \in \mathbb{R}^{(n+q)\times(n+q)}$*,* $i, j \in \mathcal{I}_{2r}$*, such that*

$$\begin{aligned} &\bar{\Phi}_{ii} \prec 0, \quad i \in \mathcal{I}_{2r}, \\ &\frac{2}{2r-1}\bar{\Phi}_{ii} + \bar{\Phi}_{ij} + \bar{\Phi}_{ji} \prec 0, \quad i, j \in \mathcal{I}_{2r},\ i \neq j, \end{aligned} \tag{II.34}$$

with

$$\bar{\Phi}_{ij} = \text{He}\begin{bmatrix} \bar{A}_i L_j + \bar{B}_i \bar{F}_j & \bar{A}_i R_j \\ \mathcal{P}_{ij} - L_j & -R_j \end{bmatrix}.$$

Then, the closed-loop system (II.18) *is admissible. Moreover, the feedback gains of the control law* (II.19) *are given in* (II.21)*.*

Proof:
In Theorem II.5, setting $T_i = S_j = 0$*, for* $\forall i, j \in \mathcal{I}_{2r}$*, it follows that* $\bar{\Phi}_{ij} = \bar{\Xi}_{ij}$*. Then, condition* (II.20) *becomes* (II.34)*. The proof is concluded following the result of Theorem II.5.*

Remark II.9. By numerical experiments in the Subsection II.3.3, we show that in many cases, the proposed quadratic control approach with specific slack variables in Theorem II.5, *i.e.*, S_i

and T_i, for $i \in \mathcal{I}_{2r}$, offered by the new modeling (II.8) can provide a better performance, in terms of conservatism reduction, compared to many existing fuzzy Lyapunov based control results in TS fuzzy control framework.

II.3.2 Control Design without Descriptor-Redundancy Approach

Hereafter, a special attention is paid to the control design of regular systems, for which the use of a descriptor-redundancy approach, *i.e.*, the extended form (I.25), is still possible but can be unnecessarily complex and conservative from a numerical viewpoint. To this end, let us consider the following descriptor nonlinear system:

$$E(z)\dot{x}(t) = A(z)x(t) + B(z)u(t), \tag{II.35}$$

where $x \in \mathbb{R}^n$, $u \in \mathbb{R}^m$, $\text{rank}(E(z)) = n$, and

$$\begin{bmatrix} E(z) & A(z) & B(z) \end{bmatrix} = \sum_{i=1}^{2r} w_i(z) \begin{bmatrix} E_i & A_i & B_i \end{bmatrix}.$$

Note that system (II.35) is admissible as long as it admits an asymptotically stable solution $x = 0$. We consider the nonlinear control law

$$u(t) = K(z)x(t). \tag{II.36}$$

The following theorem provides LMI conditions to determine a nonlinear feedback gain $K(z) \in \mathbb{R}^{m\times n}$ such that the solution $x = 0$ of system (II.35) is asymptotically stable.

Theorem II.6 *If there exist a positive definite matrix $P \in \mathbb{S}^{n\times n}$, symmetric matrices T_i, $S_i \in \mathbb{S}^{2n\times 2n}$, and matrices $F_i \in \mathbb{R}^{m\times n}$, L_i, $R_i \in \mathbb{R}^{n\times n}$, for $i \in \mathcal{I}_{2r}$, such that*

$$\begin{aligned} &\Xi_{ii} \prec 0, \quad i \in \mathcal{I}_{2r}, \\ &\frac{2}{2r-1}\Xi_{ii} + \Xi_{ij} + \Xi_{ji} \prec 0, \quad i, j \in \mathcal{I}_{2r},\ i \neq j, \end{aligned} \tag{II.37}$$

with $T_{2p} = T_{2p-1}$, $S_{2p} = S_{2p-1}$, $\forall p \in \mathcal{I}_r$, and

$$\begin{aligned} \Xi_{ij} &= \Psi_{ij} + T_i + S_j - \frac{1}{r}(T + S), \\ S &= \sum_{j=1}^{r} S_j, \quad T = \sum_{i=1}^{r} T_i, \\ \Psi_{ij} &= \text{He}\begin{bmatrix} A_iL_j + B_iF_j & A_iR_j \\ PE_i^\top - L_j & -R_j \end{bmatrix}. \end{aligned}$$

Then, the solution $x = 0$ of the regular nonlinear system (II.35) is asymptotically stable for the feedback gain of the control law (II.36) given by

$$K(z) = F(z)E(z)^{-\top}P^{-1}, \quad F(z) = \sum_{j=1}^{2r} w_j(z)F_j. \tag{II.38}$$

Proof:
Following the same steps in the proof of Theorem II.5, we can prove that LMI conditions in (II.37) guarantee

$$\text{He}\left[A(z)PE(z)^\top + B(z)F(z)\right] \prec 0. \tag{II.39}$$

Since $P \succ 0$ *and* $E(z)$ *is regular, pre- and post-multiplying* (II.39) *with* $P^{-1}E(z)^{-1}$ *and* $E(z)^{-\top}P^{-1}$*, it follows that*

$$\Pi = \mathrm{He}\left[P^{-1}E(z)^{-1}(A(z)+B(z)K(z))\right] \prec 0. \tag{II.40}$$

Condition (II.40) *ensures that* $\dot{V}(x,z) = x^\top \Pi x < 0$*, for all* $x \neq 0$*, where* $\dot{V}(x,z)$ *is the time derivative of the Lyapunov function candidate* $V(z,x) = x^\top P^{-1}x$ *along the solutions of system* (II.35)*. This concludes the proof.*

Remark II.10. The new nonlinear control law (II.36) with the feedback gain (II.38) exploits the invertibility of $E(z)$ to avoid using the extended form as in (I.25). Then, no specific matrix structure is required for the feedback gain as $\bar{K}(z)$ in (II.19) or the Lyapunov matrix as $\bar{E}^\top \mathcal{P}^{-1}(z)$ in (II.29). Compared to the conventional TS fuzzy descriptor approaches, see for instance [Tanaka and Wang, 2004; Bouarar, Guelton, and Manamanni, 2010; He et al., 2021; Zhang et al., 2017], these features can further reduce not only the numerical complexity but also the conservatism of the control results for complex regular nonlinear systems as illustrated in Example II.8.

Remark II.11. The computational complexity of LMI-based optimization problems can be evaluated with the number of scalar decision variables $\mathcal{N}_{var}$ and the number of LMI constraints $\mathcal{N}_{row}$. To illustrate the complexity reduction of the proposed method, Table II.1 shows these characteristics numbers corresponding to the LMI constraints of different control results for regular descriptor systems with $n = q$ states, m control inputs and $r = r_e + r_a$ premise variables, where r_e and r_a respectively represent the number of the premise variables in the matrix $E(z)$ and in both matrices $A(z)$ and $B(z)$. For illustrations, the evolution of $\mathcal{N}_{var}$ and $\mathcal{N}_{row}$ with respect to r for the case of stability analysis with $n = 5$ and $m = 0$ is depicted in FigureII.2. Note that for a relatively low number of premise variables, *i.e.*, $r \leq 6$, all considered methods have a similar level of numerical complexity. We can also observe an exponential growth of $\mathcal{N}_{var}$ and $\mathcal{N}_{row}$ with respect to r for TS fuzzy model-based results, which is not the case of the proposed method. Further numerical studies are performed in the next section to demonstrate the interests of the new method in reducing both computational complexity and design conservatism compared to existing TS fuzzy model-based results.

TABLE II.1: Complexity Characteristics Numbers of Different Control Results.

Control Design	Theorem II.5	Theorem II.6	[He et al., 2021, Theorem 3.3]	[Bouarar, Guelton, and Manamanni, 2010, Theorem 2]
Number of vertices	$2r$	$2r$	2^r	2^r
$\mathcal{N}_{row}$	$n(16r^2+1)$	$n(8r^2+1)$	$n(2^{r+r_a+2}+2^r+2^{r+1})$	$n(2^{r+r_a+1}+2^r+2^{r+1})+m2^{r+r_a+1}$
$\mathcal{N}_{var}$	$n^2(8r^2+32r+\frac{1}{2})$ $+n(\frac{1}{2}+4r)+2rmn$	$n^2(12r+\frac{1}{2})$ $+\frac{n}{2}+2rmn$	$n^2(\frac{5}{2}2^r+2^{r_e-1}+2^{r_a-1}+6)+$ $n(2^{r-1}+2^{r_e-1}+2^{r_a-1})+nm2^r$	$n^2(1+2^{2r_a+1}+2^{r-1})+$ $n(1+2^{r-1}+3m2^r+m2^{2r_a})+m^2 2^r$

II.3.3 Numerical Examples

This section presents three examples with different degrees of numerical complexity to illustrate the effectiveness of the proposed approach. All the involved LMI-based conditions are solved using YALMIP toolbox with SeDuMi solver [Löfberg, 2004].

Example II.6 (Admissibility Analysis)
Consider the *unforced* singular nonlinear system

$$\begin{bmatrix}1 & 0\\ 0 & 0\end{bmatrix}\begin{bmatrix}\dot{x}_1(t)\\ \dot{x}_2(t)\end{bmatrix} = \begin{bmatrix}-1 & z_1(t)+5z_2(t)\\ az_2(t) & b\end{bmatrix}\begin{bmatrix}x_1(t)\\ x_2(t)\end{bmatrix}, \tag{II.41}$$

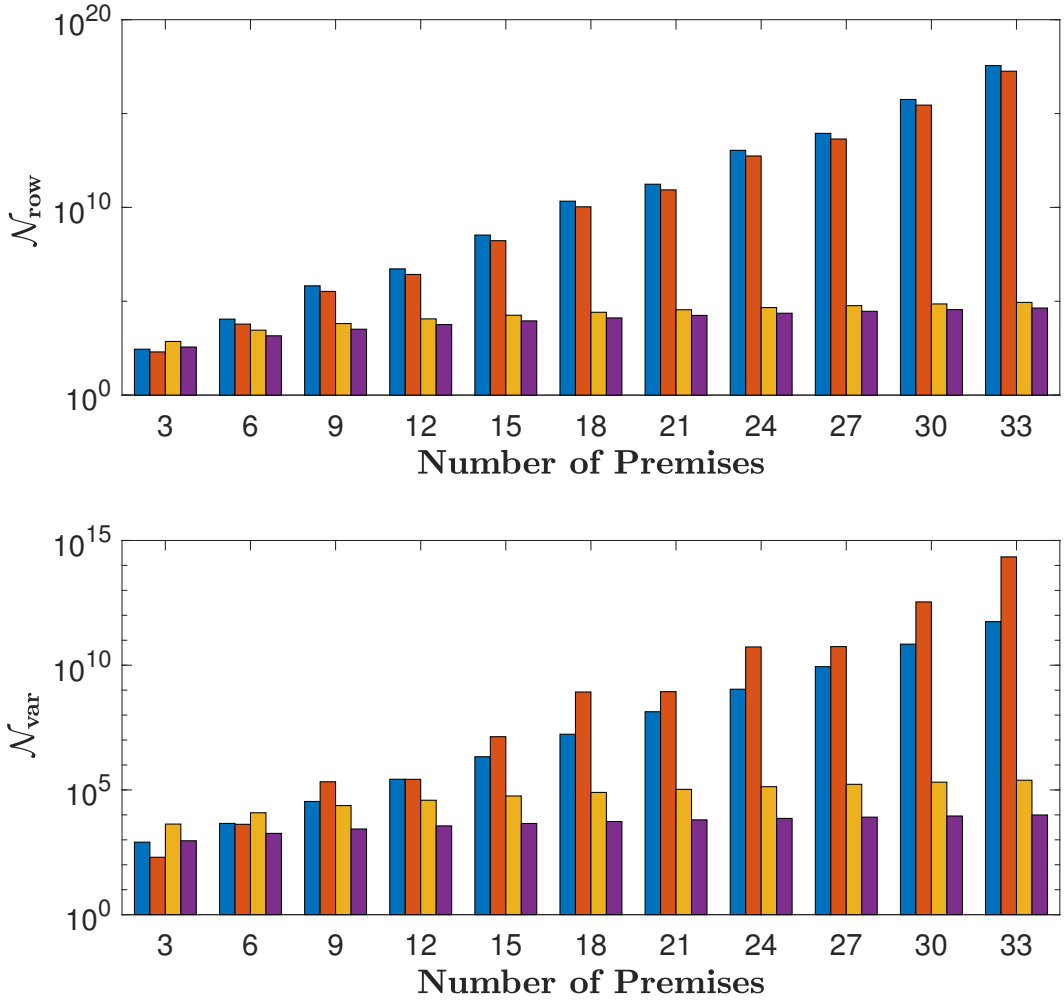

FIGURE II.2: Characteristics numbers of numerical complexity with respect to the number of premise variables r for the case $n = 5$ and $m = 0$: Theorem II.5 ■; Theorem II.6 ■; [He et al., 2021, Theorem 3.3] ■; [Bouarar, Guelton, and Manamanni, 2010, Theorem 2] ■.

where $a \in [-10, 10]$ and $b \in [-10, 10]$ are the parameters. The two premise variables are $z_1 = \cos(x_1)$ and $z_2 = \sin(x_1)$, thus $z = \begin{bmatrix} z_1 & z_2 \end{bmatrix}^\top$. The matrices of system (II.41) are given by

$$E = \begin{bmatrix} 1 & 0 \\ 0 & 0 \end{bmatrix}, \quad A(z) = \begin{bmatrix} -1 & z_1 + 5z_2 \\ az_2 & b \end{bmatrix}.$$

Applying the proposed modeling procedure in (II.8) and (II.10) to matrix $A(z)$, we obtain $2 \times r = 4$ following vertices

$$A_1 = \begin{bmatrix} -1 & -2 \\ 0 & b \end{bmatrix}, \quad A_2 = \begin{bmatrix} -1 & 2 \\ 0 & b \end{bmatrix}, \quad A_3 = \begin{bmatrix} -1 & -10 \\ -2a & b \end{bmatrix}, \quad A_4 = \begin{bmatrix} -1 & 10 \\ 2a & b \end{bmatrix}.$$

We examine the conservatism of the admissibility analysis for system (II.41) using the following approaches

- Theorem II.5 with $u(t) = 0$, *i.e*, $F_i = 0$, for $i \in \mathcal{I}_4$,

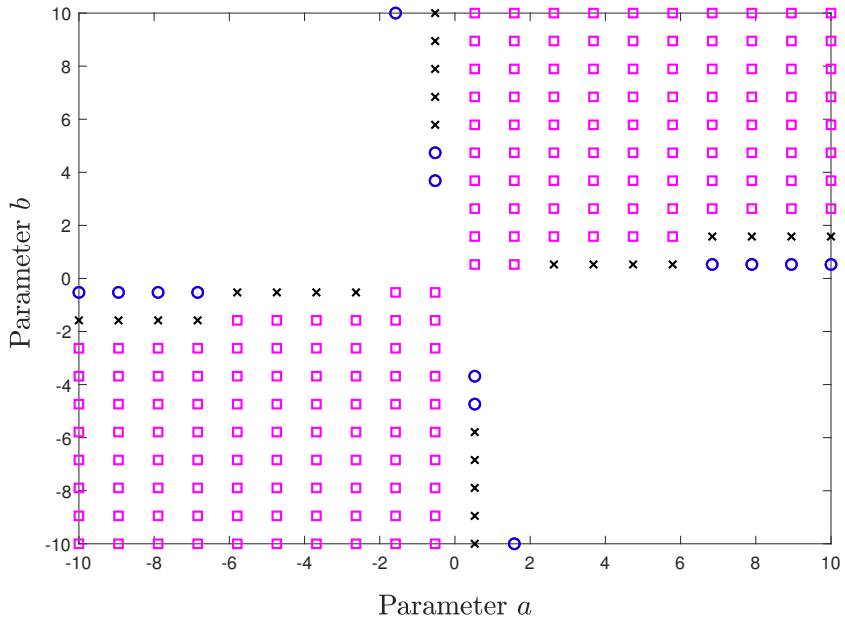

FIGURE II.3: Feasibility regions obtained with [Dehak et al., 2020, Theorem 2] (□); Corollary 1 (×,□); Theorem II.5 and [He et al., 2021, Theorem 3.3] (○,×,□).

- Corollary 1 with $u(t) = 0$, *i.e*, $F_i = 0$, for $i \in \mathcal{I}_4$,
- Affine TS fuzzy-model-based result in [Dehak et al., 2020, Theorem 2] adapted to singular systems,
- TS fuzzy-model-based result in [He et al., 2021, Theorem 3.3] with $u(t) = 0$, *i.e*, $N_{jk} = 0$, for $j, k \in \mathcal{I}_4$.

Fig.II.3 shows the feasibility regions obtained with the above results. Observe that using reduced-complexity affine representation for TS fuzzy systems, the result in [Dehak et al., 2020] leads to a conservative admissibility analysis compared to the proposed modeling method in this manuscript. Theorem II.5 provides a larger feasibility region compared to that obtained with Corollary 1. This means that using the slack variables specifically offered by the proposed modeling can contribute to reduce the conservatism induced by overbounding. For this simple singular system (II.41), the proposed approach and the recent result in [He et al., 2021] lead to the same feasibility region.

Example II.7 (Singular Descriptor System)
We consider the singular system (II.1), whose matrices are taken from [He et al., 2021] as

$$E(z) = \begin{bmatrix} 1 & 0 & 0 \\ z_1 & 1 & 0 \\ 0 & 0 & 0 \end{bmatrix}, \quad B(z) = \begin{bmatrix} 0 \\ 0.16z_3 + a \\ 0.12z_3 + b \end{bmatrix}, \quad A(z) = A_0 z_3 + \begin{bmatrix} -z_2 - 5 & 1 & z_2 \\ z_2 & bz_2 - b & 1 \\ (a+2)z_2 - 2 & 0 & 1 \end{bmatrix},$$

$$A_0 = \begin{bmatrix} 0.05 & -0.05 & 0.15 \\ 0.04 & -0.04 & 0.12 \\ 0.06 & -0.06 & 0.18 \end{bmatrix}, \tag{II.42}$$

where $a \in [-13, -8]$ and $b \in [-27, -20]$ are system parameters. The three premise variables are given by

$$z_1 = \frac{e^{-2x_1}}{1 + e^{-2x_1}}, \quad z_2 = \frac{1 + \sin^2(x_2)}{2}, \quad z_3 = \sin(0.1x_1).$$

Note that $z \in \mathscr{D}_z = \{z \in \mathbb{R}^3 : 0 \leq z_1 \leq 1,\ \frac{1}{2} \leq z_2 \leq 1,\ |z_3| \leq 1\}$. Applying the proposed modeling method, we can represent the considered system into the polytopic form (II.8) with $2 \times 3 = 6$ vertices, whose details are omitted here for brevity. We examine the design conservatism between the following control results

- LMI conditions (II.34) in Corollary 1;
- LMI conditions (II.20) in Theorem II.5;
- TS fuzzy-model-based results in [He et al., 2021, Theorem 3.3] and [Zhang et al., 2017, Theorem 3];
- TS fuzzy-model-based result in [Bouarar, Guelton, and Manamanni, 2010, Theorem 2];
- Affine TS fuzzy-model-based result in [Dehak et al., 2020, Theorem 2];

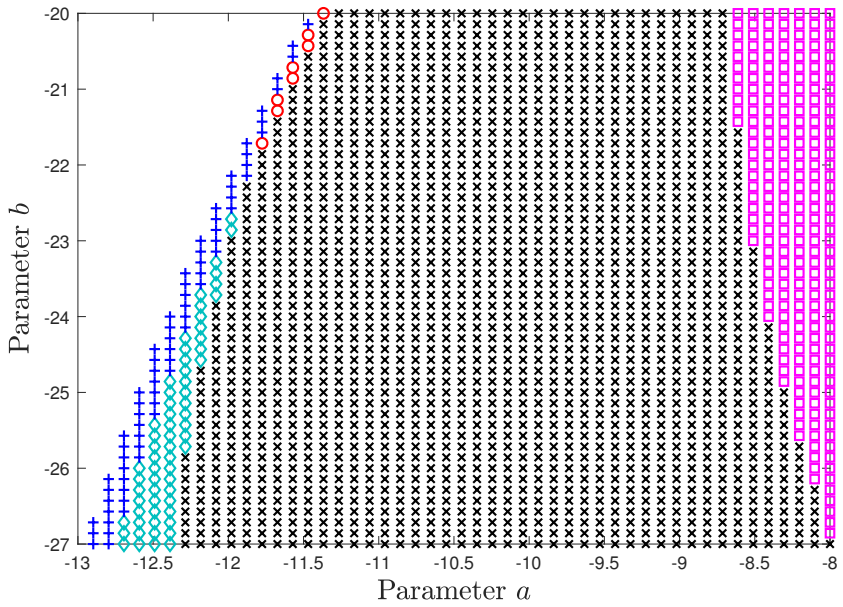

FIGURE II.4: Feasibility regions for Ex. II.7 obtained with [Dehak et al., 2020, Theorem 2] (□); [He et al., 2021, Theorem 3.3] and [Zhang et al., 2017, Theorem 3] (○,×,□); [Bouarar, Guelton, and Manamanni, 2010, Theorem 2] (◇,×,□); and Theorem II.5 (+,◇,○,×,□).

Figure II.4 depicts the feasibility regions obtained with these control results. Remark that Corollary 1 cannot provide any feasible control solution for the considered parameter space, which confirms the negative overbounding effect of the proposed modeling approach on the control design conservatism. However, taking into account the slack variables specifically introduced by this modeling, Theorem II.5 outperforms other recent TS fuzzy control results. Note that the computational complexity of LMI-based optimization problems can be evaluated with the number of scalar decision variables $\mathcal{N}_{var}$ and the number of LMI constraints $\mathcal{N}_{row}$. These characteristic numbers for the considered control results are given in Table II.2. Remark that as a price for conservatism reduction, the numerical complexity of design conditions in Theorem II.5 is slightly higher than that of other control results.

Example II.8 (3DoF Serial Robot Manipulator)
To demonstrate the interests of the proposed control approach for complex systems with a large

TABLE II.2: Numerical Complexity of Different Control Results.

Control Design	Theorem II.5	Corollary 1	[Dehak et al., 2020]	[Bouaral et al, 2010]	[He et al., 2021]
Nb. of vertices	6	6	4	8	8
$\mathcal{N}_{row}$	362	362	146	224	408
$\mathcal{N}_{var}$	1185	855	119	334	306

number of nonlinearities, we reconsider the three-degree-of-freedom (3DoF) serial robot depicted in Figure I.6, whose dynamics can be described as [Dehak et al., 2020]

$$M(\theta)\ddot{\theta}(t) + N(\theta,\dot{\theta})\dot{\theta}(t) + G(\theta) = \Gamma(t), \tag{II.43}$$

where $\theta(t) \in \mathbb{R}^3$ is the vector of generalized coordinates in joint space, $\Gamma(t) \in \mathbb{R}^3$ is the vector of generalized control forces, $M(\theta) \in \mathbb{R}^{3\times3}$ is the inertia matrix, $N(\theta,\dot{\theta}) \in \mathbb{R}^{3\times3}$ is the Coriolis/centripetal matrix plus the viscous friction coefficients of the joints, and $G(\theta) \in \mathbb{R}^n$ represents the generalized gravity forces. Since the vector-valued function $G(\theta)$ is smooth, we can then parameterize $G(\theta) = H(\theta)\theta(t)$. System (II.43) can be rewritten in the nonlinear descriptor form (I.25) with $\theta(t) = \begin{bmatrix}\theta_1(t) & \theta_2(t) & \theta_3(t)\end{bmatrix}^\top$, $u(t) = \Gamma(t)$ and

$$x(t) = \begin{bmatrix}\theta(t)\\ \dot{\theta}(t)\end{bmatrix} \in \mathbb{R}^6, \quad B(z) = \begin{bmatrix}0\\ I\end{bmatrix}, \quad E(z) = \begin{bmatrix}I & 0\\ 0 & M(z)\end{bmatrix}, \quad A_{11}(z) = \begin{bmatrix}0 & I\\ -H(z) & -N(z)\end{bmatrix}. \tag{II.44}$$

We refer to Example I.4, page 25, for the expressions of matrices $M(z)$, $N(z)$ and $H(z)$. Note that here also we consider the case without viscous friction.

With $r = 12$ premise variables, the classical TS fuzzy modeling (II.5) requires $2^{12} = 4096$ vertices to represent system (II.43)–(I.54), which is computationally complex for control design. Moreover, the corresponding TS fuzzy controller is impractical for real-time control purposes. However, the proposed modeling (II.8) leads to only $2\times12 = 24$ vertices, allowing for a practically feasible control solution. For comparison purposes, we examine the following results dedicated to *quadratic* stabilization

- LMI conditions in Theorems II.5 and II.6 with $L_j = L$, $R_j = R$, $W_{ij} = W$ and $Z_{ij} = Z$, for all $i, j \in \mathcal{I}_{24}$;
- TS fuzzy descriptor results in [Tanaka and Wang, 2004, Chapter 10] and [Bouarar, Guelton, and Manamanni, 2010, adapted Theorem 2];
- Affine TS fuzzy-model-based result in [Dehak et al., 2020, Theorem 2];

Note that the existing *nonquadratic* Lyapunov-based control approaches cannot be applied to this example due to the numerical limitations of LMI solvers. To evaluate the design conservatism, we check the existence of a stabilizing controller for the manipulator with respect to the *physical* variations of two parameters: the mass of the third arm $m_3 \in [1, 15]$ [kg], and the maximal value $\theta_{\max} \in [0, \pi]$ [rad] of the robot angular positions θ_i, that is, $|\theta_i| \leq \theta_{\max}$, for $i \in \mathcal{I}_3$. Figure II.5 shows the feasibility regions obtained with the five stabilization conditions. Remark that without including the acceleration information $\ddot{\theta}(t)$ (which is generally unavailable in practice) in the controller structure, the control result in [Dehak et al., 2020, Theorem 2] cannot provide any feasible solution. The existing TS fuzzy control results in [Tanaka and Wang, 2004; Bouarar, Guelton, and Manamanni, 2010] and Theorem II.5 lead to the same feasibility region with a very restrictive joint range, *i.e.*, $\theta_{\max} \leq \frac{\pi}{5}$ [rad]. We can observe that without using the descriptor-redundancy approach, Theorem II.6 allows finding feasible control solutions for the whole robot workspace. This clearly confirms the interest of the new control approach

TABLE II.3: Numerical Complexity of Different Control Results.

Control Design	Theorem II.5	Theorem II.6	[Dehak et al., 2020]	[Tanaka and Wang, 2004]	[Bouarar, Guelton, and Manamanni, 2010]
Nb. of vertices	24	24	13	4096	4096
$\mathcal{N}_{row}$	582	294	162	49158	61446
$\mathcal{N}_{var}$	813	525	255	73821	73821

for complex nonlinear systems in reducing the numerical complexity and design conservatism. The complexity characteristic numbers $\mathcal{N}_{row}$ and $\mathcal{N}_{var}$ for the considered control approaches are given in Table II.3.

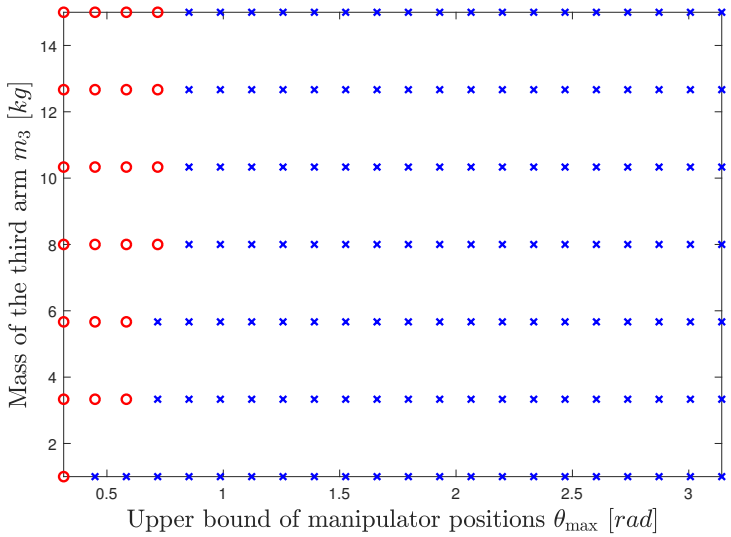

FIGURE II.5: Feasibility regions obtained with TS fuzzy approaches [Tanaka and Wang, 2004, Chapter 10] (○); [Bouarar, Guelton, and Manamanni, 2010, adapted Theorem 2] (○); Theorem II.5 (○); and Theorem II.6 (○, ×).

Remark that despite the introduction of slack variables, the computational complexity of the proposed control results are much lower compared to the existing TS fuzzy control results. The reduced-complexity affine model-based approach in [Dehak et al., 2020, Theorem 2] leads to numerically simple design conditions at the price of over-conservativeness. For illustrations, we consider the case $m_3 = 1$ [kg] and $\theta_{\max} = \pi$ [rad] for which only Theorem II.6 provide a control solution. Figure II.6 depicts the closed-loop response of the corresponding manipulator system obtained with the nonlinear control law (II.38).

II.4 Nonquadratic Control of Descriptor Systems Using Reduced-Complexity Polytopic Representation

In this section, nonquadratic stabilization of the equilibrium point $x = 0$ of system (II.1) is considered. Relying on the proposed polytopic representation (II.8), two stabilizing controller structures are proposed. The first one is based on the standard descriptor-redundancy approach [Fridman and Shaked, 2002], the second one, dedicated to the case of regular descriptor systems used a direct approach.

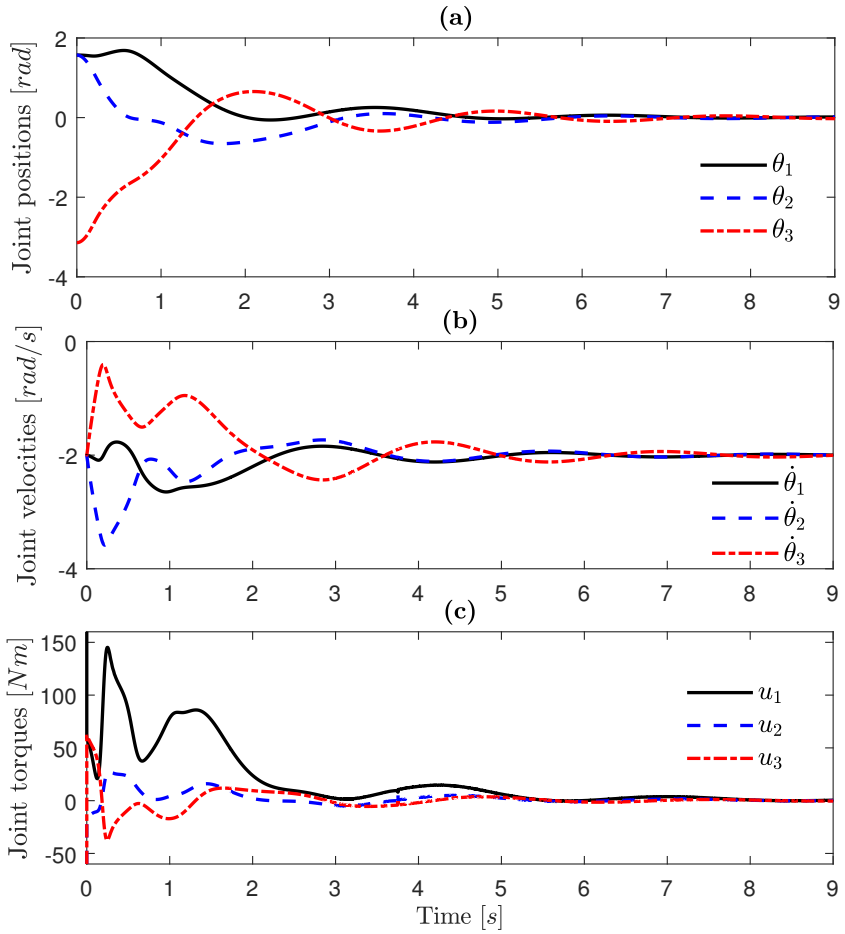

FIGURE II.6: Closed-loop response of the robot system with $m_3 = 1$ kg and $\theta_{\max} = \pi$ rad obtained with the control law (II.38).

II.4.1 Descriptor-Redundancy Based Control Design

Considering the extended form (II.18), we define the following delayed nonquadratic Lyapunov candidate functional $\mathcal{V}(z_t, x_e)$

$$\mathcal{V}(z_t, x_e) = x_e^\top \bar{E}^\top \bar{\mathcal{P}}(z_t)^{-1} x_e, \tag{II.45}$$

where

$$\bar{\mathcal{P}}(z_t) = \sum_{k=1}^{2r} \varpi_k(z_t) \bar{P}_k, \quad \bar{P}_k = \begin{bmatrix} V_k & 0 \\ W_k & Z_k \end{bmatrix}, \tag{II.46}$$

and $V_k \in \mathbb{S}^q$, $W_k \in \mathbb{R}^{n\times q}$, $Z_k \in \mathbb{R}^{n\times n}$, for $k \in \mathcal{I}_{2r}$. The functions $\varpi_k(z_t)$ are defined as in [Márquez et al., 2016] by

$$\varpi_k(z_t) = \frac{1}{\tau} \int_{t-\tau}^{t} w_k(z(\varsigma)) d\varsigma, \quad \tau > 0, \tag{II.47}$$

with $z(t) = z(0)$, for $t < 0$. The positive scalar τ is an artificial time delay. Since integration is a linear operator, it follows that $\varpi(z_t) = \left[\varpi_1(z_t), \varpi_2(z_t), \ldots, \varpi_{2r}(z_t)\right] \in \Omega$. Moreover, the time-derivative function $\dot{\varpi}_k(z_t)$ is given by

$$\dot{\varpi}_k(z_t) = \frac{1}{\tau} \left(w_k(z) - w_k(z_d)\right), \tag{II.48}$$

with $z_d(t) = z(t-\tau)$. Considering the following control law:

$$u(t) = \mathscr{F}(z_t)x_d(t) \tag{II.49}$$

The following result presents LMI-based conditions to design the nonlinear feedback gain $\mathscr{F}(z_t)$ for system (I.25).

Theorem II.7 *Given a positive scalar τ, if there exist a positive definite matrix $V_i \in \mathbb{S}^q$, symmetric matrices $T_i^{(1)}$, $T_j^{(2)}$, $T_k^{(3)}$, $T_m^{(4)} \in \mathbb{S}^{2(n+q)\times 2(n+q)}$, matrices $F_{ijk} \in \mathbb{R}^{m\times q}$, $W_i \in \mathbb{R}^{n\times q}$, $Z_i \in \mathbb{R}^{n\times n}$, $\bar{L}_{ijk}$, $\bar{R}_{ijk} \in \mathbb{R}^{2n\times 2n}$, for $i,j,k,m \in \mathcal{I}_{2r}$ such that*

$$Z_k + Z_k^\top \succ 0 \tag{II.50a}$$

$$\hat{\Xi}_{iikm} \prec 0, \quad i,k,m \in \mathcal{I}_{2r} \tag{II.50b}$$

$$\frac{2}{2r-1}\hat{\Xi}_{iikm} + \hat{\Xi}_{ijkm} + \hat{\Xi}_{jikm} \prec 0, \quad i,j,k,m \in \mathcal{I}_{2r}, \quad i \neq j, \tag{II.50c}$$

with $T_{2p}^{(\ell)} = T_{2p-1}^{(\ell)}$, $\forall p \in \mathcal{I}_r$, $\forall \ell \in \mathcal{I}_4$ and

$$\hat{\Xi}_{ijkm} = \hat{\Psi}_{ijkm} + \hat{T}_{ijkm} - \frac{1}{r}\hat{T}, \quad \hat{T}_{ijkm} = T_i^{(1)} + T_j^{(2)} + T_k^{(3)} + T_m^{(4)},$$

$$\hat{\Psi}_{ijkm} = \mathrm{He}\begin{bmatrix} \bar{A}_i\bar{L}_{jkm} + \bar{B}_i\bar{F}_{jkm} + \bar{\Theta}_{im} & \bar{A}_i\bar{R}_{jkm} \\ \bar{P}_k - \bar{L}_{jkm} & -\bar{R}_{jkm} \end{bmatrix}, \quad \hat{T} = \sum_{p=1}^{r}\sum_{\ell=1}^{4} T_{2p}^{(\ell)}$$

$$\bar{\Theta}_{im} = \frac{1}{2\tau}\,\mathrm{diag}(V_m - V_i, 0), \quad \bar{F}_{jkm} = \begin{bmatrix} F_{jkm} & 0 \end{bmatrix}.$$

where $\bar{P}_k$ is defined in (II.46). Then, the closed-loop system (II.18) is admissible for the nonlinear feedback gain of the control law (II.49) given by

$$\mathscr{F}(z_t) = F(z_t)V(z_t)^{-1}, \tag{II.51}$$

with

$$F(z_t) = \sum_{j,k,m\in\mathcal{I}_{2r}} w_j(z)\varpi_k(z_t)w_m(z_d)\; F_{jkm}, \quad V(z_t) = \sum_{k\in\mathcal{I}_{2r}} \varpi_k(z_t)V_k.$$

Proof:
For brevity, we also introduce the following notations:

$$\hat{\Xi}(z_t) = \sum_{i,j,k,m\in\mathcal{I}_{2r}} w_i(z)w_j(z)\varpi_k(z_t)w_m(z_d)\hat{\Xi}_{ijkm}, \quad \hat{\Psi}(z_t) = \sum_{i,j,k,m\in\mathcal{I}_{2r}} w_i(z)w_j(z)\varpi_k(z_t)w_m(z_d)\hat{\Psi}_{ijkm},$$

$$\bar{L}(z_t) = \sum_{j,k,m\in\mathcal{I}_{2r}} w_j(z)\varpi_k(z_t)w_m(z_d)\bar{L}_{jkm}, \qquad \bar{R}(z_t) = \sum_{j,k,m\in\mathcal{I}_{2r}} w_j(z)\varpi_k(z_t)w_m(z_d)\bar{R}_{jkm},$$

$$\bar{\Theta}(z_t) = \sum_{i,m\in\mathcal{I}_{2r}} w_i(z)w_m(z_d)\bar{\Theta}_{im}.$$

It follows directly from the definition of $\hat{\Psi}_{ijkm}$ that

$$\hat{\Psi}(z_t) = \mathrm{He}\begin{bmatrix} \Upsilon(z_t) & \bar{A}(z)\bar{R}(z_t) \\ \bar{\mathcal{P}}(z_t) - \bar{L}(z_t) & -\bar{R}(z_t) \end{bmatrix}, \tag{II.52}$$

with $\Upsilon(z_t) = \bar{A}(z)\bar{L}(z_t) + \bar{B}(z)\bar{F}(z_t) + \bar{\Theta}(z_t)$. Applying Lemma I.4 to conditions (II.50b)–(II.50c), we obtain

$$\hat{\Xi}(z_t) \prec 0. \tag{II.53}$$

Since $\varpi_k(z_t)$ also verify property (II.9b), then we have

$$\begin{aligned}\sum_{i,j,k,m\in\mathcal{I}_{2r}} w_i(z)w_j(z)\varpi_k(z_t)w_m(z_d)\ \hat{T}_{ijkm} &= \sum_{i=1}^{2r} w_i(z)T_i^{(1)} + \sum_{j=1}^{2r} w_j(z)T_j^{(2)} \\ &\quad + \sum_{k=1}^{2r} \varpi_k(z_t)T_k^{(3)} + \sum_{m=1}^{2r} w_m(z_d)T_m^{(4)} \\ &= \frac{1}{r}\sum_{p=1}^{r}\sum_{\ell=1}^{4} T_{2p}^{(\ell)} \\ &= \frac{1}{r}\hat{T} \end{aligned} \tag{II.54}$$

It follows from (II.52)–(II.54) that $\hat{\Xi}(z_t) = \hat{\Psi}(z_t)$. Hence, according to (II.53) we have

$$\hat{\Psi}(z_t) \prec 0. \tag{II.55}$$

Applying Lemma I.5 to inequality (II.55) with

$$\begin{aligned}\mathscr{A} &= \bar{A}(z), \quad \mathscr{R} = \bar{R}(z_t), \quad \mathscr{L} = \bar{L}(z_t), \\ \mathscr{P} &= \bar{\mathcal{P}}(z_t), \quad \mathscr{Q} = \bar{B}(z)\bar{F}(z_t) + \frac{1}{2}\bar{\Theta}(z_t),\end{aligned}$$

we obtain

$$\mathrm{He}\left[\bar{A}(z)\bar{\mathcal{P}}(z_t) + \bar{B}(z)\bar{F}(z_t) + \bar{\Theta}(z_t)\right] \prec 0. \tag{II.56}$$

Moreover, it follows from (II.48) that

$$\sum_{k=1}^{2r} \dot{\varpi}_k(z_t) = \frac{1}{\tau}\sum_{k=1}^{2r}(w_k(z) - w_k(z_d)),$$

which, according to (II.9a), yields that

$$\dot{\bar{\mathcal{P}}}(z_t) = \frac{1}{\tau}\sum_{i,m\in\mathcal{I}_{2r}} w_i(z)w_m(z_d)(\bar{P}_i - \bar{P}_m). \tag{II.57}$$

Note from (II.57) that $\bar{E}\dot{\bar{\mathcal{P}}}(z_t) = -2\bar{\Theta}(z_t)$. Then, inequality (II.56) can be rewritten as

$$\Phi(z_t) = \mathrm{He}\left[\bar{A}_c(z)\bar{\mathcal{P}}(z_t)\right] - \bar{E}\dot{\bar{\mathcal{P}}}(z_t) \prec 0. \tag{II.58}$$

From (II.46), we denote

$$\bar{\mathcal{P}}(z_t) = \sum_{k=1}^{2r} \varpi_k(z_t)\begin{bmatrix} V_k & 0 \\ W_k & Z_k \end{bmatrix} = \begin{bmatrix} V(z_t) & 0 \\ W(z_t) & Z(z_t) \end{bmatrix}, \tag{II.59}$$

with $N(z_t) \succ 0$. Since $\varpi_k(z_t) \in \Omega$, it follows from (II.50a) that the matrix $\bar{\mathcal{P}}(z_t)$ is regular on $\mathscr{D}_z$ with

$$\bar{\mathcal{P}}(z_t)^{-1} = \begin{bmatrix} V(z_t)^{-1} & 0 \\ -Z(z_t)^{-1}W(z_t)Z(z_t)^{-1} & Z(z_t)^{-1} \end{bmatrix}. \tag{II.60}$$

Since $\frac{\mathrm{d}}{\mathrm{d}t}\bar{\mathcal{P}}(z_t)^{-1} = -\bar{\mathcal{P}}(z_t)^{-1}\dot{\bar{\mathcal{P}}}(z_t)\bar{\mathcal{P}}(z_t)^{-1}$, *it follows that*

$$\bar{E}^\top \frac{\mathrm{d}}{\mathrm{d}t}\bar{\mathcal{P}}(z_t)^{-1} = -\bar{E}^\top\bar{\mathcal{P}}(z_t)^{-1}\dot{\bar{\mathcal{P}}}(z_t)\bar{\mathcal{P}}(z_t)^{-1} = -\bar{\mathcal{P}}(z_t)^{-\top}\bar{E}\dot{\bar{\mathcal{P}}}(z_t)\bar{\mathcal{P}}(z_t)^{-1}.$$

Note from (II.60) *that*

$$\bar{E}^\top\bar{\mathcal{P}}(z_t)^{-1} = \bar{\mathcal{P}}(z_t)^{-1}\bar{E} = \mathrm{diag}(N(z_t)^{-1}, 0).$$

Then, the nonquadratic functional $\mathcal{V}$ *defined in* (II.45) *can be rewritten as* $\mathcal{V}(z_t, x_e) = x^\top N(z_t)^{-1}x$. *Denoting* $\sigma_{\min}$ *and* $\sigma_{\max}$ *the smallest and greatest eigenvalues of all matrices* N_k, *for* $k \in \mathcal{I}_{2r}$, *it follows that*

$$\frac{1}{\sigma_{\max}}\|x\|^2 \leq \mathcal{V}(z_t, x_e) \leq \frac{1}{\sigma_{\min}}\|x\|^2. \tag{II.61}$$

Relation (II.61) *guarantees that* $\mathcal{V}(z_t, x_e)$ *is a valid Lyapunov candidate functional for system* (II.18). *Moreover, the control law* (II.49) *can be rewritten in the extended form*

$$u(t) = \bar{F}(z_t)\bar{\mathcal{P}}(z_t)^{-1}x_e(t). \tag{II.62}$$

From (II.18) *and* (II.62), *the closed-loop system can be defined as*

$$\bar{E}\dot{x}_e(t) = \bar{A}_c(z_t)x_e(t), \tag{II.63}$$

with $\bar{A}_c(z_t) = \bar{A}(z) + \bar{B}(z)\bar{F}(z_t)\bar{\mathcal{P}}(z_t)^{-1}$. *Hence, the time-derivative of* $\mathcal{V}(z_t, x_e)$ *along the trajectories of system* (II.63) *can be expressed by*

$$\dot{\mathcal{V}}(z_t, x_e) = x_e^\top\Sigma(z_t)x_e, \tag{II.64}$$

with

$$\Sigma(z_t) = \mathrm{He}\left[\bar{\mathcal{P}}(z_t)^{-\top}\bar{A}_c(z)\right] - \bar{\mathcal{P}}(z_t)^{-\top}\bar{E}\dot{\bar{\mathcal{P}}}(z_t)\bar{\mathcal{P}}(z_t)^{-1}.$$

Expression (II.64) *can be rewritten as*

$$\dot{\mathcal{V}}(z_t, x_e) = (\bar{\mathcal{P}}(z_t)x_e)^\top\Phi(z_t)(\bar{\mathcal{P}}(z_t)x_e). \tag{II.65}$$

From (II.58) *and* (II.65), *we can deduce that* $\dot{\mathcal{V}}(z_t, x_e) < 0$, *for* $x \neq 0$, *which proves the asymptotic stability of the solution* $x = 0$ *of system* (II.18). *The remainder of the proof,* i.e., $\det(A_{22}) \neq 0$, *is similar to that of Theorem II.5, which is thus omitted.*

Remark II.12. Following the same lines of Lyapunov-based control approaches for TS fuzzy systems, see [Mozelli, Palhares, and Avellar, 2009; Tognetti, Oliveira, and Peres, 2011; Zhao et al., 2014; Zhang et al., 2017; Xie et al., 2020] and related references, the Lyapunov function candidate

$$\mathscr{V}(z, x_e) = x_e^\top\bar{E}^\top\mathscr{P}(z)^{-1}x_e, \tag{II.66}$$

with

$$\mathscr{P}(z) = \begin{bmatrix} V(z) & 0 \\ W(z) & Z(z) \end{bmatrix} = \sum_{i,j\in\mathcal{I}_{2r}}^{2r} w_i(z)w_j(z)\begin{bmatrix} V_{ij} & 0 \\ W_{ij} & Z_{ij} \end{bmatrix},$$

can also be directly applied to reduce the design conservatism with respect to the quadratic approach

$$x \in \mathscr{R} = \{x \in \mathbb{R}^n : |\dot{w}_i(z)| \leq \phi_i, \quad \forall i \in \mathcal{I}_{2r}\}, \tag{II.67}$$

for some *predefined* positive scalars ϕ_i. Note that such an assumption can be only verified *a posteriori* by extensive simulations with the designed controller. Hence, as for conventional TS fuzzy control approaches [Nguyen et al., 2019], it is still not possible to *theoretically* demonstrate that control results based on $V(z, x_e)$ in (II.66) include those derived from the integral Lyapunov function $\mathcal{V}(z, x_e)$ in (II.45). This trade off comes at the expense of a more complex implementation of the controller as seen in the expression of $\mathscr{F}(z_t)$ (II.49).

Using the descriptor-redundancy approach, the feedback gain of the control law (II.49) must be extended with a special structure, *i.e.*, $\bar{\mathscr{F}}(z_t) = \begin{bmatrix}\mathscr{F}(z_t) & 0\end{bmatrix}$, to be consistent with the closed-loop system (II.18). This may lead to conservative design [Guerra, Estrada-Manzo, and Lendek, 2015; Nguyen et al., 2021b]. We avoid this drawback by expanding the non-redundant control law in (II.36) with the nonquadratic design.

II.4.2 Control Design without Descriptor-Redundancy Approach

This section presents a new nonquadratic control approach for the regular descriptor case (II.35) without requiring the classical extended form (I.25). To this end, we consider the following delayed non-quadratic Lyapunov functional candidate:

$$\mathcal{V}(z_t, x) = x^\top \mathcal{P}(z_t)^{-1} x, \tag{II.68}$$

with $\mathcal{P}(z_t) = \sum_{i=1}^{2r} \varpi_i(z_t) P_i$, and $P_i \succ 0$, for $i \in \mathcal{I}_{2r}$. For control design, we consider a new nonlinear feedback law as

$$u(t) = F(z_t) E(z)^{-\top} \mathcal{P}(z_t)^{-1} x(t), \tag{II.69}$$

The following result presents sufficient conditions to determine the gain $F(z_t)$ of the stabilizing control law (II.69) for system (II.35).

Theorem II.8 *Given a positive scalar τ, if there exist positive definite matrices $P_k \in \mathbb{S}^n$, symmetric matrices $T_i^{(1)}$, $T_j^{(2)}$, $T_k^{(3)}$, $T_m^{(4)} \in \mathbb{S}^{2n\times 2n}$, matrices L_{jkml}, $R_{jkml} \in \mathbb{R}^{n\times n}$, $F_{jkml} \in \mathbb{R}^{m\times n}$, for $i, j, k, l, m \in \mathcal{I}_{2r}$, such that*

$$\Pi_{iikml} \prec 0, \quad i, k, m, l \in \mathcal{I}_{2r} \tag{II.70a}$$

$$\frac{2}{2r-1}\Pi_{iikml} + \Pi_{ijkml} + \Pi_{jikml} \prec 0, \quad i, j, k, m, l \in \mathcal{I}_{2r} \quad i \neq j, \tag{II.70b}$$

with $T_{2p}^{(\ell)} = T_{2p-1}^{(\ell)}$, $\forall p \in \mathcal{I}_r$, $\forall \ell \in \mathcal{I}_5$, and

$$\Pi_{ijkml} = \Lambda_{ijkml} + \hat{T}_{ijkml} - \frac{1}{r}\hat{T}, \quad \hat{T}_{ijkml} = T_i^{(1)} + T_j^{(2)} + T_k^{(3)} + T_m^{(4)} + T_l^{(5)},$$

$$\Lambda_{ijkml} = \mathrm{He}\begin{bmatrix} A_i L_{jkml} + B_i F_{jkml} + \Gamma_{ijml} & A_i R_{jkml} \\ P_k E_i^\top - L_{jkml} & -R_{jkml} \end{bmatrix}, \quad \hat{T} = \sum_{p=1}^{r}\sum_{\ell=1}^{4} T_{2p}^{(\ell)}$$

$$\Gamma_{ijml} = -\frac{1}{2\tau} E_l (P_i - P_m) E_j^\top$$

Then, the solution $x = 0$ of the regular nonlinear system (II.35)–(II.69) is asymptotically stable for the feedback gain $F(z_t)$ given by

$$F(z_t) = \sum_{j,k,m,l\in\mathcal{I}_{2r}} w_j(z)\varpi_k(z_t) w_m(z_d) w_l(z) F_{jkml}. \tag{II.71}$$

Proof:
Similarly to the proof of Theorem 1, according to Lemmas I.4 and I.5, we can prove that

conditions (II.70a) *and* (II.70b) *yield the following inequality*

$$\text{He}\left[A(z)\mathcal{P}(z_t)E(z)^\top + B(z)F(z_t) + \Gamma(z_t)\right] \prec 0, \tag{II.72}$$

with

$$\Gamma(z_t) = \sum_{i,j,m,l\in\mathcal{I}_{2r}} w_i(z)w_j(z)w_m(z_d)w_l(z)\Gamma_{ijml}.$$

From the definition of Γ_{ijml}*, we can deduce that*

$$E(z)\dot{\mathcal{P}}(z_t)E(z)^\top = -2\Gamma(z_t). \tag{II.73}$$

Combining (II.73) *with* (II.72)*, it follows that*

$$\text{He}\left[A(z)\mathcal{P}(z_t)E(z)^\top + B(z)F(z_t) - \frac{1}{2}E(z)\dot{\mathcal{P}}(z_t)E(z)^\top\right] \prec 0. \tag{II.74}$$

The time-derivative of the Lyapunov functional $\mathcal{V}(z_t, x)$*, defined in* (II.68)*, along the trajectories of* (II.35) *is given by*

$$\begin{aligned}\dot{\mathcal{V}}(z_t,x) = x^\top \text{He}\Big[&\mathcal{P}(z_t)^{-\top}E(z)^{-1}A(z) + \mathcal{P}(z_t)^{-\top}E(z)^{-1}B(z)F(z_t)E(z)^{-\top}\mathcal{P}(z_t)^{-1}\\ &- \frac{1}{2}\mathcal{P}(z_t)^{-1}\dot{\mathcal{P}}(z_t)\mathcal{P}(z_t)^{-1}\Big]x\\ = \xi^\top \text{He}&\left[A(z)\mathcal{P}(z_t)E(z)^\top + B(z)F(z_t) - \frac{1}{2}E(z)\dot{\mathcal{P}}(z_t)E(z)^\top\right]\xi,\end{aligned} \tag{II.75}$$

with $\xi = E(z)^{-\top}\mathcal{P}(z_t)^{-1}x$*. It follows from* (II.74) *and* (II.75) *that* $\dot{\mathcal{V}}(z_t, x) < 0$*, for all* $x \neq 0$*, which proves the asymptotic stability of the solution* $x = 0$ *of system* (II.35) *with the control law* (II.69)*.*

II.4.3 Numerical Examples

This section presents an example to illustrate the performance and complexity of the non-quadratic design for the proposed polytopic representation (II.8) in comparison with the previous results on quadratic stabilization and other works from literature. All the involved LMI-based conditions are solved using YALMIP toolbox with SeDuMi solver [Löfberg, 2004].

Example II.9 (Comparative Study)
To illustrate the design conservatism of the proposed approach, let us revisit the academic nonlinear descriptor system in Example I.1. The parameter ranges of system (I.10) are defined as $a \in [-8, 8]$ and $b \in [-20, 20]$. For comparison purposes, we examine the design conservatism between six control results

- Nonquadratic conditions (II.50) in Theorem II.7;
- Quadratic conditions (II.20) in Theorem II.5;
- Nonquadratic conditions (II.70) in Theorem II.8;
- Quadratic conditions (II.37) in Theorem II.6;
- Nonquadratic in [He et al., 2021, Theorem 2] with $|\dot{\mu}_i(z)| \leq 0.5$ for $i \in \mathcal{I}_8$;
- Quadratic conditions in [Guerra et al., 2007, Theorem 1];

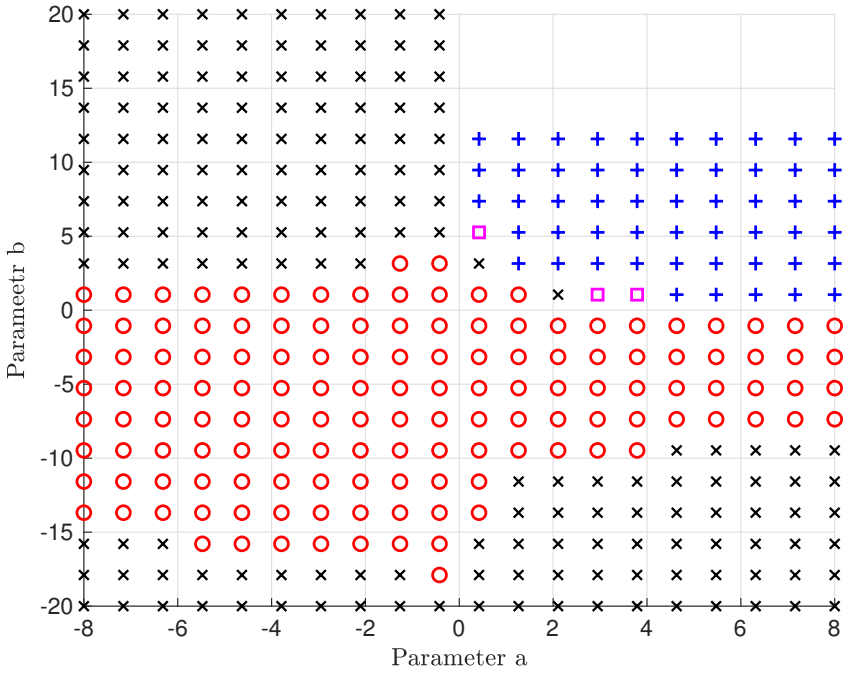

FIGURE II.7: Feasibility regions obtained with [Zhang et al., 2017, Theorem 2] ("∘"); [Guerra et al., 2007, Theorem 1] ("∘","×"); Theorem II.5 and Theorem II.6 ("∘", "×", "□"); Theorem II.7 and Theorem II.8 with $\tau = 5 \times 10^{-6}$ ("∘", "×", □, "+").

Figure (II.7) shows the feasibility regions obtained with these six control results. Remark that compared to the existing control approaches, the proposed one leads to less conservative results for both quadratic and nonquadratic based control designs. We can also observe the interest of using nonquadratic Lyapunov functionals in Theorems II.7 and II.8 to further reduce the design conservatism compared to their quadratic counterparts in Theorems II.5 and II.6, respectively. For this example, the proposed conditions provide the same feasibility regions with or without using the descriptor-redundancy approach.

Note that the computational complexity of LMI-based optimization problems can be evaluated with the number of scalar decision variables $\mathcal{N}_{var}$ and the number of LMI constraints $\mathcal{N}_{lmi}$. These characteristic numbers and also the number of slack variables $\mathcal{N}_{slack}$ introduced into the design conditions of the six considered quasi-LPV control results are given in Table II.4. Remark that as a price for conservatism reduction, the numerical complexity of design conditions in Theorems II.7 and II.8 are higher than that of other control results. Observe also that with a significantly reduced-complexity, Theorem II.6 can provide less conservative results compared to existing related works [Zhang et al., 2017; Guerra et al., 2007].

TABLE II.4: Numerical Complexity of Six quasi-LPV Control Results.

Control Design	Th II.7	Th II.5	Th II.8	Th II.6	Th 2 [He et al., 2021]	Th 1 [Guerra et al., 2007]
Nb. of vertices	6	6	6	6	8	8
$\mathcal{N}_{slack}$	2916	324	2430	90	0	0
$\mathcal{N}_{var}$	10326	539	4608	153	258	547
$\mathcal{N}_{lmi}$	82993	2313	124441	581	8961	2053

II.5 Conclusions

A polytopic quasi-LPV approach has been proposed for a class of nonlinear descriptor systems. Compared to classical polytopic quasi-LPV approaches, the numerical complexity of the new representation grows proportionally, rather than exponentially, with respect to the number of scheduling parameters. This is particularly interesting when dealing with complex descriptor systems with a large number of nonlinearities. Moreover, the system vertices obtained from the proposed representation approach are not unique even with the same predefined MFs. This non-uniqueness representation feature allows introducing slack variables into quasi-LPV models, which can contribute to reduce the control design conservatism that maybe caused by the overbounding phenomena illustrated in Example II.5.

Based on the proposed quasi-LPV representation, delayed Lyapunov candidate functionals have been exploited to derive sufficient stabilization conditions for nonlinear descriptor systems with or without using the descriptor-redundancy approach. Both nonquadratic control designs are reformulated as convex optimization problems under LMI constraints. It is proved with theoretical arguments and numerical illustrations that the control results of the new nonquadratic approach include those derived from a quadratic Lyapunov function.

The proposed quasi-LPV representation approach provides a solid alternative for modeling complex nonlinear systems with a high number of nonlinear terms. In the next chapter we will tackle the problems of robust trajectory tracking and observer design for robotic systems.

Chapter III

Robust Trajectory Tracking for Uncertain Descriptor Systems

> "Thoroughly conscious ignorance is the prelude to every real advance in science."
>
> James Clerk Maxwell

Contents

III.1 Introduction **55**

III.2 Uncertain Polytopic Quasi-LPV Modeling for Nonlinear Descriptor Systems **55**

III.2.1 Uncertain Quasi-LPV Modeling 56

III.2.2 Robust Stabilization of Uncertain Descriptor Systems 58

III.2.3 Control Design Based on System Redundancy 59

III.3 Trajectory Tracking for Serial Manipulators **65**

III.3.1 Uncertain Robot Manipulator Dynamics 66

III.3.2 $\mathcal{H}_\infty$-Performance Trajectory Tracking Control 67

III.3.3 Application of $\mathcal{H}_\infty$ Control to a 3DoF Serial Manipulator 70

III.4 The Case of Unmeasured Scheduling Variables **76**

III.5 Conclusions **77**

III.1 Introduction

Trajectory tracking control is one of the most active research topics in robotics, especially for industrial manipulators [Mouhacine, 2004; Lochan and Roy, 2015; Andreev and Peregudova, 2019; Yuan et al., 2020; Makni et al., 2021]. The control objective is to achieve high-precision tracking control performance for a desired reference trajectory [Voglewede, Smith, and Monti, 2009]. Despite significant advances in control theory, classical control approaches such as proportional-integral-derivative (PID) controllers or computed torque controllers (CTC) [Piltan et al., 2012] still remain the most commonly used in practice. The main reason behind such an interest relies in the simplicity of their design and real-time implementation [Hamamci, 2007; Efe, 2011]. However, several problems arise in the designs of these classical control approaches, including lack of robustness, design oversimplification, noise degradation in the derivative control and loss of performance [Han, 2009]. Significant research efforts have been made in order to improve the robustness and performance of both PID and CTC controllers, for instance fractional-order PID control [Keyser, Muresan, and Ionescu, 2018], or robust CTC designs [Lee and Cheng, 1996; Song et al., 2005]. However, the existing control schemes still show some limitations, in particular when dealing with highly coupled nonlinear systems such as robot manipulators. Other control theories have been applied to perform trajectory tracking, namely fuzzy-model-based control [Nguyen et al., 2018; Nguyen et al., 2019], adaptive robust control [Ren et al., 2018], neural networks based control [Zhao-Hui and Taiki, 2008] and so on. It is important to note that many of these approaches require full-state information for feedback control. However, the online measurement of both the positions and the velocities of the robots can lead to problems related to the accuracy of industrial tachometers [Fantuzzi, Secchi, and Visioli, 2003].

Moreover, these existing control designs are rather involved with generally complex control structures for real-time implementation, especially for robot manipulators with high degrees of freedom. These disadvantages point out a need for more effective control schemes relying only on the measurement of robot joint positions, which can achieve a desired tracking control performance. Additionally, the presence of structural uncertainties can heavily impact the desired performance of trajectory tracking control. For model based approaches, due to uncertainties, the mathematical model may not reflect closely the real physical behavior of the system. The proposed solution in literature [Nguyen et al., 2019], which relies on the knowledge of the uncertainty bounds to derive LMI conditions for a robust control design, can prove to be conservative in term of finding feasible solutions to the design conditions.

Motivated by the above theoretical and practical robotics control issues, we first propose in this chapter a new approach for dealing with parametric uncertainties exploiting properties of the quasi-LPV approach (II.8) proposed in Chapter II. This solution is compared to the literature using two examples of singular descriptor systems. Then we shift our focus to the problem of robust trajectory tracking of a 3-DoF serial manipulator exploiting the novel uncertain quasi-LPV modeling approach. We consider the presence of modeling uncertainties and unknown disturbances and suppose initially that the measurement of both angular position and velocity are rendered available. The case where the velocity measurement is unavailable is discussed alongside the resulting issue of unmeasured premise variables and the viability of a mixed controller/observer design.

III.2 Uncertain Polytopic Quasi-LPV Modeling for Nonlinear Descriptor Systems

The aim of this section is to extend the quasi-LPV representation (II.8) to nonlinear uncertain

systems. As will be seen later, the proposed polytopic modeling allows a new way of dealing with parametric uncertainties providing extra flexibility for the control design.

III.2.1 Uncertain Quasi-LPV Modeling

Consider the following uncertain descriptor system

$$E(z)\dot{x}(t) = \big(A(z) + \Delta A(z)\big)x(t) + \big(B(z) + \Delta B(z)\big)u(t) \tag{III.1}$$

with $E(z) = \mathrm{diag}(E_1(z), 0)$, $\mathrm{rank}(E_1(z)) = q$. We define the following decomposition for the premise vector $z(t) = \begin{bmatrix} z_s^\top(t) & z_\delta^\top(t) \end{bmatrix}^\top \in \mathbb{R}^{r+\ell}$, where $z_s(t) \in \mathbb{R}^r$ is the known scheduling variable vector which can continuously depends on the differential states $x_d(t)$ and/or other time-varying parameters and the vector $z_\delta(t) \in \mathbb{R}^\ell$ composed of uncertain terms whose explicit expressions are unknown. All the components of $z(t)$ are assumed bounded, that is $z \in \mathscr{D}_z$ with

$$\mathscr{D}_z = \left\{ z \in \mathbb{R}^{r+\ell} : z_i^0 \leq z_i \leq z_i^1,\ i = 1, 2, \ldots, r+\ell \right\}, \tag{III.2}$$

where z_i is the i-th entry of vectors z, z_i^0 and z_i^1 are some given bounds. The matrices $E(z) \in \mathbb{R}^{n\times n}$, $A(z) \in \mathbb{R}^{n\times n}$, and $B(z) \in \mathbb{R}^{m\times n}$ depend affinely on z_s while the matrices $\Delta A(z) \in \mathbb{R}^{n\times n}$ and $\Delta B(z) \in \mathbb{R}^{m\times n}$ depend affinely on z_δ. Note that various nonlinear systems in mechatronics and robotics can be naturally modeled in the form (III.1), for instance Lagrangian-Euler systems under algebraic constraints [Kamman and Huston, 1984; Bayo, Garcia De Jalon, and Serna, 1988].

Similarly to the affine polytopic decomposition (II.6), we define the following uncertain polytopic representation for the system matrices of (III.1)

$$X(z) + \Delta X(z) = \bar{X}_0 + \Delta\bar{X}_0 + \sum_{p=1}^{r+\ell} z_p(\bar{X}_p + \Delta\bar{X}_p) \tag{III.3}$$

with $X \in \{E, A, B\}$, $\Delta X \in \{\Delta A, \Delta B\}$ and

$$\bar{X}_p = 0, \quad \forall p \in \mathcal{I}_{r+\ell\backslash r}, \qquad \Delta\bar{X}_p = 0, \quad \forall p \in \mathcal{I}_r$$

with $\bar{E}_p \in \mathbb{R}^{n\times n}$, $\bar{A}_p \in \mathbb{R}^{n\times n}$, $\bar{B}_p \in \mathbb{R}^{m\times n}$, for $p \in \mathcal{I}_r \cup \{0\}$ $\Delta\bar{A}_p \in \mathbb{R}^{n\times n}$, $\Delta\bar{B}_p \in \mathbb{R}^{m\times n}$ for $p \in \mathcal{I}_{r+\ell\backslash r} \cup \{0\}$. As z belongs to the bounded set $\mathscr{D}_z$, using the sector nonlinearity approach [Taniguchi et al., 2001], both the state-dependent and uncertain terms $z_p(x)$ can be rewritten as a convex combination of their bounds, as in (I.4). Then, it follows that (III.3) is equivalent to the following polytopic decomposition

$$\begin{aligned}
X(z) + \Delta X(z) &= \bar{X}_0 + \Delta\bar{X}_0 + \sum_{p=1}^{r+\ell} \left(\omega_p^1(z_p)z_p^1 + \omega_p^0(z_p)z_p^0\right)(\bar{X}_p + \Delta\bar{X}_p) \\
&= \sum_{p=1}^{r+\ell} \left(\frac{\omega_p^1(z_p)}{r+\ell} \left(\bar{X}_0 + \Delta\bar{X}_0 + (r+\ell)z_p^1(\bar{X}_p + \Delta\bar{X}_p) \right) \right. \\
&\quad \left. + \frac{\omega_p^0(z_p)}{r+\ell} \left(\bar{X}_0 + \Delta\bar{X}_0 + (r+\ell)z_p^0(\bar{X}_p + \Delta\bar{X}_p) \right) \right) \\
&= \sum_{i=1}^{2(r+\ell)} w_i(z)(X_i + \Delta X_i),
\end{aligned} \tag{III.4}$$

with

$$w_{2p-1}(z) = \frac{1}{r+\ell}\omega_p^1(z_p), \quad w_{2p}(z) = \frac{1}{r+\ell}\omega_p^0(z_p), \tag{III.5}$$

and

$$X_{2p-1} = \bar{X}_0 + (r+\ell)z_p^1\bar{X}_p, \qquad X_{2p} = \bar{X}_0 + (r+\ell)z_p^0\bar{X}_p$$
$$\Delta X_{2p-1} = \Delta\bar{X}_0 + (r+\ell)z_p^1\Delta\bar{X}_p, \qquad \Delta X_{2p} = \Delta\bar{X}_0 + (r+\ell)z_p^0\Delta\bar{X}_p,$$

Applying the matrix decomposition (III.4), the uncertain quasi-LPV descriptor system (III.1) can be equivalently represented in the following uncertain polytopic form

$$\sum_{i=1}^{2(r+\ell)} w_i(z)E_i\dot{x}(t) = \sum_{i=1}^{2(r+\ell)} w_i(z)\Big((A_i+\Delta A_i)x(t) + (B_i+\Delta B_i)u(t)\Big). \tag{III.6}$$

The weights $w_i(z)$, for $i \in \mathcal{I}_{2(r+\ell)}$, satisfy the following property

$$\sum_{i=1}^{2(r+\ell)} w_i(z) = 1, \quad 0 \le w_i(z) \le 1, \tag{III.7a}$$
$$w_{2p-1}(z) + w_{2p}(z) = \frac{1}{r+\ell}, \quad \forall p \in \mathcal{I}_{r+\ell}. \tag{III.7b}$$

The vertex X_i can be directly derived from $X(z)$, for $X \in \{E, A, B\}$ and $i \in \mathcal{I}_{2(r+\ell)}$ while the vertex ΔX_i can be directly derived from $\Delta X(z)$, for $\Delta X \in \{\Delta A, \Delta B\}$ and $i \in \mathcal{I}_{2(r+\ell)}$. To this end, we define the vectors $\zeta^1, \ldots, \zeta^{r+\ell}$ forming the canonical basis of $\mathbb{R}^{r+\ell}$ as

$$\zeta^i = [0, \ldots, 0, \overbrace{1}^{i\text{th}}, 0, \ldots, 0]^\top, \quad i \in \mathcal{I}_{r+\ell}.$$

Then, for $i \in \mathcal{I}_{2(r+\ell)}$, the vertices X_i and ΔX_i of system (III.6) are directly obtained from $X(z)$ and $\Delta X(z)$ respectively, for $X \in \{E, A, B\}$ and $\Delta X \in \{\Delta A, \Delta B\}$, as

$$X_i = \begin{cases} X\big((r+\ell)z_p^1\zeta^p\big), & \text{if } i = 2p-1, \text{ and } p \in \mathcal{I}_r \\ X\big((r+\ell)z_p^0\zeta^p\big), & \text{if } i = 2p, \text{ and } p \in \mathcal{I}_r \\ X(0 \times \zeta^p), & \text{if } i \in \mathcal{I}_{(2r+\ell)\backslash 2r} \end{cases} \tag{III.8}$$

$$\Delta X_i = \begin{cases} \Delta X\big((r+\ell)z_p^1\zeta^p\big), & \text{if } i = 2p-1, \text{ and } p \in \mathcal{I}_{r+\ell\backslash r} \\ \Delta X\big((r+\ell)z_p^0\zeta^p\big), & \text{if } i = 2p, \text{ and } p \in \mathcal{I}_{r+\ell\backslash r} \\ \Delta X(0 \times \zeta^p), & \text{if } i \in \mathcal{I}_{2r} \end{cases} \tag{III.9}$$

With the uncertain polytopic representation (III.6), the weights $w_i(z)$ defined in (III.5) depend only on one component of the premise vector $z(t)$ ($z_{i/2}$ or $z_{(i+1)/2}$ according to the parity of i) *i.e.* they do not required a combination product as in [Taniguchi et al., 2001]. As only the $2r$ first weights $w_i(z)$ have a known expression, any stabilizing control law can exclusively depends on these weights and the internal variables. The polytopic form (III.6) has $2(r+l)$ vertices, which may significantly reduce the numerical complexity compared to the classical polytopic representation with 2^r vertices [Taniguchi et al., 2001; Tanaka and Wang, 2004]. This feature is particularly interesting when dealing with nonlinear systems with large numbers r of scheduling variables and l of uncertain terms.

Example III.10 (Illustrative Uncertain System)
We consider system (III.1) with the following state-dependent matrices taken from [He et al., 2021]. The structure of the uncertainties is modified so that it depends uniquely and affinely on the uncertain terms

$$E(z) = \begin{bmatrix} 1 & 0 & 0 \\ z_1 & 1 & 0 \\ 0 & 0 & 0 \end{bmatrix}, \quad A(z) = \begin{bmatrix} -z_2 - 5 & 1 & z_2 \\ z_2 & -b + bz_2 & 1 \\ (a+2)z_2 - 2 & 0 & 1 \end{bmatrix}, \quad B = \begin{bmatrix} 0 \\ a \\ b \end{bmatrix}, \tag{III.10}$$

where a and b are some constant parameters. The uncertain terms matrices are given as such $\Delta A(z) = H_a z_3 W_a$ and $\Delta B(z) = H_b z_3 W_b$ with $W_a = W_{a_1} - W_{a_2}$ and

$$H_a = \begin{bmatrix} 0.5 \\ 0.4 \\ 0.6 \end{bmatrix}, \quad W_{a_1}^\top = \begin{bmatrix} 0.3 \\ 0.1 \\ 0.3 \end{bmatrix}, \quad W_{a_2}^\top = \begin{bmatrix} 0.2 \\ 0.2 \\ 0 \end{bmatrix}, \quad H_b = \begin{bmatrix} 0 \\ 0.4 \\ 0.3 \end{bmatrix}, \quad W_b = 0.4 \tag{III.11}$$

The full scheduling vector is defined as $z = \begin{bmatrix} z_1 & z_2 & z_3 \end{bmatrix}^\top$ with $z_s = \begin{bmatrix} z_1 & z_2 \end{bmatrix}^\top$, $z_\delta = z_3$ and

$$z_1 = \frac{e^{-2x_1}}{1 + e^{-2x_1}}, \quad z_2 = \frac{1 + \sin^2(x_2)}{2}, \quad z_3 = \sin(0.1t).$$

Note that $z_s \in \mathscr{D}_z$ and $z_\delta \in \mathscr{D}_z$ with

$$\mathscr{D}_z = \{z \in \mathbb{R}^3 : 0 \leq z_i \leq 1,\ i \in \mathcal{I}_2,\ -1 \leq z_3 \leq 1\}$$

The number of vertices is $2(r + \ell) = 6$. For illustrations, the system matrices and the weights of two vertices of the proposed uncertain polytopic approach (III.6) are given by

$$E_2 = E(\begin{bmatrix} z_1^1 & 0 & 0 \end{bmatrix}) = \begin{bmatrix} 1 & 0 & 0 \\ 4 & 1 & 0 \\ 0 & 0 & 0 \end{bmatrix}, \qquad E_4 = E(\begin{bmatrix} 0 & z_2^1 & 0 \end{bmatrix}) = \begin{bmatrix} 1 & 0 & 0 \\ 0 & 1 & 0 \\ 0 & 0 & 0 \end{bmatrix},$$

$$A_2 = A(\begin{bmatrix} z_1^1 & 0 & 0 \end{bmatrix}) = \begin{bmatrix} -5 & 1 & 0 \\ 0 & -b & 1 \\ -2 & 0 & 1 \end{bmatrix}, \qquad A_4 = A(\begin{bmatrix} 0 & z_2^1 & 0 \end{bmatrix}) = \begin{bmatrix} -9 & 1 & 4 \\ 4 & 2b & 1 \\ 3a+4 & 0 & 1 \end{bmatrix},$$

$$\Delta A_2 = \Delta A(\begin{bmatrix} z_1^1 & 0 & 0 \end{bmatrix}) = \begin{bmatrix} 0 & 0 & 0 \\ 0 & 0 & 0 \\ 0 & 0 & 0 \end{bmatrix}, \qquad \Delta A_5 = \Delta A(\begin{bmatrix} 0 & 0 & z_3^0 \end{bmatrix}) = \begin{bmatrix} -0.10 & -0.10 & 0 \\ -0.08 & -0.08 & 0 \\ -0.12 & -0.12 & 0 \end{bmatrix},$$

$$\Delta B_2 = \Delta B(\begin{bmatrix} z_1^1 & 0 & 0 \end{bmatrix}) = \begin{bmatrix} 0 \\ 0 \\ 0 \end{bmatrix}, \qquad \Delta B_5 = \Delta B(\begin{bmatrix} 0 & 0 & z_3^0 \end{bmatrix}) = \begin{bmatrix} 0 \\ -0.48 \\ -0.36 \end{bmatrix},$$

$$w_3(z) = \frac{1 + \sin^2(x_1)}{6}, \qquad w_4(z) = \frac{1 - \sin^2(x_2)}{6}.$$

III.2.2 Robust Stabilization of Uncertain Descriptor Systems

This section presents the synthesis of a controller that quadratically stabilizes system (III.1) using the proposed modeling approach (III.6). Furthermore, exploiting the additional property (III.7b), a specific nonlinear feedback is proposed to deal with uncertainties.

Consider the descriptor system expressed in the extended form (I.38) rewritten as

$$\bar{E}_o \dot{x}_e(t) = \bar{\mathcal{A}}(z) x_e(t) + \bar{\mathcal{B}}(z) u(t) \tag{III.12}$$

with

$$\bar{\mathcal{A}}(z) = \bar{A}(z) + \Delta\bar{A}(z), \quad \bar{\mathcal{B}}(z) = \bar{B}(z) + \Delta\bar{B}(z).$$

It follows from the expression (III.6) that the extended descriptor form (III.12) can be rewritten as

$$\bar{E}_o\dot{x}_e(t) = \sum_{i=1}^{2(r+\ell)} w_i(z)(\bar{\mathcal{A}}_i x_e(t) + \bar{\mathcal{B}}_i u(t)). \tag{III.13}$$

We define the following control law

$$u(t) = \bar{K}(z)x_e(t) \tag{III.14}$$

with $\bar{K}(z) = \begin{bmatrix} K(z) & 0 \end{bmatrix}$ and $K(z) \in \mathbb{R}^{m\times q}$. The closed-loop system (III.12)–(III.14) is then given by

$$\bar{E}_o\dot{x}_e(t) = \mathcal{A}_c(z)x_e(t) \tag{III.15}$$

with $\mathcal{A}_c(z) = \bar{\mathcal{A}}(z) + \bar{\mathcal{B}}(z)\bar{K}(z)$. Considering the decomposition of the state vector $x_e = \begin{bmatrix} x_d^\top & \dot{x}_d^\top & x_a^\top \end{bmatrix}^\top$, the closed-loop matrix $\mathcal{A}_c(z)$ admits the following decomposition

$$\mathcal{A}_c(z) = \begin{bmatrix} 0 & I & 0 \\ \mathcal{A}_{11}(z) + \mathcal{B}_1(z)K(z) & -E_1(z) & \mathcal{A}_{12}(z) \\ \mathcal{A}_{21}(z) + \mathcal{B}_2(z)K(z) & 0 & \mathcal{A}_{22}(z) \end{bmatrix} \tag{III.16}$$

where

$$\begin{aligned} &\mathcal{A}_{11}(z) = A_{11}(z) + \Delta A_{11}(z), \quad \mathcal{A}_{12}(z) = A_{12}(z) + \Delta A_{12}(z), \quad \mathcal{A}_{21}(z) = A_{21}(z) + \Delta A_{21}(z), \\ &\mathcal{A}_{22}(z) = A_{22}(z) + \Delta A_{22}(z), \quad \mathcal{B}_1(z) = B_1(z) + \Delta B_1(z), \quad \mathcal{B}_2(z) = B_2(z) + \Delta B_2(z), \end{aligned}$$

and $\mathcal{A}_{11} \in \mathbb{R}^{q\times q}$, $\mathcal{A}_{12} \in \mathbb{R}^{q\times s}$, $\mathcal{A}_{21} \in \mathbb{R}^{s\times q}$, $\mathcal{A}_{22} \in \mathbb{R}^{s\times s}$, $\mathcal{B}_1 \in \mathbb{R}^{q\times m}$, and $\mathcal{B}_2 \in \mathbb{R}^{s\times m}$.

III.2.3 Control Design Based on System Redundancy

We consider the following Lyapunov candidate function

$$\mathcal{V}(z, x_e) = x_e^\top \bar{E}_o^\top \mathcal{P}(z)^{-1} x_e \tag{III.17}$$

with

$$\mathcal{P}(z) = \begin{bmatrix} V(z) & 0 \\ W(z) & Z(z) \end{bmatrix} = \sum_{p=1}^{2(r+\ell)} w_j(z)P_j, \quad P_j = \begin{bmatrix} V_j & 0 \\ W_j & Z_j \end{bmatrix}, \quad P_{2p-1} = P_{2p}, \quad \forall p \in \mathcal{I}_{r+\ell} \tag{III.18}$$

where $V(z) \in \mathbb{R}^{q\times q}$ is positive definite and $Z(z)$ invertible for all $z \in \mathscr{D}_z$. It follows that the matrix $\mathcal{P}(z)$ is non singular on $\mathscr{D}_z$ with

$$\mathcal{P}(z)^{-1} = \begin{bmatrix} V(z)^{-1} & 0 \\ -Z(z)^{-1}W(z)V(z)^{-1} & Z(z)^{-1} \end{bmatrix}. \tag{III.19}$$

Note that from the definition of $\bar{E}_o$ and (III.19), we have

$$\bar{E}_o^\top \mathcal{P}(z)^{-1} = \mathcal{P}(z)^{-1}\bar{E}_o = \begin{bmatrix} V(z)^{-1} & 0 \\ 0 & 0 \end{bmatrix} \succeq 0.$$

Then, the proposed function $\mathcal{V}$ defined in (III.17) can be rewritten as $\mathcal{V}(z, x_e) = x_d^\top V(z)^{-1} x_d$ and thus is a positive-definite function of x_d. Considering the additional property (III.7b) and the definition of $\mathcal{P}(z)$ in (III.18), we have

$$\begin{aligned} \mathcal{P}(z) = \sum_{j=1}^{2(r+\ell)} w_j(z) P_j &= \sum_{p=1}^{r+\ell} w_{2p-1}(z) P_{2p-1} + w_{2p}(z) P_{2p} \\ &= \sum_{p=1}^{r+\ell} \left(w_{2p-1}(z) + w_{2p}(z)\right) P_{2p} \\ &= \frac{1}{r+\ell} \sum_{p=1}^{r+\ell} P_{2p} \end{aligned} \tag{III.20}$$

and thus the proposed function $\mathcal{V}$ defined in (III.17) is in fact quadratic, leading to $\dot{\mathcal{P}}(z) = 0$ and

$$\dot{\mathcal{V}}(z, x_e) = \mathrm{He}\left[x_e^\top \mathcal{P}(z)^{-\top} \bar{E}_o \dot{x}_e\right] \tag{III.21}$$

The proposed Lyapunov candidate function exploits the additional property (III.7b) to introduce $r + \ell$ matrices P_j while maintaining a quadratic expression needing no additional assumptions on the derivatives of the weights $w_i(z)$ as in the nonquadratic Lyapunov case [Mozelli, Palhares, and Avellar, 2009].

Considering the control law (III.14), we define the nonlinear gain $\bar{K}(z)$ as such

$$\bar{K}(z) = \bar{H}(z)\mathcal{P}(z)^{-1}, \tag{III.22}$$

with $\bar{H}(z) = \begin{bmatrix} H(z) & 0 \end{bmatrix}$, $H(z) \in \mathbb{R}^{m \times q}$ and

$$H(z) = \sum_{j=1}^{2(r+\ell)} w_j(z) H_j, \quad H_{2p-1} = H_{2p}, \quad \forall p \in \mathcal{I}_{r+\ell \setminus r} \tag{III.23}$$

The weights $w_j(z)$ for $j \in \mathcal{I}_{2(r+\ell)\setminus 2r}$ in the expression of $H(z)$ depend on the uncertain vector $z_\delta(t)$ and, as such, are unknown and cannot be used in the control law. However, since they also verify the additional property (III.7b) and $H_{2p-1} = H_{2p}$, $\forall p \in \mathcal{I}_{r+\ell\setminus r}$, we have

$$\begin{aligned} H(z) = \sum_{i=1}^{2(r+\ell)} w_i(z) H_i &= \sum_{j=1}^{2r} w_j(z_s) H_j + \sum_{k=2r+1}^{2(r+\ell)} w_k(z_\delta) H_k \\ &= \sum_{j=1}^{2r} w_j(z_s) H_j + \sum_{p=r+1}^{r+\ell} w_{2p-1}(z_\delta) H_p + w_{2p}(z_\delta) H_p \\ &= \sum_{j=1}^{2r} w_j(z_s) H_j + \frac{1}{r+\ell} \sum_{p=r+1}^{r+\ell} H_p \end{aligned}$$

thus $H(z)$ depends only on the known scheduling variables z_s, and the knowledge of the weights $w_j(z_\delta)$ for $j \in \mathcal{I}_{2(r+\ell)\setminus 2r}$ is as a matter of fact not required.

Theorem III.9

If there exist matrices $W_j \in \mathbb{R}^{n\times q}$, $Z_j \in \mathbb{R}^{n\times n}$, L_j and $R_j \in \mathbb{R}^{(n+q)\times(n+q)}$, $H_j \in \mathbb{R}^{m\times q}$, and symmetric matrices $V_j \in \mathbb{S}^{q\times q}$, T_j, $S_j \in \mathbb{S}^{2(n+q)\times 2(n+q)}$ for $j \in \mathcal{I}_{2(r+\ell)}$ such that

$$\frac{1}{r+\ell}\sum_{p=1}^{r+\ell} V_{2p} \succ 0 \tag{III.24a}$$

$$\Xi_{ii} \prec 0, \quad \forall i \in \mathcal{I}_{2(r+\ell)}, \tag{III.24b}$$

$$\frac{2}{2(r+\ell)-1}\Xi_{ii} + \Xi_{ij} + \Xi_{ji} \prec 0, \quad \forall i,j \in \mathcal{I}_{2(r+\ell)}, \quad i \neq j, \tag{III.24c}$$

where

$$\Xi_{ij} = \Psi_{ij} + T_i + S_j - \frac{1}{r+\ell}(T+S), \quad T = \sum_{p=1}^{r+\ell} T_{2p}, \quad S = \sum_{p=1}^{r+\ell} S_{2p},$$

$$\Psi_{ij} = \mathrm{He}\begin{bmatrix} \bar{\mathcal{A}}_i L_j + \bar{\mathcal{B}}_i \bar{H}_j & \bar{\mathcal{A}}_i R_j \\ P_j - L_j & -R_j \end{bmatrix}, \quad \bar{H}_j = \begin{bmatrix} H_j & 0 \end{bmatrix}, \quad P_{2p} = \begin{bmatrix} V_{2p} & 0 \\ W_{2p} & Z_{2p} \end{bmatrix},$$

$$P_{2p-1} = P_{2p}, \quad T_{2p-1} = T_{2p}, \quad S_{2p-1} = S_{2p}, \quad \forall p \in \mathcal{I}_{r+\ell}, \quad H_{2\rho-1} = H_{2\rho}, \quad \forall \rho \in \mathcal{I}_{r+\ell\setminus r}.$$

Then, the system (III.1) is admissibilizable and a stabilizing control law is given by (III.22) with the nonlinear feedback gain

$$\bar{K}(z) = \bar{H}(z)\mathcal{P}(z)^{-1}, \tag{III.25}$$

where $\bar{H}(z)$ is defined in (III.23).

Proof:

For brevity, we introduce the following notations

$$\Xi(z) = \sum_{i,j\in\mathcal{I}_{2(r+\ell)}} w_i(z)w_j(z)\Xi_{ij}, \quad \Psi(z) = \sum_{i,j\in\mathcal{I}_{2(r+\ell)}} w_i(z)w_j(z)\Psi_{ij},$$

$$L(z) = \sum_{j\in\mathcal{I}_{2(r+\ell)}} w_j(z)L_j, \qquad R(z) = \sum_{j\in\mathcal{I}_{2(r+\ell)}} w_j(z)R_j,$$

It follows directly from the definition of Ψ_{ij} that

$$\Psi(z) = \mathrm{He}\begin{bmatrix} \bar{\mathcal{A}}(z)L(z) + \bar{\mathcal{B}}(z)\bar{H}(z) & \bar{\mathcal{A}}(z)R(z) \\ \mathcal{P}(z) - L(z) & -R(z) \end{bmatrix}, \tag{III.26}$$

From Lemma I.4 and conditions (III.24b)–(III.24c), we obtain

$$\Xi(z) \prec 0. \tag{III.27}$$

According to Property (III.7), it follows that

$$\sum_{i=1}^{2(r+\ell)}\sum_{j=1}^{2(r+\ell)} w_i(z)w_j(z)(T_i + S_j) = \sum_{k=1}^{2(r+\ell)} w_k(z)(T_k + S_k)$$

$$
\begin{aligned}
&= \sum_{p=1}^{r+\ell} w_{2p-1}(z)(T_{2p-1} + S_{2p-1}) + w_{2p}(z)(T_{2p} + S_{2p}) \\
&= \sum_{p=1}^{r+\ell} (w_{2p-1}(z) + w_{2p}(z))(T_{2p} + S_{2p}) \\
&= \frac{1}{r+\ell}(T + S). \qquad \text{(III.28)}
\end{aligned}
$$

Then according to (III.26) *and* (III.28) *we have* $\Xi(z) = \Psi(z)$. *It follows from* (III.27) *that*

$$\Psi(z) \prec 0. \qquad \text{(III.29)}$$

Applying Lemma I.5 to inequality (III.29) *with*

$$\mathscr{A} = \bar{\mathcal{A}}(z), \quad \mathscr{R} = R(z), \quad \mathscr{L} = L(z), \quad \mathscr{P} = \mathcal{P}(z), \quad \mathscr{Q} = \bar{\mathcal{B}}(z)\bar{H}(z),$$

we obtain

$$\mathrm{He}\left[\bar{\mathcal{A}}(z)\mathcal{P}(z) + \bar{\mathcal{B}}(z)\bar{H}(z)\right] \prec 0. \qquad \text{(III.30)}$$

On the other hand, according to the partitions (III.16) *and* (III.19), *we have*

$$\mathrm{He}\left[\bar{\mathcal{A}}(z)\mathcal{P}(z) + \bar{\mathcal{B}}(z)\bar{H}(z)\right] = \begin{bmatrix} \bullet & \bullet \\ \bullet & \mathrm{He}[A_{22}(z)Z(z)] \end{bmatrix} \prec 0 \qquad \text{(III.31)}$$

which implies that both matrices $Z(z)$ *and* A_{22} *are invertible. This last point shows that the closed-loop form* (III.15) *is of index* 1. *Additionally, according to* (III.20) *and* (III.24a) *we have* $V(z) = \frac{1}{r+\ell}\sum_{p=1}^{r+\ell} V_{2p} \succ 0$ *which in turn implies that* $\mathcal{P}(z)$ *is invertible. Then pre- and post-multiplying* (III.30) *with* $\mathcal{P}(z)^{-\top}$ *and* $\mathcal{P}(z)^{-1}$ *respectively we obtain*

$$\mathrm{He}\left[P(z)^{-\top}(\bar{\mathcal{A}}(z) + \bar{\mathcal{B}}(z)\bar{K}(z))\right] \prec 0, \qquad \text{(III.32)}$$

with $\bar{K}(z)$ *as defined in* (III.25). *According to* (III.15) *and* (III.21) *the function* $\mathcal{V}$ *and its time derivative have for expressions*

$$\mathcal{V}(z, x_e) = x_d^\top V(z)^{-1} x_d, \qquad \dot{\mathcal{V}}(z, x_e) = \mathrm{He}\left[x_e^\top P(z)^{-\top} \mathcal{A}_c(z) x_e\right]$$

with $\mathcal{A}_c(z) = \bar{\mathcal{A}}(z) + \bar{\mathcal{B}}(z)\bar{K}(z)$. *It follows from* (III.32) *that* $\dot{\mathcal{V}}(z, x_e) < 0$, $\forall x_d \neq 0$ *and since* $V(z) \succ 0$, *then* $\mathcal{V}(z, x_e) > 0$, $\forall x_d \neq 0$. *As such, the asymptotic stability of the solution* $x_e = 0$ *of* (III.15) *is proven, and thus the system* (III.12) *is admissibilizable. This concludes the proof.* □

Example III.11 (Comparative Study)

To assess the conservatism of the proposed approach, let us reconsider the academic nonlinear descriptor system described in Example III.10. The parameter ranges of system (III.10) are $a \in [-14, -8]$ and $b \in [-25, -15]$. For comparison purposes, we examine the design conservatism between our Theorem III.9 and Theorem 3.1 in [He et al., 2021].

Figure III.1 shows the feasibility regions obtained with these two methods. Remark that the region achieved by the proposed uncertainty treatment in Theorem III.9 nearly doubles the size of the region obtained with the classical treatment of uncertainty using the TS modeling in Theorem 3.1 [He et al., 2021]. This example illustrate the proposed approach potential in reducing the design conservatism with respect to parametric uncertainties.

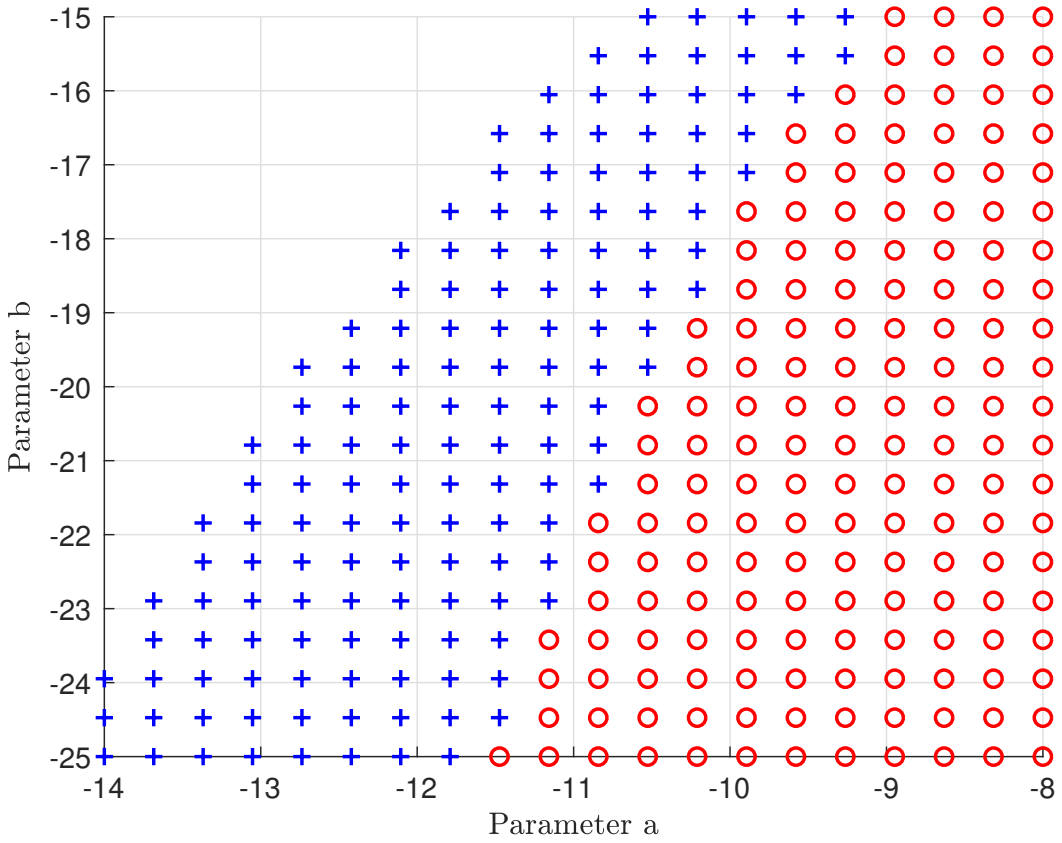

FIGURE III.1: Feasibility regions obtained with Theorem III.9 ("+","∘"), and Theorem 3.1 in [He et al., 2021] ("∘").

Example III.12 (Nonlinear Damped-Spring-Disc System)

Consider the nonlinear damped-spring-disc system taken from [Arceo et al., 2019] and [Di Franco, Scarciotti, and Astolfi, 2020], and depicted in Figure III.2. It is assumed that the disc rolls without slipping, in absence of gravity, and it is connected to a wall by a linear damper with coefficient $b = 2$ N.m^{-1}.s, a linear spring with coefficient $k_1 = 1$ N.m^{-1}, and a nonlinear spring with coefficient $k_2 = 1$ N.m^{-3}. The values of the parameters have been taken from [Arceo et al., 2019]. The system motion is described by the following set of equations

$$\begin{aligned}
\dot{x}_1 &= x_2 \\
\dot{x}_2 &= -\frac{k_1}{M}x_1 - \frac{k_2}{M}x_1^3 - \frac{b}{M}x_2 + \frac{\lambda}{M} \\
\dot{x}_3 &= -\frac{r}{J_\delta}\lambda + \frac{1}{J_\delta}u \\
0 &= x_2 - rx_3
\end{aligned} \tag{III.33}$$

with $x_1(t)$ is the distance from the rest position to the disc center, $x_2(t)$ is the corresponding velocity, and $x_3(t)$ is the disc angular velocity. The contact force between the disc and the surface is $\lambda(t)$. The disc has a radius $r = 2$ m. Its mass M is known belonging to the range $[0.1, 15]$ kg. The value of the disk inertia J_δ is uncertain and may be expressed as $J_\delta = \frac{Jr^2}{r^2+\delta J}$ and $J = 4$ kg.m^2 and $0 \leq \delta \leq c$.

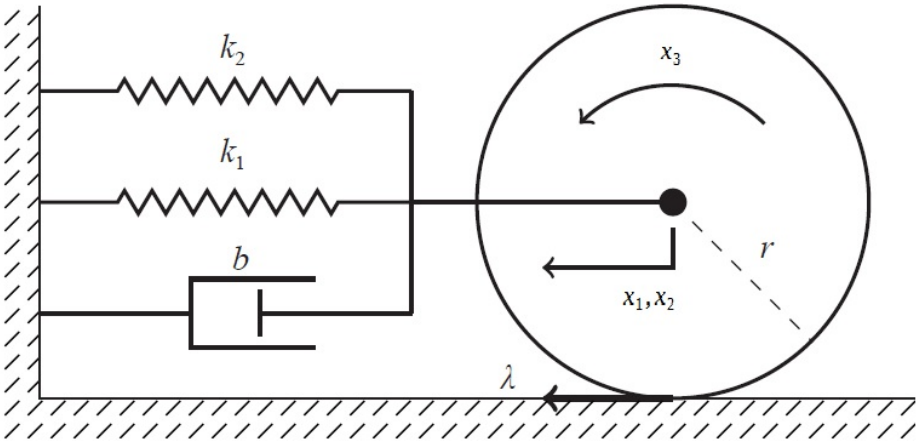

FIGURE III.2: Nonlinear damped spring disc system.

The system (III.33) is then rewritten into the uncertain descriptor form (III.13) with $x(t) = \begin{bmatrix} x_1 & x_2 & x_3 & \lambda \end{bmatrix}^\top$, $z_1 = x_1^2$, $z_2 = \delta$ and

$$E(z) = \begin{bmatrix} 1 & 0 & 0 & 0 \\ 0 & 1 & 0 & 0 \\ 0 & 0 & 0 & 0 \\ 0 & 0 & 0 & 0 \end{bmatrix}, \ \bar{\mathcal{A}}(z) = A(z) + \Delta A(z), \ \bar{\mathcal{B}}(z) = B + \Delta B(z), \ B = \begin{bmatrix} 0 \\ 0 \\ 0 \\ \frac{-r}{J} \end{bmatrix}, \ \Delta B(z) = \begin{bmatrix} 0 \\ 0 \\ 0 \\ \frac{z_2}{r} \end{bmatrix},$$

$$A(z) = \begin{bmatrix} 0 & 1 & 0 & 0 \\ -\frac{k_1}{M} - \frac{k_2}{M} z_1 & -\frac{b}{M} & 0 & \frac{1}{M} \\ 0 & 1 & -r & 0 \\ -\frac{k_1}{M} - \frac{k_2}{M} z_1 & -\frac{b}{M} & 0 & \frac{r^2}{J} + \frac{1}{M} \end{bmatrix}, \ \Delta A(z) = \begin{bmatrix} 0 & 0 & 0 & 0 \\ 0 & 0 & 0 & 0 \\ 0 & 0 & 0 & 0 \\ 0 & 0 & 0 & -z_2 \end{bmatrix}.$$

The differential state vector is defined as $x_d = \begin{bmatrix} x_1 & x_2 \end{bmatrix}^\top$ while the vector of algebraic variables is defined as $x_a = \begin{bmatrix} x_3 & \lambda \end{bmatrix}^\top$. Applying again Theorem III.9 and Theorem 3.1 in [He et al., 2021], the feasibility regions for the parameters M and c are plotted in Figure III.3. As it can be observed, the proposed approach (Theorem III.9) yields better results.

A Matlab simulation achieved with the *Simulink Simscape Mechanics Library* has been done for a mass $M = 0.1\ kg$ and an inertia $J_\delta = 1\text{kg.m}^2$ (corresponding to $\delta = 3$). The trajectories of the damped spring disc system are presented in Figure III.4. The initial values chosen for the differential states are $x_{d_0} = \begin{bmatrix} -5 & 10 \end{bmatrix}^\top$, while the initial values for the algebraic variables are deduced from the *Simulink Simscape* model which embodies the algebraic constraints necessary to determine the angular velocity $x_3(t)$ and the contact force $\lambda(t)$.

As can be seen, the state converges asymptotically towards the equilibrium $x = 0$ while the value of the algebraic equation in (III.33) is virtually null alongside the trajectories illustrating that the algebraic constraints of the system are fully respected.

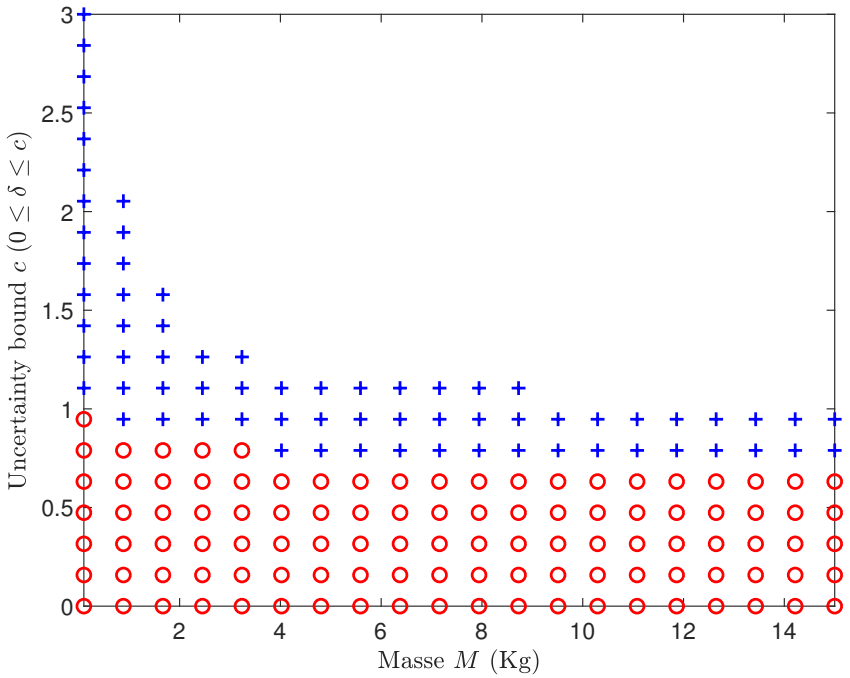

FIGURE III.3: Feasibility regions obtained with Theorem III.9 ("+", "∘"), and Theorem 3.1 in [He et al., 2021] ("∘").

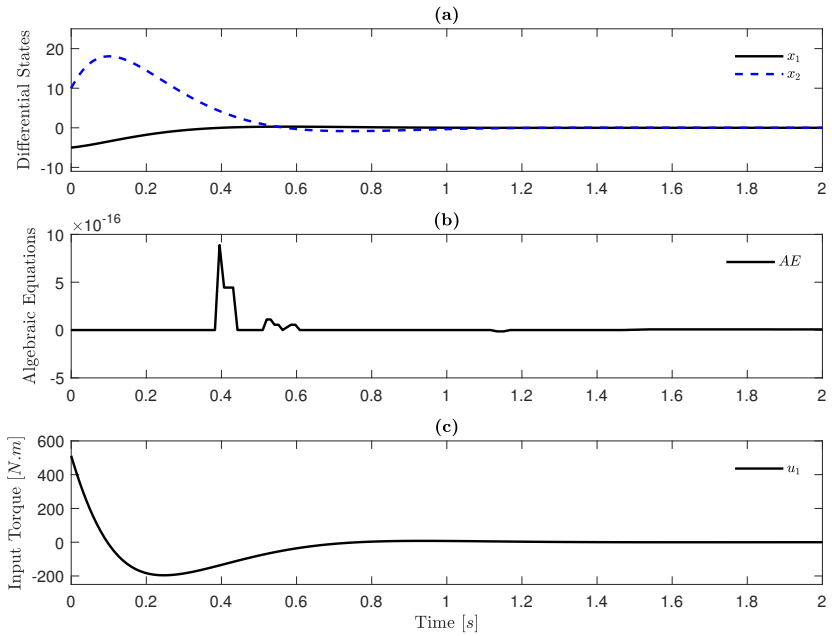

FIGURE III.4: (a) Trajectories of the nonlinear damped spring disc system, (b) numerical behavior of the algebraic constraint, (c) obtained control torque

III.3 Trajectory Tracking for Serial Manipulators

We tackle in this section the problem of high precision trajectory tracking for a class of physical descriptor systems. The objective is to validate the proposed uncertain polytopic modeling

approach (III.6) for tracking control tasks with the presence of uncertainties and external disturbances. To that end, we consider a robotic serial manipulator as our point of interest given the importance of trajectory tracking control as a key issue in the field of robot manipulator motion planning [Nubert et al., 2020; Jie et al., 2020; Thakar et al., 2022]. Additionally, even robot manipulators with a relatively low degrees of freedom yield significantly complex dynamic models as previously shown by the 3DoF example (I.4) in Chapter I, which renders the tracking task even more challenging.

III.3.1 Uncertain Robot Manipulator Dynamics

We consider this time the dynamics of general robot manipulators while taking into consideration the presence of uncertainties and external disturbances. In such case, the fundamental mechanical equation (I.35) can be rewritten as

$$M(\theta)\ddot{\theta}(t) + \hat{N}(\theta,\dot{\theta})\dot{\theta}(t) + \hat{G}(\theta) = \Gamma(t) + \Gamma_{\text{ext}}(t), \tag{III.34}$$

with

$$\hat{N}(\theta,\dot{\theta}) = N(\theta,\dot{\theta}) + \Delta N(\theta,\dot{\theta}), \quad \hat{G}(\theta) = G(\theta) + \Delta G(\theta).$$

where $\theta \in \mathbb{R}^n$ is the vector of generalized joint-space coordinates, $M(\theta) \in \mathbb{R}^{n\times n}$ is the inertia matrix, $N(\theta,\dot{\theta}) \in \mathbb{R}^{n\times n}$ is the Coriolis-centripetal matrix plus the viscous friction coefficients of the joints, $G(\theta) \in \mathbb{R}^n$ represents the generalized gravity torque, $\Gamma(t) \in \mathbb{R}^n$ is the vector of the generalized control torques applied to the joints, and $\Gamma_{\text{ext}}(t) \in \mathbb{R}^n$ is the vector of external disturbances. It is assumed that the vectors of manipulator position $\theta(t)$ and manipulator velocity $\dot{\theta}(t)$ respectively belong to the following bounded sets

$$\begin{aligned} \theta(t) &\in \mathscr{D}_\theta = \{\theta \in \mathbb{R}^n : \ \theta_{i\,\min} \le \theta_i \le \theta_{i\,\max}, \ \forall i \in \mathcal{I}_n\} \\ \dot{\theta}(t) &\in \mathscr{D}_{\dot{\theta}} = \{\dot{\theta} \in \mathbb{R}^n : \ \dot{\theta}_{i\,\min} \le \dot{\theta}_i \le \dot{\theta}_{i\,\max}, \ \forall i \in \mathcal{I}_n\} \end{aligned} \tag{III.35}$$

where the bounds of the robot manipulator $\theta_{i\,\min}$, $\theta_{i\,\max}$, $\dot{\theta}_{i\,\min}$ and $\dot{\theta}_{i\,\max}$ are physically defined according to the robot workspace and operating characteristics.

Remark III.13. Note that the considered class of uncertain robot manipulators in this chapter (III.34), do not take into consideration the presence of uncertainties in the inertia matrix $M(\theta)$. This is due to the structure of the considered control input (II.36) where the inertia matrix is exploited for the non-redundant control design. This limitation is surmounted in the next chapter.

Given that $\hat{G}(\theta)$ depends smoothly on the articular positions $\theta(t)$ and assuming that $\hat{G}(0) = 0$, then the gravity matrix admits the decomposition $\hat{G}(\theta) = (H(\theta) + \Delta H(\theta))\theta(t)$. This allows for the uncertain manipulator systems (III.34) to be rewritten under the uncertain descriptor form

$$E(z_s)\dot{x}(t) = (A(z_s) + \Delta A(z_\delta))x(t) + B(u(t) + d_e(t)) \tag{III.36}$$

where $\text{rank}(E(z_s)) = 2n$, $x(t) = \begin{bmatrix}\theta^\top(t) & \dot{\theta}^\top(t)\end{bmatrix}^\top$, $z = \begin{bmatrix}z_s^\top & z_\delta^\top\end{bmatrix}^\top \in \mathbb{R}^{r+\ell}$ is the scheduling vector composed of known premise variables $z_s \in \mathbb{R}^r$ and uncertain terms $z_\delta \in \mathbb{R}^\ell$, $u(t)$ is the control input, and $d_e(t)$ is the external disturbance signal. The expressions of the system matrices are

$$E(z_s) = \begin{bmatrix} I & 0 \\ 0 & M(\theta) \end{bmatrix}, \ A(z_s) = \begin{bmatrix} 0 & I \\ -H(\theta) & -N(\theta,\dot{\theta}) \end{bmatrix}, \ B = \begin{bmatrix} 0 \\ I \end{bmatrix}, \ \Delta A(z_\delta) = \begin{bmatrix} 0 & 0 \\ \Delta H(\theta) & \Delta N(\theta,\dot{\theta}) \end{bmatrix},$$

Note that it is a regular descriptor system (III.36) so that assumption 1 holds. In the next part, we formulate the tracking control problem under $\mathcal{L}_2$-norm performance criterion for serial manipulators represented by the uncertain descriptor form (III.36) and using the aforementioned uncertain polytopic representation (III.6) for the control design.

III.3.2 $\mathcal{H}_\infty$-Performance Trajectory Tracking Control

Consider the descriptor system (III.36). We suppose that both the joints positions $\theta(t)$ and velocities $\dot{\theta}(t)$ are measured (*i.e.*, $y(t) = x(t)$). We define the tracking error in the generalized coordinates as $e(t) = x(t) - x_r(t)$, where $x_r(t) = \begin{bmatrix}\theta_r^\top(t) & \dot{\theta}_r^\top(t)\end{bmatrix}^\top$ is the vector of the joint coordinates corresponding to the desired trajectory r. Then, the tracking error dynamics can be defined from (III.36) as

$$\begin{aligned} E(z_s)\dot{e}(t) &= \big(A(z_s) + \Delta A(z_\delta)\big)e(t) + B\big(u(t) + d_e(t)\big) + d_r(t), \\ d_r(t) &= \big(A(z_s) + \Delta A(z_\delta)\big)x_r(t) - E(z_s)\dot{x}_r(t) \\ \psi(t) &= Ce(t), \end{aligned} \tag{III.37}$$

where $\psi(t) \in \mathbb{R}^n$ is the targeted performance vector, and $d_r(t)$ is the remaining trajectory related terms. Note that according to the structure of the system matrices and uncertainties, $d_r(t)$ can be represented as

$$d_r(t) = BB^\dagger d_r(t)$$

where $B^\dagger = (B^\top B)^{-1}B^\top$ is the pseudo-inverse of B. Then, the dynamic error (III.37) can be rewritten as

$$\begin{aligned} E(z_s)\dot{e}(t) &= \big(A(z_s) + \Delta A(z_\delta)\big)e(t) + B\big(u(t) + d(t)\big) \\ \psi(t) &= Ce(t), \end{aligned} \tag{III.38}$$

where $d(t) = d_e(t) + B^\dagger d_r(t)$ is the lumped disturbance composed of the external disturbances and reference related terms. To ensure the precision of the trajectory tracking performance with respect to the disturbance we impose an $\mathcal{H}_\infty$-criterion for the tracking error dynamics (III.38). To that end we consider the control law

$$u(t) = K_p(z)e(t) + K_I(z)e_I(t) \tag{III.39}$$

where $e_I(t)$ is the integral of the tracking error dynamics (*i.e.*, $\dot{e}_I(t) = Ce(t)$). The extended closed-loop tracking error dynamics can then be expressed as

$$\begin{aligned} \bar{E}(z)\dot{\xi}(t) &= \big(\bar{A}(z) + \bar{B}\bar{K}(z)\big)\xi(t) + \bar{B}d(t) \\ \psi(t) &= \bar{C}\xi(t), \end{aligned} \tag{III.40}$$

where

$$\xi(t) = \begin{bmatrix} e(t) \\ e_I(t) \end{bmatrix}, \quad \bar{E}(z) = \begin{bmatrix} E(z_s) & 0 \\ 0 & I \end{bmatrix}, \quad \bar{A}(z) = \begin{bmatrix} A(z_s) + \Delta A(z_\delta) & 0 \\ C & 0 \end{bmatrix}, \quad \bar{B} = \begin{bmatrix} B \\ 0 \end{bmatrix},$$

$$\bar{K}(z) = \begin{bmatrix} K_p(z) & K_I(z) \end{bmatrix}, \qquad \bar{C} = \begin{bmatrix} C & 0 \end{bmatrix}.$$

Problem 1. Consider the robot model (III.34). Determine the gains $K_p(z)$ and $K_I(z)$ of the controller (III.39) such that the extended descriptor system (III.40) verifies the following closed-loop properties.

(P1) For $d(t) = 0$, $\forall t \geq 0$, the zero solution of system (III.40) is exponentially stable with some decay rate $\alpha > 0$.

(P2) For $d(\cdot) \in \mathcal{L}_2$, system (III.40) under zero initial condition $\xi(0) = 0$, the induced $\mathcal{L}_2-$norm of the performance vector ψ is bounded as

$$\int_0^{+\infty} \psi^\top(t)\psi(t)\,dt \leq \gamma \int_0^{+\infty} d^\top(t)d(t)\,dt, \tag{III.41}$$

where γ is a positive scalar.

Theorem III.10

If there exist symmetric matrices $P \in \mathbb{S}^{3n}$, $T_i \in \mathbb{S}^{8n+2m}$, matrices L and $R \in \mathbb{R}^{(4n+m)\times(4n+m)}$, $\bar{Y}_i \in \mathbb{R}^{m\times 3n}$, for $i \in \mathcal{I}_{2(r+\ell)}$, and a positive scalar α such that

$$P \succ 0 \tag{III.42a}$$

$$\Xi_i \prec 0, \quad \forall i \in \mathcal{I}_{2(r+\ell)}, \tag{III.42b}$$

where

$$\Xi_i = \Psi_i + T_i - \frac{1}{r+\ell}\,T, \quad \Psi_i = \mathrm{He}\begin{bmatrix} \mathcal{A}_i L + \Sigma_i & \mathcal{A}_i R \\ \mathcal{P}_i - L & -R \end{bmatrix}, \quad T = \sum_{p=1}^{r+\ell} T_{2p},$$

$$\mathcal{A}_i = \begin{bmatrix} \bar{A}_i + \alpha\bar{E}_i & 0 & 0 \\ 0 & 0 & 0 \\ \bar{C} & 0 & 0 \end{bmatrix}, \quad \Sigma_i = \begin{bmatrix} \bar{B}\bar{Y}_i & \bar{B} & 0 \\ 0 & -\frac{\gamma}{2}I & 0 \\ 0 & 0 & -\frac{1}{2}I \end{bmatrix}, \quad \mathcal{P}_i = \begin{bmatrix} P\bar{E}_i^\top & 0 & 0 \\ 0 & I & 0 \\ 0 & 0 & I \end{bmatrix},$$

$$T_{2p-1} = T_{2p}, \quad \forall p \in \mathcal{I}_{r+\ell}, \quad \bar{Y}_{2\rho-1} = \bar{Y}_{2\rho}, \quad \forall \rho \in \mathcal{I}_{r+\ell\setminus r}.$$

Then, for the control law (III.39) with the gains $\bar{K}(z) = \begin{bmatrix} K_p(z) & K_I(z) \end{bmatrix}$ given by

$$\bar{K}(z) = \bar{Y}(z)\bar{E}(z)^{-\top}P^{-1}, \quad \bar{Y}(z) = \sum_{i=1}^{2(r+\ell)} w_i(z)\bar{Y}_i, \tag{III.43}$$

the closed-loop system (III.40) verifies properties (P1) and (P2) specified in Problem 1, with a guaranteed $\mathcal{L}_2-$gain $\gamma_s = \sqrt{\gamma}$.

Proof:

Let us denote

$$\Xi(z) = \sum_{i=1}^{2(r+\ell)} w_i(z)\Xi_i, \quad \Psi(z) = \sum_{i=1}^{2(r+\ell)} w_i(z)\Psi_i, \quad \Sigma(z) = \sum_{i=1}^{2(r+\ell)} w_i(z)\Sigma i, \quad \mathcal{P}(z) = \sum_{i=1}^{2(r+\ell)} w_i(z)\mathcal{P}_i.$$

It follows directly from the definition of Ψ_i and $\mathcal{P}_i$ that

$$\Psi(z) = \mathrm{He}\begin{bmatrix} \mathcal{A}(z)L + \Sigma(z) & \mathcal{A}(z)R \\ \mathcal{P}(z) - L & -R \end{bmatrix}, \quad \mathcal{P}(z) = \begin{bmatrix} P\bar{E}(z)^\top & 0 & 0 \\ 0 & I & 0 \\ 0 & 0 & I \end{bmatrix} \tag{III.44}$$

According to Property (III.7), it follows that

$$\sum_{i=1}^{2(r+\ell)} w_i(z)T_i = \sum_{p=1}^{r+\ell} w_{2p-1}(z)T_{2p-1} + w_{2p}(z)T_{2p}$$

$$= \sum_{p=1}^{r+\ell} (w_{2p-1}(z) + w_{2p}(z)) T_{2p}$$
$$= \frac{1}{r+\ell} T, \tag{III.45}$$

and, so $\Xi(z) = \Psi(z)$. *By convexity, inequalities* (III.42b) *imply* $\Xi(z) \prec 0$, *hence*

$$\Psi(z) \prec 0, \tag{III.46}$$

and applying Lemma I.5 to this inequality with

$$\mathscr{A} = \mathcal{A}(z), \qquad \mathscr{R} = R, \qquad \mathscr{L} = L, \qquad \mathscr{P} = \mathcal{P}(z), \qquad \mathscr{Q} = \Sigma(z) + \Sigma(z)^\top,$$

we obtain

$$\mathrm{He}\left[\mathcal{A}(z)\mathcal{P}(z) + \Sigma(z)\right] \prec 0. \tag{III.47}$$

Pre- and post-multiplying this last inequality with $\mathcal{P}(z)^{-\top}$ *and its transpose respectively, we obtain that* $\mathrm{He}\left[\mathcal{P}(z)^{-\top}(\mathcal{A}(z) + \Sigma(z)\mathcal{P}(z)^{-1})\right] \prec 0$, *that is*

$$\mathrm{He}\begin{bmatrix} P^{-1}\bar{E}(z)^{-1}(\bar{A}(z) + \bar{B}\bar{K}(z) + \alpha\bar{E}(z)) & P^{-1}\bar{E}(z)^{-1}\bar{B} & 0 \\ 0 & -\frac{\gamma}{2}I & 0 \\ \bar{C} & 0 & -\frac{1}{2}I \end{bmatrix} \prec 0. \tag{III.48}$$

then applying the Schur Complement lemma I.2 we obtain

$$\Pi(z) := \mathrm{He}\begin{bmatrix} P^{-1}\bar{E}(z)^{-1}\Big(\bar{A}(z) + \bar{B}\bar{K}(z) + \alpha\bar{E}(z)\Big) + \frac{1}{2}\bar{C}^\top\bar{C} & P^{-1}\bar{E}(z)^{-1}\bar{B} \\ 0 & -\frac{\gamma}{2} \end{bmatrix} \prec 0. \tag{III.49}$$

Let $\mathcal{V}(\xi) = \xi^\top P^{-1}\xi$. *Then, according to* (III.42a), $\mathcal{V}$ *is a positive definite function. The derivative of* $\mathcal{V}$ *along the trajectories of* (III.40) *has for expression*

$$\dot{\mathcal{V}}(\xi) = \mathrm{He}\left[\xi^\top P^{-1}\bar{E}(z)^{-1}\Big(\bar{A}(z) + \bar{B}\bar{K}(z)\Big)\xi + P^{-1}\bar{B}d\right].$$

Now, from (III.49), *it comes that*

$$\zeta^\top \Pi(z)\zeta = \dot{\mathcal{V}}(\xi) + 2\alpha\mathcal{V}(\xi) + \psi^\top\psi - \gamma d^\top d < 0 \tag{III.50}$$

for $\zeta^\top = \begin{bmatrix} \xi^\top & d^\top \end{bmatrix} \neq 0$.

- *If* $d(.) = 0$, *we have* $\dot{\mathcal{V}}(\xi) \leq -2\alpha\mathcal{V}(\xi)$, *and then, from the comparison lemma, the solution* $\xi = 0$ *of the undisturbed system* (III.40) *is exponentially stable with a decay rate* α, *that is property (P1) of Problem 1 holds.*
- *If* $d(.) \in \mathcal{L}_2$, *from* (III.50), *we deduce that*

$$\dot{\mathcal{V}}(\xi) < \gamma d^\top d - \psi^\top\psi. \tag{III.51}$$

For any $T_s > 0$, *integrating both sides of this inequality from* 0 *to* T_s *gives*

$$\mathcal{V}(\xi(T_s)) - \mathcal{V}(0) < \int_0^{T_s} (\gamma d^\top(t)d(t) - \psi^\top(t)\psi(t))\, dt. \tag{III.52}$$

Assuming zero initial conditions, since $\mathcal{V}(\xi(T_s)) > 0$*, it follows that*

$$\int_0^{T_s} \psi^\top(t)\psi(t)\,dt < \gamma \int_0^{T_s} d^\top(t)d(t)\,dt \leq \gamma \|d(\cdot)\|_2^2,$$

which guarantees Property (P2) for the closed-loop system (III.40)*. This concludes the proof.*

III.3.3 Application of $\mathcal{H}_\infty$ Control to a 3DoF Serial Manipulator

This section illustrates the tracking control problem for the 3Dof robot manipulator given in Example I.4. The dynamics of the system are given by equation (III.34). The nominal values of the robot parameters are given in Table I.4, while the expressions of the nonlinearities z_i, for $i \in \mathcal{I}_{12}$, are given in Table I.3. The lumped disturbance d considers an external force Γ_{ext} exerted on the end of effector and given by

$$\Gamma_{ext} = \begin{bmatrix} \Gamma_{ext1} \\ \Gamma_{ext2} \\ \Gamma_{ext3} \end{bmatrix} = \begin{bmatrix} 450\sin(15t) \\ 375\sin(15t) \\ 300\sin(15t) \end{bmatrix} \tag{III.53}$$

We consider in addition to the effect of the external disturbance Γ_{ext}, the following parametric uncertainties

$$\Delta N(\theta,\dot{\theta}) = \begin{bmatrix} \delta_2 & 0 & 0 \\ 0 & \delta_3 & 0 \\ 0 & 0 & \delta_4 \end{bmatrix}, \qquad \Delta G(\theta) = \begin{bmatrix} -c_1\delta_1 & 0 & 0 \\ 0 & 0 & 0 \\ 0 & 0 & 0 \end{bmatrix}$$

where $|\delta_1| \leq 1.2$ represents an increase of $+120\%$ in the mass m_1 of the first joint link and $|\delta_i| \leq 10$ represents uncertain friction coefficients. Considering the vector of premise variables $z_s \in \mathbb{R}^{12}$ as given in Table I.3 and the vector of uncertain terms $z_\delta = \begin{bmatrix} \delta_1 & \delta_2 & \delta_3 & \delta_4 \end{bmatrix} \in \mathbb{R}^2$, then the total premise vector for the uncertain polytopic representation (III.6) is $z = \begin{bmatrix} z_s & z_\delta \end{bmatrix} \in \mathbb{R}^{16}$.

In practice, the measurement of joints velocities is obtained via numerical derivation of the joints positions. This however induces a numerical error on the measured signals. To account for this effect in our simulation, we consider that the joint velocities measurements are disturbed by a white noise. The measured signal is then filtered by a first-order low pass filter. We compare the proposed approach in this section to a PID controller combined with a feedforward action [Paccot, Andreff, and Martinet, 2009] and a computed-torque control (CTC) approach combined with disturbance estimation [Mohammadi et al., 2013]. The PID control law combined with a feedforward action is given by

$$\begin{aligned} u_{PID}(t) &= k_p e_\theta(t) + k_d e_{\dot{\theta}}(t) + k_i \int_0^t e_\theta(\tau)\partial\tau + u_{ff}, \\ u_{ff} &= M(\theta)\ddot{\theta}_r + N(\theta,\dot{\theta})\dot{\theta}_r + G(\theta). \end{aligned} \tag{III.54}$$

Its control gains are given by

$$\begin{aligned} k_p = 10^4 \begin{bmatrix} 24.280 & 6.413 & 0.866 \end{bmatrix}, \qquad k_d = 10^4 \begin{bmatrix} 0.51524 & 0.13608 & 0.01838 \end{bmatrix}, \\ k_i = 10^4 \begin{bmatrix} 381.39 & 100.73 & 13.60 \end{bmatrix}. \end{aligned} \tag{III.55}$$

While the CTC control law is given by

$$\begin{aligned} u_{CTC}(t) &= M(\theta)v(t) + N(\theta,\dot{\theta})\dot{\theta}(t) + G(\theta) + \hat{d}_{CTC}, \\ v(t) &= \ddot{\theta}_r + g_p e_\theta(t) + g_d e_{\dot{\theta}}(t) + g_i \int_0^t e_\theta(\tau)\partial\tau. \end{aligned} \tag{III.56}$$

Its gains are given by

$$\begin{aligned} g_p = 10^3 \begin{bmatrix} 6.6620 & 6.6620 & 6.6620 \end{bmatrix}, \qquad g_d = \begin{bmatrix} 141.3717 & 141.3717 & 141.3717 \end{bmatrix}, \\ g_i = 10^5 \begin{bmatrix} 1.0465 & 1.0465 & 0.0465 \end{bmatrix}. \end{aligned} \tag{III.57}$$

For the tracking control design proposed in this section, the chosen value for the decay rate of the feedback control design is $\alpha = 8.5$. The achieved $\mathcal{L}_2$-gain is equal to $\gamma = 8 \times 10^{-4}$. The simulation period is set for $T_s = 3$ s. For illustration, here are some control gains obtained with Theorem I.2

$$K_{p_{11}} = 10^7 \begin{bmatrix} 2.6854 & -0.7192 & -0.1320 & 2.6854 & -0.7192 & -0.1320 \\ 4.0000 & -0.7086 & -0.1164 & -0.3650 & -0.0564 & -0.0856 \\ 5.3155 & -0.1508 & -0.1358 & -0.1832 & -0.0784 & 0.0307 \end{bmatrix},$$

$$K_{I_{11}} = 10^7 \begin{bmatrix} -0.0003 & 0.3429 & -1.4606 \\ -0.0006 & 1.2819 & -0.6341 \\ -0.0006 & 1.7636 & 0.0233 \end{bmatrix},$$

$$K_{p_{28}} = 10^7 \begin{bmatrix} -3.2812 & -0.1687 & -0.0240 & -0.8502 & -0.1794 & -0.0514 \\ -0.6910 & -0.1626 & -0.0224 & -0.1794 & -0.2675 & -0.0564 \\ -0.0539 & -0.0258 & -0.0228 & -0.0514 & -0.0564 & -0.0436 \end{bmatrix},$$

$$K_{I_{28}} = 10^7 \begin{bmatrix} 0.0004 & -1.1719 & -0.6249 \\ 0.0000 & -0.2369 & -0.1910 \\ 0.0000 & -0.0302 & 0.1065 \end{bmatrix}.$$

For a quantitative performance analysis, we define the following performance indicators.

- Root mean square (RMS $[m]$) of the end-effector position error along both axes X and Y

$$\text{RMS}_X = \sqrt{\frac{1}{T_s}\int_0^{T_s} (X(t) - X_r(t))^2 dt}, \qquad \text{RMS}_Y = \sqrt{\frac{1}{T_s}\int_0^{T_s} (Y(t) - Y_r(t))^2 dt},$$

  where T_s is the simulation time.

- Maximal absolute value (MAV $[m]$) of the end-effector position error along both axes X and Y

$$\text{MAV}_X = \max_{t\in[0,T_s]} |X(t) - X_r(t)|, \qquad \text{MAV}_Y = \max_{t\in[0,T_s]} |Y(t) - Y_r(t)|.$$

- Mean square root (RMS_u [Nm]) of the control input

$$\text{RMS}_u = \sqrt{\frac{1}{T_s}\sum_{i=1}^{3}\int_0^{T_s} u_i(t)^2 dt}.$$

We consider the tracking of two different types of trajectories. The first trajectory is linear and constitutes a square contained in the XY plane with the gravity $\overrightarrow{g} = -g\,\overrightarrow{y}$. The second trajectory is curved and constitutes 3 quarters of a circle also contained in the same XY plane. The following subsections presents the simulation results and a comparison of the tracking performance.

a) Square Trajectory Tracking

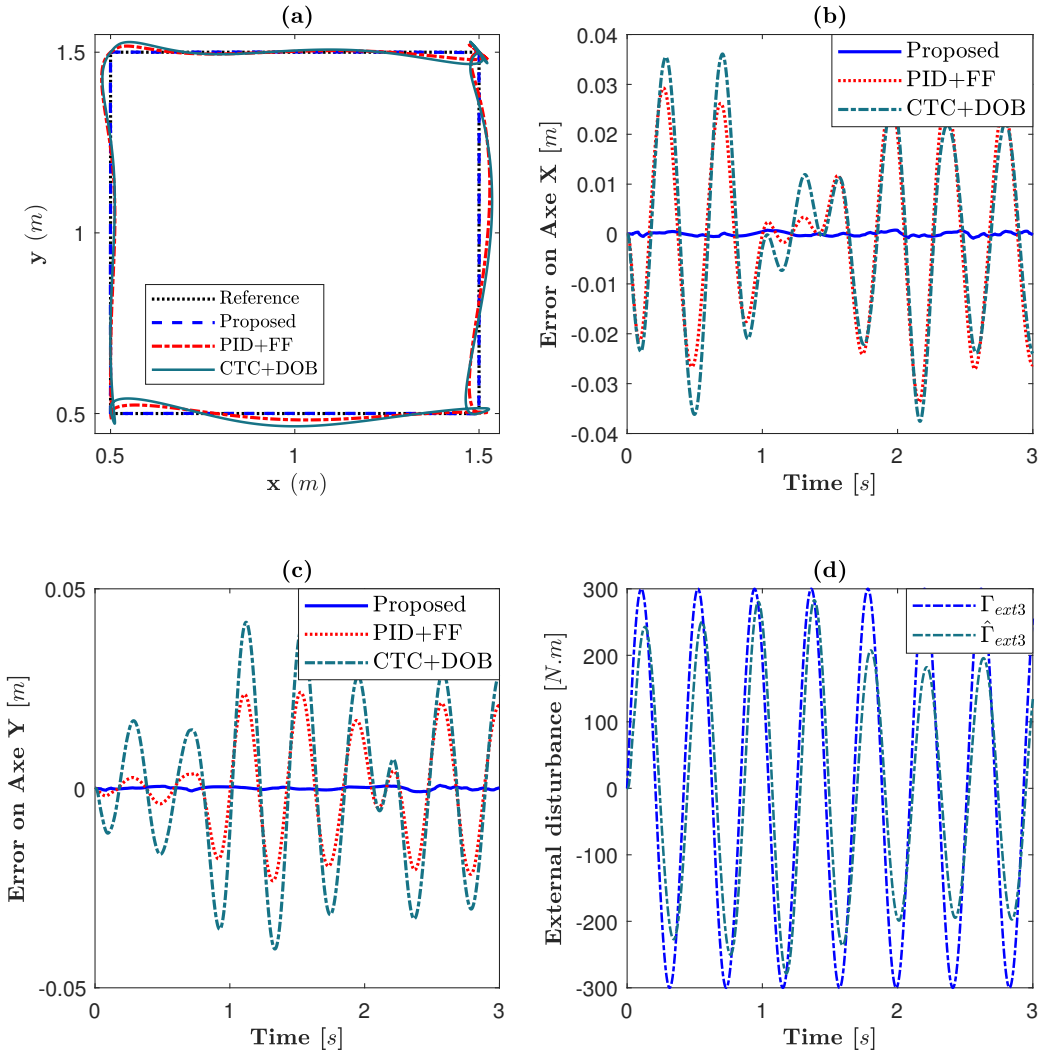

FIGURE III.5: Comparison of tracking performance: (a) Linear trajectory tracking result in XY plane. (b) Tracking error alongside axe X. (c) Tracking error alongside axe Y. (d) Considered external disturbance Γ_{ext3} and its estimation according to [Mohammadi et al., 2013].

Figure III.5 shows that the proposed control scheme allows for a better trajectory tracking achieving minimal errors alongside the axes X and Y. Both the root mean square (RMS) and the maximal absolute value (MAV) errors indicate the superiority of the proposed control scheme with respect to the PID [Paccot, Andreff, and Martinet, 2009] combined with the feedforward action and the CTC approach combined with DOB [Mohammadi et al., 2013].

According to Figure III.6, the obtained control inputs with the proposed design are impacted by the noise in the velocity measurement due to the high values of the controller gains. This impact is reflected in the shape of the control law as well as the value of the mean square root of the integral of input signal (RMS_u) given in Table III.1. However, the proposed control approach performs better across the remaining performance indicators in Table III.1.

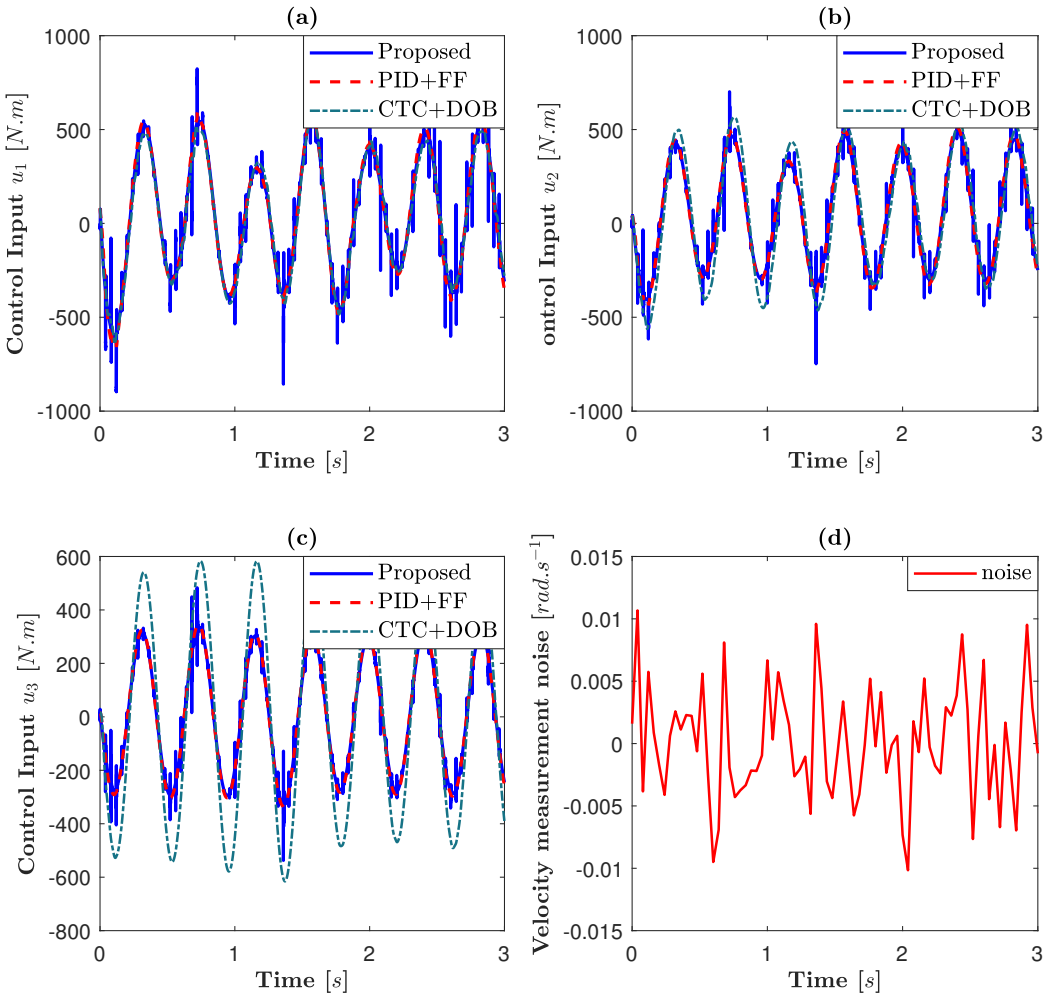

FIGURE III.6: Comparison of control inputs and velocity estimation error for linear trajectory.

TABLE III.1: Linear trajectory tracking performance

Criterion	FF-based PID	DOB-based CTC	Proposed Approach
RMS_X	1.66×10^{-2}	1.79×10^{-2}	3.21×10^{-4}
RMS_Y	1.16×10^{-2}	2.04×10^{-2}	2.52×10^{-4}
MAV_X	3.37×10^{-2}	3.76×10^{-2}	8.86×10^{-4}
MAV_Y	2.41×10^{-2}	4.16×10^{-2}	7.73×10^{-4}
RMS_u	1.36×10^{4}	1.62×10^{4}	$3.02š \times 10^{4}$

b) Circular Trajectory Tracking

Figure III.7 shows that the PID [Paccot, Andreff, and Martinet, 2009] and CTC [Mohammadi et al., 2013] controllers perform slightly better with respect to their performance on the linear trajectory alongside the axe X. This observation is confirmed by the values of the root mean square error (RMS_X) and the maximal absolute value (MAV_X). On the other hand, the tracking performance alongside the axe Y is slightly degraded on both the root mean square error (RMS_Y) and the maximal absolute value (MAV_Y). The proposed approach behaves similarly although

still manages to outperform the other approaches with respect to tracking errors as shown in Table III.2.

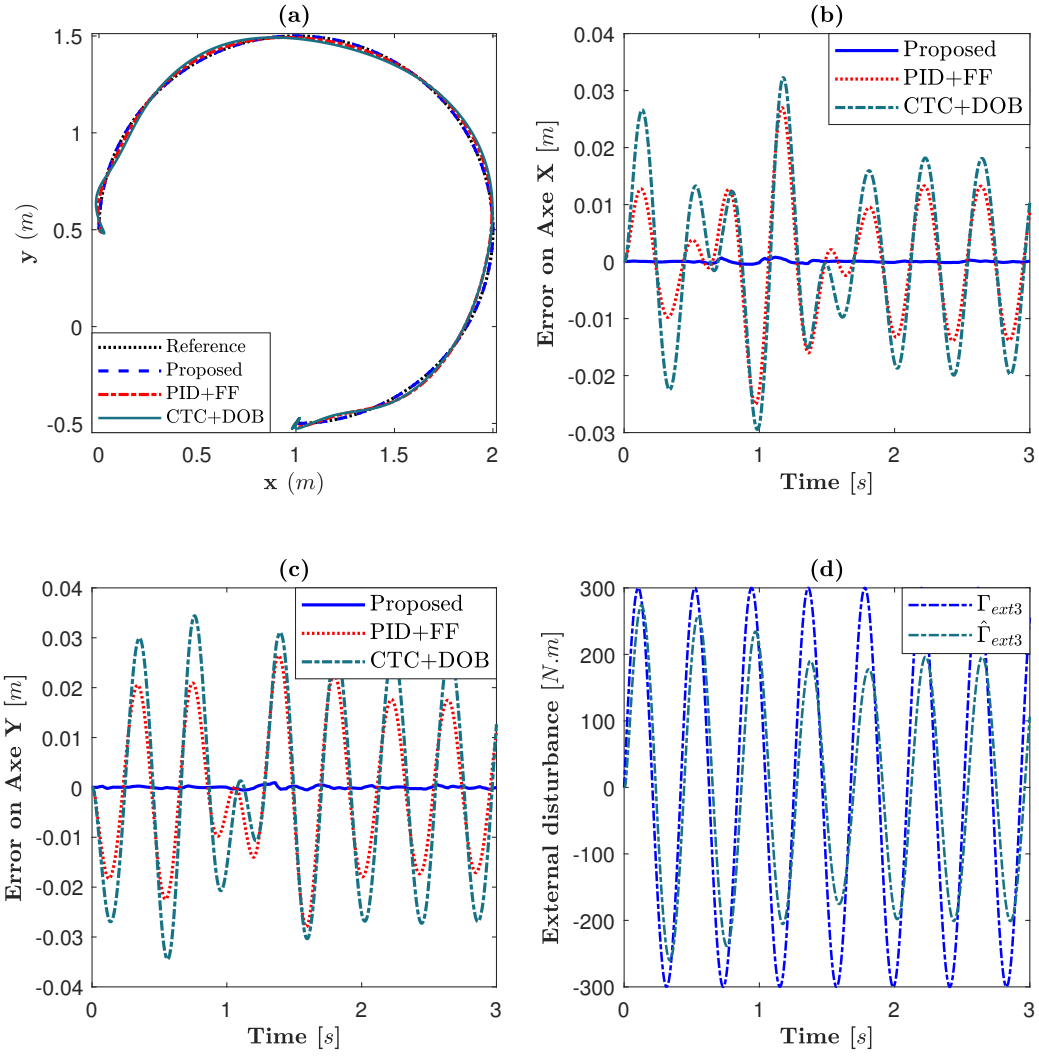

FIGURE III.7: Comparison of tracking performance: (a) Curved trajectory tracking result in XY plane. (b) Tracking error alongside axe X. (c) Tracking error alongside axe Y. (d) Considered external disturbance Γ_{ext3} and its estimation according to [Mohammadi et al., 2013].

TABLE III.2: Circular trajectory tracking performance

Criterion	FF-based PID	DOB-based CTC	Proposed Approach
RMS_X	10^{-2}	1.35×10^{-2}	1.84×10^{-4}
RMS_Y	1.38×10^{-2}	1.92×10^{-2}	2.33×10^{-4}
MAV_X	2.7×10^{-2}	3.23×10^{-2}	7.64×10^{-4}
MAV_X	2.8×10^{-2}	3.45×10^{-2}	9.37×10^{-4}
RMS_u	1.32×10^{4}	1.63×10^{4}	2.74×10^{4}

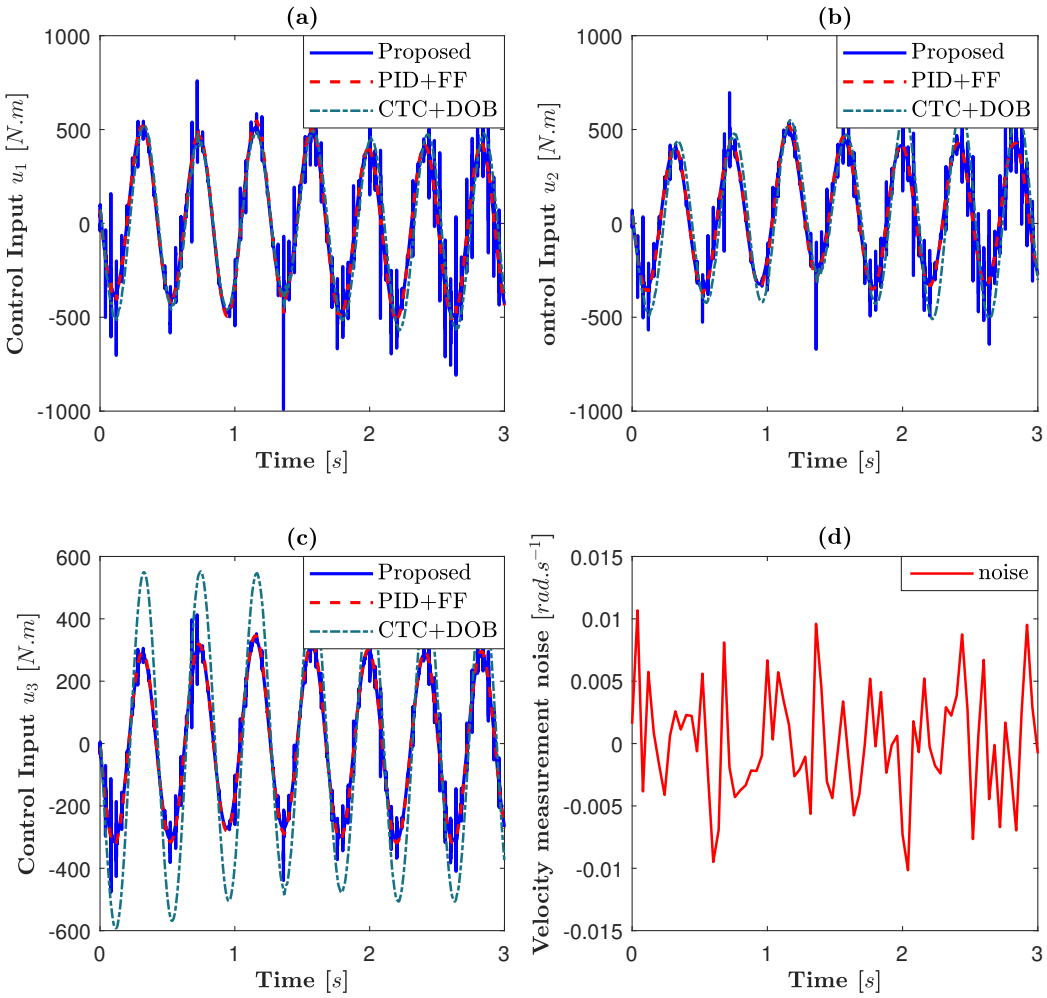

FIGURE III.8: Comparison of control inputs and velocity estimation error for circular trajectory.

Figure III.8 shows the resulting control inputs for each approach. Here once more due to the high values of the controller gains, the input signals for the proposed approach are slightly impacted by the noise measurement as shown by the value of the mean square root of the integral of input signal (RMS_u) given in Table III.2. On the other hand, the values of RMS_u across all approaches for the curved trajectory tracking are lower than the case of linear trajectory.

Remark III.14. Note that the impact of the noise measurement on the control inputs of the proposed control design can be avoided using an estimation of the velocity via an observer design instead of relying on the noisy measurement. However, given that some scheduling variables depend on the velocity components, operating without their measurements can complicate the control design. Moreover, the mixed controller-observer design is also impacted by the presence of unmeasured scheduling variables. The next section of this chapter aims at evaluating the complexity of the design in presence of said unmeasured scheduling variables as well as the viability of a separation principle in such a case.

III.4 The Case of Unmeasured Scheduling Variables

Considering the nonlinear descriptor system (II.1), we propose the following nonlinear observer

$$E(\hat{z})\dot{\hat{x}}(t) = A(\hat{z})\hat{x}(t) + B(\hat{z})u(t) + L(\hat{z})C(x(t) - \hat{x}(t)) \tag{III.58}$$

$$\hat{y}(t) = C\hat{x}(t) \tag{III.59}$$

where $\hat{x}(t) \in \mathbb{R}^n$ is the state estimation, $y(t) \in \mathbb{R}^p$ is the system's measured output, $\hat{y}(t) = C\hat{x}(t) \in \mathbb{R}^p$ is the output estimation, and $\hat{z}$ is the estimation of the premise vector z. Considering a reconstructed state control input $u(t) = K(\hat{z})\hat{x}(t)$, then the estimation error $\varepsilon(t) = x(t) - \hat{x}(t)$ and the nonlinear descriptor system (II.1) dynamics are given by the following extended form

$$\begin{bmatrix} E(z) & 0 \\ \Delta E & E(\hat{z}) \end{bmatrix} \begin{bmatrix} \dot{x}(t) \\ \dot{\varepsilon}(t) \end{bmatrix} = \begin{bmatrix} A(z) + B(z)K(\hat{z}) & -B(z)K(\hat{z}) \\ \Delta A + \Delta BK(\hat{z}) & A(\hat{z}) - L(\hat{z})C - \Delta BK(\hat{z}) \end{bmatrix} \begin{bmatrix} x(t) \\ \varepsilon(t) \end{bmatrix} \tag{III.60}$$

where

$$\Delta E = E(z) - E(\hat{z}), \qquad \Delta A = A(z) - A(\hat{z}), \qquad \Delta B = B(z) - B(\hat{z}).$$

Note that if all of the premise vector components are measured, then we have $z = \hat{z}$ and $\Delta X = 0$ for $X \in \{E, A, B\}$. Then, the extended form (III.60) becomes

$$\begin{bmatrix} E(z) & 0 \\ 0 & E(z) \end{bmatrix} \begin{bmatrix} \dot{x}(t) \\ \dot{\varepsilon}(t) \end{bmatrix} = \begin{bmatrix} A(z) + B(z)K(z) & -B(z)K(z) \\ 0 & A(z) - L(z)C \end{bmatrix} \begin{bmatrix} x(t) \\ \varepsilon(t) \end{bmatrix} \tag{III.61}$$

In such case, due to the diagonal and upper triangular structures of the derivative and state matrices of system (III.61), respectively, it is possible to prove the separation principle as in Xie et al., 2018 and derive separate LMI design conditions for both the controller and observer gains. However, as seen in Table I.3, while the descriptor matrix $E(z)$ of the robot manipulator dynamics exclusively contains fully measured premise variables and the input matrix $B(z) = B$ being constant, the matrix $A(z)$ on the other hand contains premise variables that depend on the velocity which we suppose is unavailable through measurement in this chapter. This implies that in (III.60) we have $\Delta A \neq 0$ and as such the state matrix is no longer upper triangular rendering the principle of separation inapplicable.

Considering $\Delta A = A(z) - A(\hat{z})$ as a parametric uncertainty to be modeled using the uncertain polytopic approach (III.6) does solve the separation problem, rendering the mixed observer-controller design a bilinear problem. Alternatively, in this case the system (III.60) can be rewritten as such

$$\begin{bmatrix} E(z) & 0 \\ 0 & E(z) \end{bmatrix} \begin{bmatrix} \dot{x}(t) \\ \dot{\varepsilon}(t) \end{bmatrix} = \begin{bmatrix} A(z) + B(z)K(z) & -B(z)K(z) \\ 0 & A(z) - L(z)C \end{bmatrix} \begin{bmatrix} x(t) \\ \varepsilon(t) \end{bmatrix} + f(x) - f(\hat{x}) \tag{III.62}$$

where $f(\cdot)$ is a nonlinear function such that $f(x) - f(\hat{x}) = \begin{bmatrix} 0 \\ \Delta A \end{bmatrix} x(t)$. Assuming that $f(\cdot)$ is either *bounded Jacobian*, *Lipschitz continuous*, *one-sided Lipschitz*, *quadratically inner-bounded*, or *quadratically bounded*, we obtain the following mathematical properties [Nugroho, Taha, and Hoang, 2021]

Exploiting the mathematical proprieties in Table III.3, similar LMI conditions to [Nugroho, Taha, and Hoang, 2021] for the mixed controller-observer design can be extended to the polytopic model representation (II.8). The bounds in Table III.3 are exploited to give the term $f(x) - f(\hat{x})$ in (III.62) a similar treatment to the parametric uncertainties in Theorem (I.3). However, computing an exact bound as shown in [Nugroho, Taha, and Hoang, 2021] can be challenging and the resulting design conservative. In the next chapter, we proposed a specific treatment

TABLE III.3: Functions sets of nonlinearity considered for $f(\cdot)$

Class	**Mathematical property**
Bounded Jacobian	$-\infty < f_{ij}^0 \leq \frac{\partial f}{\partial x_j}(x) \leq f_{ij}^1 < +\infty$, $x, \hat{x} \in \mathscr{D}_f$, $f_{ij}^0, f_{ij}^0 \in \mathbb{R}$
Lipschitz Continuous	$\|f(x) - f(\hat{x})\|_2 \leq \gamma_l \|x - \hat{x}\|_2$, $x, \hat{x} \in \mathscr{D}_f$, $\gamma_l \in \mathbb{R}^+$
One-sided Lipschitz	$\langle f(x) - f(\hat{x}), x - \hat{x} \rangle \leq \gamma_l \|x - \hat{x}\|_2^2$, $x, \hat{x} \in \mathscr{D}_f$, $\gamma_l \in \mathbb{R}$
Quadratically Inner-bounded	$\langle f(x) - f(\hat{x}), f(x) - f(\hat{x}) \rangle \leq \gamma_1 \|x - \hat{x}\|_2^2 + \gamma_2 \langle f(x) - f(\hat{x}), x - \hat{x} \rangle$, $x \in \mathscr{D}_f$, $\Lambda \in \mathbb{R}^{\varsigma \times n}$
Quadratically Bounded	$\langle f(x), f(x) \rangle \leq x^\top \Lambda^\top \Lambda x$, $x \in \mathscr{D}_f$, $\Lambda \in \mathbb{R}^{\varsigma \times n}$

for the unmeasured premise variables exploiting the structure of robot manipulators where no bounds are required for the mixed controller-observer design.

III.5 Conclusions

In this chapter we have extended the proposed quasi-LPV modeling approach (II.8) to uncertain descriptor systems and provided a new treatment for parametric uncertainties where due to the unique additional properties of the polytopic approach, the parametric uncertainties can be modeled into the polytopic form (III.6). A new feedback control was proposed which ensures the stability of the resulting uncertain polytopic model. A comparison of the proposed approach to the classical treatment of uncertainties on two different examples of uncertain singular systems was provided, and the results have proven the proposed approach to be less conservative in finding a stabilizing feedback control.

Additionally, we have targeted in this chapter the problem of high precision trajectory tracking control for serial manipulators with full measurement of the states and where the presence of parametric uncertainties and unknown disturbances is considered. The proposed uncertain quasi-LPV approach (III.6) was shown to yield better tracking results in comparison with a combined PID and feedforward action [Paccot, Andreff, and Martinet, 2009] as well as a combined CTC and DOB approach [Mohammadi et al., 2013]. However, due to the slightly high gains of the proposed control design, the resulting control inputs are impacted by the presence of noise in the measurement of joint-velocities.

To surpass this issue, we evaluated the possibility of a mixed controller-observer design to provide a noise free estimation of the velocity. With no available measurements of joint velocities, the problem of unmeasured scheduling variables arises for the mixed design. The existence of a separation principle in the design of the controller and observer gains in presence of unmeasured scheduling variables was explored as well.

In the next chapter, we propose exploiting the inherent mechanical nature of robot manipulators to offer a solution to the mixed controller-observer design in the presence of unmeasured scheduling variables. The validity of the proposed solution is then examined on both serial and parallel kinematic manipulators.

Chapter IV

Disturbance-Observer Based Tracking Control for Robot Manipulators

"Research is what I'm doing when I don't know what I am doing."

Werner von Braun

Contents

IV.1 Introduction 79
IV.2 Robot Modeling 80
IV.2.1 Mathematical Model of Robot Manipulators 80
IV.2.2 Tracking Control Goal and Robot Model Transformation 83
IV.3 Observer-Based Tracking Control Problem Formulation 84
IV.3.1 Feedforward Control 85
IV.3.2 Disturbance-Observer-Based Control 86
IV.3.3 Feedback Control 87
IV.4 Convex Design for Observer-Based Output Feedback Tracking Control 88
IV.5 Illustrations and Performance Evaluation 92
IV.5.1 A Serial Manipulator Example 93
IV.5.2 A Parallel Manipulator Example 102
IV.6 Discussions on Control Performance with respect to Unknown Disturbances 109
IV.7 Conclusions 113

IV.1 Introduction

The design of robot controllers [Mohammadi et al., 2013; Briot and Khalil, 2015] is usually based on complete state feedback, the measurements of both joint angular positions and joint angular velocities are required. The joint angular position measurements are generally obtained by means of either encoders or resolvers, which yield reliable and accurate measurements of the joint displacements. However, the same cannot be said for joint angular velocities obtained with tachometers or, more recently via numerical differentiation, both of which are often contaminated by noise. This can significantly affect the tracking precision for robot manipulators in particular. One solution to this problem is to deploy linear and nonlinear filters for noise cancellation or the extraction of desired frequency signals [Anderson and Moore, 1979; Chen et al., 2015]. In [Ahrens and Khalil, 2009] the reduced order high-gain observer allows to cancel high-frequency noises. In [Iwasaki and Skelton, 1994], an LMI formulation for $\mathcal{H}_\infty$-optimization design is proposed. In contrast, another solution that does not require the use of filters or high-gain feedback is to reconstruct the joint angular velocity signal via an observer [Jiang, Deghat, and Anderson, 2017; Magnis and Petit, 2016; Piperakis, Koskinopoulou, and Trahanias, 2018] and then exploit it for the control design.

In general, a robot is essentially a multibody dynamic system. Thus, a unified multibody dynamic model for both serial and parallel kinematic manipulators can be built based on differential-algebraic equations (DAEs) with nonindependent generalized coordinates. However, robot dynamic systems described by DAEs bring new challenges for the trajectory tracking control problems such is the case for parallel kinematic manipulators. The challenge primarily comes from the fact that numerical integration of the dynamical equations is a difficult problem because of the inherent instability due to the high-index problem for DAEs [Blajer, 1992]. Thus, the control design for such DAE systems is difficult to achieve. Most existing control design methods, specifically the well established control results for open kinematic chains, are only applicable to state-space models. For this reason, the state-space representation became a popular choice for representing the dynamics of a robot. In this regard, the proposed reduced model in [Ghorbel et al., 2000] was expressed in terms of independent generalized coordinates and it was shown to retain several structural properties of open chain manipulators. On the other hand, the reduced model assumes a transformation from independent coordinates to dependent coordinates, which is local and implicit. This implicit transformation needs to be solved in real-time for model-based control implementation. In [Wang and Ghorbel, 2004] the algebraic constraint equation in an index-1 DAE model is replaced by an asymptotically stable fast dynamics ODE.Thus, no online resolution of the algebraic constraints is required. However, this approach is based on differential-index-reduction which not only requires extensive algebraic calculations but also leads to regular descriptor models with an excessive number of nonlinearities for model-based robot control design [Allouche, 2016]. Alternatively, reduced order models are obtained by projecting the differential equations of the DAE system into a constraint free subspace [Blajer and Kolodziejczyk, 2004] but such an approach may require solving complex nonlinear matrices equations to determine the projecting matrix. Numerical discrete methods for controlled DAEs have also been proposed in [Peng et al., 2020; Shi et al., 2021]. However, such approaches relies on precise measurement of the joints coordinates and may prove to be vulnerable with respect to the system uncertainties.

Motivated by the above theoretical and practical robotics control issues, we propose in this chapter a disturbance-observer based (DOB) output feedback control scheme for uncertain robot manipulators considering both serial and parallel architectures using the proposed modeling approach in (II.8). The main contributions of this chapters are summarized as follows

- We propose design conditions for the mixed controller/observer problem in the case of

uncertain descriptor systems. To this aim, we prove the principle of separation allowing for an LMI formulation to the design of both the controller and observer gains.

- We exploit the specific structure of the robot manipulator dynamic model in the design of a DOB control scheme to minimize the effects of modeling uncertainties and unknown disturbances as well as resolve the issue of unmeasured premise variables [Nguyen et al., 2021a].
- The proposed DOB control scheme presents an extended observer with a virtual variable in order to further relax the design conditions. Additionally, the proposed DOB scheme allows for the complexity reduction for the class of robot manipulators systems.
- Finally, the proposed approach in this chapter represents a unified framework for the control design of both serial and parallel robot manipulators alike relying only on the measurement of the active joints position. The proposed approach is validated on high fidelity simulation models of both a serial and parallel robot manipulators.

IV.2 Robot Modeling

This section presents the modeling of uncertain robot manipulators with unmeasured premise variables. The specific structure of the robot manipulators is exploited to obtain an uncertainty free model with measured premises and a lumped disturbance term. Then, the robot model is transformed into the proposed polytopic representation (II.8), which is appropriate for the purpose of nonlinear output feedback tracking control design.

IV.2.1 Mathematical Model of Robot Manipulators

The general dynamics of a rigid manipulator under algebraic constraints can be described as [Briot and Khalil, 2015]

$$\begin{aligned} &\hat{M}(\phi)\ddot{\phi}(t) + \hat{N}(\phi,\dot{\phi})\dot{\phi}(t) + \hat{G}(\phi) = \mathfrak{B}(\phi)(\Gamma(t) + \Gamma_{ext}(t)) + \mathcal{J}(\phi)^\top \lambda(t), \\ &\mathfrak{h}(\phi) = 0, \qquad \frac{\partial}{\partial \phi}\mathfrak{h}(\phi) = \mathcal{J}(\phi). \end{aligned} \tag{IV.1}$$

where $\phi(t) = \begin{bmatrix}\theta^\top(t) & q^\top(t)\end{bmatrix}^\top \in \mathbb{R}^\kappa$ is the vector of joint-space coordinates, $\theta(t) \in \mathbb{R}^n$ and $q(t) \in \mathbb{R}^\nu$ are respectively the active and passive joint-space coordinates, with $\kappa = n + \nu$. $\hat{M}(\phi) \in \mathbb{R}^{\kappa\times\kappa}$ is the inertia matrix, $\hat{N}(q,\dot{q}) \in \mathbb{R}^{\kappa\times\kappa}$ is the Coriolis-centripetal matrix plus the viscous friction coefficients of the joints, $\hat{G}(\phi) \in \mathbb{R}^\kappa$ represents the generalized gravity torque. The actuation force and torque distribution is represented by $\mathfrak{B}(\phi) = \begin{bmatrix}\beta(\theta)^\top & 0\end{bmatrix}^\top$, where $\beta(\theta) \in \mathbb{R}^{n\times n}$ is assumed to be invertible for fully actuated robot systems, *i.e.*, $\det(\beta(\theta)) \neq 0$. $\mathfrak{h}(\phi) \in \mathbb{R}^\nu$ represents the kinematic constraints imposed by the manipulator linkage considered at least twice differentiable, and whose Jacobian is defined as $\mathcal{J}(\phi) \in \mathbb{R}^{\kappa\times\nu}$. The Lagrangian multiplier $\lambda(t) \in \mathbb{R}^\nu$ represents the internal forces caused by the algebraic constraints. $\Gamma(t) \in \mathbb{R}^n$ is the vector of the generalized control torques applied to the joints whereas $\Gamma_{ext}(t) \in \mathbb{R}^n$ is the vector of external disturbances such as joint dry friction. Note that the dynamics of serial robot manipulators can be directly obtained from (IV.1) with $q(t) \in \emptyset$, $\nu = 0$ and $\kappa = n$. For the general case, the robot dynamics (IV.1) can be equivalently decomposed as

$$\mathcal{F}_a(t) = \beta(\theta)(\Gamma(t) + \Gamma_{ext}(t)) + \mathcal{J}_a(\theta)^\top \lambda(t), \tag{IV.2a}$$

$$\mathcal{F}_b(t) = \mathcal{J}_b(q)^\top \lambda(t), \tag{IV.2b}$$

with

$$\mathcal{F}_a(t)=\hat{M}_a(\theta)\ddot{\theta}(t)+\hat{M}_{ab}(\phi)\ddot{q}(t)+\hat{N}_a(\theta,\dot{\theta})\dot{\theta}(t)+\hat{N}_{ab}(\phi,\dot{\phi})\dot{q}(t)+\hat{G}_a(\theta),$$
$$\mathcal{F}_b(t)=\hat{M}_b(q)\ddot{q}(t)+\hat{M}_{ab}(\phi)\ddot{\theta}(t)+\hat{N}_b(q,\dot{q})\dot{q}(t)+\hat{N}_{ba}(\phi,\dot{\phi})\dot{\theta}(t)+\hat{G}_b(q),$$

and

$$\hat{M}(\phi)=\begin{bmatrix}\hat{M}_a(\theta) & \hat{M}_{ab}(\phi)\\ \hat{M}_{ab}(\phi) & \hat{M}_b(q)\end{bmatrix}, \tag{IV.3}$$

$$\hat{N}(\phi,\dot{\phi})=\begin{bmatrix}\hat{N}_a(\theta,\dot{\theta}) & \hat{N}_{ab}(\phi,\dot{\phi})\\ \hat{N}_{ba}(\phi,\dot{\phi}) & \hat{N}_b(q,\dot{q})\end{bmatrix}, \tag{IV.4}$$

$$\hat{G}(\phi)=\begin{bmatrix}G_a(\theta)\\ G_b(q)\end{bmatrix},\quad \mathcal{J}(\phi)=\begin{bmatrix}\mathcal{J}_a(\phi)\\ \mathcal{J}_b(\phi)\end{bmatrix}. \tag{IV.5}$$

The following set defines the reachable robot workspace:

$$\mathcal{R}=\{\phi\in\mathbb{R}^{\kappa}:\ \mathfrak{h}(\phi)=0\}\subset\mathbb{R}^{\kappa}. \tag{IV.6}$$

Since function $\mathfrak{h}(\phi)$ is at least twice continuously differentiable, we can deduce from $\mathfrak{h}(\phi)=0$ that

$$\mathcal{J}_a(\phi)\dot{\theta}(t)+\mathcal{J}_b(\phi)\dot{q}(t)=0, \tag{IV.7}$$

$$\mathcal{J}_a(\phi)\ddot{\theta}(t)+\mathcal{J}_b(\phi)\ddot{q}(t)+\frac{d\mathcal{J}_a(\phi)}{dt}\dot{\theta}(t)+\frac{d\mathcal{J}_b(\phi)}{dt}\dot{q}(t)=0. \tag{IV.8}$$

It follows from (IV.7) that if $\mathcal{J}_b(\phi)\in\mathbb{R}^{\nu\times\nu}$ is invertible, then the velocity $\dot{q}(t)$ and the acceleration $\ddot{q}(t)$ of the passive joints can be explicitly expressed as functions of the generalized coordinates $\phi(t)$ and the active joint velocities $\dot{\theta}(t)$ and accelerations $\ddot{\theta}(t)$. As a result, we can define a singularity-free workspace for a joint space control problem as

$$\mathcal{S}=\{\phi\in\mathbb{R}^{\kappa}:\ \det(\mathcal{J}_b(\phi))\neq 0\}\subset\mathbb{R}^{\kappa}. \tag{IV.9}$$

Assumption 2. For tracking control, we assume in this work that the desired trajectory is planned such that the generalized coordinates are within the reachable workspace while avoiding singular configurations [Ghorbel et al., 2000; Wang and Ghorbel, 2004], *i.e.*, $\phi\in\mathcal{R}\cap\mathcal{S}$, where the sets $\mathcal{R}$ and $\mathcal{S}$ are respectively defined in (IV.6) and (IV.9).

Remark IV.15. The control design for systems in the algebro-differential form (IV.2) is particularly challenging [Blajer, 1992; Ghorbel et al., 2000; Peng et al., 2020; Shi et al., 2021]. Moreover, in practice, the passive-joint variable $q(t)$ and its time-derivative $\dot{q}(t)$ are not available for control implementation. Reducing the differential index has been proposed to deal with these major issues [Ghorbel et al., 2000; Wang and Ghorbel, 2004; Liu et al., 2021]. To this end, it is assumed that $\mathcal{J}_b(\phi)^{\top}$ is invertible. Then, the vector of internal forces $\lambda(t)$ can be computed from (IV.2b) as

$$\lambda=\mathcal{J}_b(\phi)^{-\top}\mathcal{F}_b(t). \tag{IV.10}$$

Exploiting the algebraic constraints $\mathfrak{h}(\phi)=0$ and its time derivatives, the passive-joint variable $q(t)$, and its derivatives $\dot{q}(t)$ and $\ddot{q}(t)$ can be expressed as a function of $\theta(t)$, $\dot{\theta}(t)$ and $\ddot{\theta}(t)$. Then, substituting (IV.10) into (IV.2a) yields a robot model with only active-joint coordinates $\theta(t)$ and its derivatives as shown in [Ghorbel et al., 2000; Wang and Ghorbel, 2004; Liu et al., 2021]. This latter model enables the design of a practical controller for system (III.34), or its algebro-differential form (IV.2). However, such a differential-index-reduction-based control approach not only requires extensive algebraic calculations but also leads to regular descriptor models with a

number of nonlinearities that can be excessive for the robot control design [Wang and Ghorbel, 2004].

Consider the robot dynamics (IV.2a) with parameter uncertainties, including the uncertain inertia matrix $\Delta M_a(\theta) \in \mathbb{R}^{n\times n}$, the uncertain Coriolis-centrifugal matrix $\Delta N_a(\theta,\dot\theta) \in \mathbb{R}^{n\times n}$, and the uncertain gravity torque $\Delta G_a(\theta) \in \mathbb{R}^n$, *i.e.*,

$$\begin{aligned} \hat M_a(\theta) &= M_a(\theta) + \Delta M_a(\theta), \\ \hat N_a(\theta,\dot\theta) &= N_a(\theta,\dot\theta) + \Delta N_a(\theta,\dot\theta), \\ \hat G_a(\theta) &= G_a(\theta) + \Delta G_a(\theta). \end{aligned} \tag{IV.11}$$

The uncertainty vector can be defined as

$$\Gamma_\delta(t) = \Delta M_a(\theta)\ddot\theta(t) + \Delta N_a(\theta,\dot\theta)\dot\theta(t) + \Delta G_a(\theta). \tag{IV.12}$$

Moreover, due to the nature of the robot dynamics (IV.2), we can regroup all the terms dependent on the variables related to the passive joints as

$$\Gamma_q(t) = \mathcal{J}_a(\phi)^\top \lambda(t) - \hat M_{ab}(\phi)\ddot q(t) - \hat N_{ab}(\phi,\dot\phi)\dot q(t). \tag{IV.13}$$

Let us define a lumped disturbance vector as

$$\Gamma_d(t) = \Gamma_q(t) + \beta(\theta)\Gamma_{ext}(t) - \Gamma_\delta(t). \tag{IV.14}$$

Substituting (IV.11), (IV.12), (IV.13) and (IV.14) into (IV.2), under Assumption 2 the uncertain robot dynamics (IV.1) restrained to the active joints-space can be presented by

$$M_a(\theta)\ddot\theta(t) + N_a(\theta,\dot\theta)\dot\theta(t) + G_a(\theta) = \beta(\theta)\Gamma(t) + \Gamma_d(t) \tag{IV.15}$$

Hence, model (IV.15) can be used for the robot manipulator control design under multiple uncertainties and disturbances. It is assumed that the vectors of manipulator position $\theta(t)$ and manipulator velocity $\dot\theta(t)$ respectively belong to the following bounded sets

$$\begin{aligned} \theta(t) &\in \mathscr{D}_\theta = \{\theta \in \mathbb{R}^n : \ \ \theta_{i\min} \le \theta_i \le \theta_{i\max},\ \forall i \in \mathcal{I}_n\} \\ \dot\theta(t) &\in \mathscr{D}_{\dot\theta} = \{\dot\theta \in \mathbb{R}^n : \ \ \dot\theta_{i\min} \le \dot\theta_i \le \dot\theta_{i\max},\ \forall i \in \mathcal{I}_n\} \end{aligned} \tag{IV.16}$$

where the bounds of the robot manipulator $\theta_{i\min}$, $\theta_{i\max}$, $\dot\theta_{i\min}$ and $\dot\theta_{i\max}$ are defined according to the robot workspace and operating characteristics. The following inherent property is useful for robot control design and analysis.

Property 1 ([Lewis, Dawson, and Abdallah, 2003])**.** The inertia matrix $M(\theta)$ is symmetric positive definite and verifies

$$\alpha_1 I \le M_a(\theta) \le \alpha_2 I, \tag{IV.17}$$

where α_1 and α_2 are two positive scalars.

In this chapter, we assume that only the manipulator position $\theta(t)$ can be measured to perform the tracking control tasks. Then, for control design the robot model (IV.15) is reformulated in the descriptor form as

$$\begin{aligned} E(\sigma)\dot x(t) &= A(\sigma)x(t) + B\big(u(t) + d_t(t)\big) \\ y(t) &= Cx(t) \end{aligned} \tag{IV.18}$$

where $x(t) = \begin{bmatrix}\theta^\top(t) & \dot{\theta}^\top(t)\end{bmatrix}^\top \in \mathbb{R}^{2n}$ is the state vector, $u(t) = \beta(\phi)^{-1}(\Gamma(t) - G_a(\theta)) \in \mathbb{R}^n$ is the control input, and $d_t(t) = \Gamma_d(t) \in \mathbb{R}^n$ is the disturbance vector. The state-space matrices are defined as

$$E(\sigma) = \begin{bmatrix} I & 0 \\ 0 & M_a(\theta) \end{bmatrix}, \quad A(\sigma) = \begin{bmatrix} 0 & I \\ 0 & -N_a(\theta, \dot{\theta}) \end{bmatrix}, \quad B = \begin{bmatrix} 0 & I \end{bmatrix}^\top, \quad C = \begin{bmatrix} I & 0 \end{bmatrix}, \tag{IV.19}$$

where $\sigma(t) \in \mathbb{R}^r$ is the vector of r premise variables, *i.e.*, system nonlinearities, identified in the robot dynamics, that continuously depend on the state $x(t)$. Since $\theta(t) \in \mathscr{D}_\theta$ and $\dot{\theta}(t) \in \mathscr{D}_{\dot{\theta}}$ as defined in (IV.16), we can straightforwardly derive the bounded set of $\sigma(t)$ from the mathematical expression of each nonlinearity σ_i, for $i \in \mathcal{I}_r$, *i.e.*,

$$\sigma(t) \in \mathscr{D}_\sigma = \{\sigma \in \mathbb{R}^r : \sigma_{i\min} \leq \sigma_i \leq \sigma_{i\max},\ \forall i \in \mathcal{I}_m\}, \tag{IV.20}$$

where $\sigma_{i\min}$ and $\sigma_{i\max}$ are the bounds derived from (IV.16). Note that the matrices $E(\sigma) \in \mathbb{R}^{2n\times 2n}$ and $A(\sigma) \in \mathbb{R}^{2n\times 2n}$ depend affinely on $\sigma(t)$, *i.e.*,

$$E(\sigma) = E_0 + \sum_{i=1}^{r} \sigma_i(t) E_i, \quad A(\sigma) = A_0 + \sum_{i=1}^{r} \sigma_i(t) A_i \tag{IV.21}$$

where E_i and A_i for $i \in \mathcal{I}_r \cup \{0\}$ are known constant matrices of appropriate dimensions. Moreover, due to property (IV.17), the matrix $E(\sigma)$ is regular, for all $\sigma(t) \in \mathscr{D}_\sigma$.

IV.2.2 Tracking Control Goal and Robot Model Transformation

Our main goal is to design a disturbance-observer-based output controller such that the end-effector of the robot described in (IV.15) tracks a desired trajectory with a high precision and a fast convergence, despite the presence of uncertain dynamics, unknown gravitational and disturbance torques.

Note that the Coriolis-centrifugal matrix $N(\theta, \dot{\theta})$ involved in $A(\sigma)$ has *unmeasured* nonlinear elements due to its dependency on $\dot{\theta}(t)$. This may lead to technical challenges in designing nonlinear controllers and observers for system (IV.18) as discussed in [Nguyen et al., 2021b]. To avoid these difficulties, we divide the set of premise variables into two subsets, *i.e.*, $\sigma(t) = \begin{bmatrix} z^\top(t) & \bar{z}^\top(t) \end{bmatrix}^\top$ with

$$z \in \mathcal{M} = \{\sigma_i \in \sigma :\ \sigma_i \text{ is measurable}, i \in \mathcal{I}_p\}, \tag{IV.22}$$

$$\bar{z} \in \mathcal{U} = \left\{\sigma_j \in \sigma :\ \sigma_j \text{ is unmeasurable}, j \in \mathcal{I}_{r\backslash p}\right\}, \tag{IV.23}$$

with $p \in \mathbb{Z}_+$ and $p \leq r$. Then, only the premise variables belonging to $\mathcal{M}$ are used to construct the nonlinear observer-based tracking controller. Each unmeasurable premise variable belonging to $\mathcal{U}$ can be rewritten as

$$\sigma_j(t) = \sigma_{jc} + \delta_j(t)\sigma_{jd}, \quad \forall j \in \mathcal{I}_{r\backslash p}, \tag{IV.24}$$

where $\delta_j(t) \in [-1, 1]$, and

$$\sigma_{jc} = \frac{\sigma_{j\max} + \sigma_{j\min}}{2}, \quad \sigma_{jd} = \frac{\sigma_{j\max} - \sigma_{j\min}}{2}.$$

It follows from (IV.21) and (IV.24) that

$$A(\sigma) = A_0 + \sum_{i=1}^{p} \sigma_i(t) A_i + \sum_{j=p+1}^{r} \sigma_j(t) A_j$$

$$= A_0 + \sum_{i=1}^{p} \sigma_i(t) A_i + \sum_{j=p+1}^{r} \sigma_{jc} A_j + \sum_{j=p+1}^{r} \delta_j(t) \sigma_{jd} A_j$$
$$= \bar{A}_0 + \sum_{i=1}^{p} \sigma_i(t) A_i + \Delta A(t), \tag{IV.25}$$

with $\bar{A}_0 = A_0 + \sum_{j=p+1}^{r} \sigma_{jc} A_j$ is a *known* constant matrix, and $\Delta A(t) = \sum_{j=p+1}^{r} \delta_j(t) \sigma_{jd} A_j$ is an *uncertain* matrix caused by unmeasured premise variables. It follows from (IV.25) that $A(\sigma) = A(z) + \Delta A(t)$. Note that due to the structure of matrices $A(\sigma)$ and B in (IV.19), $\Delta A(t)$ can be rewritten as

$$\Delta A(t) = B B^{\dagger} \Delta A(t), \tag{IV.26}$$

where $B^{\dagger} = (B^{\top} B)^{-1} B^{\top}$ is the pseudo-inverse of B. Let us define $d_l(t) = B^{\dagger} \Delta A(t)$. Then, from (IV.25) and (IV.26), the robot descriptor model (IV.18) can be rewritten as

$$\begin{aligned} E(z)\dot{x}(t) &= A(z)x(t) + B\big(u(t) + d(t)\big), \\ y(t) &= Cx(t), \end{aligned} \tag{IV.27}$$

where $d(t) = d_t(t) + d_l(t)$ is the vector of lumped disturbances. We have $E(\sigma) = E(z)$ since all of the premise variables contained in the inertia matrix are measured.

Remark IV.16. We transform the uncertain robot model (IV.15) with unmeasured premise variables $\sigma(t)$ into the uncertain descriptor model (IV.27) with only measured premise variables z. This model transformation plays a key role in the control approach in this section to avoid the major issue of unmeasured premise variables for nonlinear observer design [Pan et al., 2021; Nguyen et al., 2021b] and to be able to prove the separation principle for nonlinear observer-based control of uncertain descriptor systems.

Using the proposed polytopic approach (II.8), the nonlinear system (IV.27) can be rewritten as

$$\sum_{i=1}^{2p} w_i(z) E_i \dot{x}(t) = \sum_{i=1}^{2p} w_i(z) A_i x(t) + B\big(u(t) + d(t)\big). \tag{IV.28}$$

The nonlinear weights $w_i(z)$, for $i \in \mathcal{I}_{2p}$, satisfy the convex sum property (II.9a) and the additional property (II.9b). Let Ω be the set of the nonlinear weights satisfying (II.9), *i.e.*, $w = [w_1(z), w_2(z), \ldots, w_{2p}(z)] \in \Omega$. As we have proven in Chapter II, using the proposed modeling approach (II.8), the reduced complexity polytopic representation (IV.28) is an *equivalent* representation of model (IV.27), *i.e.*, there is no modeling approximation between these two nonlinear models, within the compact set $\mathscr{D}_{\sigma}$ defined in (IV.20).

Remark IV.17. To further simplify the proposed polytopic model (IV.28), some premise variables, including measured premise variables, can be interpreted as "modeling uncertainties" via expression (IV.24) as in [Nguyen et al., 2019]. Such model uncertainties can be then lumped into the disturbance vector $d(t)$ similarly to the model transformation discussed in Remark IV.16. Hence, despite its simplicity, the proposed model transformation has two major advantages for nonlinear observer-based control design: i) derive uncertain robot model with only measured premise variables, ii) derive tractable control-based model with a significantly reduced complexity.

IV.3 Observer-Based Tracking Control Problem Formulation

This section formulates the tracking control problem of the uncertain robot system (IV.15), described in the proposed polytopic form (IV.28). To this end, we define the tracking error in

the generalized coordinate as $e(t) = x(t) - x_r(t)$, where $x_r(t) = \begin{bmatrix} \theta_r^\top(t) & \dot{\theta}_r^\top(t) \end{bmatrix}^\top$ is the vector of the joint coordinates corresponding to the desired trajectory $r_e(t)$. This latter is expressed in the robot workspace using the end-effector coordinates.Then, the tracking error dynamics can be defined from (IV.27) as

$$\begin{aligned} E(z)\dot{e}(t) &= A(z)e(t) + B\big(u(t) + d(t)\big) + A(z)x_r(t) - E(z)\dot{x}_r(t), \\ \psi(t) &= Ce(t), \end{aligned} \tag{IV.29}$$

where $\psi(t)$ is the targeted performance vector. To effectively deal with the modeling uncertainties and disturbances, we propose a composite nonlinear tracking control law composed of the three following control components

$$u(t) = u_{ff}(t) + u_{dc}(t) + u_{fb}(t), \tag{IV.30}$$

where $u_{ff}(t)$ is the feedforward control action, $u_{dc}(t)$ is the disturbance-observer-based control action, and $u_{fb}(t)$ is the feedback control action. The proposed tracking control scheme is illustrated in Figure IV.1.

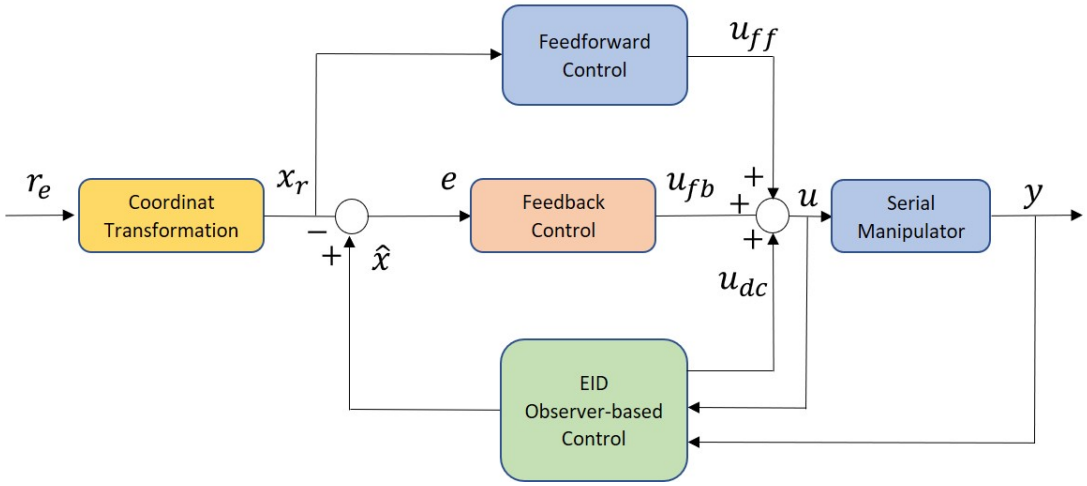

FIGURE IV.1: Disturbance-observer based tracking control structure for serial manipulators.

IV.3.1 Feedforward Control

Since the desired trajectory for tracking tasks of robot manipulators are generally planned in advance, the reference signal $r_e(t)$ and its derivative can be obtained in real-time. Note that the desired trajectory is planned such that the singular points in the robot workspace are avoided. Following the robot kinematics developments, the reference signal $r_e(t)$ can be defined with end-effector trajectory as $r_e(t) = \mathcal{Y}(\theta_r)$, where $\mathcal{Y}(\theta_r)$ is the forward geometric model that express the end-effector coordinates as a function of active joint coordinates. Then, the desired joint coordinates can be computed as $\theta_r(t) = \mathcal{Y}^{-1}(r_e)$ and

$$\dot{\theta}_r(t) = J_r(\theta_r)^{-1}\dot{r}_e(t), \qquad \ddot{\theta}_r(t) = \frac{\mathrm{d}J_r(\theta)^{-1}}{\mathrm{dt}}\dot{r}_e(t) + J_r(\theta)^{-1}\ddot{r}_e(t), \tag{IV.31}$$

where $J_r(\theta) = \frac{\partial}{\partial\theta}\mathcal{Y}(\theta)$ is the is the Jacobian of the forward kinematic model. Note that the Jacobian is of full rank since the trajectory is chosen to fulfil a singularity-free path in the end-effector workspace. As a result, $\dot{x}_r(t)$ can be obtained for control design. The feedforward control action is designed to account for the effect of $x_r(t)$ and its derivative, considered as

known disturbances, on the error dynamics (IV.29) such that

$$Bu_{ff}(t) = -\big(A(z)x_r(t) - E(z)\dot{x}_r(t)\big). \tag{IV.32}$$

Then, the feedforward action can be designed from (IV.32) as

$$u_{ff}(t) = -B^{\dagger}\big(A(z)x_r(t) - E(z)\dot{x}_r(t)\big). \tag{IV.33}$$

Remark IV.18. The feedfoward action allows to simplify the tracking error dynamics by compensating the terms related to the reference signal allowing for a more efficient design of the feedback control law.

IV.3.2 Disturbance-Observer-Based Control

Note from (IV.29) that the lumped disturbance d affects the error dynamics via the same channel as the control input u, *i.e.*, matching disturbance. Hence, the disturbance-observer-based control action can be designed as

$$u_{dc}(t) = -\hat{d}_f(t), \tag{IV.34}$$

where $\hat{d}_f(t)$ is a filtered estimate of the disturbance $d(t)$. In fact, we assume that for the disturbance estimation we have $d(t)$ as a low-frequency signal, whose dynamics can be captured using a piecewise second-order polynomial signal [Koenig, 2006]. To this point, based on the equivalent-input-disturbance approach [She, Xin, and Pan, 2010; Li et al., 2022], the following low-pass filter is incorporated to limit the angular-frequency band of the disturbance estimate

$$F(s) = \frac{K_f}{1 + T_f s} I, \tag{IV.35}$$

where s is the Laplace variable, T_f is the time constant of the filter. Then, the disturbance model is given as

$$\dot{d}_e(t) = D d_e(t), \tag{IV.36}$$

with

$$d_e(t) = \begin{bmatrix} d_f(t) \\ d(t) \\ \dot{d}(t) \end{bmatrix}, \quad D = \begin{bmatrix} -\frac{1}{T_f} I & \frac{K_f}{T_f} I & 0 \\ 0 & 0 & I \\ 0 & 0 & 0 \end{bmatrix}.$$

Motivated by the extended-descriptor-based observer design in [Guerra, Estrada-Manzo, and Lendek, 2015; Nguyen et al., 2021b], from (IV.27) and (IV.36), we propose the following Luenberger-like observer to simultaneously estimate the state and the unknown disturbance

$$\begin{aligned} E(z)\dot{\hat{x}}(t) &= A(z)\hat{x}(t) + B\big(u(t) + \hat{d}(t)\big) + \big(L_x(z) + E(z)L_\eta(z)\big)\big(y(t) - \hat{y}(t)\big), \\ \eta(t) &= \dot{\hat{x}} - L_\eta(z)\big(y(t) - \hat{y}(t)\big), \\ \dot{\hat{d}}_e(t) &= D\hat{d}_e(t) + L_d(z)\big(y(t) - \hat{y}(t)\big), \qquad \text{(IV.37)} \\ \hat{y}(t) &= C\hat{x}(t), \qquad \text{(IV.38)} \end{aligned}$$

where $\hat{x}(t)$ is the estimate of $x(t)$, $\hat{d}(t)$ is the estimate of $d(t)$, and $\hat{d}_e(t)$ is the estimate of $d_e(t)$. The fictive variable $\eta(t)$, considered as an "image" of the estimate of $\dot{x}(t)$, is introduced in the observer structure (IV.37) to facilitate the nonlinear descriptor observer design [Guerra, Estrada-Manzo, and Lendek, 2015]. The nonlinear observer gains $L_x(z) \in \mathbb{R}^{2n\times n}$, $L_\eta(z) \in \mathbb{R}^{2n\times n}$ and $L_d(z) \in \mathbb{R}^{3n\times n}$ are to be determined.

Remark IV.19. Observer (IV.37) integrates the parameters of the filter $F(s)$ into the design of observer gains to offer a degree of freedom in adjusting the angular-frequency band for the disturbance rejection. The value of T_f can then be selected such that $T_f \in \left[\frac{1}{10w_f}, \frac{1}{5w_f}\right]$, where w_f is the highest angular frequency selected for disturbance rejection purposes [She, Xin, and Pan, 2010].

From (IV.27) and (IV.37), it follows that

$$E(z)(\dot{x}(t) - \dot{\hat{x}}(t)) = (A(z) - L(z)C)(x(t) - \hat{x}(t)) + B_o(d_e(t) - \hat{d}_e(t)) \tag{IV.39}$$

with $L(z) = L_x(z) + E(z)L_\eta(z)$ and $B_o = \begin{bmatrix} 0 & B & 0 \end{bmatrix}$. From the definition of $\eta(t)$ in (IV.37), it follows from (IV.39) that

$$E(z)(\dot{x}(t) - \eta(t)) = (A(z) - L_x(z)C)(x(t) - \hat{x}(t)) + B_o(d_e(t) - \hat{d}_e(t)) \tag{IV.40}$$

We define the estimation errors as $e_x(t) = x(t) - \hat{x}(t)$, $e_d(t) = d_e(t) - \hat{d}_e(t)$, $e_\eta(t) = \dot{x}(t) - \eta(t)$ and $\varepsilon(t) = \begin{bmatrix} e_x^\top(t) & e_d^\top(t) & e_\eta^\top(t) \end{bmatrix}^\top$. Then, the estimation error dynamics are defined from (IV.27), (IV.36), (IV.37) and (IV.40) as

$$E_o\dot{\varepsilon}(t) = (A_o(z) - L_o(z)C_o)\varepsilon(t), \tag{IV.41}$$

with

$$E_o = \mathrm{diag}(I, I, 0), \quad A_o(z) = \begin{bmatrix} 0 & 0 & I \\ 0 & D & 0 \\ A(z) & B_o & -E(z) \end{bmatrix}, \quad L_o(z) = \begin{bmatrix} L_\eta(z) \\ L_d(z) \\ L_x(z) \end{bmatrix}, \quad C_o = \begin{bmatrix} C & 0 & 0 \end{bmatrix}.$$

Remark IV.20. Note that the nonlinear observer (IV.37) provides the estimation of both $\hat{d}_f(t)$ for the disturbance-observer-based control (IV.34) and $\hat{x}(t)$ for the feedback control (IV.42) described in the following section. The injection of the estimated disturbance in the control input $u_{dc}(t)$ aims at reducing the impact of the disturbance on the trajectory tracking and improve the performance of the $\mathcal{L}_2$-gain design of the feedback control.

IV.3.3 Feedback Control

The feedback control guarantees the closed-loop stability and the robustness of the tracking performance with respect to disturbances and uncertainties. To this end, we consider the following nonlinear proportional-integral-type control law

$$u_{fb}(t) = K_p(z)(\hat{x}(t) - x_r(t)) + K_I(z)e_I(t), \tag{IV.42}$$

where $K_p(z) \in \mathbb{R}^{n\times 2n}$ and $K_I(z) \in \mathbb{R}^{n\times n}$ are the nonlinear gains to be determined. The dynamics of $e_I(t)$ is defined as

$$\dot{e}_I(t) = C(x(t) - x_r(t)).$$

With the three control components $u_{ff}(t)$, $u_{dc}(t)$ and $u_{fb}(t)$ of the control law (IV.30), respectively defined in (IV.33), (IV.34) and (IV.42), the closed-loop tracking error dynamics (IV.29) can be reformulated in the following extended descriptor form

$$E_c\dot{\xi}(t) = (A_c(z) + B_cK_c(z))\xi(t) + \bar{B}_p(z)\varepsilon(t) + B_cw_d(t), \tag{IV.43}$$

where $\xi(t) = \begin{bmatrix} e^\top(t) & e_I^\top(t) & \dot{e}^\top(t) \end{bmatrix}^\top$ and

$$E_c = \begin{bmatrix} I & 0 & 0 \\ 0 & I & 0 \\ 0 & 0 & 0 \end{bmatrix}, \quad A_c(z) = \begin{bmatrix} 0 & 0 & I \\ C & 0 & 0 \\ A(z) & 0 & -E(z) \end{bmatrix}, \quad K_c(z) = \begin{bmatrix} K_p(z) & K_I(z) & 0 \end{bmatrix},$$

$$\bar{B}_p(z) = \begin{bmatrix} 0 & 0 & 0 \\ 0 & 0 & 0 \\ -BK_p(z) & 0 & 0 \end{bmatrix}, \quad B_c = \begin{bmatrix} 0 \\ 0 \\ B \end{bmatrix}.$$

Note that the disturbance $w_d(t) \in \mathbb{R}^n$ is introduced into the closed-loop dynamics (IV.43) to take into account the high-frequency disturbances/uncertainties, *e.g.*, model uncertainties stemmed from (IV.24) or high-frequency excitation of dry friction included in the disturbance $\Gamma_d(t)$, that cannot be estimated by observer (IV.37) due to the low-frequency assumption on $d(t)$.

The extended error dynamics of both tracking error and estimation error can be defined from (IV.41) and (IV.43) as

$$\begin{aligned} \begin{bmatrix} E_c & 0 \\ 0 & E_o \end{bmatrix} \dot{x}_e(t) &= \begin{bmatrix} \bar{A}_c(z) & \bar{B}_p(z) \\ 0 & \bar{A}_o(z) \end{bmatrix} x_e(t) + \begin{bmatrix} B_c \\ 0 \end{bmatrix} w_d(t), \\ \psi(t) &= \bar{C} x_e(t), \end{aligned} \tag{IV.44}$$

where $x_e(t) = \begin{bmatrix} \xi^\top(t) & \varepsilon^\top(t) \end{bmatrix}^\top$, $\bar{C} = \begin{bmatrix} C & 0 \end{bmatrix}$, and

$$\bar{A}_c(z) = A_c(z) + B_c K_c(z), \quad \bar{A}_o(z) = A_o(z) - L_o(z) C_o.$$

We are ready to reformulate the following observer-based feedback control problem.

Problem 2. Consider the robot model (IV.15), reformulated in the proposed polytopic form (IV.28). Determine the gains $K_p(z)$ and $K_I(z)$ (respectively $L_x(z)$, $L_d(z)$ and $L_\eta(z)$) of controller (IV.42) (respectively observer (IV.37)) such that the extended descriptor system (IV.44) verifies the following closed-loop properties.

(P1) For $w_d(.) = 0$, system (IV.44) is exponentially stable with a decay rate $\alpha > 0$.

(P2) For $w_d(.) \in \mathcal{L}_2$ and under zero initial condition $x_e(0) = 0$, the induced $\mathcal{L}_2-$norm of the performance vector $\psi(t)$ is bounded as

$$\int_0^{T_s} \psi^\top(t)\psi(t)dt < \gamma \int_0^{T_s} w_d^\top(t) w_d(t) dt, \ \forall T_s > 0, \tag{IV.45}$$

where γ is a positive scalar.

Remark IV.21. Note that minimizing γ in (IV.45) leads to a minimization of the negative effect of the disturbance $w(t)$ on $\psi(t)$ which help to further improve the closed-loop tracking performance.

IV.4 Convex Design for Observer-Based Output Feedback Tracking Control

This section presents convex conditions to design both controller (IV.42) and observer (IV.37) for the robot tracking control. The following theorem provides LMI-based conditions to solve Problem 1.

Theorem IV.11 *If there exist symmetric positive definite matrices $Q_1 \in \mathbb{S}^{5n}$, $P_1 \in \mathbb{S}^{3n}$, symmetric matrices $T_{o_i} \in \mathbb{S}^{14n}$, $S_{o_j} \in \mathbb{S}^{14n}$, $T_{c_i} \in \mathbb{S}^{10n}$, $S_{c_j} \in \mathbb{S}^{10n}$, matrices $H_{o_i}, R_{o_i} \in \mathbb{R}^{7n\times 7n}$, $H_{c_i}, R_{c_i} \in \mathbb{R}^{5n\times 5n}$, $W_{ij} \in \mathbb{R}^{7n\times n}$, $Y_{ij} \in \mathbb{R}^{n\times 3n}$, $Q_{2_{ij}} \in \mathbb{R}^{2n\times 5n}$, $P_{2_{ij}} \in \mathbb{R}^{2n\times 3n}$, $P_{3_{ij}} \in \mathbb{R}^{2n\times 2n}$, and $Q_{3_{ij}} \in \mathbb{R}^{2n\times 2n}$, for $i, j \in \mathcal{I}_{2p}$, positive scalars α_c, α_o such that $\alpha_c < \alpha_o$ and*

$$\Upsilon_{ii} \prec 0, \quad \forall i \in \mathcal{I}_q \tag{IV.46}$$

$$\frac{2}{q-1}\Upsilon_{ii} + \Upsilon_{ij} + \Upsilon_{ji} \prec 0, \quad \forall i, j \in \mathcal{I}_q, \quad i \neq j \tag{IV.47}$$

$$\Xi_{ij} \prec 0, \quad \forall i \in \mathcal{I}_q \tag{IV.48}$$

$$\frac{2}{q-1}\Xi_{ii} + \Xi_{ij} + \Xi_{ji} \prec 0, \quad \forall i, j \in \mathcal{I}_q, \quad i \neq j \tag{IV.49}$$

where

$$\Upsilon_{ij} = \Lambda_{ij} + T_{o_i} + S_{oj} - \frac{1}{p}(T_o + S_o), \quad T_o = \sum_{k=1}^{p} T_{o_{2k}}, \quad S_o = \sum_{k=1}^{p} S_{o_{2k}},$$

$$\Xi_{ij} = \digamma_{ij} + T_{c_i} + S_{c_j} - \frac{1}{p}(T_c + S_c), \quad T_c = \sum_{k=1}^{r} T_{c_{2k}}, \quad S = \sum_{k=1}^{r} S_{c_{2k}},$$

$$\Lambda_{ij} = \mathrm{He}\begin{bmatrix} \mathcal{A}_{o_i}^\top H_{o_j} - C_o^\top W_{ij}^\top & \mathcal{A}_{o_i}^\top R_{o_j} \\ \mathcal{Q}_{ij} - H_{o_j} & -R_{o_j} \end{bmatrix}, \quad \digamma_{ij} = \mathrm{He}\begin{bmatrix} \mathcal{A}_{c_i} H_{c_j} + \Sigma_{ij} & \mathcal{A}_{c_i} R_{c_j} \\ \mathscr{P}_{ij} - H_{c_j} & -R_{c_j} \end{bmatrix},$$

$$\mathcal{P}_{ij} = \begin{bmatrix} P_1 & 0 \\ P_{2_{ij}} & P_{3_{ij}} \end{bmatrix}, \quad \mathcal{Q}_{ij} = \begin{bmatrix} Q_1 & 0 \\ Q_{2_{ij}} & Q_{3_{ij}} \end{bmatrix}, \quad \mathcal{A}_{o_i} = A_{o_i} + \alpha_o E_o, \quad \mathscr{P}_{ij} = \mathrm{diag}(\mathcal{P}_{ij}, I, I),$$

$$\mathcal{A}_{c_i} = \begin{bmatrix} A_{c_i} + \alpha_c E_c & 0 & C^\top \\ 0 & 0 & 0 \\ 0 & 0 & 0 \end{bmatrix}, \quad \Sigma_{ij} = \begin{bmatrix} B_c \bar{Y}_{ij} & B_d & 0 \\ 0 & -\frac{\gamma}{2} I & 0 \\ 0 & 0 & -\frac{1}{2} I \end{bmatrix}, \quad \bar{Y}_{ij} = \begin{bmatrix} Y_{ij} & 0 \end{bmatrix},$$

$$T_{o_{2k-1}} = T_{o_{2k}}, \quad S_{o_{2k-1}} = T_{o_{2k}}, \quad T_{c_{2k-1}} = T_{c_{2k}}, \quad S_{c_{2k-1}} = T_{c_{2k}}, \quad \forall k \in \mathcal{I}_p$$

Then, the closed-loop system (IV.44) verifies properties (P1) and (P2) specified in Problem 1, with a guaranteed $\mathcal{L}_2-$gain $\gamma_s = \sqrt{\gamma}$. Moreover, the gain expressions $K_c(z)$ and $L_o(z)$ of controller (IV.42) and observer (IV.37), respectively, are given by

$$K_c(z) = Y(z)P_1^{-1}, \quad L_o(z) = \mathcal{Q}(z)^{-\top} W(z). \tag{IV.50}$$

Proof:
For stability analysis of the closed-loop system (IV.44), we consider the following extended Lyapunov function:

$$\mathcal{V}(x_e) = x_e^\top \begin{bmatrix} \tau E_c^\top \mathcal{P}(z)^{-1} & 0 \\ 0 & E_o^\top \mathcal{Q}(z) \end{bmatrix} x_e, \tag{IV.51}$$

with $\tau > 0$. Note that

$$E_c^\top \mathcal{P}(z)^{-1} = \mathrm{diag}\left(P_1^{-1}, 0\right) \succeq 0, \quad E_o^\top \mathcal{Q}(z) = \mathrm{diag}\left(Q_1, 0\right) \succeq 0.$$

Since $T_{o_{2k-1}} = T_{o_{2k}}$, $\forall k \in \mathcal{I}_p$, then according to properties (II.9) on the weights $w_i(z)$ we have

$$\sum_{i=1}^{2p} w_i(z)(T_{o_p} - \frac{1}{p}T_o) \quad = \quad \sum_{k=1}^{p} w_{2k-1}(z)T_{o_{2k-1}} + w_{2k}T_{o_{2k}} - \frac{1}{p}T_o$$

$$= \frac{1}{p}\sum_{k=1}^{p}(z)T_{o_{2k}} - \frac{1}{p}T_o$$

$$= 0$$

Similarly, it follows that

$$\sum_{i=1}^{2p} w_i(z)(S_{o_p} - \frac{1}{p}S_o) = 0, \quad \sum_{i=1}^{2p} w_i(z)(T_{c_p} - \frac{1}{p}T_c) = 0, \quad \sum_{i=1}^{2p} w_i(z)(S_{c_p} - \frac{1}{p}S_o) = 0. \tag{IV.52}$$

Then, applying Lemma I.4 to conditions (IV.46) and (IV.47) yields

$$\Upsilon(z) = \Lambda(z) = \mathrm{He}\begin{bmatrix} \mathcal{A}_o(z)^\top H_o(z) - C_o^\top W(z)^\top & \mathcal{A}_o(z)^\top R_o(z) \\ \mathcal{Q}(z) - H_o(z) & -R_o(z) \end{bmatrix} \prec 0. \tag{IV.53}$$

Pre- and post-multiplying this inequality with $\begin{bmatrix} I & \mathcal{A}(z)^\top \end{bmatrix}$ *and its transpose, it follows that*

$$\mathrm{He}\left[\mathcal{A}(z)^\top \mathcal{Q}(z) - C_o^\top W(z)^\top\right] \prec 0. \tag{IV.54}$$

Note that

$$\mathrm{He}\left[\mathcal{A}(z)^\top \mathcal{Q}(z) - C_o^\top W(z)^\top\right] = \mathrm{He}\begin{bmatrix} \bullet & \bullet \\ \bullet & -E(z)^\top \mathcal{Q}(z) \end{bmatrix} \tag{IV.55}$$

where "$\bullet$" denotes some matrix terms. Then, it follows from (IV.54) and (IV.55) that

$$\det\left(-E(z)^{-\top}\mathcal{Q}(z)\right) \neq 0. \tag{IV.56}$$

We deduce from (IV.56) that $\mathcal{Q}(z)$ is invertible, thus the gain expression $L_o(z)$ given in (IV.50) is well-defined. Moreover, with this expression of $L_o(z)$, inequality (IV.54) can be rewritten as

$$\mathrm{He}\left[(A(z) - L_o(z)C_o + \alpha_o E_o)^\top \mathcal{Q}(z)\right] \prec 0. \tag{IV.57}$$

Using again Lemma I.4 while exploiting the result (IV.52), it follows from (IV.48) and (IV.49) that

$$\Xi(z) = \digamma(z) = \mathrm{He}\begin{bmatrix} \mathcal{A}(z)H(z) + \Sigma(z) & \mathcal{A}(z)R(z) \\ \mathscr{P}(z) - H(z) & -R(z) \end{bmatrix} \prec 0. \tag{IV.58}$$

Pre- and post-multiplying inequality (IV.58) with $\begin{bmatrix} I & \mathcal{A}(z)^\top \end{bmatrix}$ *and its transpose, it follows that*

$$\mathrm{He}\left[\mathcal{A}(z)\mathscr{P}(z) + \Sigma(z)\right] \prec 0, \tag{IV.59}$$

which, in turn, can be rewritten as

$$\begin{bmatrix} \Theta(z) & B_d & \mathcal{P}(z)^\top C^\top \\ \star & -\gamma I & 0 \\ \star & \star & -I \end{bmatrix} \prec 0, \tag{IV.60}$$

with $\Theta(z) = \mathrm{He}\left[(A(z)+\alpha_c E_c)\mathcal{P}(z) + B_c\bar{Y}(z)\right]$. *We note from* (IV.60) *that*

$$\Theta(z) = \mathrm{He}\begin{bmatrix}\bullet & \bullet \\ \bullet & -E(z)\mathcal{P}(z)\end{bmatrix} \prec 0. \tag{IV.61}$$

It follows from (IV.61) *that* $\det(\mathcal{P}(z)) \neq 0$, *thus* $\mathcal{P}(z)$ *is invertible. Then, note also that the gain expression* $K_c(z)$ *defined in* (IV.50) *can be rewritten as*

$$K_c(z) = \bar{Y}(z)\mathcal{P}(z)^{-1}. \tag{IV.62}$$

Pre- and post-multiplying inequality (IV.60) *with* $\mathscr{P}(z)^{-\top}$ *and its transpose while taking into expression* (IV.62), *it follows that*

$$\begin{bmatrix}\Psi(z) & \mathcal{P}(z)^{-\top}B_d & C^\top \\ \star & -\gamma I & 0 \\ \star & \star & -I\end{bmatrix} \prec 0, \tag{IV.63}$$

with $\Psi(z) = \mathrm{He}\left[\mathcal{P}(z)^{-\top}(A(z)+B_cK_c(z)+\alpha_cE_c)\right]$. *By Schur complement lemma [Boyd et al., 1994], we can prove that condition* (IV.63) *is equivalent to*

$$\begin{bmatrix}\Psi(z)+C^\top C & \mathcal{P}(z)^{-\top}B_d \\ \star & -\gamma I\end{bmatrix} \prec 0. \tag{IV.64}$$

Let us denote

$$\begin{aligned}\Pi_o &= \mathrm{He}[(A_o(z)-L_o(z)C_o)^\top\mathcal{Q}(z)], \\ \Pi_c &= \begin{bmatrix}\mathrm{He}\left[\mathcal{P}(z)^{-\top}(A(z)+B_cK_c(z))\right]+C^\top C & \mathcal{P}(z)^{-\top}B_d \\ \star & -\gamma I\end{bmatrix}.\end{aligned} \tag{IV.65}$$

Since $\alpha_o E_o^\top \mathcal{Q}(z) \succeq 0$, *it follows from* (IV.57) *that* $\Pi_o \prec 0$. *Similarly, since* $\alpha_c E_c^\top \mathcal{P}(z)^{-1} \succeq 0$, *it follows from* (IV.64) *that* $\Pi_c \prec 0$. *Moreover, note that* Π_o *only depends on the observer gain* $L_o(z)$ *and matrix* $\mathcal{Q}(z)$, *while* Π_c *only depends on the control gain* $K_c(z)$ *and matrix* $\mathcal{P}(z)$. *Then, there always exists a positive scalar* $\tau > 0$, *sufficiently small, such that*

$$\Pi_o \prec \tau\Phi\Pi_c^{-1}\Phi^\top, \tag{IV.66}$$

with $\Phi = \begin{bmatrix}\bar{B}_p(z)^\top\mathcal{P}(z)^{-1} & 0\end{bmatrix}$. *By Schur complement lemma, we can show that* (IV.66) *is equivalent to*

$$\begin{bmatrix}\tau\Pi_c & \tau\Phi^\top \\ \star & \Pi_o\end{bmatrix} \prec 0. \tag{IV.67}$$

Following similar arguments to obtain (IV.66) *for* $\Psi(z)$, Π_o *and* $\bar{B}_p(z)$, *it follows that* $\Pi_o \prec \tau\bar{B}_p(z)^\top\mathcal{P}(z)^{-1}\Psi(z)^{-1}\mathcal{P}(z)^{-\top}\bar{B}_p(z)$, *or equivalently*

$$\begin{bmatrix}\tau\Psi(z) & \tau\mathcal{P}(z)^{-\top}\bar{B}_p(z) \\ \star & \Pi_o\end{bmatrix} \prec 0. \tag{IV.68}$$

From now, we distinguish the two following cases

- *Case 1: system* (IV.44) *with* $w_d(.) = 0$,
- *Case 2: system* (IV.44) *with* $w_d(.) \in \mathcal{L}_2$.

For Case 1, pre- and post-multiplying (IV.68) *with* $\begin{bmatrix}\xi^\top & \varepsilon^\top\end{bmatrix}$ *and its transpose, it follows that*

$$\xi^\top \tau\Psi(z)\xi + \mathrm{He}[\xi^\top \mathcal{P}(z)^{-\top}\bar{B}_p(z)\varepsilon] + \varepsilon^\top \Pi_o \varepsilon < 0. \tag{IV.69}$$

Taking into account the definitions of $\Psi(z)$, Π_o *and* $\bar{B}_p(z)$, *after some algebraic manipulations condition* (IV.69) *can be rewritten as*

$$\dot{\mathcal{V}}(x_e) + 2\tau\alpha_c \xi^\top E_c^\top \mathcal{P}(z)^{-1}\xi + 2\alpha_o \varepsilon^\top E_o^\top \mathcal{Q}(z)\varepsilon < 0, \tag{IV.70}$$

where $\dot{\mathcal{V}}(x_e)$ *is the time-derivative of the Lyapunov function* $\mathcal{V}(x_e)$, *defined in* (IV.51), *along the solution of the closed-loop system* (IV.44) *with* $w_d(t) = 0$. *Since* $0 < \alpha_c < \alpha_o$ *and* $E_o^\top \mathcal{Q} \succeq 0$, *it follows from* (IV.70) *that*

$$\dot{\mathcal{V}}(x_e) + 2\tau\alpha_c \xi^\top E_c^\top \mathcal{P}(z)^{-1}\xi + 2\alpha_c \varepsilon^\top E_o^\top \mathcal{Q}(z)\varepsilon < 0,$$

or equivalently $\dot{\mathcal{V}}(x_e) + 2\alpha_c \mathcal{V}(x_e) < 0$. *This latter guarantees Property (P1),* i.e., *system* (IV.44) *is exponentially stable with a decay rate* $\alpha = \alpha_c > 0$.
For Case 2, pre- and post-multiplying condition (IV.67) *with* $\begin{bmatrix}\xi^\top & w_d^\top & \varepsilon^\top\end{bmatrix}$ *and its transpose, we can obtain the following condition after some algebraic manipulations*

$$\begin{aligned}&\tau\xi^\top \mathrm{He}\left[\mathcal{P}(z)^{-\top}(A(z) + B_c K_c(z))\right]\xi + \tau\,\mathrm{He}\left[\xi^\top \mathcal{P}(z)^{-\top}\bar{B}_p(z)\varepsilon\right] \\ &+ \tau\,\mathrm{He}\left[\xi^\top \mathcal{P}(z)^{-\top} B_d w_d\right] + \varepsilon^\top \Pi_o \varepsilon + \psi^\top\psi - \gamma w_d^\top w_d < 0.\end{aligned} \tag{IV.71}$$

Condition (IV.71) *can be rewritten in the compact form*

$$\dot{\mathcal{V}}(x_e) + \psi^\top\psi - \gamma^2 w_d^\top w_d < 0. \tag{IV.72}$$

Integrating both sides of (IV.72) *from 0 to* T_s, *for any* $T_s > 0$, *under zero initial condition,* i.e., $\mathcal{V}(x_e(0)) = 0$, *we have*

$$\mathcal{V}(x_e(T_s)) < \int_0^{T_s} (\gamma w_d^\top(t) w_d(t) - \psi^\top(t)\psi(t))dt. \tag{IV.73}$$

Since $\mathcal{V}(x_e(T_s)) > 0$, *it follows from* (IV.73) *that*

$$\int_0^{T_s} \psi^\top(t)\psi(t)dt < \gamma \int_0^{T_s} w_d^\top(t) w_d(t)dt,$$

which guarantees Property (P2) for the closed-loop system (IV.44). *This concludes the proof.*

Remark IV.22. The positive scalar τ is introduced in the construction of the extended Lyapunov function $\mathcal{V}(x_e)$, defined in (IV.51), to facilitate the obtaining of strict LMI-based conditions to design an observer-based output tracking controller for uncertain polytopic descriptor systems of the form (IV.28). This scalar τ is not involved in the design conditions in Theorem IV.11 but rather serves as a rigorous proof element of the separation principle [Xie et al., 2018] which holds mainly due to the diagonal and upper triangular structures of the derivative and state matrices of system (IV.44), respectively.

IV.5 Illustrations and Performance Evaluation

In this section we present the results of the proposed observer-based control design applied to two different types of robot manipulators. In the first example, we consider the trajectory tracking for a serial manipulator on both linear and curved trajectories. The second example considers

a parallel robot manipulator where the dynamics are rewritten as in (IV.15) and the tracking performance is evaluated on a spiral trajectory. We consider the presence of uncertainties and external disturbances and the proposed control scheme is compared to a PID controller combined with a feedforward action [Paccot, Andreff, and Martinet, 2009] for both examples, a CTC controller combined with a DOB input [Mohammadi et al., 2013] for the serial manipulator, and a simple CTC controller [Briot and Khalil, 2015] for the parallel manipulator.

IV.5.1 A Serial Manipulator Example

Let us denote the vector of angular positions as $\theta(t) = \begin{bmatrix}\theta_1(t) & \theta_2(t) & \theta_3(t)\end{bmatrix}^\top \in \mathbb{R}^3$. Then, the uncertain dynamics of the serial robot as depicted in Figure IV.2 can be represented by (IV.1) where the nominal system is given by

$$M(\theta) = \begin{bmatrix} m_{11} & m_{12} & m_{13} \\ \star & 2c_6\sigma_2 + c_8 & c_6\sigma_2 + I_3 \\ \star & \star & I_3 \end{bmatrix}, \quad N(\theta,\dot\theta) = \begin{bmatrix} n_{11} & n_{12} & n_{13} \\ n_{21} & n_{22} & -c_6\sigma_8 \\ n_{31} & c_6\sigma_7 & 0 \end{bmatrix},$$
$$G(\theta) = \begin{bmatrix} c_1\sigma_{10} + c_2\sigma_{11} + c_3\sigma_{12} \\ c_2\sigma_{11} + c_3\sigma_{12} \\ c_3\sigma_{12} \end{bmatrix},$$

with

$$\begin{aligned}
&m_{11} = 2(c_4\sigma_1 + c_6\sigma_2 + c_5\sigma_3 + c_7), && m_{12} = c_4\sigma_1 + 2c_6\sigma_2 + c_5\sigma_3 + c_8, && m_{13} = c_6\sigma_2 + c_5\sigma_3 + I_3,\\
&n_{11} = c_5(\sigma_6 - \sigma_9) + c_6(\sigma_7 - \sigma_8), && n_{12} = -c_4\sigma_4 + c_6(\sigma_7 - \sigma_8) - c_5\sigma_9, && n_{13} = -c_6\sigma_8 - c_5\sigma_9,\\
&n_{21} = c_4\sigma_5 + c_5\sigma_6 + c_6(\sigma_7 - \sigma_8), && n_{22} = c_6(\sigma_7 - \sigma_8), && n_{31} = c_5\sigma_6 + c_6\sigma_7,\\
&c_1 = g(L_1m_2 + L_1m_3 + m_1r_1), && c_2 = g(L_2m_3 + m_2r_2), && c_3 = gm_3r_3,\\
&c_4 = L_1(L_2m_3 + m_2r_2), && c_5 = L_1m_3r_3, && c_6 = L_2m_3r_3,\\
&c_7 = (m_2 + m_3)L_1^2 + L_2^2m_3 + I_t, && c_8 = L_2^2m_3 + I_2 + I_3, && I_t = I_1 + I_2 + I_3.
\end{aligned}$$

For this serial manipulator, since there is no algebraic constraint, then it follows from (IV.1) that the vector of passive joints is empty $q \in \emptyset$ and we have $\phi = \theta$, $\mathfrak{B}(\phi) = \beta(\phi) = I$, $\mathcal{J} = 0$, and $\mathfrak{h}(\phi) \in \emptyset$. The nominal values of the robot parameters are given in Table I.4, while the expressions of the nonlinearities σ_i, for $i \in \mathcal{I}_{12}$, are given in Table I.3. We denote $x = \begin{bmatrix}\theta^\top & \dot\theta^\top\end{bmatrix}^\top \in \mathbb{R}^6$ and $u = \Gamma - G(\theta) \in \mathbb{R}^3$. Then, the considered robot model can be rewritten in the nonlinear descriptor form (IV.18) with

$$E(\sigma) = \begin{bmatrix} I & 0 \\ 0 & M(\theta) \end{bmatrix}, \quad A(\sigma) = \begin{bmatrix} 0 & I \\ 0 & -N(\theta,\dot\theta) \end{bmatrix}, \quad B = \begin{bmatrix} 0 \\ I \end{bmatrix}. \tag{IV.74}$$

Note that since $G(\theta)$ is fully compensated by the control input, the remaining premises in the descriptor form (IV.18) are σ_i for $i \in \mathcal{I}_9$. The premise vector σ is divided, according to (IV.22), into two subsets of measurable premises $z \in \mathcal{M}$ and unmeasured premise variables $\bar z \in \mathcal{U}$ as such

$$z = \begin{bmatrix}\sigma_2 & \sigma_3\end{bmatrix}^\top, \qquad \bar z = \begin{bmatrix}\sigma_1 & \sigma_4 & \sigma_5 & \sigma_6 & \sigma_7 & \sigma_8 & \sigma_9\end{bmatrix}^\top \tag{IV.75}$$

Although the premise variable σ_1 can be measurable, we include it as a component of $\bar z(t)$. This allows to represent the uncertain robot model (IV.18) in the proposed quasi-LPV descriptor form (IV.28), where all the vertices M_{ai} of the inertia matrix $M_a(\theta)$ in $E(z)$ verify Property 1. Note that since $z(t) \in \mathbb{R}^2$, then the proposed quasi-LPV model of the robot manipulator has $2 \times 2 = 4$ vertices. The lumped disturbance $d(t)$ in (IV.28) includes the external force $\Gamma_{ext}(t)$

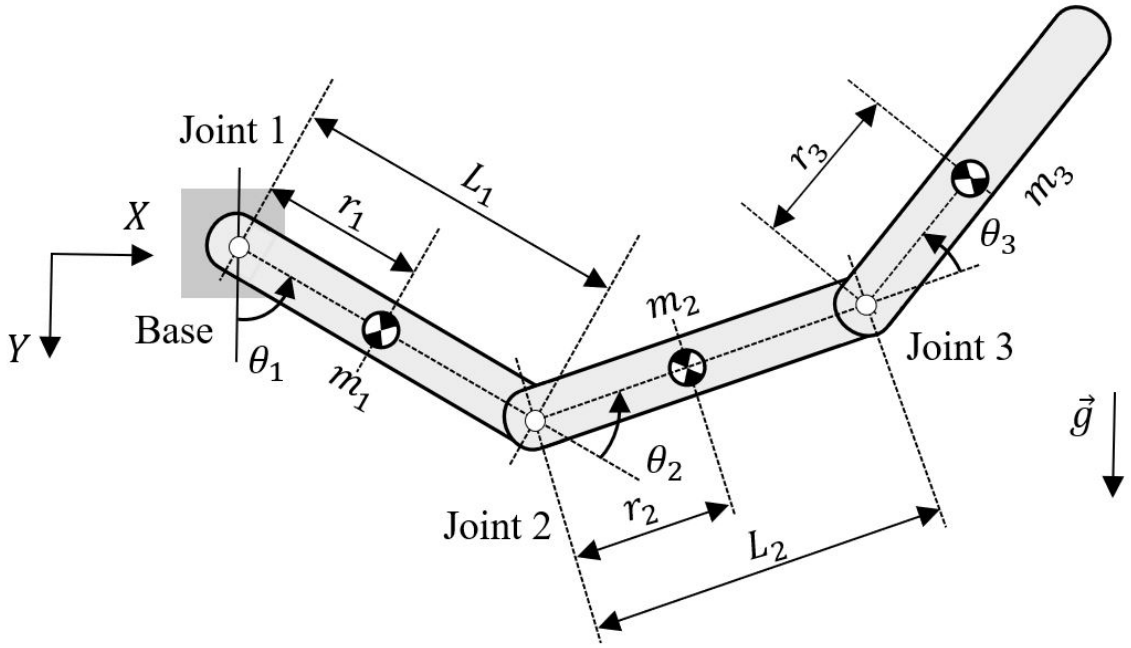

FIGURE IV.2: Schematic of the 3DoF robot in the vertical plane.

exerted on the end of effector as in (III.53). We consider in addition to the effect of the external disturbance Γ_{ext}, the following parametric uncertainties

$$\begin{aligned} \Delta m_1 &= +40\%\ m_1, & \Delta m_2 &= +40\%\ m_2, & \Delta m_3 &= +120\%\ m_3, \\ \Delta r_1 &= +40\%\ r_1, & \Delta r_2 &= +40\%\ r_2, & \Delta r_3 &= +120\%\ r_3, \end{aligned}$$

Uncertainties on end-effector payload are included in the parameters Δm_3 and Δr_3. To demonstrate the effectiveness of the new control results, we perform a comparison between the following robot tracking control approaches:

- Approach 1: Proportional-integral-derivative (PID) control combined with a feedforward action (FF) [Paccot, Andreff, and Martinet, 2009].
- Approach 2: Computed-torque control (CTC) combined with a disturbance observer (DOB) [Mohammadi et al., 2013].
- Approach 3: Quasi-LPV disturbance-observer-based output tracking control proposed in Theorem IV.11.

The PID control law is given by (III.54) and its controller gains are the same as (III.3.3). Likewise, the CTC control law is given by (III.56) and its controller gains are the same as (III.3.3). It is important to note that the PID controller in (III.54) and the CTC controller in (III.56) require the measurement of the angular velocity $\dot{\theta}$ for control implementation, which is not the case for Approach 3. For the control design of the proposed tracking controller, the values of the decay rates are selected as $\alpha_c = 3.1$ and $\alpha_o = 3.15$. The parameters of the disturbance filter $F(s)$ in (IV.35) are $T_f = 10^{-3}$ s and $K_f = 1$ as suggested in Remark IV.19. Then, solving the design conditions in Theorem I.2, an observer-based tracking controller can be obtained with an $\mathcal{L}_{2e}-$gain of $\gamma = 10^{-3}$. For illustrations, some of the feedback gains obtained

with Theorem IV.11 are given by

$$K_{p_1} = 10^4 \begin{bmatrix} -137.333 & 44.836 & 57.672 & -0.122 & 0.032 & 0.05 \\ 39.029 & 28.003 & 40.272 & 0.025 & 0.019 & 0.04 \\ 61.917 & 39.547 & -17.053 & 0.047 & 0.0294 & -0.018 \end{bmatrix},$$

$$K_{I_1} = 10^4 \begin{bmatrix} 28.543 & 1801.312 & 1321.886 \\ 1553.144 & 1149.974 & 751.612 \\ 1373.537 & 664.491 & -89.389 \end{bmatrix},$$

$$K_{p_2} = 10^4 \begin{bmatrix} -427.049 & -232.151 & -71.723 & -0.345 & -0.201 & -0.051 \\ -250.686 & -248.986 & -89.13 & -0.198 & -0.213 & -0.061 \\ -82.656 & -97.176 & -19.325 & -0.065 & -0.083 & -0.012 \end{bmatrix},$$

$$K_{I_2} = 10^4 \begin{bmatrix} -0.051 & -4735.064 & -2740.235 & -801.48 \\ -0.0613 & -3210.4345 & -3391.605 & -1371.861 \\ -0.012 & -1002.291 & -1579.95- & 124.168 \end{bmatrix}.$$

For a quantitative performance analysis, we recall the performance indicators previously defined in the former chapter section III.3.3

- Root mean square (RMS $[m]$) of the end-effector position error along both axes X and Y

$$\mathrm{RMS}_X = \sqrt{\frac{1}{T_s}\int_0^{T_s} (X(t) - X_r(t))^2 dt}, \qquad \mathrm{RMS}_Y = \sqrt{\frac{1}{T_s}\int_0^{T_s} (Y(t) - Y_r(t))^2 dt},$$

  where T_s is the simulation time.

- Maximal absolute value (MAV $[m]$) of the end-effector position error along both axes X and Y

$$\mathrm{MAV}_X = \max_{t\in[0,T_s]} |X(t) - X_r(t)|, \qquad \mathrm{MAV}_Y = \max_{t\in[0,T_s]} |Y(t) - Y_r(t)|.$$

- Mean square root (RMS_u [Nm]) of the control input

$$\mathrm{RMS}_u = \sqrt{\frac{1}{T_s}\sum_{i=1}^{3}\int_0^{T_s} u_i(t)^2 dt}.$$

We consider the tracking of two different types of trajectories. The first trajectory is linear and constitutes a square contained in the XY plane with the gravity $\overrightarrow{g} = -g\overrightarrow{y}$. The second trajectory is curved and constitutes 3 quarters of a circle also contained in the same XY plane. The following subsections present the simulation results and a comparison of the tracking performance.

a) Square Trajectory Tracking

The tracking control performance with a square trajectory obtained with the three control methods is depicted in Figure IV.3. We can see that the proposed quasi-LPV controller yields a much better tracking performance compared to the two other controllers, which provide themselves similar control results. As confirmed by the results in Table IV.1, both the RMS error and the MAV error indicate the superiority of the proposed tracking control scheme over the FF-based PID control in [Paccot, Andreff, and Martinet, 2009] and the DOB-based CTC control in [Mohammadi et al., 2013].

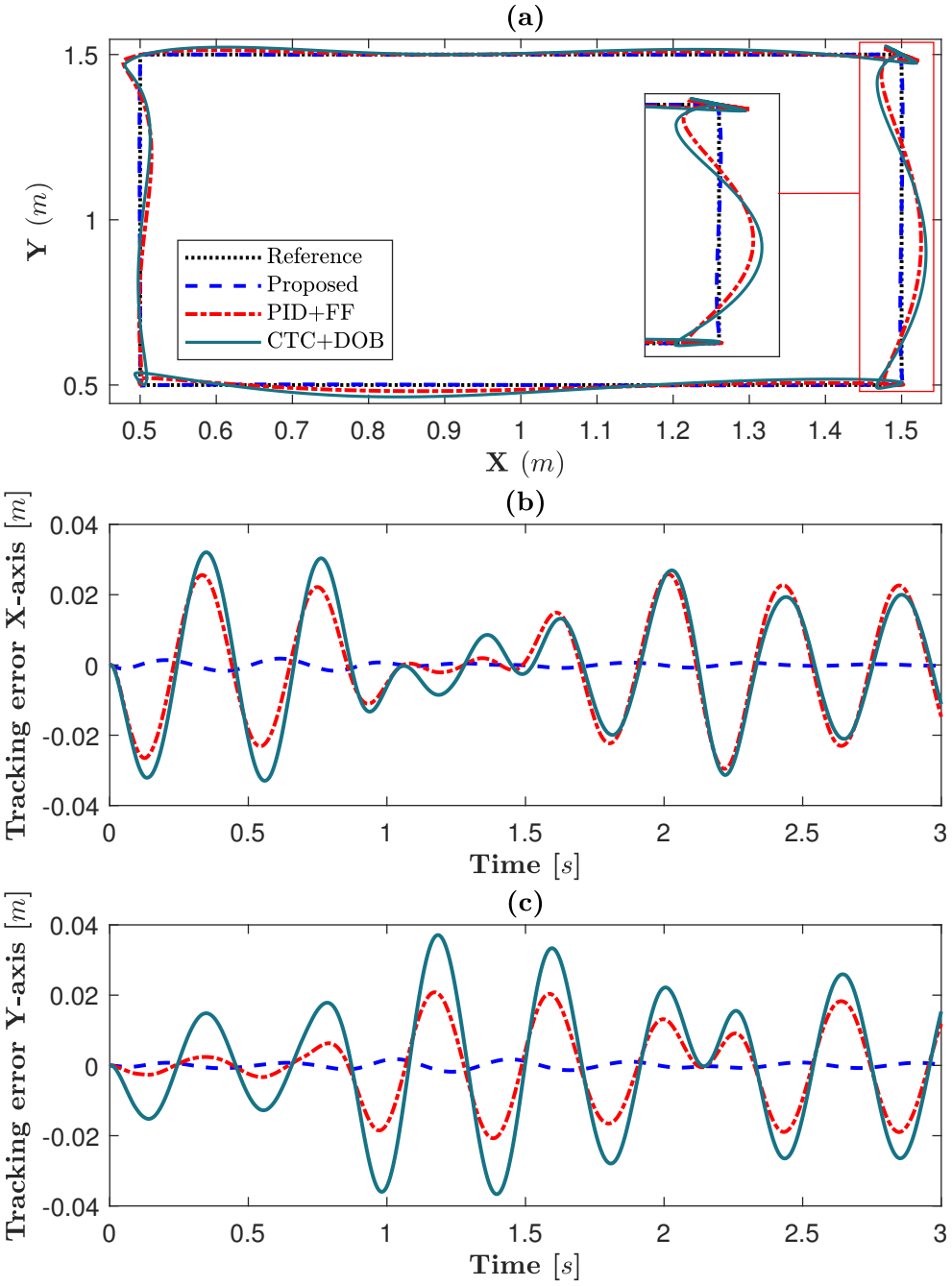

FIGURE IV.3: Comparison of tracking control performance. (a) Linear trajectory tracking in XY plane. (b) Tracking error along X-axis. (c) Tracking error along Y-axis.

As shown in Figure IV.4, the control inputs obtained with the proposed control scheme are of similar shapes to those of the two other control approaches. Table IV.1 also indicates that the proposed approach yields a lower torque control input in terms of RMS_u.

Figure IV.5 presents a comparison of the velocity estimation errors to evaluate the interest of the proposed disturbance compensation input $u_{dc}(t) = -\hat{d}_f$. We can see that the estimation performance can be significantly improved in the presence of DOB, which allows for an improvement of the overall tracking control performance. Table IV.1 presents the results of the chosen performance indicators. Comparing the results of the proposed DOB control in this chapter to the $\mathcal{H}_\infty$-performance robust tracking control design of the previous chapter in Table III.1,

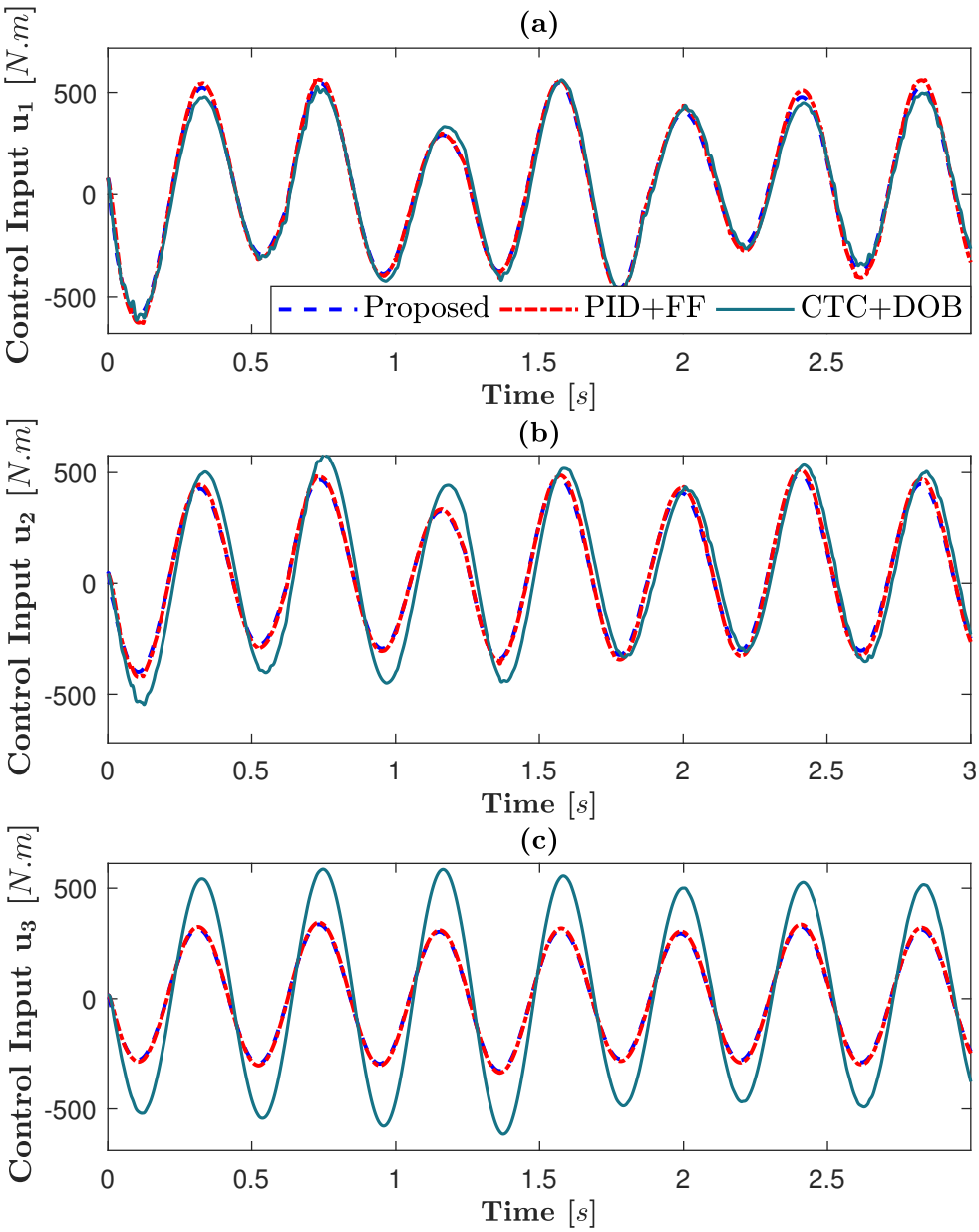

FIGURE IV.4: Comparison of control inputs in the case of linear trajectory tracking.

TABLE IV.1: Linear trajectory tracking performance.

Indicator	FF-based PID	DOB-based CTC	Theorem I.2
RMS_X $[m]$	1.66×10^{-2}	1.79×10^{-2}	4.86×10^{-4}
RMS_Y $[m]$	1.16×10^{-2}	2.04×10^{-2}	3.64×10^{-4}
MAV_X $[m]$	3.37×10^{-2}	3.76×10^{-2}	1.2×10^{-3}
MAV_Y $[m]$	2.41×10^{-2}	4.16×10^{-2}	9.10×10^{-4}
RMS_u $[Nm]$	1.29×10^{4}	1.65×10^{4}	1.24×10^{4}

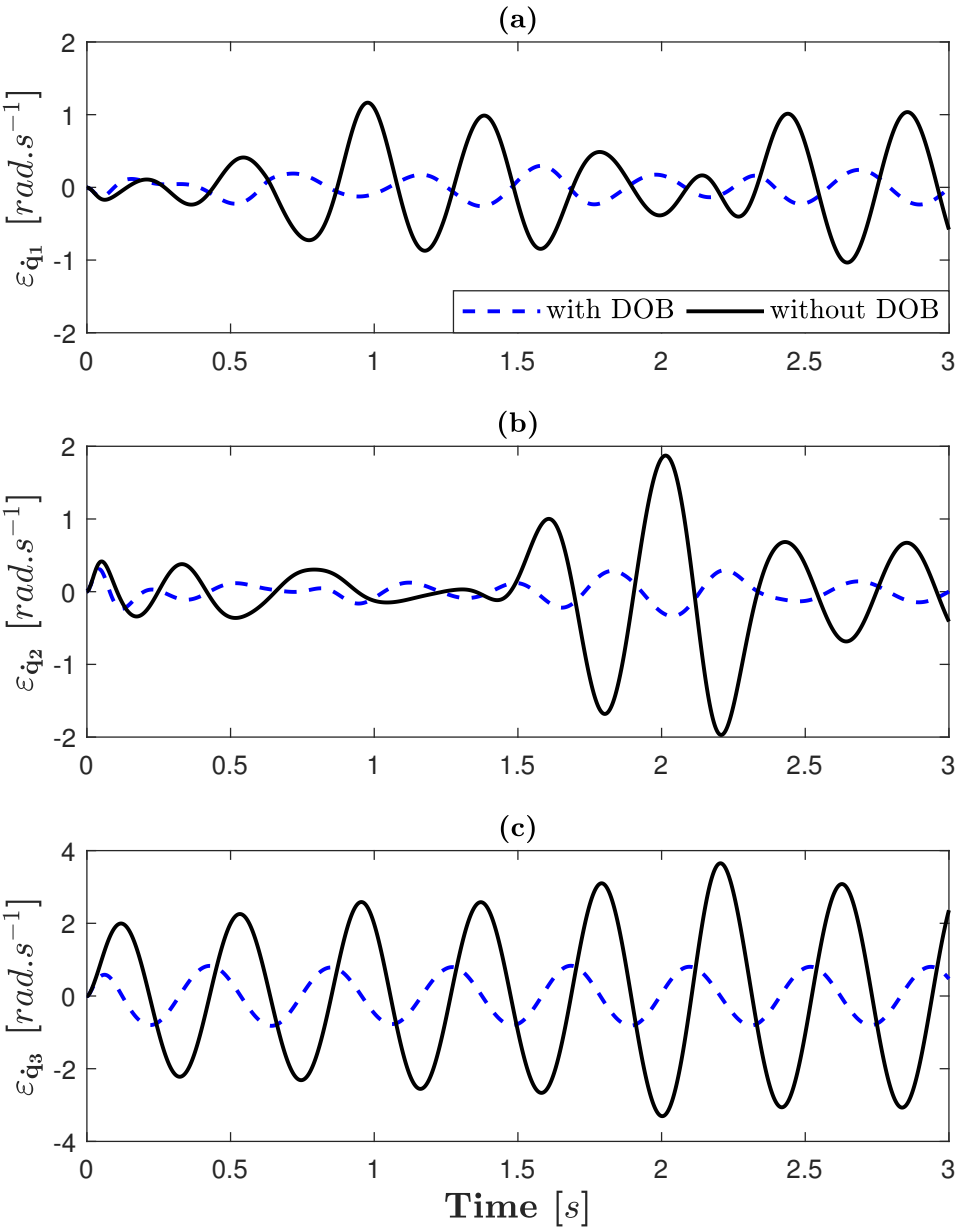

FIGURE IV.5: Velocity estimation error for linear trajectory with and without the proposed DOB.

we see that while the current approach slightly under performs with respect to the root mean square (RMS $[m]$) as well as the maximal absolute value (MAV $[m]$) of the end-effector position error along both axes X and Y, it performs much better with respect to the mean square root (RMS_u [Nm]) of the control input. This is due to the smooth shape of the estimated velocity in contrast with the noised velocity measurement.

b) Circular Trajectory Tracking

Figure IV.6 shows that the PID [Paccot, Andreff, and Martinet, 2009] and CTC [Mohammadi et al., 2013] controllers performs slightly better with respect to their performance on the linear trajectory alongside the X-axis. This observation is confirmed by the values of the root mean

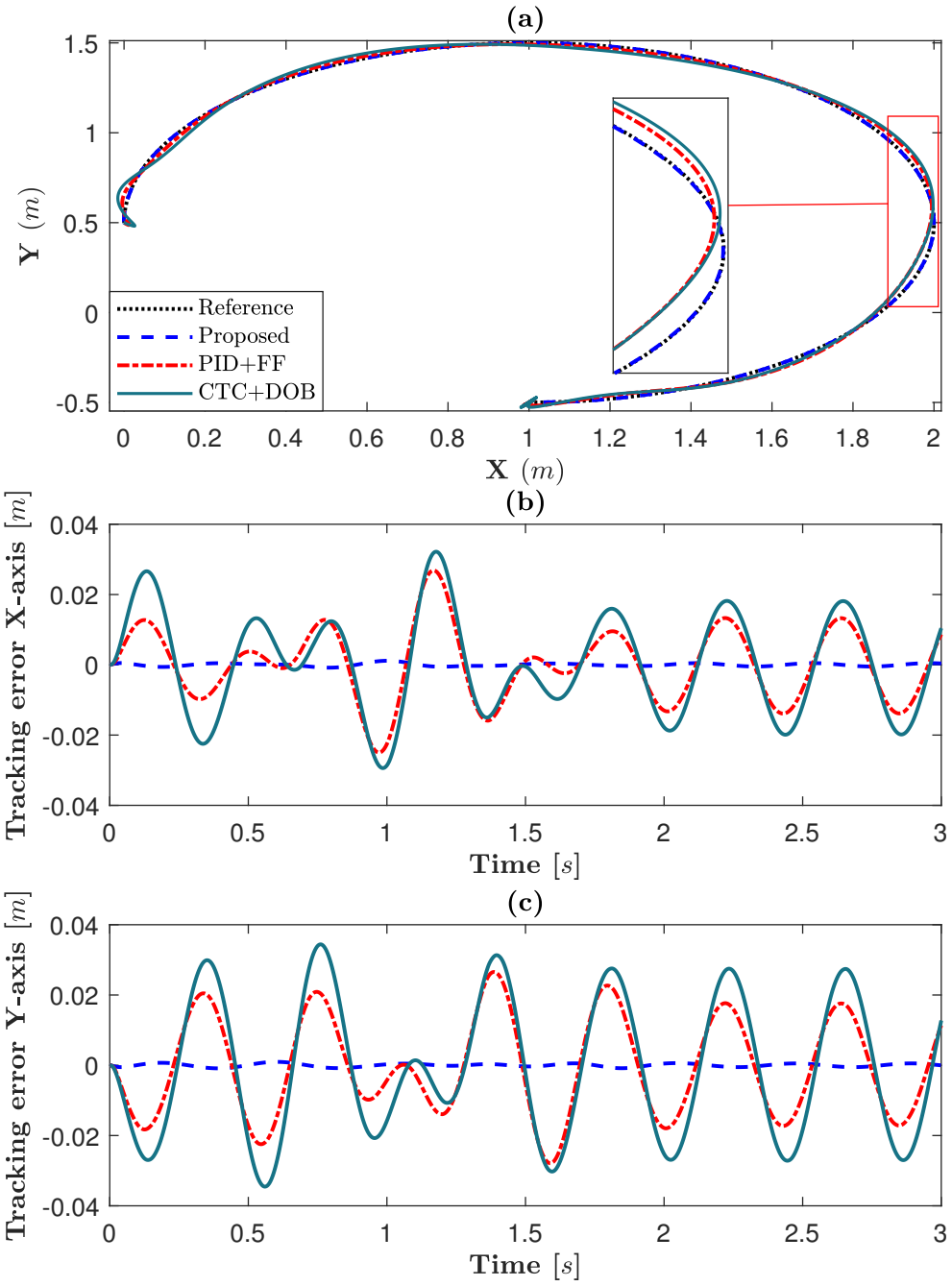

FIGURE IV.6: Comparison of tracking performance: (a) Curved trajectory tracking result in XY plane. (b) Tracking error alongside X-axis. (c) Tracking error alongside Y-axis. (d) Disturbance estimation by proposed DOB and [Mohammadi et al., 2013].

square error (RMS_X) and the maximal absolute value (MAV_X). On the other hand, the tracking performance alongside the Y-axis is slightly degraded on both the root mean square error (RMS_Y) and the maximal absolute value (MAV_Y). The proposed approach behaves similarly although still manages to outperform the other approaches with respect to tracking errors as shown in Table IV.2. Figure IV.7 shows the resulting control inputs for each approach tracking a curved trajectory. The shape of the control inputs is similar to the case of a linear trajectory with slightly different amplitudes. The values of RMS_u across all approaches for the curved trajectory tracking are lower than the case of linear trajectory as shown in Table IV.2, where

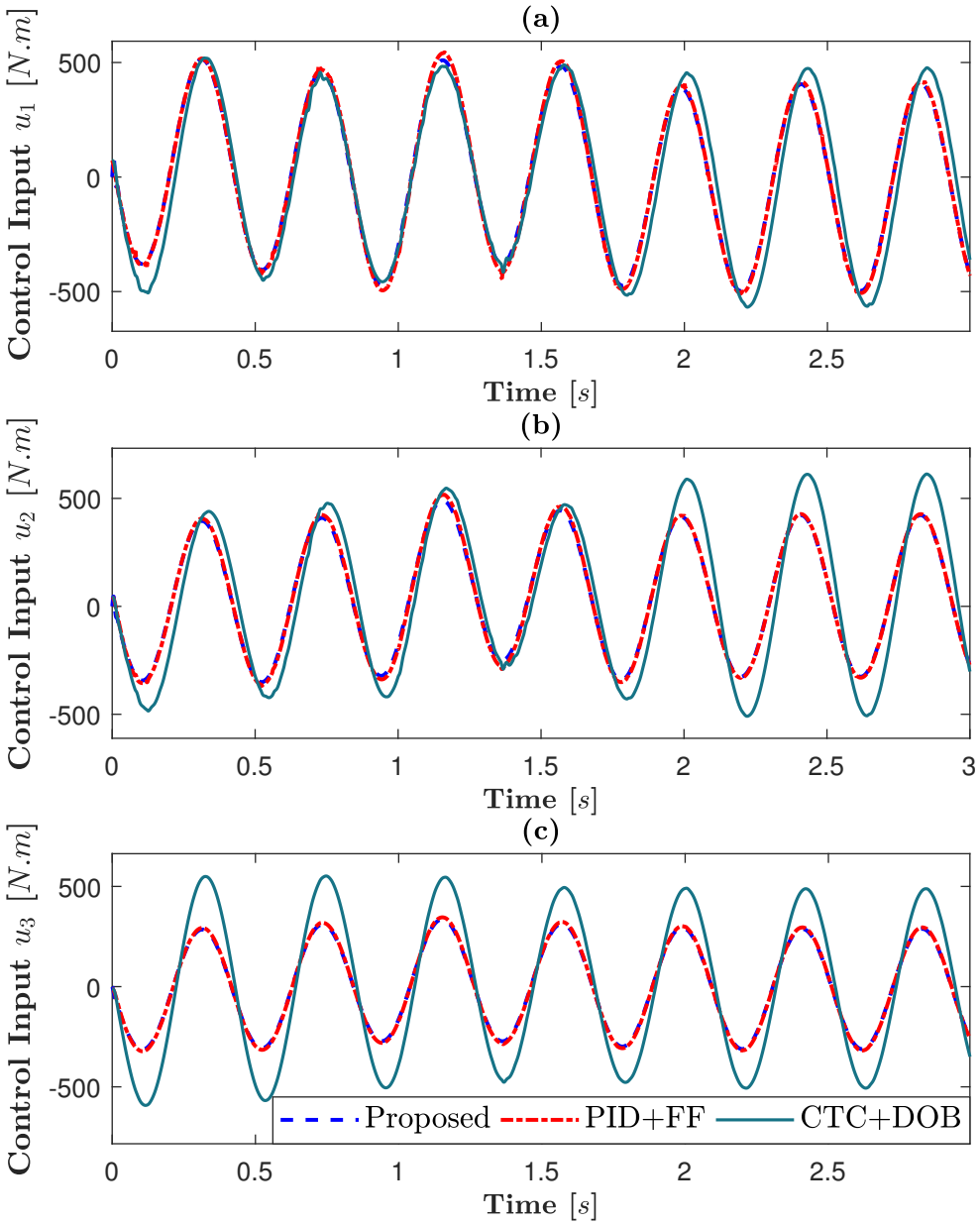

FIGURE IV.7: Comparison of control inputs and velocity estimation error for circular trajectory.

the proposed approach yields a lower input energy.

By comparing the result of the proposed observer-based tracking control design in this chapter to the performance of the $\mathcal{H}_\infty$-Performance approach in the previous chapter, we observe again a slight increase in both of the root mean square and the maximal absolute values alongside both axes X and Y.

As for the control input signal, a smooth shape is obtained in contrast with the control input of the $\mathcal{H}_\infty$-Performance design while the control gains of both approaches are of similar magnitude. This is mainly due to the observer-based approach not relying on the noised measurement of velocities and as result the mean input energy (RMS_u) is much lower.

TABLE IV.2: Circular trajectory tracking performance

Criterion	PID	CTC	$\mathcal{H}_\infty$-Design	Proposed DOB
RMS_X	10^{-2}	1.34×10^{-2}	1.84×10^{-4}	4.01×10^{-4}
RMS_Y	1.37×10^{-2}	1.89×10^{-2}	2.33×10^{-4}	4.28×10^{-4}
MAV_X	2.69×10^{-2}	3.22×10^{-2}	7.64×10^{-4}	1.2×10^{-3}
MAV_X	2.79×10^{-2}	3.45×10^{-2}	9.37×10^{-4}	9.65×10^{-4}
RMS_u	1.21×10^4	1.52×10^4	2.74×10^4	1.13×10^4

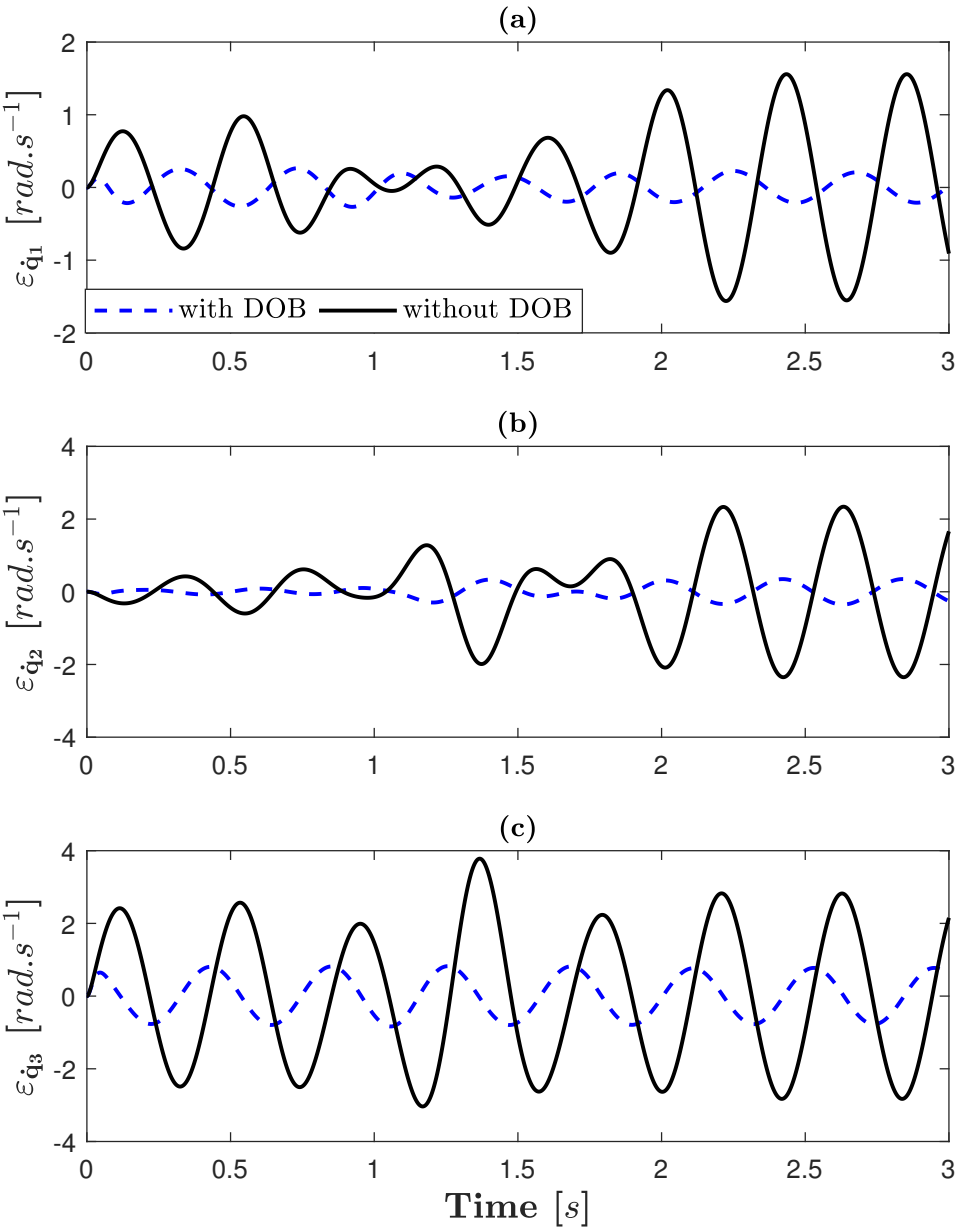

FIGURE IV.8: Velocity estimation error for circular trajectory with and without proposed DOB.

Remark IV.23. While the proposed observer-based approach under-performs in comparison with the $\mathcal{H}_\infty$-performance of the previous chapter, it remains a better alternative to both the PID and CTC controllers. Moreover, the reconstructed state control allows to negate the effect of noised velocity measurement, compensate the effect of external disturbances, and deal effectively with the considered parametric uncertainties and disregarded unmeasured premise variables.

Remark IV.24. Note that the disturbance model proposed in IV.36 supposes that its second time derivative is null *i.e.*, $\ddot{d}(t)$=0. However, due to the non-monotonic nature of the unmeasured premise variables $\bar{z}$ in the expression IV.75, this assumption does not hold. As a consequence, the precision on the estimation of the lumped disturbance $\hat{d}$ is lacking as shown in Figure IV.8. While the disturbance estimation is not accurate, it still offers an improvement via the compensating input $u_{dc}(t) = -\hat{d}_f(t)$ as it verifies $|d(t) - \hat{d}_f(t) < d(t)$. The tracking performance is ensured by the feedback control.

IV.5.2 A Parallel Manipulator Example

This section illustrates the tracking control problem for an uncertain 2-DoF planar parallel robot named "five-bar mechanism" [Briot and Khalil, 2015]. The robot is endowed with a Delta-like architecture and is composed of two identical 2DoF serial arm links joined at the point "S" as depicted in Figure IV.9. The dynamics of the robot are given by (IV.1) with

$$\hat{M}(\phi) = \begin{bmatrix} \hat{M}_a & \hat{M}_{ab} \\ \star & \hat{M}_b \end{bmatrix}, \quad \hat{N}(\phi, \dot{\phi}) = \begin{bmatrix} \hat{N}_a & \hat{N}_{ab} \\ \hat{N}_{ba} & \hat{N}_b \end{bmatrix}, \quad \hat{G}(\phi) = \begin{bmatrix} G_a \\ G_b \end{bmatrix}, \quad \mathcal{J}(\phi) = \begin{bmatrix} \mathcal{J}_a \\ -\mathcal{J}_b \end{bmatrix},$$

$$\hat{M}_a = \begin{bmatrix} c_4 & c_4\sigma_1 \\ 0 & c_4 \end{bmatrix}, \quad \hat{N}_a = 0, \quad \hat{G}_a = \begin{bmatrix} c_1\sigma_1 + c_1\sigma_{21} \\ c_1\sigma_2 \end{bmatrix}, \quad \hat{N}_{ab} = \begin{bmatrix} -c_3\sigma_7 & -c3\sigma\sigma_{20} \\ 0 & -c_3\sigma_8 \end{bmatrix}$$

$$\hat{M}_b = \begin{bmatrix} c_5 & -c_5\sigma_1 \\ 0 & c_5 \end{bmatrix}, \quad \hat{N}_b = 0, \quad \hat{G}_b = \begin{bmatrix} c_2\sigma_3 - c2\sigma_{23} \\ c_2\sigma_4 \end{bmatrix}, \quad \hat{N}_{ba} = \begin{bmatrix} c_3\sigma_9 & -c_3\sigma_{22} \\ 0 & c_3\sigma_{10} \end{bmatrix},$$

$$\hat{M}_{ab} = \begin{bmatrix} c_3\sigma_5 & c3\sigma_{19} \\ 0 & c_3\sigma_6 \end{bmatrix}, \quad \mathcal{J}_a = a \begin{bmatrix} -\sigma_1 + \sigma_{15} & \sigma_2 - \sigma_{16} \\ \sigma_{11} & -\sigma_{12} \end{bmatrix}, \quad \mathcal{J}_b = b \begin{bmatrix} \sigma_3 - \sigma_{17} & -\sigma_4 + \sigma_{18} \\ -\sigma_{13} & \sigma_{14} \end{bmatrix},$$

$$\mathfrak{h}(\phi) = \begin{bmatrix} a(\sigma_{11} - \sigma_{12}) + b(\sigma_{13} - \sigma_{14}) \\ a(\sigma_1 - \sigma_2) + b(\sigma_3 - \sigma_4) \end{bmatrix}, \quad \beta(\theta) = \begin{bmatrix} 1 & \sigma_1 \\ 0 & 1 \end{bmatrix},$$

where $\phi(t) = \begin{bmatrix} \theta(t)^\top & q(t)^\top \end{bmatrix}^\top \in \mathbb{R}^4$ is the vector of joint-space coordinates, $\theta(t) \in \mathbb{R}^2$ and $q(t) \in \mathbb{R}^2$ are respectively the active and passive joint positions, $\lambda(t)$ is the vector of internal forces acting on the joint point 'S', $\mathfrak{h}(\phi)$ is the vector of algebraic constraints caused by the closed kinematic loop of the parallel manipulator, $\mathcal{J}(\phi)$ is the Jacobian matrix of $\mathfrak{h}(\phi)$ with respect to $\phi(t)$, and

$$c_1 = g(m_a r_a + m_b a), \quad c_2 = g m_b r_b, \quad c_3 = m_b r_b a,$$
$$c_4 = I_a + m_a r_a^2 + m_b a^2, \quad c_5 = I_b + m_b r_b,$$

The nominal values of the robot parameters are given in Table IV.3, while the expressions of the nonlinearities σ_i, for $i \in \mathcal{I}_{23}$, are given in Table IV.4.

Remark IV.25. By writing the dynamics of a parallel manipulator under the algebraic differential form (IV.2), where the active joints are directly controlled and the passive joints are indirectly moved, it is possible to restraint the dynamics of the robot to the active joint-space coordinates yielding a serial manipulator like dynamics (IV.15). However, the process significantly

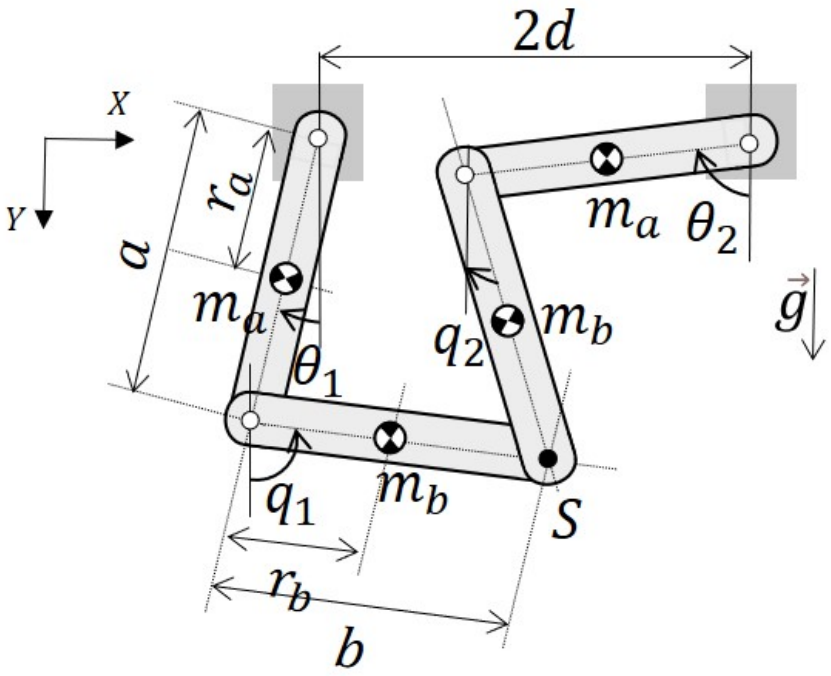

FIGURE IV.9: Schematic of the 2DoF parallel robot in the vertical plane.

TABLE IV.3: Parallel robot parameters.

Symbol	Description	Nominal value
g	Gravitational constant	9.81 [m/s^2]
a	Length of active arm links	0.165 [m]
b	Length of passive arm links	0.165 [m]
I_a	Inertia of active joints	0.0011 [kg.m^2]
I_b	Inertia of passive joints	0.0007 [kg.m^2]
m_a	Mass of active arm links	0.0825 [kg]
m_b	Mass of passive arm links	0.0825 [kg]
r_a	Center distance of active arm links	0.0825 [m]
r_b	Center distance of passive arm links	0.0825 [m]

increase the number of nonlinear terms in the system as it involves the inversion and product of nonlinear matrices. Indeed, for the case of serial manipulators the passive joint coordinates vector is null $q(t) \in \emptyset$ where $\phi(t) = \theta(t)$ and $\lambda(t) = 0$.

We denote $x(t) = \begin{bmatrix}\theta(t)^\top & \dot{\theta}(t)^\top\end{bmatrix}^\top \in \mathbb{R}^4$ and $u(t) = \beta(\theta)\Gamma(t) - G(\theta) \in \mathbb{R}^2$. Then, the considered robot model can be rewritten in the nonlinear descriptor form (IV.18) with

$$E(\sigma) = \begin{bmatrix} I & 0 \\ 0 & M_a \end{bmatrix}, \quad A(\sigma) = \begin{bmatrix} 0 & I \\ 0 & -N_a \end{bmatrix}, \quad B = \begin{bmatrix} 0 \\ I \end{bmatrix}. \tag{IV.76}$$

Note that since all parametric uncertainties and passive-joints related nonlinear terms are grouped in the lumped disturbance vector d in (IV.18) and $G_a(\theta)$ is fully incorporated in the virtual control input u, there remains only one measured premise variable $z(t) = \sigma_1(t)$ in the robot matrices defined in (IV.76). Then, this uncertain robot model can be represented in the quasi-LPV form (IV.28) with only $2^1 = 2$ submodels, *i.e.*, 2 vertices. The lumped disturbance

TABLE IV.4: Expressions of parallel robot nonlinearities.

Nonlinearity	Expression
σ_1	$\sin(\theta_1)$
σ_2	$\sin(\theta_2)$
σ_3	$\sin(q_1)$
σ_4	$\sin(q_2)$
σ_5	$\cos(q_1 - \theta_1)$
σ_6	$\cos(q_2 - \theta_2)$
σ_7	$\dot{q}_1 \sin(q_1 - \theta_1)$
σ_8	$\dot{q}_2 \sin(q_2 - \theta_2)$
σ_9	$\dot{\theta}_1 \sin(q_1 - \theta_1)$
σ_{10}	$\dot{\theta}_2 \sin(q_2 - \theta_2)$
σ_{11}	$\cos(\theta_1)$
σ_{12}	$\cos(\theta_2)$
σ_{13}	$\cos(q_1)$
σ_{14}	$\cos(q_2)$
σ_{15}	$\sin(\theta_1)\cos(\theta_1)$
σ_{16}	$\sin(\theta_1)\cos(\theta_2)$
σ_{17}	$\sin(\theta_1)\cos(q_1)$
σ_{18}	$\sin(\theta_1)\cos(q_2)$
σ_{19}	$\sin(\theta_1)\cos(q_2 - \theta_2)$
σ_{20}	$\dot{q}_2 \sin(\theta_1)\sin(q_2 - \theta_2)$
σ_{21}	$\sin(\theta_1)\sin(\theta_2)$
σ_{22}	$\dot{\theta}_2 \sin(\theta_1)\sin(q_2 - \theta_2)$
σ_{23}	$\sin(\theta_1)\sin(q_2)$

d in (IV.28) also includes the external force $\Gamma_{ext}(t)$ exerted on the joint 'S', given by

$$\Gamma_{ext}(t) = \begin{bmatrix} 15\sin(50t) \\ 15\sin(5t) \end{bmatrix}, \tag{IV.77}$$

and the uncertainty vector Γ_δ defined in (IV.12) with the following parametric uncertainties:

$$\Delta m_a = 40\%\ m_1, \quad \Delta m_b = 120\%\ m_2.$$

Uncertainties on end-effector payload are included in the parameters Δm_b. Similarly to the previous example, we perform a performance comparison between three control approaches

- Approach 1: FF-based PID control [Paccot, Andreff, and Martinet, 2009],
- Approach 2: CTC control [Briot and Khalil, 2015],
- Approach 3: quasi-LPV disturbance-observer-based control proposed in Theorem IV.11.

For Approach 1, the PID control law is given by (III.54) with

$$k_p = \begin{bmatrix} 634.71 & 634.71 \end{bmatrix}, \quad k_d = 10^4 \begin{bmatrix} 2.5254 & 2.5254 \end{bmatrix}, \quad k_i = 10^4 \begin{bmatrix} 5.3173 & 5.3173 \end{bmatrix}.$$

For Approach 2, the CTC control law is given by

$$\begin{aligned} u_{ctc}(t) &= M_\phi\ v(t) + N_{\phi,\dot{\phi}}\ \dot{\phi}(t) + G_\phi, \\ v(t) &= \ddot{\theta}_r 5T + g_p e_\theta(t) + g_d e_{\dot{\theta}}(t) + g_i \int_0^t e_\theta(\tau) d\tau, \end{aligned} \tag{IV.78}$$

where

$$
\begin{aligned}
&M_\phi = M_a + M_{ab}\mathcal{J}_b^{-1}\mathcal{J}_a + \mathcal{J}_a^\top \mathcal{J}_b^{-\top}(M_b\mathcal{J}_b^{-1}\mathcal{J}_a + M_{ab}),\\
&N_{\phi,\dot\phi} = \begin{bmatrix} N_{\theta,\dot\theta} & N_{q,\dot q}\end{bmatrix}, \quad G_\phi = G_a + G_q\\
&N_{\theta,\dot\theta} = M_{ab}\mathcal{J}_b^{-1}\dot{\mathcal{J}}_a + N_a + \mathcal{J}_a^\top \mathcal{J}_b^{-\top}(M_b\mathcal{J}_b^{-1}\dot{\mathcal{J}}_a + N_{ba}),\\
&N_{q,\dot q} = N_{ab} - M_{ab}\mathcal{J}_b^{-1}\dot{\mathcal{J}}_b - \mathcal{J}_a^\top \mathcal{J}_b^{-\top}(M_b\mathcal{J}_b^{-1}\dot{\mathcal{J}}_b + N_b),\\
&G_q = \mathcal{J}_a^\top \mathcal{J}_b^{-\top} G_b.
\end{aligned}
$$

The control gains of the CTC law are as such

$$
g_p = 10^4\begin{bmatrix}18.95 & 18.95\end{bmatrix}, \quad g_d = 10^4\begin{bmatrix}753.9822 & 753.9822\end{bmatrix}, \quad g_i = 10^4\begin{bmatrix}1587.5 & 1587.5\end{bmatrix}.
$$

It is important to note that the PID controller (III.54) and the CTC controller (IV.78) require the measurement of the active angular velocity $\dot\theta(t)$ for control implementation, which is not the case for Approach 3. For Approaches 1 and 2, the measurement of the velocities is made available with a small noise disturbance. Moreover, the CTC controller (IV.78) requires the online computation of the passive-joints position $q(t)$ and velocity $\dot q(t)$ as well as the inverse of the Jacobian matrix $\mathcal{J}_b$ and the first time derivatives $\dot{\mathcal{J}}_a$ and $\dot{\mathcal{J}}_b$.

For the control design of the proposed tracking controller, the values of the decay rates are selected as $\alpha_c = 15$ and $\alpha_o = 20$. The parameters of the disturbance filter $F(s)$ in (IV.35) are selected as $T_f = 10^{-3}$ and $K_f = 100$ as suggested in Remark IV.19. Then, solving the design conditions in Theorem I.2, an observer-based tracking controller can be obtained with an $\mathcal{L}_{2e}-$gain of $\gamma = 5\times 10^{-4}$. For illustrations, some of the feedback gains obtained with Theorem I.2 are given by

$$
\begin{aligned}
K_{p1} &= 10^4\begin{bmatrix}-1.238 & 0.365 & -0.006 & 0.001\\ -1.702 & -1.512 & -0.009 & -0.007\end{bmatrix},\\
K_{p2} &= 10^4\begin{bmatrix}-1.24 & 0.369 & -0.006 & 0.001\\ -1.7 & -1.514 & -0.009 & -0.007\end{bmatrix},\\
K_{I1} &= 10^4\begin{bmatrix}-51.697 & 15.621\\ -70.381 & -63.038\end{bmatrix},\\
K_{I2} &= 10^4\begin{bmatrix}-51.8 & 15.77\\ -70.316 & -63.144\end{bmatrix}.
\end{aligned}
$$

To illustrate the tracking performance of the three control approaches, the following tests are performed with a spiral trajectory using Simscape Multibody simulation environment in Matlab/Simulink.

a) Simulation Results and Comparative Study

Figure IV.10 shows that the proposed control scheme allows for a better trajectory tracking achieving smallest errors along X and Y axes compared to two other approaches. As also indicated in Table IV.5, both tracking error RMS and MAV show the superiority of the proposed approach over FF-based PID controller and DOB-based CTC controller. In addition to the tracking performance, the propose approach in this chapter relies solely on the measurement of the active joints position rendering the approach cost effective with respect to real time implementation. According to Figure IV.11, the behaviors of the control inputs obtained with the three control approaches are very similar, which is also confirmed by the comparison results in Table IV.5 where the three approaches yield a similar magnitude of torque inputs. While the FF-based PID control does not include a DOB compensation input, we observe that the feedback action instinctively seeks to compensate the lumped disturbance given its matching

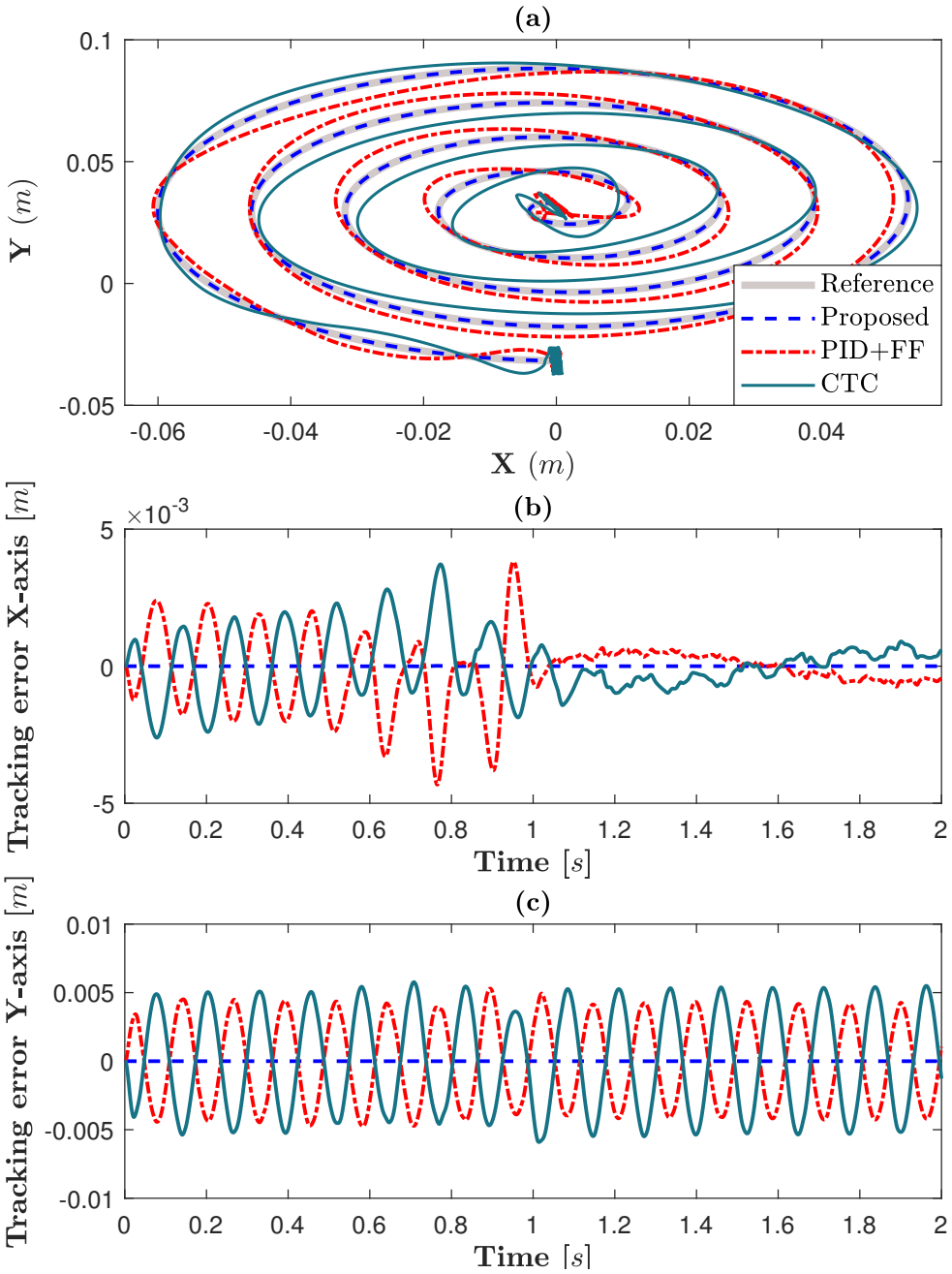

FIGURE IV.10: Comparison of tracking performance. (a) Spiral trajectory tracking in plan XY. (b) Tracking error along X-axis. (c) Tracking error along Y-axis.

nature with the input matrix. The DOB action offers a better compensation and hence improve upon the tracking performance.

Figure IV.12 presents a comparison of the active-joint angular velocity estimation errors for the parallel robot manipulator where the results indicate that the estimation is significantly improved when including the DOB input $u_{dc}(t)$. Note that the estimation can be improved upon by further tuning the static gain K_f of the estimated disturbance filter. While the estimated velocities are not exact it provides a better alternative to the noised measurement.

Moreover, the algebraic constraints of the parallel robot over time are fully respected as shown Figure IV.13. This validates the proposed approach where only the dynamics of the active joints are exploited for the control design while the algebraic constraints are only required

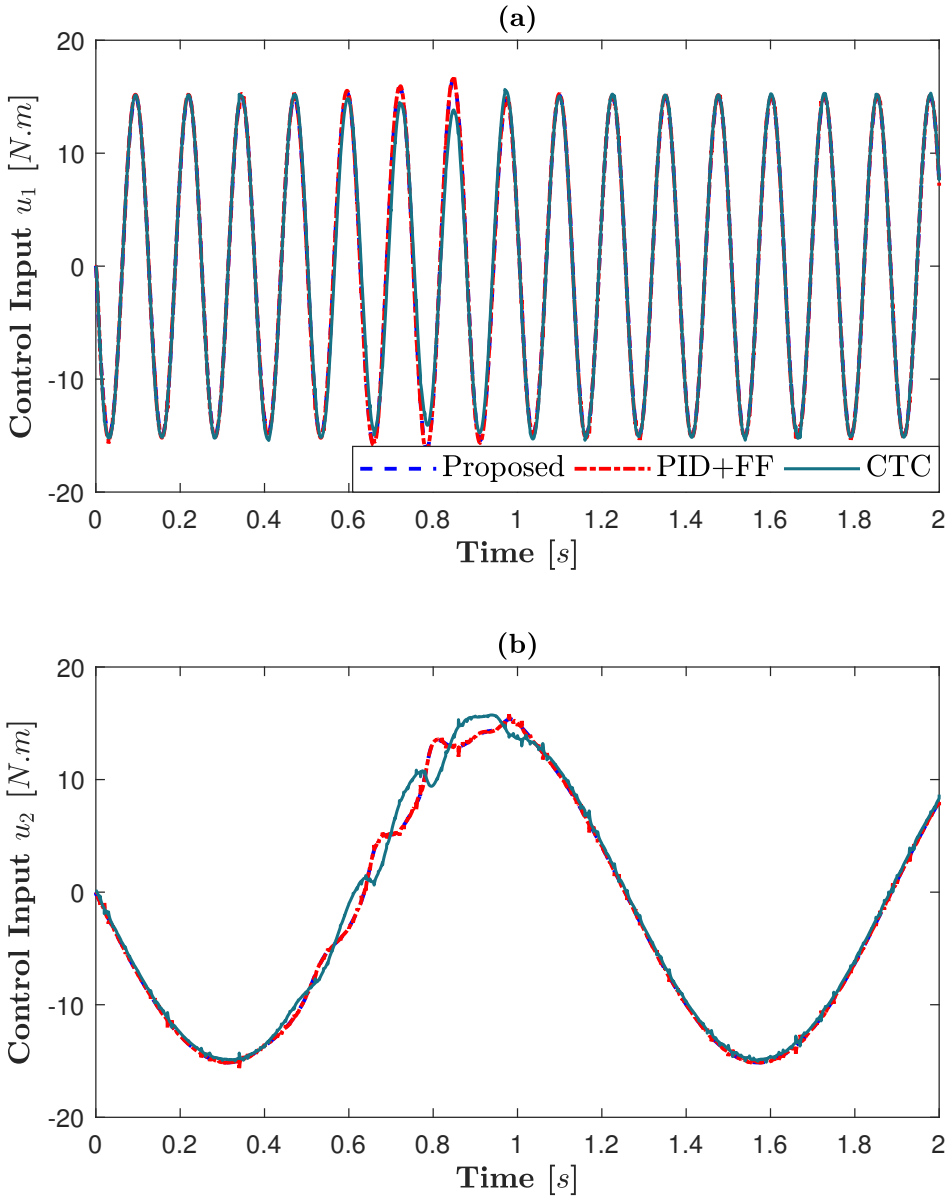

FIGURE IV.11: Comparison of control inputs in the case of spiral trajectory tracking.

TABLE IV.5: Spiral trajectory tracking performance

Criterion	PID	CTC	Proposed DOB
RMS_X $[m]$	1.2×10^{-3}	1.1×10^{-3}	1.25×10^{-4}
RMS_Y $[m]$	3×10^{-3}	3.6×10^{-3}	1.45×10^{-4}
MAV_X[m]	4.3×10^{-3}	3.7×10^{-3}	3.42×10^{-4}
MAV_X[m]	5.3×10^{-3}	5.9×10^{-3}	3.18×10^{-4}
RMS_u $[Nm]$	10.54	10.43	10.84

to determine a singularity-free desired reference trajectory.

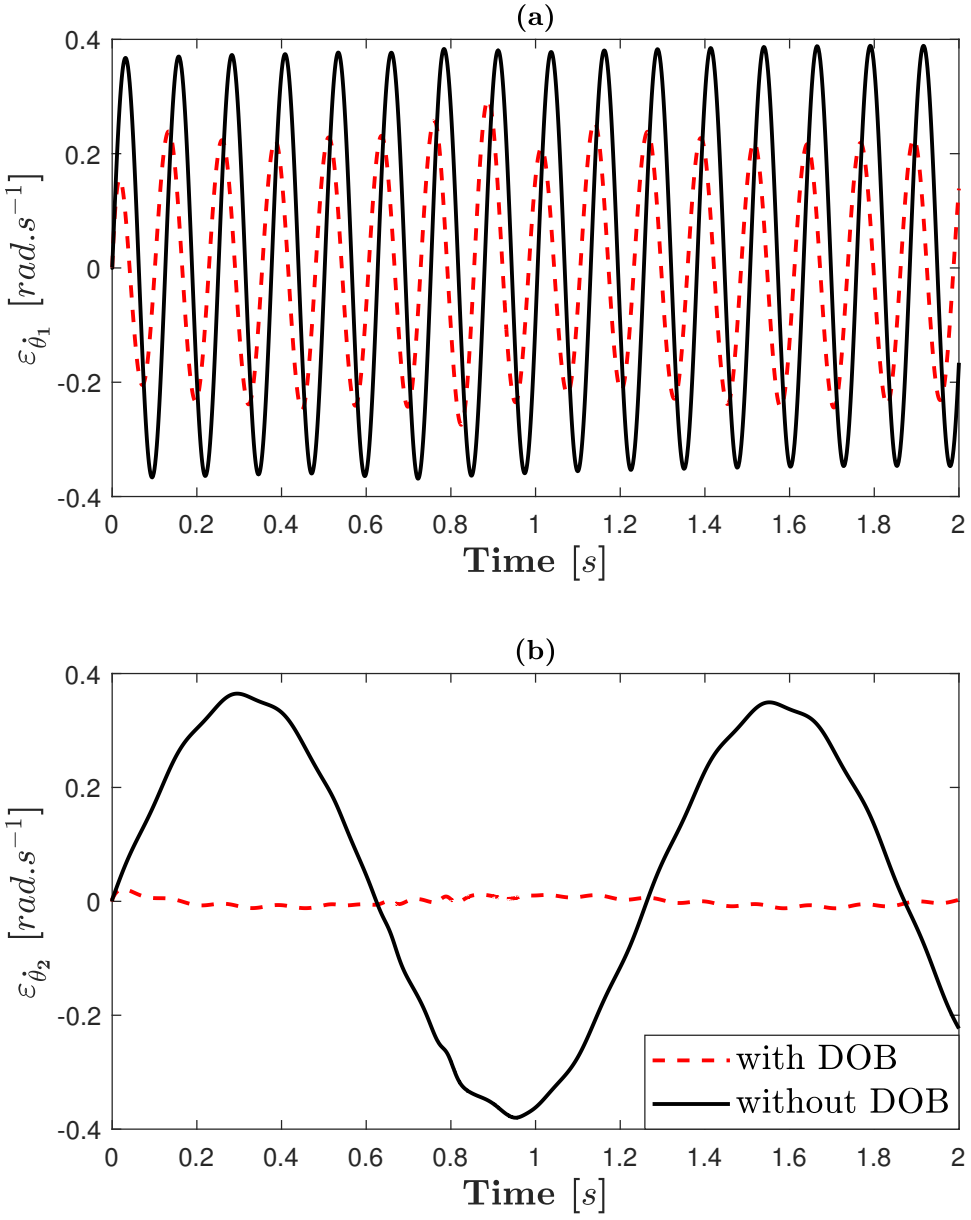

FIGURE IV.12: Active-joints angular velocities estimation error for spiral trajectory with and without proposed DOB.

To further highlight the contribution of the DOB-based compensation input $u_{dc}(t) = -\hat{d}_e(t)$, the following high-amplitude external force is considered in place of (IV.77):

$$\Gamma_{ext}(t) = \begin{bmatrix} 100\sin(50t) \\ 100\sin(50t) \end{bmatrix}.$$

The corresponding simulation results for the spiral trajectory tracking with and without DOB are depicted in Figure IV.14. We can clearly see the interest of the DOB-based compensation input to improve the robustness performance in terms of minimizing the disturbances effects. Indeed, the tracking errors along both X and Y axes are significantly lower in the presence of

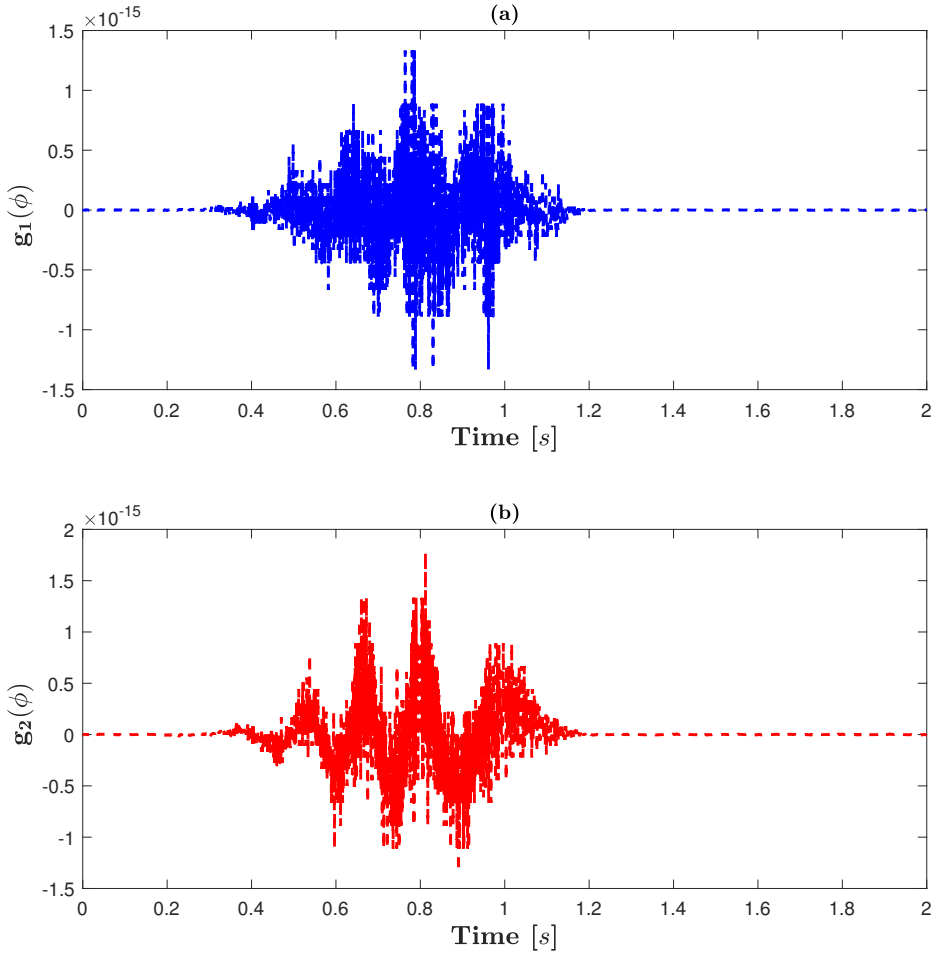

FIGURE IV.13: Value of the algebraic constraints over time.

the DOB-based compensation.

IV.6 Discussions on Control Performance with respect to Unknown Disturbances

The proposed quasi-LPV disturbance-observer-based control approach fundamentally relies on the model transformation from the algebro-differential model (IV.1) into the descriptor model (I.25). Despite its simplicity, the proposed approach allows deriving uncertain robot models with only measured premise variables, leading to tractable design conditions with a significantly reduced complexity. However, it is important to evaluate the extent to which the DOB-based approach can be effectively exploited for the compensation of unmodeled dynamics while maintaining an acceptable tracking control performance. For this purpose and for illustrations, we propose to evaluate the tracking performance, disturbance estimation, and state estimation of the previous 3DoF serial manipulator. For this robot system, the vector of premise variables σ was divided, according to (IV.22), into two subsets of measurable premises $z \in \mathcal{M}$ and unmeasured premise variables $\bar{z} \in \mathcal{U}$ as given in (IV.75). To evaluate the robustness performance with respect to unknown disturbances, we consider the two following cases where measured premise variables are further transformed as "unknown uncertainties" using (IV.24):

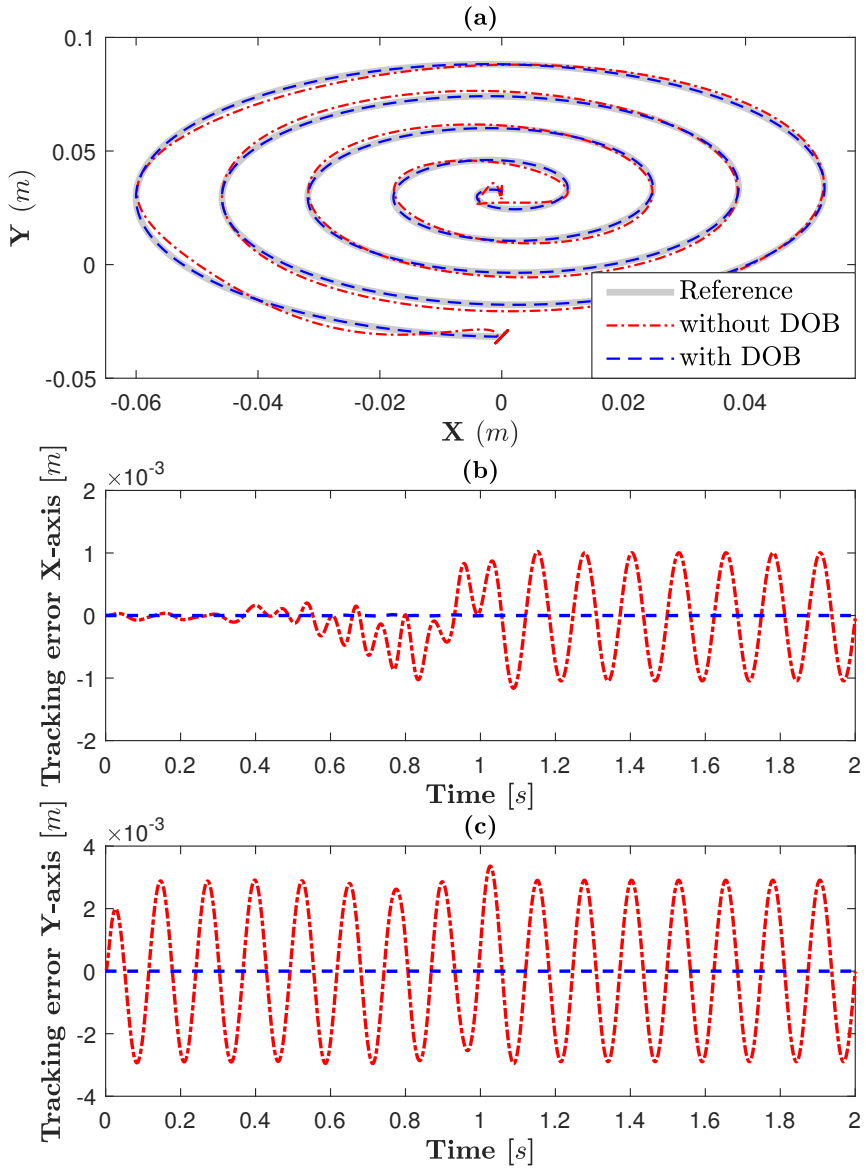

FIGURE IV.14: Comparison of tracking performance with a high-amplitude external force. (a) Circular trajectory tracking result in XY plan. (b) Tracking error along X-axis. (c) Tracking error along Y-axis.

- Uncertain robot model (I.25) with only one measured premise variable, *i.e.*,

$$z = \sigma_3,\ \bar{z} = \begin{bmatrix}\sigma_1 & \sigma_2 & \sigma_4 & \sigma_5 & \sigma_6 & \sigma_7 & \sigma_8 & \sigma_9\end{bmatrix}$$

- Uncertain robot model (I.25) without measured premise variable resulting in a linear uncertain model, *i.e.*,

$$z \in \emptyset,\ \bar{z} = \begin{bmatrix}\sigma_1 & \sigma_2 & \sigma_3 & \sigma_4 & \sigma_5 & \sigma_6 & \sigma_7 & \sigma_8 & \sigma_9\end{bmatrix}$$

Figure IV.15 shows that considering two measured premise variables for the polytopic modeling (IV.28) yields a better tracking performance than considering only one measured premises. However, the latter case still outperforms the CTC and PID controllers as shown in Table IV.6. On the other hand, the linear model obtained from considering all measured premises as unmodeled dynamics, yields the worst performance overall. We observe that the more we

consider measured premises as unmodeled dynamics to be lumped into the disturbance vector $d(t)$, the worse becomes the tracking performance. This aligns with the comparison with the $\mathcal{H}_\infty$-performance in the previous chapter where all premises are considered to be measured. We observe a similar behavior concerning the estimation of the lumped disturbance $d(t)$.

Figure IV.16 shows that considering more measured premises as unmodeled dynamics severally impacts the precision of states estimation with the best estimation obtained with two measured premises in the polytopic modeling (IV.28) and the worst estimation when zero measured premises are considered. The error on the estimation of the system states negatively impact the tracking precision. However, due to the robust feedback control the resulting performs is still superior to classic approaches with the exception of the linear model obtained by considering all measured premises as unmodeled dynamics.

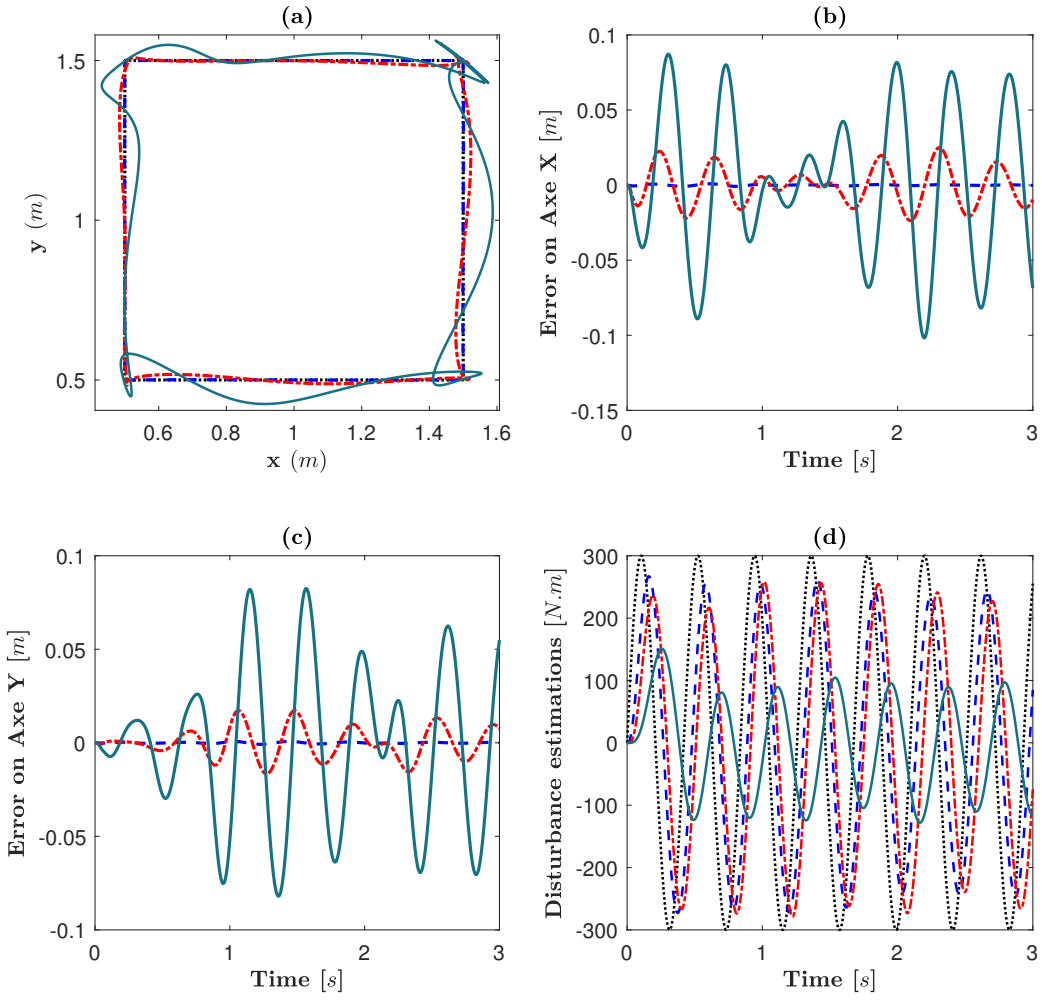

FIGURE IV.15: Comparison of disturbance-observer-based tracking control performance for different choices of partition of premise variables. (a) Linear trajectory tracking. (b) Tracking error along X-axis. (c) Tracking error along Y-axis. (d) Disturbance estimation. Reference (·····), two measured premise variables (- - -), one measured premise variable (–·–), without measured premise (——).

Remark IV.26. The proposed disturbance-observer approach presents an effective solution in dealing with parametric uncertainties and unmeasured premise variables as well as external disturbances. However, the approach requires the use of a robust feedback controller to guarantee

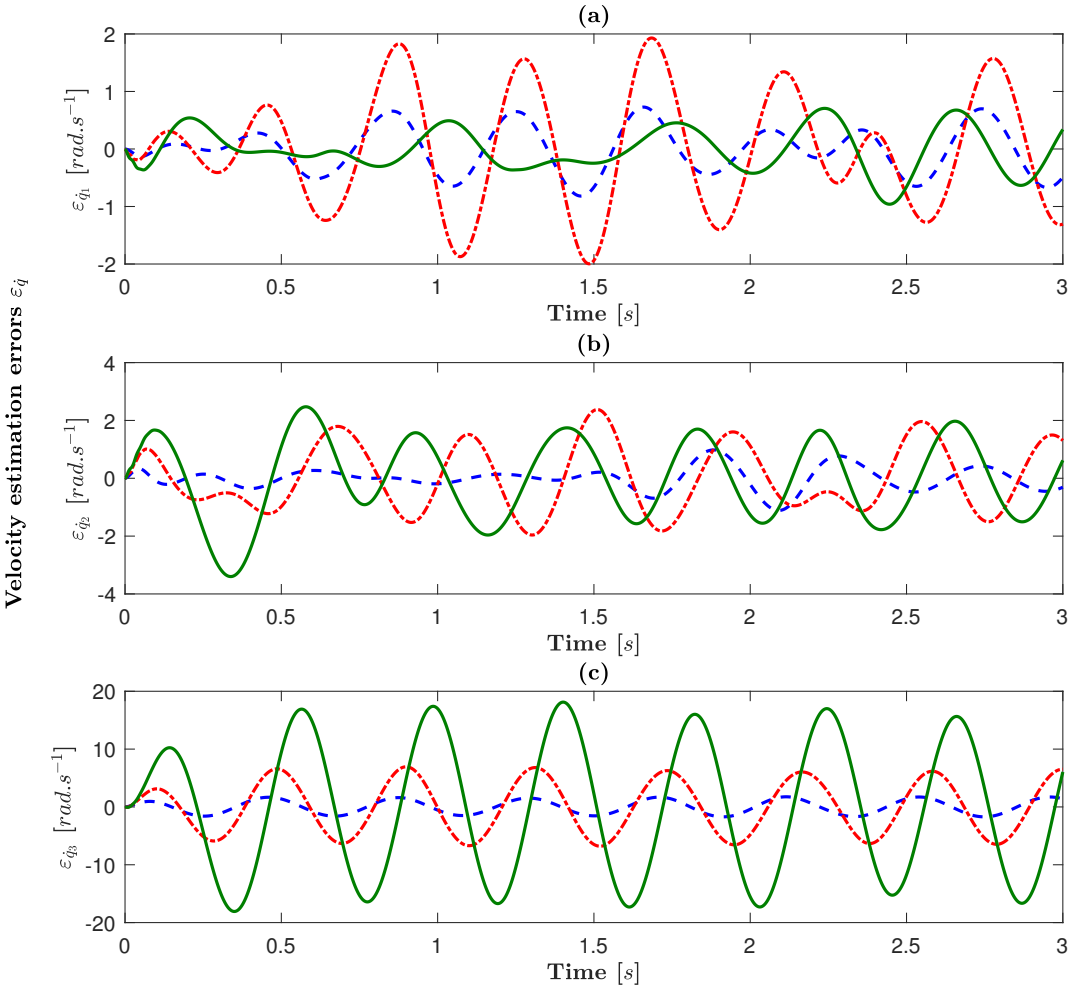

FIGURE IV.16: Comparison of disturbance-observer-based estimation precision for different choices of partition of premise variables. (a) Estimation error of angular velocity $\varepsilon_{\dot{\theta}_1}$. (b) Estimation error of angular velocity $\varepsilon_{\dot{\theta}_2}$. (c) Estimation error of angular velocity $\varepsilon_{\dot{\theta}_3}$. Two measured premise variables (- - -), one measured premise variable (–·–), without measured premise (——).

TABLE IV.6: Square trajectory tracking performance

Criterion	Two measured premise variables	One measured premise variable	Zero measured premise variables
RMS_X $[m]$	4.86×10^{-4}	1.17×10^{-2}	4.48×10^{-2}
RMS_Y $[m]$	3.64×10^{-4}	7.9×10^{-3}	3.84×10^{-2}
MAV_X $[m]$	1.2×10^{-3}	2.5×10^{-2}	1.02×10^{-1}
MAV_Y $[m]$	9.10×10^{-4}	1.73×10^{-2}	8.25×10^{-2}
RMS_u $[N.m]$	1.24×10^{4}	1.27×10^{4}	1.32×10^{4}

the tracking precision. While the approach allowed to derive uncertain robot model with only measured premise variables and derive tractable control-based model with a significantly reduced complexity, we have shown that the reduction of complexity in this case can result in a significant decrease in tracking performance. As such for an optimal tracking performance and design complexity it is best to moderate the re-partition of the premises and to only consider the unmeasured premise variables as unmodeled dynamics while keeping the measured nonlinear

terms of the system as much as possible for the polytopic model representation (II.8).

The proposed disturbance-observer approach presents an effective solution in dealing with parametric uncertainties and unmeasured premise variables as well as external disturbances. However, the approach requires the use of a robust feedback controller to guarantee the tracking precision. While the approach allowed to derive uncertain robot model with only measured premise variables and derive tractable control-based model with a significantly reduced complexity, we have shown that the reduction of complexity in this case can result in a significant decrease in tracking performance. As such for an optimal tracking performance and design complexity it is best to moderate the re-partition of the premises and to only consider the unmeasured premise variables as unmodelled dynamics while keeping the measured nonlinear terms of the system as much as possible for the polytopic model representation (II.8).

IV.7 Conclusions

In this chapter, we have tackled the problem of high precision trajectory tracking control for robot manipulators under algebraic constraints where the states are partially measured and presence of parametric uncertainties and unknown disturbances is considered. Dividing the total joint-space coordinates into active joint coordinates that are directly affected by the control input and passive joint coordinates that are directly unaffected by the control input, we proposed to restrain the system to only consider active joints-coordinates resulting into a regular descriptor system with no algebraic constraint. All related passive dynamics are represented by a single passive term which allowed for a seamless treatment of both serial and parallel manipulators alike.

Exploiting the particular structure of robot manipulators, the unmeasured scheduling variables alongside the structural uncertainties, the passive term and the external disturbances were grouped into a single lumped disturbance allowing for the DOB observer to estimate then compensate it accordingly. An elaborate mixed controller-observer design was proposed applying the DOB approach for reconstructing the state and compensating the disturbances. The DOB output feedback has been elaborated using the proposed polytopic form (IV.28) where the control law was composed of three separate inputs: a feedforward input, a disturbance-observer-based compensating input, and a robust estimated states feedback control action. The principle of separation was deployed to allow for a convex LMI design of both observer and controller gains. Its tracking performance was compared to classical PID with nonlinear feedforward and CTC controllers on both serial and parallel manipulators.

Despite its simplicity, the proposed approach allowed to derive uncertain robot model with only measured premise variables and derive tractable control-based model with a significantly reduced complexity. However, upon evaluating the extent to which the DOB approach can be effectively exploited for the compensation of unmodelled dynamics while maintaining peak tracking performance, we concluded that for an optimal tracking performance and design complexity, it is best to moderate the re-partition of the premises. The key is to only consider the unmeasured premise variables as unmodelled dynamics to be estimated and compensated while keeping the measured nonlinear terms of the system, as much as possible, for the polytopic model representation (IV.28).

Concluding Remarks & Perspectives

These thesis dissertation presents our contribution to model-based control of nonlinear singular systems and high precision trajectory tracking of robot manipulators.

Initially, we introduced the framework of model-based nonlinear control via convex optimization and the challenges it faces for highly nonlinear systems with respect to numerical complexity and conservatism of controller/observer designs, both from a feasibility standpoint as well as practical implementation. We limited our interest to a class of nonlinear singular systems that covers a large number of engineering applications. This framework include also regular systems, such as serial manipulators without algebraic constraint.

Chapter I of this dissertation was dedicated for a brief overview of TS Fuzzy modeling approach based on sector nonlinearity for the convex representation of nonlinear singular systems. Applying the definition of differential index, we have extended the notions of admissibility and stabilization of linear descriptor systems to the nonlinear singular case. A brief overview of LMI problem formulation was established. Then, LMI conditions for admissibility and stabilization of descriptor TS Fuzzy systems were presented using the direct Lyapunov method and the descriptor-redundancy approach. Next, we discussed the notion of robust control design with respect to parametric uncertainty and its linkage to the aforementioned model complexity of exact convex representation of nonlinear system. Finally, a reduced complexity affine TS modeling approach was proposed where a reduction of the vertices in the TS convex representation, from 2^r to $r+1$, was achieved where r is the number of premises. The proposed reduced complexity affine TS approach maintained an *exact* representation of the nonlinear singular system with a number of vertices that grows proportionally to the number of premises. However, the conservatism of the proposed reduced method with respect to the feasibility of design conditions was shown to be quite limiting. Furthermore, the proposed approach depends on the TS convex representation for the process of vertices reduction rendering the approach an unreliable option for the reduction of model complexity.

In Chapter II, we proposed a new polytopic quasi-LPV framework for nonlinear systems. Compared to the classical TS fuzzy-model-based control approaches, the numerical complexity of the new approach grows proportionally, rather than exponentially, with respect to the number of premise variables. This is particularly interesting when dealing with complex descriptor systems with a large number of nonlinearities. The issue of overbounding with respect to the vertices of the polytopic representation was evaluated and revealed to be the source of the conservatism in design condition. However, the system vertices obtained from the novel polytopic representation are not unique even with the same predefined set of premise variables. This non-uniqueness representation feature allows introducing specific slack variables into the control design to reduce the conservatism of the proposed approach. Strict LMI conditions are derived via Lyapunov stability theory for control design and admissibility analysis. A special attention is paid to the control design of regular nonlinear systems, for which the descriptor-redundancy approach is not required to further reduce the design complexity and conservatism. The interests of the new control results are clearly demonstrated with both numerical and physically motivated examples. From numerical experiments, it is observed that for nonlinear systems with a low number of premise variables the proposed method leads to admissibility analysis and control design results with a similar level of conservatism and numerical complexity as related existing TS fuzzy model-based approaches. However, when the number of premise variables becomes

sufficiently large, as illustrated in Example II.8, the strong interest of the new method related to numerical complexity and design conservatism reduction over TS fuzzy model-based approaches is put in evidence.

In Chapter III we have extended the proposed quasi-LPV modeling approach (II.8) to uncertain descriptor systems and provided a new treatment for parametric uncertainties where due to the unique additional properties of the polytopic approach, the parametric uncertainties can be modeled into the polytopic form (III.6). A new feedback control was proposed which ensures the stability of the resulting uncertain polytopic model. A comparison of the proposed approach to the classical treatment of uncertainties on two different examples of uncertain singular systems was provided, and the results have proven the proposed approach to be less conservative in finding a stabilizing feedback control. Additionally, we have targeted in this chapter the problem of high precision trajectory tracking control for serial manipulators with full measurement of the states and where the presence of parametric uncertainties and unknown disturbances is considerate. The proposed uncertain quasi-LPV approach (III.6) was shown to yield better tracking results in comparison with a combined PID and feedforward action [Paccot, Andreff, and Martinet, 2009] as well as a combined CTC and DOB approach [Mohammadi et al., 2013]. However, due to the slightly elevated gains of the proposed control design, the resulting control inputs are impacted by the presence of noise in the measurement of joint-velocities. To surpass this issue, we evaluated the possibility of a mixed controller-observer design to provide a noise free estimation of the velocity. Disregarding the measurement of joint-velocities introduced the problem of unmeasured scheduling variables to the mix. The viability of a separation in the design of the controller and observer gains in presence of said unmeasured scheduling variables was explored as well.

Finally, in Chapter IV, we have focused on the problem of high precision trajectory tracking control for robot manipulators under algebraic constraints where the states are partially measured and the presence of parametric uncertainties and unknown disturbances is considerate. Dividing the total joint-space coordinates into active joints coordinates that are directly affected by the control input and passive joints coordinates that are unaffected by the control input, we proposed to restrain the system to consider only active joints-coordinates resulting into a regular descriptor system with no algebraic constraint. All related passive dynamics are represented by a single passive term which allowed for a seamless treatment of both serial and parallel manipulators alike. Exploiting the particular structure of robot manipulators, the unmeasured scheduling variables alongside the structural uncertainties, the passive term, and the external disturbances were grouped into a single lumped disturbance allowing for the DOB observer to estimate then compensate it accordingly. An elaborate mixed controller-observer design was proposed applying the DOB approach for reconstructing the state and compensating the disturbances. The DOB output feedback has been elaborated using the proposed polytopic form (IV.28) where the control law was composed of three separate inputs: a previewed-feedforward input, a disturbance-observer-based compensating input, and a robust estimated state feedback control action. The principle of separation was deployed to allow for a convex LMI design of both observer and controller gains. Its tracking performance was compared to classical PID and CTC controllers on both serial and parallel manipulators. Despite its simplicity, the proposed approach allowed to derive uncertain robot model with only measured premise variables and derive tractable control-based model with a significantly reduced complexity. However, after evaluating the extent to which the DOB approach can be effectively exploited for the compensation of unmodelled dynamics while maintaining peak tracking performance, we concluded that for an optimal tracking performance and design complexity, it is best to moderate the repartition of the premises. The key is to only consider the unmeasured premises as unmodelled dynamics to be estimated and compensated while keeping the measured nonlinear terms of the system, as much as possible, for establishing the polytopic model representation (IV.28).

The work presented in this thesis opens up several development perspectives.

Short- to Medium-Term Perspectives

- A physical platform of the parallel delta robot in Figure IV.9 has been made available for conducting practical experiments. The aim is to validate the proposed DOB approach in real physical conditions and reproduce the simulation results obtained on the high fidelity *Simmechanics Multibody* simulation model on *Matlab*. We hope to finalize the experiment results in time to present at the thesis defense presentation.

- Extending the proposed polytopic model representation (II.8) to the discrete domain is also envisaged. Given that for the implementation of a sampled control input, a discrete controller is proven to be more efficient and yields better experimental results.

Long-Term Perspectives

- Due to the compensation of unmodelled dynamics, the estimations of the system state variables obtained via the observer are not accurate. While the estimation error did not affect the stability of the systems used as examples thanks to the robust feedback control action, we cannot prove that it will be the case for any given system. Additionally, for applications where the aim is to design accurate observers for either diagnostics or data analysis, it is worthwhile to seek alternative treatment of the unmeasured premises such as [Nguyen et al., 2021a] in order to fully exploit the proposed exact polytopic model representation (II.8).

- Given the recent results in the identification of LPV systems [Liu et al., 2014; Bombois et al., 2018; Ghosh et al., 2018], combining the process of identification with the proposed polytopic model representation can yield interesting results especially if the additional property II.9b and the introduction of the slack variables can be exploited to decrease the identification error.

RÉSUMÉ ÉTENDU EN FRANÇAIS

Introduction Générale et Contexte de la Thèse

Les travaux présentés dans cette thèse ont pour objectif l'évaluation de la viabilité de l'approche basée sur l'utilisation d'un modèle de Takagi-Sugeno (TS) pour la synthèse de lois de commande ou d'observation de systèmes robotiques complexes caractérisés par un nombre élevé de non-linéarités. Il s'agit alors de développer de nouveaux outils théoriques pour réduire la complexité numérique et le conservatisme de cette méthode tant dans la recherche de solution (étude de la faisabilité du problème d'optimisation associé) que dans l'implémentation du contrôleur/observateur. Nous considérons une classe de systèmes descripteurs non linéaires couvrant un grand nombre d'applications technologiques comprenant les manipulateurs robotiques sous contraintes algébriques.

Les robots manipulateurs sont largement utilisés dans différentes applications, que ce soit dans l'industrie comme l'automatisation du soudage et les chaînes de montage, en médecine comme la chirurgie robotique et les exosquelettes, ou pour les loisirs. La modélisation dynamique d'un robot manipulateur définit la relation entre la position angulaire de l'articulation, sa vitesse angulaire, son accélération angulaire et le couple nécessaire pour atteindre la position, la vitesse et l'accélération souhaitées pour l'effecteur terminal. L'application de la mécanique de Lagrange permet d'obtenir de manière systématique un modèle décrivant le mouvement du système sous forme d'équations différentielles couplées à des équations algébriques représentant les différentes contraintes mécaniques au sein du système. Ces équations différentielles algébriques, également appelées représentation d'état généralisée ou systèmes singuliers, fournissent un cadre naturel pour représenter et analyser un grand nombre d'applications d'ingénierie. Cependant, elles nécessitent des techniques plus complexes que les représentations d'état classiques, car outre la stabilité, les propriétés de régularité et d'admissibilité doivent être prises en compte. L'analyse de la stabilité des systèmes descripteurs est classiquement basée sur la notion d'indice de différentiation ou de technique de réduction de coordonnées. Néanmoins, ces méthodes nécessitent de nombreuses manipulations algébriques pouvant se révéler inadaptées pour une large classe de problèmes concrets. Pour éviter cet inconvénient, des méthodes de Lyapunov spécifiques aux systèmes descripteurs ont été proposées. Enfin, malgré des avancées significatives en analyse numérique, le problème de la stabilisation des systèmes descripteurs généraux reste un défi, en particulier pour les systèmes comportant un grand nombre de termes non linéaires.

La modélisation d'un système technologique en utilisant les principes de la physique conduit à une représentation du système avec des variables d'état possédant un sens physique. De manière pragmatique, il est possible de supposer que leurs amplitudes sont limitées. Sous cette hypothèse, une nouvelle description du modèle sous formes de systèmes linéaires (ou quasi-linéaire) à paramètres variant dans le temps de type polytopique. Ceci a motivé le développement de méthodes de synthèse de commande ou d'observation de type LPV (pour *linéaires à paramètres variant*) ou de Takagi-Sugeno (TS) performantes et robustes basées

sur l'utilisation de tels modèles et des techniques de l'optimisation semi-définie positive. La méthodologie TS est devenue l'une des techniques les plus populaires pour la commande des systèmes non linéaires comme l'atteste le grand nombre de publications illustrant l'efficacité pratique de l'approche pour des cas d'application réels. D'un point de vue théorique, il est possible d'obtenir des conditions de stabilité asymptotiquement nécessaires et suffisantes pour les systèmes TS. Néanmoins, en pratique, ces conditions de stabilité sont plus conceptuelles que pratiques puisque la charge de calcul augmente rapidement de sorte que la plupart des solveurs numériques se bloquent. Cela conduit à un autre défi des approches TS consistant à obtenir des conditions suffisantes les moins conservatrices possibles pour l'analyse de stabilité des systèmes non linéaires ou la synthèse de contrôleurs, avec une charge numérique raisonnable.

Les contributions récentes dans le domaine se concentrent sur l'introduction de nouvelles conditions LMI pour améliorer la faisabilité et réduire le conservatisme en introduisant des fonctions de Lyapunov non quadratiques [Lee, Park, and Joo, 2012; Guerra and Vermeiren, 2004; Mozelli, Palhares, and Avellar, 2009; Nguyen, Guerra, and Campos, 2019] ou des techniques de relaxation à sommes multiples [Sala and Ariño, 2007; Coutinho et al., 2020]. Cependant, un problème sous-jacent avec l'approche de modélisation TS est la relation de type exponentiel entre le nombre de sous-modèles linéaires locaux utilisés pour construire le modèle d'état et le nombre de variables de prémisse. Ainsi, si le modèle TS est basé sur p termes non linéaires, alors le nombre de sous-modèles est 2^p. La complexité induite peut rendre l'application de l'approche TS limitée aux systèmes ayant un petit nombre de non-linéarités. Pour surmonter cette sévère limitation, plusieurs approches ont été proposées comme l'utilisation de la décomposition en valeurs singulières des matrices du système conduisant, après troncature, à un modèle TS plus simple ou encore l'assimilation d'un certain nombre de non-linéarités du système à des termes incertains. Alternativement, des méthodes basées sur les données ont été proposées pour la réduction de la dimension des variables de prémisse comme, *par exemple*, l'analyse en composantes principales ou l'emploi de réseaux neuronaux profonds. Cependant, ces méthodes de modélisation altèrent le modèle initial, elles peuvent donc s'avérer inadaptées lorsque des performances dynamiques poussées sont attendues. En particulier, les approches basées sur les données reposent fondamentalement sur des données expérimentales obtenues à partir de trajectoires typiques des variables du système ou à travers des simulations approfondies pour collecter des données. Ce qui peut entraîner un coût de calcul important, en particulier lorsqu'il s'agit de systèmes non linéaires ayant un grand nombre de variables d'état ou nombre de terme non linéaire. De plus, en raison de la dépendence sur la qualité des données pour ces approches "basée sur les données" pour la concepton du modèle, l'analyse de la stabilité et les performances de contrôle obtenues avec les modèles résultants dépendent aussi fortement des données représentatives collectées.

Pour cette thèse, de nouvelles approches représentant d'une manière exacte et équivalente les systèmes non linéaires sous formes polytopiques convexe ont été proposées. l'objectif est réduire à la fois la complexité numérique et le conservatisme du design des contrôleurs/observateurs par rapport à l'implémentation en pratique et à la faisabilité de la solution. Des conditions LMI pour l'analyse d'admissibilité et la stabilisation des systèmes singuliers non linéaires sont développés en utilisant les représentations polytopiques exactes proposées. Plusieurs exemples numériques avec différents degrés de complexité numérique seront présentées pour illustrer l'efficacité des approches proposées. Nous ciblons également le problème du suivi de trajectoire à haute précision des robots manipulateurs avec la présence d'incertitudes structurelles et de perturbations externes en se basant uniquement sur la mesure de position.

Structure de la Thèse

La thèse est composée de quatre chapitres :

- Chapitre I : Introduction à la modélisation Takagi-Sugeno par secteur non-linéaire.
- Chapitre II : Un nouveau cadre quasi-LPV polytopique pour les systèmes non linéaires.
- Chapitre III : Suivi de trajectoire robuste pour les systèmes descripteurs incertains.
- Chapitre IV : Suivi de trajectoire basé sur un observateur de perturbations pour les robots manipulateurs.

Chapter I : Modélisation Takagi-Sugeno par secteur non-linéaire

La théorie des ensembles flous a été développée par [Zadeh, 1965] dans les années soixante, et constitue un outil puissant pour la représentation de classes ambiguës d'objets physiques. Cette approche découle de la capacité de l'homme à décider et à agir de manière intelligente, basée sur des capacités d'observation et une tendance naturelle à catégoriser et classer les objets et les expériences. Dans le domaine de l'automatique, la théorie a été introduite comme un outil permettant à un expert de mettre en œuvre méthodiquement ses connaissances et son expertise pour le contrôle de systèmes physiques complexes ou difficilement modélisables. Le premier article sur la commande floue a été publié en 1975 par [Mamdani and Assilian, 1975] posant les bases et les principes de l'application de la logique floue à la conception d'nu correcteur. La mise en œuvre réussie de la commande floue sur le métro de Sendai au Japon a rendu l'approche célèbre et suscité l'intérêt de nombreux chercheurs dont les apports relatifs dans ce domaine ne cessent de croître à ce jour. L'un des avantages historiques de cette approche est qu'elle ne nécessite pas de modèle mathématique pour la conception de la commande, ce qui rend l'approche attrayante lorsqu'il s'agit de systèmes physiques difficiles à modéliser ou qui produisent des modèles mathématiques complexes [Takagi and Sugeno, 1985]. Cependant, le caractère heuristique de l'approche est problématique lorsqu'il s'agit d'applications pour lesquelles une certaine garantie de robustesse et une preuve de stabilité de la conception de la commande sont cruciales. Pour rompre les liens avec la nature heuristique de l'approche de commande floue, [Tanaka and Sugeno, 1992] a proposé une approche alternative basée sur un modèle tout en conservant la même philosophie de conception de la logique floue. L'approche qui en a résulté présentait une grande similitude dans sa formulation mathématique avec les modèles LPV [Sala, Guerra, and Babuška, 2005] permettant l'utilisation d'outils théoriques de base en automatique comme la théorie de la stabilité de Lyapunov et la formulation LMI.

Au cours des dernières décennies, les modèles TS ont été largement utilisés pour la représentation des systèmes non linéaires. Caractérisée par un ensemble de règles floues Si-Alors dont les parties conséquentes sont des représentations linéaires locales, l'approche de modélisation floue TS peut représenter un système non linéaire par une combinaison convexe de modèles linéaires [Tanaka, Ikeda, and Wang, 1998; Sala and Ariño, 2009]. Le passage du modèle non linéaire à la représentation TS peut s'effectuer par linéarisation autour de plusieurs points de fonctionnement [Johansen, Shorten, and Murray-Smith, 2000] ou par l'utilisation de l'approche par secteur non linéaire [Ohtake, Tanaka, and Wang, 2003]. Éprouvée comme constituant une classe d'approximations universelles [Tanaka and Wang, 2004], l'approche du modèle flou fournit une solution puissante pour le développement de l'approximation de fonctions, l'identification de systèmes ainsi que des techniques systématiques d'analyse de stabilité et de synthèse de lois de commande. En fait, pour des systèmes non linéaires suffisamment lisses, une représentation équivalente peut être obtenue de manière semi-globale en utilisant l'approche de modélisation TS basée sur la décomposition en secteurs non linéaires.

L'étude de la stabilité ou de la stabilisation des modèles TS est généralement basée sur le choix d'une fonction de Lyapunov candidate. En imposant un comportement dissipatif à cette fonction, on aboutit souvent à des conditions de stabilité sous forme d'inégalités matricielles linéaires [Tanaka and Wang, 2004]. Une fois ces conditions établies, des algorithmes d'optimisation convexe sont utilisés pour résoudre le problème semi-défini ainsi formulé [Gahinet et al., 1995; Boyd et al., 1994].

L'objectif de ce chapitre est de fournir un bref aperçu des différents résultats pour les modèles TS continus basés sur l'approche des secteurs non linéaires. Tout d'abord, une description de l'approche TS ainsi que la procédure de modélisation d'une classe de systèmes non linéaires sont données. Dans la deuxième partie, nous passons en revue les principaux résultats en stabilité, stabilisation et robustesse pertinents pour les travaux présentés dans la suite de ce manuscrit. Nous discutons ensuite du principal inconvénient de toutes les approches polytopiques de modélisation exacte, y compris l'approche floue TS, c'est-à-dire la complexité de la modélisation qui

croît de façon exponentielle avec le nombre des paramètres variants. Nous discutons des solutions suggérées dans la littérature et proposons une première tentative pour réduire systématiquement la complexité des modèles TS.

Chapter II : Un nouveau cadre quasi-LPV polytopique pour les systèmes non linéaires

Pour les approches LPV polytopiques existantes, la complexité numérique de l'analyse de stabilité, de l'observation et des conditions de conception de contrôle *exponentiellement* augmente par rapport au nombre des paramètres variants [Rizvi et al., 2016]. Cela limite l'applicabilité de telles approches à des systèmes avec seulement peu de non-linéarités ou de paramètres variant dans le temps [Hoffmann and Werner, 2015]. Pour pallier cet inconvénient majeur, des méthodes basées sur les données ont été proposées pour réduire le nombre des paramètres variants dans les modèles LPV polytopiques, comme, par exemple, l'analyse en composantes principales (ACP) [Kwiatkowski and Werner, 2008], l'ACP du noyau [Rizvi et al., 2016], les réseaux de neurones profonds [Koelewijn and Tóth, 2020]. Cependant, ces méthodes souffrent de quelques inconvénients majeurs. Premièrement, nous ne pouvons traiter des systèmes non linéaires qu'au sens de l'approximation, ce qui pourrait être inadapté aux systèmes dynamiques non linéaires rapides. Deuxièmement, ces méthodes de réduction des paramètres reposent fondamentalement sur des données expérimentales obtenues à partir de trajectoires des prémisses typiques, qui nécessitent non seulement des étapes d'optimisation supplémentaires, mais également des simulations approfondies pour collecter des données. Troisièmement, en raison de la fonctionnalité "basée sur les données", les performances obtenues avec les modèles LPV résultants dépendent fortement des données collectées.

D'un point de vue théorique, il est possible de dériver des conditions de stabilité nécessaires et suffisantes pour les systèmes quasi-LPV [Sala and Ariño, 2007]. Néanmoins, en pratique, ces conditions de stabilité sont plus conceptuelles qu'implémentables puisque la charge de calcul augmente si rapidement la plupart des solveurs numériques échouent à obtenir une solution numérique [Nguyen et al., 2019]. Cela conduit à un autre défi des approches LPV dans la dérivation de conditions suffisantes moins conservatrices pour l'analyse de stabilité des systèmes non linéaires et la synthèse des gains du correcteur/observateur avec une charge numérique raisonnable. Ensuite, pour réduire le conservatisme de conception, diverses fonctions de Lyapunov poly-quadratiques ont été efficacement exploitées dans la littérature pour les systèmes LPV [Briat, 2014; Nguyen, Chevrel, and Claveau, 2018; Mohammadpour and Scherer, 2012]. Contrairement à la stabilité quadratique, l'exploitation des informations sur les paramètres variants et leurs taux de variation joue un rôle clé pour la stabilité poly-quadratique des systèmes LPV [Wu et al., 1996; Apkarian, Gahinet, and Becker, 1995; Sato, 2011; Nguyen, Chevrel, and Claveau, 2018]. Cependant, dans le cadre quasi-LPV, les paramètres variants dépendent du vecteur d'état. Les informations sur la dérivée temporelle des paramètres variants ne sont généralement pas disponibles pour la conception de commande de systèmes singuliers. Cela implique beaucoup plus de difficultés numériques ou théoriques lors de l'utilisation de fonctions de Lyapunov polyquadratiques, également appelées fonctions de Lyapunov non quadratiques ou multiples [Tanaka, Ohtake, and Wang, 2007; Mozelli, Palhares, and Avellar, 2009; Márquez et al., 2016], pour l'analyse de stabilité et la synthèse de commande de systèmes quasi-LPV en temps continu. La plupart des résultats de commande existants sont formulés à l'aide de paramètres d'analyse *local* avec différents degrés de prudence [Nguyen et al., 2019]. Notez que dans le cadre de commande quasi-LPV polytopique local, il n'est toujours pas possible de **théoriquement** démontrer que les résultats non quadratiques incluent ceux dérivés des fonctions de Lyapunov quadratiques.

Ce chapitre présente une solution à deux principaux inconvénients de l'approche polytopique quasi-LPV que sont la complexité numérique des conditions permettant le calculs des différents paramètres de la loi de commande et le conservatisme des lois de commande résultantes. Nous introduisons ainsi dans ce chapitre un nouveau modèle systématique de représentation polytopique quasi-LPV des systèmes non linéaires où le nombre de sommets ne croît que de manière *proportionnelle* en fonction du nombre de prémisses. De plus, pour un même ensemble prédéfini de variables de prémisse, les sommets des modèles polytopiques obtenus ne sont pas fixés de manière

unique et peuvent admettre un nombre *infini* de représentations . Ceci permet d'introduire certaines variables de relaxation spécifiques à l'étape de modélisation afin de réduire le conservatisme de la conception de la commande. Sur la base de la représentation polytopique proposée et de la théorie de la stabilité de Lyapunov, nous dérivons une analyse d'admissibilité à complexité réduite et des conditions de synthèse de correcteurs, exprimées en termes d'inégalités matricielles linéaires, pour la classe de systèmes descripteurs considérée. Enfin, une nouvelle loi de commande non linéaire est proposée pour les systèmes descripteurs réguliers permettant d'éviter l'utilisation classique de la forme de redondance étendue, qui peut produire des résultats numériquement complexes et conservateurs en raison de la structure de commande spéciale imposée. Des exemples tant académiques que pratiques sont donnés pour démontrer l'intérêt de la nouvelle approche de commande par rapport aux résultats existants basés sur un modèle TS.

Considérant le système LPV suivant :

$$E(\alpha)\dot{x}(t) = A(\alpha)x(t) + B(\alpha)u(t) \tag{IV.79}$$

où $\alpha(t) \in \mathbb{R}^r$ est le vecteur des paramètres variables. La représentation polytopique équivalente du système LPV (IV.79) est donnée par :

$$\sum_{i=1}^{n_r} h_i(\alpha)\tilde{E}_i\dot{x}(t) = \sum_{i=1}^{n_r} h_i(\alpha)(\tilde{A}_i x(t) + \tilde{B}_i u(t)) \tag{IV.80}$$

avec un nombre de sommets $n_r = 2^r$ et pour tout $j \in \{1, 2, \ldots, q\}$

$$h_i(\alpha) = \prod_{j=1}^{r} \omega_j^{i_j}(\alpha_j), \quad \omega_j^0(\alpha_j) = \frac{\alpha_j^1 - \alpha_j}{\alpha_j^1 - \alpha_j^0}, \quad \omega_j^1(\alpha_j) = 1 - \omega_j^0(\alpha_j),$$
$$\sum_{i=1}^{n_r} h_i(\alpha) = 1, \quad 0 \le h_i(\alpha) \le 1, \quad \forall i \in \{1, 2, \ldots, n_r\}$$

et $i = 1 + i_1 + i_2 \times 2 + \cdots + i_r \times 2^{r-1}$, $i_p \in \{0, 1\}$ (c'est-à-dire $i_r i_{r-1} \ldots i_1$ est la représentation binaire du nombre entier $i - 1$). En revanche, l'approche quasi-LPV proposé dans cette thèse aboutit à la représentation polytopique *équivalente* suivante :

$$\sum_{i=1}^{2r} w_i(\alpha)E_i\dot{x}(t) = \sum_{i=1}^{2r} w_i(\alpha)(A_i x(t) + B_i u(t)) \tag{IV.81}$$

avec

$$w_{2p-1}(\alpha) = \frac{1}{r}\frac{\alpha_j^1 - \alpha_j}{\alpha_j^1 - \alpha_j^0}, \quad w_{2p-1}(\alpha) + w_{2p}(\alpha) = \frac{1}{r}, \quad \forall p \in \{1, 2, \ldots, r\}$$
$$\sum_{i=1}^{2r} w_i(\alpha) = 1, \quad 0 \le w_i(\alpha) \le \frac{1}{r}, \quad \forall i \in \{1, 2, \ldots, 2r\}$$

La représentation polytopique proposée (IV.81) contient un nombre de prémisse égale à $2r$ qui évolue d'une manière proportionnel en fonction du nombre des paramètres variables contrairement à la forme polytopique classique (IV.80) où le nombre de sommet évolue d'une manière exponentiel en fonction du nombre des paramètres variables. D'autre part, les poids non linéaire de la forme polytopique proposée, en plus de vérifier la somme convexe, sont dotés d'une propriété additionnel permettant l'introduction de variables de relaxation afin de réduire le conservatisme du design indépendamment du choix de la fonction de Lyapunov ou du contrôleur/observateur.

La figure IV.17 illustre l'évolution des variables de décisions $\mathcal{N}_{var}$ et le nombre des contraintes LMI $\mathcal{N}_{row}$ pour les conditions d'analyse avec l'approche polytopique proposée. On présente le

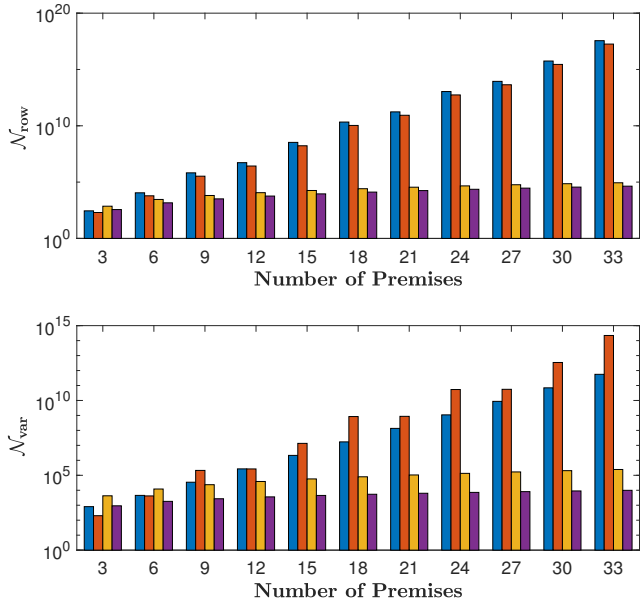

FIGURE IV.17: Nombres caractéristiques de complexité numérique par rapport au nombre de variables de prémisse r pour le cas $n = 5$ et $m = 0$: Théorème 1 proposé ■ ; Théorème 2 proposé ■ ; He et al., 2021, Theorem 3.3 ■ ; Bouarar, Guelton, and Manamanni, 2010, Théorème 2 ■.

Théorème 1 utilisant une forme descripteur étendue et le Théorème 2 sous forme descripteur non redondante en comparaison avec des approches de la littérature

Chapter III : Suivi de trajectoire robuste pour les systèmes descripteurs incertains

La commande du suivi de trajectoire est l'un des sujets de recherche les plus actifs en robotique, en particulier pour les manipulateurs industriels [Mouhacine, 2004; Lochan and Roy, 2015; Andreev and Peregudova, 2019; Yuan et al., 2020]. L'objectif de la commande est d'obtenir des performances de suivi de haute précision pour une trajectoire de référence souhaitée [Voglewede, Smith, and Monti, 2009]. Malgré des avancées significatives en automatique, les approches classiques telles que les correcteurs proportionnels-intégraux-dérivés (PID) ou la commande du couple calculé (CTC) [Piltan et al., 2012] restent les plus utilisées en pratique. La principale raison d'un tel intérêt réside dans la simplicité de leur conception et de leur mise en œuvre en temps réel [Hamamci, 2007; Efe, 2011]. Cependant, plusieurs problèmes surviennent pour ces approches de commande, notamment le manque de robustesse, une simplification excessive dans leurs calculs, la dégradation due aux bruits par l'action dérivée et la perte de performances [Han, 2009]. Des efforts de recherche importants ont été déployés afin d'améliorer la robustesse et les performances des correcteurs PID et CTC, par exemple la commande PID d'ordre fractionnaire [Keyser, Muresan, and Ionescu, 2018], ou des lois de commande CTC robustes [Lee and Cheng, 1996; Song et al., 2005]. Cependant, les schémas de commande existants présentent encore certaines limites, en particulier lorsqu'il s'agit de systèmes non linéaires fortement couplés tels que les robots manipulateurs. D'autres méthodes de commande ont été appliquées pour effectuer le suivi de trajectoire, à savoir la commande basée sur un modèle flou [Nguyen et al., 2018; Nguyen et al., 2019], la commande adaptative robuste [Ren et al., 2018], la commande basée sur des réseaux de neurones [Zhao-Hui and Taiki, 2008] et ainsi de suite. Il est important de noter que bon nombre de ces approches nécessitent des informations sur l'état complet pour la commande par retour d'état. Cependant, la mesure en ligne à la fois des positions et des vitesses des robots peut entraîner des problèmes liés à la précision des tachymètres industriels [Fantuzzi, Secchi, and Visioli, 2003]. De plus, les structures de commande sont généralement complexes pour une mise en œuvre en temps réel, en particulier pour les robots manipulateurs à degrés de liberté élevés. Ces inconvénients soulignent le besoin de schémas de commande plus efficaces reposant uniquement sur la mesure des positions articulaires du robot pouvant atteindre les performances de suivi souhaitées.

La présence d'incertitudes structurelles peut également avoir un impact important sur les performances souhaitées en suivi de trajectoire. Pour les approches basées sur un modèle, en raison des incertitudes, le modèle mathématique peut ne pas refléter fidèlement le comportement physique réel du système. Des techniques de commande robustes basées sur des conditions LMI exploitant la connaissance de bornes des différents termes incertains ont été développés [Nguyen et al., 2019]. Elles peuvent cependant s'avérer trop pessimistes. Pour les manipulateurs en série, la structure particulière de ces systèmes mécaniques permet de regrouper les incertitudes structurelles et les perturbations correspondantes dans un seul signal qui peut ensuite être estimé à l'aide d'un observateur à entrée inconnue. Le signal estimé peut ensuite être injecté dans l'entrée de commande dans ce que l'on appelle l'approche équivalente de perturbation d'entrée (EID) [She, Xin, and Pan, 2011] afin de compenser les incertitudes considérées et d'atténuer l'effet de la perturbation sur les performances de suivi.

Motivés par les problèmes théoriques et pratiques de commande robotique ci-dessus, nous proposons dans ce chapitre une nouvelle approche pour traiter les incertitudes paramétriques exploitant les propriétés supplémentaires et uniques de l'approche quasi-LPV proposée. En effet, les incertitudes paramétriques sont modélisées dans une forme polytopique convexe au lieu d'être exclus. Une nouvelle loi de commande par retour d'état est proposée qui assure la stabilité du modèle polytopique incertain résultant. Une comparaison de l'approche proposée au traitement classique des incertitudes sur deux exemples différents de systèmes singuliers incertains est fournie et montre que notre approche est moins conservatrice pour trouver un retour d'état stabilisant. De plus, nous nous concentrons dans ce chapitre sur le problème du

suivi de trajectoire haute précision pour les manipulateurs en série en présence d'incertitudes paramétriques et de perturbations inconnues. Nous supposons initialement que les mesures de la position angulaire et de la vitesse sont disponibles. Le cas où la vitesse n'est pas mesurée est aussi présenté mettant en exergue les problèmes résultants des prémisses non mesurées et de la viabilité de la synthèse simultanée d'un correcteur et d'un observateur.

La dynamique du robot sérial à 3ddl considéré pour le suivi de trajectoire dans ce chapitre est donnée par [Spong and Vidyasagar, 2008] :

$$M(q)\ddot{q} + N(q,\dot{q})\dot{q} + G(q) = \Gamma(t) + \Gamma_{ext}(t), \tag{IV.82}$$

où $q(t) \in \mathbb{R}^3$ est le vecteur des coordonnées généralisées dans l'espace articulaire, $\Gamma(t) \in \mathbb{R}^3$ est le vecteur des forces de contrôle généralisées, $\Gamma_{ext}(t) \in \mathbb{R}^3$ représente la pertubation externe, $M(q) \in \mathbb{R}^{3\times3}$ est la matrice d'inertie, $N(q,\dot{q}) \in \mathbb{R}^{3\times3}$ est la matrice des forces de Coriolis/centripète plus les coefficients de frottement visqueux des articulation, et $G(q) \in \mathbb{R}^2$ représente la matrice de gravité :

$$M(\theta) = \begin{bmatrix} m_{11} & m_{12} & m_{13} \\ \star & 2c_6\sigma_2 + c_8 & c_6\sigma_2 + I_3 \\ \star & \star & I_3 \end{bmatrix}, \quad N(\theta,\dot{\theta}) = \begin{bmatrix} n_{11} & n_{12} & n_{13} \\ n_{21} & n_{22} & -c_6\sigma_8 \\ n_{31} & c_6\sigma_7 & 0 \end{bmatrix},$$
$$G(\theta) = \begin{bmatrix} c_1\sigma_{10} + c_2\sigma_{11} + c_3\sigma_{12} \\ c_2\sigma_{11} + c_3\sigma_{12} \\ c_3\sigma_{12} \end{bmatrix}, \quad \Gamma_{ext} = \begin{bmatrix} \Gamma_{ext1} \\ \Gamma_{ext2} \\ \Gamma_{ext3} \end{bmatrix} = \begin{bmatrix} 450\sin(15t) \\ 375\sin(15t) \\ 300\sin(15t) \end{bmatrix}$$

avec

$$\begin{aligned}
&m_{11} = 2(c_4\sigma_1 + c_6\sigma_2 + c_5\sigma_3 + c_7), && m_{12} = c_4\sigma_1 + 2c_6\sigma_2 + c_5\sigma_3 + c_8, && m_{13} = c_6\sigma_2 + c_5\sigma_3 + I_3,\\
&n_{11} = c_5(\sigma_6 - \sigma_9) + c_6(\sigma_7 - \sigma_8), && n_{12} = -c_4\sigma_4 + c_6(\sigma_7 - \sigma_8) - c_5\sigma_9, && n_{13} = -c_6\sigma_8 - c_5\sigma_9,\\
&n_{21} = c_4\sigma_5 + c_5\sigma_6 + c_6(\sigma_7 - \sigma_8), && n_{22} = c_6(\sigma_7 - \sigma_8), && n_{31} = c_5\sigma_6 + c_6\sigma_7,\\
&c_1 = g(L_1m_2 + L_1m_3 + m_1r_1), && c_2 = g(L_2m_3 + m_2r_2), && c_3 = gm_3r_3,\\
&c_4 = L_1(L_2m_3 + m_2r_2), && c_5 = L_1m_3r_3, && c_6 = L_2m_3r_3,\\
&c_7 = (m_2 + m_3)L_1^2 + L_2^2m_3 + I_t, && c_8 = L_2^2m_3 + I_2 + I_3, && I_t = I_1 + I_2 + I_3.
\end{aligned}$$

Le robot est illustré par la Figure IV.18 et la Table IV.7 représente les non-linéarités du système :

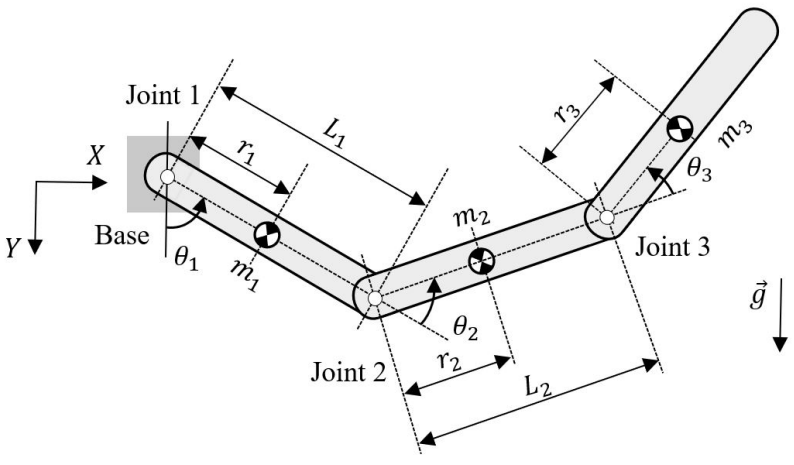

FIGURE IV.18: Schéma du robot manipulateur 3ddl dans le plan vertical.

TABLE IV.7: Non-linéarités du robot manipulateur 3ddl.

Paramètre variable	Expression
σ_1	$\cos(\theta_2)$
σ_2	$\cos(\theta_3)$
σ_3	$\cos(\theta_2 + \theta_3)$
σ_4	$2\dot{\theta}_1 + \dot{\theta}_2 \sin(\theta_2)$
σ_5	$\dot{\theta}_1 \sin(\theta_2)$
σ_6	$\dot{\theta}_1 \sin(\theta_2 + \theta_3)$
σ_7	$(\dot{\theta}_1 + \dot{\theta}_2) \sin(\theta_3)$
σ_8	$(\dot{\theta}_1 + \dot{\theta}_2 + \dot{\theta}_3) \sin(\theta_3)$
σ_9	$(\dot{\theta}_1 + \dot{\theta}_2 + \dot{\theta}_3) \sin(\theta_2 + \theta_3)$
σ_{10}	$\text{sinc}(\theta_1)$
σ_{11}	$\text{sinc}(\theta_1 + \theta_2)$
σ_{12}	$\text{sinc}(\theta_1 + \theta_2 + \theta_3)$

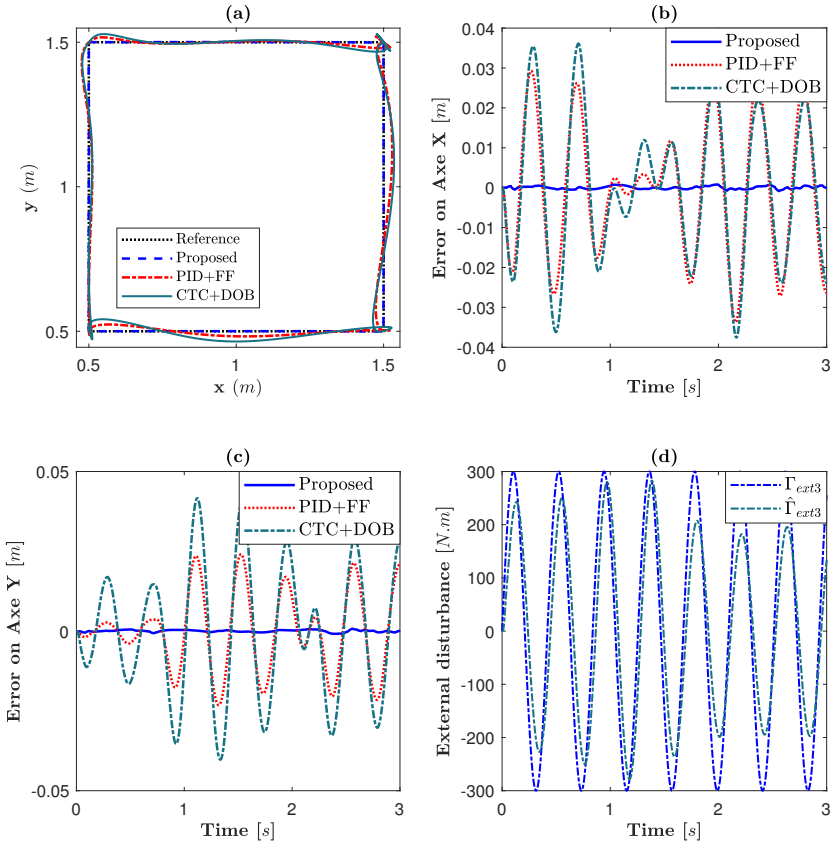

FIGURE IV.19: Comparaison des performances du suivi. (a) Résultat du suivi de trajectoire linéaire dans le plan XY. (b) Erreur de suivi le long de l'axe X. (c) Erreur de suivi le long de l'axe Y. (d) Perturbation externe Γ_{ext3} considérée

Le résultat du suivi de trajectoire est illustré dans la Figure IV.19 où on observe que l'approche de commande à base de l'estimation de perturbations proposée obtient une performance supérieure en terme de suivi par rapport aux autres approches de commande CTC et PID.

Chapter IV : Suivi de trajectoire basé sur un observateur de perturbations pour les robots manipulateurs

La conception des correcteurs pour un robot [Mohammadi et al., 2013; Briot and Khalil, 2015] est généralement basée sur un retour d'état complet nécessitant les mesures des positions et des vitesses angulaires articulaires. Les mesures de position angulaire de l'articulation sont généralement obtenues à l'aide de codeurs ou de résolveurs permettant des mesures fiables et précises. Cependant, il n'en est pas de même des vitesses angulaires articulaires obtenues avec des tachymètres souvent polluées par le bruit. Cela peut affecter considérablement la précision de suivi des robots manipulateurs. Une solution à ce problème consiste à déployer des filtres linéaires ou non pour l'annulation du bruit ou l'extraction des signaux de fréquences souhaitées [Anderson and Moore, 1979; Chen et al., 2015]. Dans [Ahrens and Khalil, 2009] un observateur à gain élevé d'ordre réduit permet d'annuler les bruits à haute fréquence. Dans [Iwasaki and Skelton, 1994], une formulation LMI pour la synthèse $\mathcal{H}_\infty$ est proposée. Une autre solution qui ne nécessite pas l'utilisation de filtres consiste à reconstruire le signal de vitesse angulaire articulaire via un observateur [Jiang, Deghat, and Anderson, 2017; Magnis and Petit, 2016; Piperakis, Koskinopoulou, and Trahanias, 2018], puis à l'exploiter pour la commande. Un robot est essentiellement un système multicorps. Ainsi, un modèle dynamique multicorps unifié pour un robot peut être construit sur la base d'équations algébro-différentielles (DAE) avec des coordonnées généralisées non indépendantes. Cependant, les systèmes dynamiques de robots décrits par des DAE apportent de nouveaux défis pour les problèmes de commande de suivi de trajectoire. Un des principaux verrous vient principalement du fait que l'intégration numérique des équations dynamiques est un problème difficile lorsque l'indice de différentiation est élevé [Blajer, 1992]. Ainsi, la synthèse de la commande pour de tels systèmes DAE est difficile à réaliser. La plupart des méthodes existantes, principalement pour les chaînes cinématiques ouvertes, ne sont applicables qu'aux représentation du système dans un espace d'état. Pour cette raison, la représentation d'état est devenue un choix populaire pour modéliser la dynamique du robot. À cet égard, le modèle réduit proposé dans [Ghorbel et al., 2000] est exprimé en termes de coordonnées généralisées indépendantes et conserve plusieurs propriétés structurelles des manipulateurs à chaîne ouverte. Le modèle réduit suppose une transformation de coordonnées indépendantes en coordonnées dépendantes, qui est locale et implicite. Cette transformation implicite doit être résolue en temps réel pour la mise en œuvre de la commande. Dans [Wang and Ghorbel, 2004] l'équation de contrainte algébrique pour un modèle d'indice 1 est remplacée par une équation différentielle de dynamique rapide asymptotiquement stable de façon à garantir le respect des contraintes cinématiques. Cette approche est cependant basée sur la réduction au préalable de l'indice de différentiation qui nécessite non seulement un certain de transformations algébriques, mais conduit également à des modèles descripteurs réguliers avec un nombre élevé de non-linéarités. Alternativement, des modèles d'ordre réduit sont obtenus en projetant les équations différentielles du système DAE dans un sous-espace sans contrainte [Li et al., 2021; Blajer and Kolodziejczyk, 2004] mais une telle approche nécessite la résolution pouvant se révéler complexes d'équations matricielles non linéaires. Des méthodes discrètes numériques pour les DAE commandés ont également été proposées dans [Peng et al., 2020; Shi et al., 2021]. Cependant, de telles approches reposent sur une mesure précise des coordonnées des articulations et peuvent s'avérer vulnérables vis-à-vis des incertitudes du système.

Outre le problème du bruit sur les mesures, la présence de multiples sources de perturbations est préoccupante car elle peut entraîner une dégradation des performances voire une instabilité [Guo and Cao, 2014]. Les perturbations dans les systèmes robotiques correspondent à de multiples phénomènes d'origine interne (frottement, dynamique non modélisée) ou externe via l'interaction avec l'environnement (collisions), présentant des comportements et des caractéristiques différents, généralement non prévisibles ou difficilement modélisables. De plus, les perturbations peuvent ne pas vérifier la condition de recouvrement (ou "matching ") ce qui conduit à une difficulté accrue pour le rejet des perturbations. Comment traiter efficacement les multiples

perturbations est une clé pour améliorer les performances de commande. De grands efforts ont été déployés au sein de la communauté automaticienne pour résoudre ce problème, l'accent a été mis sur la robustesse des techniques de rejet de perturbations [Wang et al., 2010; Castañeda, Luviano-Juárez, and Chairez, 2015]. Une de ces techniques repose sur la notion d'observateurs de perturbations (DO) déployées dans une variété d'applications avec différents objectifs : estimation du couple exercé dans les exosquelettes des membres inférieurs [Mohammed et al., 2016] ; compensation des dynamiques non modélisées dans les robots humanoïdes Bae and Oh, 2017 ou même pour améliorer l'approche de commande aux frontières des manipulateurs flexibles [Zhao, Ahn, and Li, 2020]. Dans les manipulateurs robotiques, l'utilisation de stratégies DO a été principalement utilisée pour les tâches de suivi de trajectoire haute précision [Mohammadi et al., 2013]. Cependant, le rejet des perturbations implique généralement de faire certaines hypothèses sur les caractéristiques de la perturbation. En raison de la nature hautement non linéaire des manipulateurs robotiques, l'utilisation de techniques d'analyse et de conception linéaires pour DO a été limitée à certaines stratégies standard telles que la linéarisation autour d'un point de fonctionnement. Dans ce cas, une performance optimale locale peut être obtenue en utilisant un filtre de Kalman étendu par exemple comme dans [Mohammadi et al., 2013]. Plus récemment, des stratégies DO ont été développés dans le cadre de techniques de commande des systèmes non linéaires, comme la commande par mode glissant ou les approches LPV ou de Takagi–Sugeno.

Motivés par les problèmes de commande robotique théoriques et pratiques ci-dessus, un modèle d'ordre réduit pour les robots manipulateurs incertains utilisant un schéma d'observateur de de perturbation est proposé. Des résultats de commande adaptées aux manipulateurs à chaîne ouverte peuvent être transposés à la commande des manipulateurs à chaîne fermée sans avoir besoin d'une résolution en temps réel des contraintes algébriques. L'approche développée présente une commande par retour d'état de sortie basée sur un observateur étendu utilisant la nouvelle approche de modélisation quasi-LPV. La loi de suivi proposée est basée sur trois composants principaux, à savoir une action anticipatrice, une action corrective de tendance basée sur l'observateur de perturbation et un retour d'état reconstruit. La première action cherche à compenser les termes liés à la référence dans la dynamique de l'erreur de suivi, tandis que la seconde [Sariyildiz, Oboe, and Ohnishi, 2020] est utilisée pour minimiser les effets des incertitudes de modélisation et des perturbations inconnues ainsi que pour résoudre le problème de prémisses non mesurées [Nguyen et al., 2021a] pour ce type particulier de systèmes. La synthèse est basée sur l'exploitation de la structure et des propriétés intrinsèques du système robotique. La loi de commande par retour d'état reconstruit garantit les propriétés de stabilité et de robustesse en boucle fermée via la théorie de la stabilité de Lyapunov. L'approche proposée est ensuite validée sur des modèles de simulation haute fidélité de robots manipulateurs série et parallèle. La viabilité du schéma de rejet des perturbations pour la réduction du modèle en ce qui concerne les performances de suivi et l'estimation de l'état est évaluée, et une conclusion sur le choix optimal pour l'observateur de perturbation mixte et la synthèse de lois de commande basée sur le modèle quasi-LPV est fournie.

Le schéma de commande basé sur un observateur étendu estimant l'état et la perturbation est donné par la Figure IV.20.

$$u(t) = u_{ff}(t) + u_{dc}(t) + u_{fb}(t),$$

dont

$$\begin{aligned} u_{ff}(t) &= -B^{\dagger}\big(A(z)x_r(t) - E(z)\dot{x}_r(t)\big), \\ u_{fb}(t) &= K_p(z)\big(\hat{x}(t) - x_r(t)\big) + K_I(z)e_I(t), \\ u_{dc}(t) &= -\hat{d}(t). \end{aligned} \tag{IV.83}$$

L'entrée $u_{ff}(t)$ représente l'action anticipatrice qui permet de compenser les termes liés au modèle de référence figurant la dynamique de l'erreur de poursuite. L'entrée $u_{dc}(t)$ représente l'action

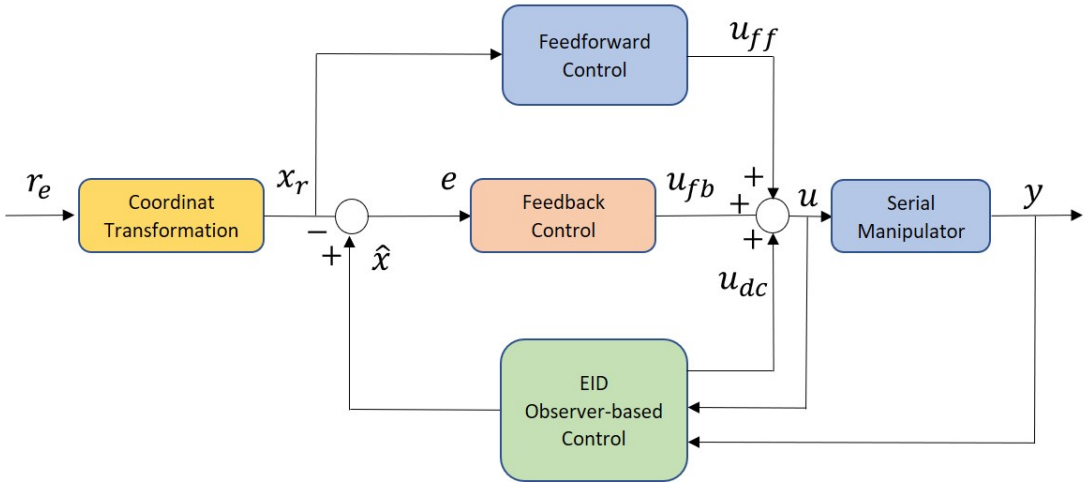

FIGURE IV.20: Structure de contrôle du suivi de trajectoire basée sur l'observateur de perturbations pour les manipulateurs en série.

corrective de tendance basée sur l'observateur de perturbation qui permet d'atténuer l'impact des termes incertains, non-linéarités non mesurables, et des perturbations exogènes. L'entrée $u_{fb}(t)$ représente le retour d'état reconstruit et assure la robustesse de la loi de commande. Le schéma du robot parallèle considéré est illustré par la Figure IV.21 et le résultat du suivi correspondant est montré dans la Figure IV.22:

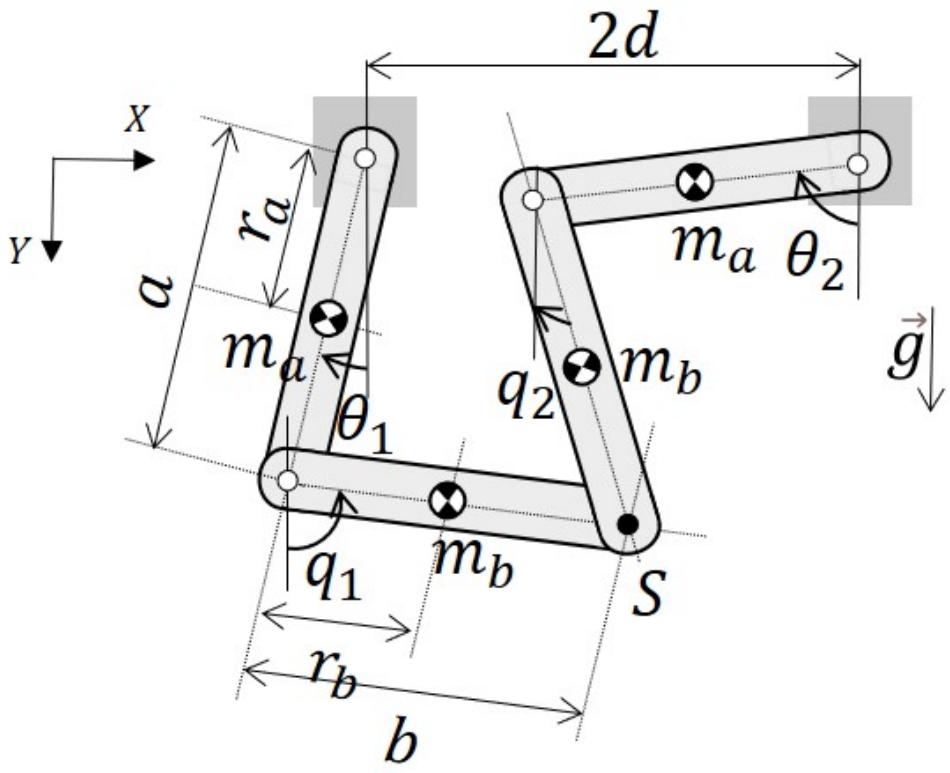

FIGURE IV.21: Schéma du robot parallèle 2ddl dans le plan vertical.

On constate que la performance du suivi de trajectoire obtenue par l'approche proposée dépasse largement les performances de la commande CTC et du PID combiné avec l'action anticipatrice.

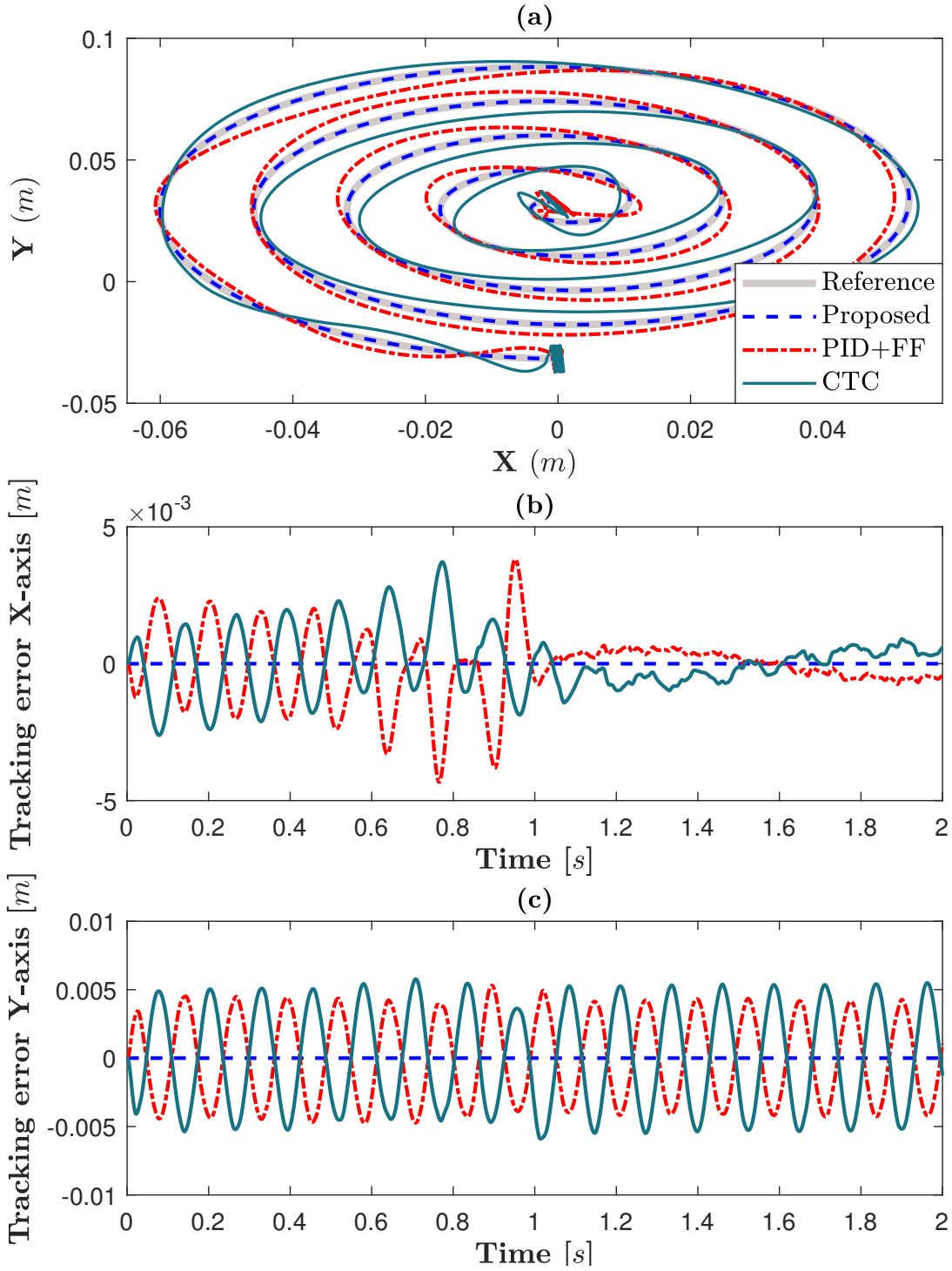

FIGURE IV.22: Comparaison des performances de suivi. (a) Suivi de trajectoire en spirale dans le plan XY. (b) Erreur de suivi le long de l'axe X. (c) Erreur de suivi le long de l'axe Y.

Contributions

- La principale contribution de cette thèse consiste en une nouvelle représentation polytopique d'un système non linéaire et à son potentiel pour les techniques de commande à base de modèle, en particulier pour les systèmes fortement non linéaires où le besoin d'observateurs non linéaires efficaces et de lois de commande robustes est nécessaire.
- Une nouvelle loi de commande est proposée pour les systèmes descripteurs réguliers avec une réduction significative du conservatisme et de la complexité par rapport à l'approche basée sur un modèle augmenté du système.
- Un traitement alternatif des incertitudes structurelles est rendu possible grâce aux propriétés supplémentaires de la représentation polytopique proposée.
- La technique de l'observateur de perturbations est exploitée pour traiter des prémisses non mesurées pour l'observation des robots manipulateurs.

Perspectives

a) Pistes de recherche court à moyen terme

- Une plate-forme physique d'un robot delta parallèle a été mise à disposition pour mener des expériences pratiques. L'objectif est de valider l'approche basée sur l'observateur de perturbation proposée en conditions physiques réelles et les comparer aux résultats de simulation obtenus sur un modèle haute fidélité implanté sur *Simscape Multibody* de *Matlab*. Nous espérons finaliser les résultats de l'expérience à temps pour les présenter lors de la soutenance de thèse.
- Une extension de la représentation polytopique proposée aux systèmes à temps discret est également envisagée, étant donnée que pour la mise en œuvre d'une loi de commande échantillonnée, un correcteur discret s'avère plus efficace et donne de meilleurs résultats expérimentaux.

b) Pistes de recherche long terme

- En raison des dynamiques non modélisées ou des incertitudes du modèle, les estimations des variables d'état du système obtenues via l'observateur ne sont pas précises. La stabilité du système commandée est garantie pour des perturbations évoluant de manière affine avec le temps. Il n'en va pas de même pour d'autres types de perturbations pour lesquelles il serait utile de rechercher un traitement alternatif des prémisses non mesurées telles que [Nguyen et al., 2021a] afin d'exploiter pleinement la représentation exacte du modèle sous la forme polytopique proposée. Outre l'application aux problèmes de commande, ces travaux peuvent être appliquées à la conception d'observateurs précis pour le diagnostic ou l'analyse des données.
- Compte tenu des récents résultats dans l'identification des systèmes LPV [Liu et al., 2014; Bombois et al., 2018; Ghosh et al., 2018], combiner le processus d'identification avec la représentation polytopique proposée peut donner des résultats intéressants surtout si la propriété supplémentaire et l'introduction des variables de relaxation peuvent être exploitées pour diminuer l'erreur d'identification.

Publications

Revues

1. A. Dehak, A.-T. Nguyen, A. Dequidt, L. Vermeiren, M. Dambrine (2022). "Reduced-complexity LMI conditions for admissibility analysis and control design of singular nonlinear systems". IEEE Transactions on Fuzzy Systems. **(en révision)**

2. A. Dehak, A.-T. Nguyen, A. Dequidt, L. Vermeiren, M. Dambrine (2022). "Takagi-Sugeno fuzzy disturbance-observer-based output tracking control for robot manipulators: Design and experiments". IEEE Transactions on Control Systems Technology. **(en préparation)**

Conférences

1. A. Dehak, A.-T. Nguyen, A. Dequidt, L. Vermeiren, M. Dambrine (2019). "Disturbance-observer based tracking control of industrial SCARA robot manipulators". 45th Annual Conference of the IEEE Industrial Electronics, Lisbon, Portugal, Octobre.

2. A. Dehak, A.-T. Nguyen, A. Dequidt, L. Vermeiren, M. Dambrine (2020). "Reduced-complexity affine representation for Takagi-Sugeno fuzzy systems". 21st IFAC World Congress, Berlin, Germany, Juillet.

3. A. Dehak, A.-T. Nguyen, A. Dequidt, L. Vermeiren, M. Dambrine (2020). "Stability Analysis of TS Systems via Reduced-Complexity Affine Representation". Rencontres Francophones sur la Logique Floue et ses Applications (Sète, France), pp. 109-114, Cépaduès Editions, I.S.B.N. : 9782364938663.

Bibliography

Ahrens, J. and H. Khalil (2009). "High-gain observers in the presence of measurement noise: A switched-gain approach". In: *Automatica (Oxf)* 45.4, pp. 936–943.

Allouche, B. (2016). "Modélisation et commande des robots : nouvelles approches basées sur les modèles Takagi-Sugeno". PhD thesis. Polytechnic University of Hauts-de-France.

Anderson, B. and J. Moore (1979). *Optimal Filtering*. Prentice-Hall.

Andreev, A. and O. Peregudova (2019). "Trajectory tracking control for robot manipulators using only position measurements". In: *Int. J. Control* 92.7, pp. 1490–1496.

Apkarian, P., P. Gahinet, and G. Becker (1995). "Self-scheduled $\mathscr{H}_\infty$ control of linear parameter-varying systems: a design example". In: *Automatica (Oxf)* 31.9, pp. 1251–1261. ISSN: 0005-1098.

Arceo, Juan Carlos et al. (2019). "Convex stability analysis of nonlinear singular systems via lnear matrix inequalities". In: *IEEE Trans. Automat. Contr* 64.4, pp. 1740–1745.

Bae, H. and J.-H. Oh (2017). "Novel state estimation framework for humanoid robot". In: *Rob. Auton. Syst.* 98, pp. 258–275.

Bayo, E., J. Garcia De Jalon, and M.A. Serna (1988). "A modified lagrangian formulation for the dynamic analysis of constrained mechanical systems". In: *Comput Methods Appl Mech Eng* 71.2, pp. 183–195. ISSN: 0045-7825.

Blajer, W. (1992). "Index of differential-algebraic equations governing the dynamics of constrained mechanical systems". In: *Appl. Math. Model.* 16.2, pp. 70–77.

Blajer, W. and K. Kolodziejczyk (2004). "A geometric approach to solving problems of control constraints: Theory and a DAE framework". In: *Multibody Syst. Dyn.* 11, pp. 343–364.

Bombois, X. et al. (2018). "Optimal identification experiment design for the interconnection of locally controlled systems". In: *Automatica (Oxf)* 89, pp. 169–179.

Bouali, A., M. Yagoubi, and P. Chevrel (2008). "Gain scheduled observer state feedback controller for rational LPV systems". In: *IFAC Proceedings Volumes* 41, pp. 4922–4927.

Bouarar, T., K. Guelton, and N. Manamanni (2010). "Robust fuzzy Lyapunov stabilization for uncertain and disturbed Takagi–Sugeno descriptors". In: *ISA Trans.* 49.4, pp. 447–461. ISSN: 0019-0578.

Boyd, S. et al. (1994). *Linear Matrix Inequalities in System and Control Theory*. Vol. 15. Philadelphia: SIAM.

Briat, C. (2014). *Linear parameter-varying and time-delay systems: Analysis, observation, filtering & control*. Springer, Berlin, Heidelberg.

Briot, S. and W. Khalil (Sept. 2015). *Dynamics of Parallel Robots*. Vol. 35, p. 80.

Cardim, R. et al. (2007). "Design of state-derivative feedback controllers using a state feedback control design". In: *IFAC Proceedings Volumes* 40.20. 3rd IFAC Symposium on System Structure and Control, pp. 22–27. ISSN: 1474-6670.

Castañeda, L., A. Luviano-Juárez, and I. Chairez (2015). "Robust trajectory tracking of a delta robot through adaptive active disturbance rejection control". In: *IEEE Trans. Control Syst. Technol.* 23.4, pp. 1387–1398.

Chen, Y. et al. (2015). "Toward adaptive robust state estimation based on MCC by using the generalized Gaussian density as kernel functions". In: *Int. J. Electr. Power Energy Syst.* 71.C, pp. 297–304.

Coutinho, P. et al. (2020). "A multiple-parameterization approach for local stabilization of constrained Takagi-Sugeno fuzzy systems with nonlinear consequents". In: *Inf. Sci.* 506, pp. 295–307.

Dehak, A. et al. (2020). "Reduced-complexity affine representation for Takagi-Sugeno fuzzy systems". In: *21st IFAC World Congress*. Berlin, Germany.

Di Franco, P., G. Scarciotti, and A. Astolfi (2020). "Stability of nonlinear differential-algebraic systems via additive identity". In: *IEEE/CAA J. Autom. Sin* 7.4, pp. 929–941.

Efe, M. (2011). "Neural network assisted computationally simple $PI^{\lambda}D^{\mu}$ control of a quadrotor UAV". In: *IEEE Trans. Indus. Inform.* 7.2, pp. 354–361.

Fantuzzi, C., C. Secchi, and A. Visioli (2003). "On the fault detection and isolation of industrial robot manipulators". In: *IFAC Proc. Vol.* 36.17, pp. 399–404.

Fridman, E. and U. Shaked (2002). "A descriptor system approach to $\mathscr{H}_\infty$ control of linear time-delay systems". In: *IEEE Trans. Autom. Control* 47.2, pp. 253–270.

Gahinet, P. et al. (1995). *LMI Control Toolbox*. The Math Works Inc.

Ghorbel, F. et al. (2000). "Modeling and set point control of closed-chain mechanisms: theory and experiment". In: *IEEE Trans. Control Syst. Technol.* 8.5, pp. 801–815.

Ghosh, D. et al. (2018). "Optimal identification experiment design for LPV systems using the local approach". In: *Automatica (Oxf)* 87, pp. 258–266.

Guelton, K., S. Delprat, and T.-M. Guerra (2008). "An alternative to inverse dynamics joint torques estimation in human stance based on a Takagi-Sugeno unknown-inputs observer in the descriptor form". In: *Control Eng. Pract.* 16.12, pp. 1414–1426.

Guerra, T.-M., V. Estrada-Manzo, and Z. Lendek (2015). "Observer design for Takagi–Sugeno descriptor models: An LMI approach". In: *Automatica (Oxf)* 52, pp. 154–159.

Guerra, T.-M. and L. Vermeiren (2001). "Control laws for Takagi-Sugeno fuzzy models". In: *Fuzzy Sets Syst* 120.1, pp. 95–108.

— (2004). "LMI-based relaxed non-quadratic stabilization conditions for nonlinear systems in the Takagi-Sugeno's form". In: *Automatica (Oxf)* 40.5, pp. 823–829.

Guerra, T.-M. et al. (2007). "A way to improve results for the stabilization of continuous-time fuzzy descriptor models". In: *46th IEEE Conf. Decision Control*. New Orleans, LA, USA, pp. 5960–5964.

Guo, L. and S. Cao (2014). "Anti-disturbance control theory for systems with multiple disturbances: A survey". In: *ISA Trans.* 53.4, pp. 846–849.

Hamamci, S. (2007). "an algorithm for stabilization of fractional-order time delay systems using fractional-order PID controllers". In: *IEEE Trans. Autom. Control* 52.10, pp. 1964–1969.

Han, J. (2009). "From PID to active disturbance rejection control". In: *IEEE Trans. Indus. Electron.* 56.3, pp. 900–906.

He, J. et al. (2021). "Admissibility analysis and robust $\mathscr{H}_\infty$ control for T–S fuzzy descriptor systems with structured parametric uncertainties". In: *IEEE Trans. Fuzzy Syst.* 9.1, pp. 192–200.

Hoffmann, C. and H. Werner (2015). "A survey of linear parameter-varying control applications validated by experiments or high-fidelity simulations". In: *IEEE Trans. Control Syst. Technol.* 23.2, pp. 416–433.

Iwasaki, T. and R. Skelton (1994). "All controllers for the general H_∞ control problem: LMI existence conditions and state space formulas". In: *Automatica (Oxf)* 30.8, pp. 1307–1317. ISSN: 0005-1098.

Jiang, B., M. Deghat, and B. Anderson (2017). "Simultaneous velocity and position estimation via distance-only measurements with application to multi-agent system control". In: *IEEE Trans. Autom. Control* 62.2, pp. 869–875.

Jie, W. et al. (2020). "Trajectory tracking control using fractional-order terminal sliding mode control with sliding perturbation observer for a 7-DoF robot manipulator". In: *IEEE ASME Trans Mechatron* 25.4, pp. 1886–1893.

Johansen, T.A., R. Shorten, and R. Murray-Smith (2000). "On the interpretation and identification of dynamic Takagi-Sugeno fuzzy models". In: *IEEE Trans. Fuzzy Syst.* 8.3, pp. 297–313.

Kamman, J.W. and R.L. Huston (1984). "Constrained multibody system dynamics an automated approach". In: *Computers & Structures* 18.6, pp. 999–1003. ISSN: 0045-7949.

Keyser, R., C. Muresan, and C. Ionescu (2018). "Autotuning of a robust fractional order PID controller". In: *IFAC-PapersOnLine* 51.25, pp. 466–471.

Koelewijn, P. and R. Tóth (2020). "Scheduling dimension reduction of LPV models – A deep neural network approach". In: *American Control Conf.* Denver, CO, USA, pp. 1111–1117.

Koenig, D. (2006). "Observer design for unknown input nonlinear descriptor systems via convex optimization". In: *IEEE Trans. Autom. Control* 51.6, pp. 1047–1052.

Krishnan, H. and H. Mcclamroch (1994). "Tracking in nonlinear differential-algebraic control systems with applications to constrained robot systems". In: *Automatica* 30.12, pp. 1885–1897.

Kumar, A. and P. Daoutidis (2020). *Control of Nonlinear Differential Algebraic Equation Systems: with Applications to Chemical Processes*. Chapman and Hall/CRC.

Kwiatkowski, A. and H. Werner (2008). "PCA-based parameter set mappings for LPV models with fewer parameters and less overbounding". In: *IEEE Trans. Control Syst. Technol.* 16.4, pp. 781–788.

Lee, D., J. Park, and Y.H. Joo (Feb. 2012). "A fuzzy Lyapunov function approach to estimating the domain of attraction for continuous-time Takagi-Sugeno fuzzy systems". In: *Inf. Sci.* 185, pp. 230–248.

Lee, G.-W. and F. Cheng (Feb. 1996). "Robust control of manipulators using the computed torque plus $\mathcal{H}_\infty$ compensation method". In: *IET Control Theory Appl.* 143, pp. 64 –72.

Lendek, Z. et al. (2011). *Stability Analysis and Nonlinear Observer Design Using Takagi-Sugeno Fuzzy Models*. Springer.

Lewis, F., D. Dawson, and C. Abdallah (2003). *Robot Manipulator Control: Theory and Practice*. New York, USA: CRC Press.

Li, J. et al. (2021). "Neural networks-based sliding mode tracking control for the four wheel-legged robot under uncertain interaction". In: *Int. J. Robust Nonlinear Control.* 31, pp. 4306 –4323.

Li, S. et al. (2022). "Equivalent-input-disturbance based dynamic tracking control for soft robots via reduced order finite element models". In: *IEEE ASME Trans Mechatron.*

Lin, D. and M.J. Er (2001). "A new approach for stabilizing nonlinear systems with time delay". In: *2001 ECC*, pp. 114–119.

Liu, Q. et al. (2014). "A local approach for the LPV identification of an actuated beam using piezoelectric actuators and sensors". In: *Mechatronics* 24.4. Vibration control systems, pp. 289–297. ISSN: 0957-4158.

Liu, Z. et al. (2021). "Real-time dynamics of cable-driven continuum robots considering the cable constraint and friction effect". In: *IEEE Robot. Autom. Lett.* 6.4, pp. 6235–6242.

Lochan, K. and B.K. Roy (2015). "Control of two-link 2-DoF robot manipulator using fuzzy logic techniques: A review". In: *SocProS 2014*. Ed. by Kedar Nath Das et al. New Delhi: Springer India, pp. 499–511.

Löfberg, J. (2004). "YALMIP: A toolbox for modeling and optimization in Matlab". In: *IEEE Int. Symp. Comput. Aided Control Syst. Des.* Taipei, pp. 284–289.

Ma, X.-J., Z.-Q. Sun, and Y.-Y. He (1998). "Analysis and design of fuzzy controller and fuzzy observer". In: *IEEE Trans. Fuzzy Syst.* 6.1, pp. 41–51.

Magnis, L. and N. Petit (2016). "Angular velocity nonlinear observer from single vector measurements". In: *IEEE Trans. Autom. Control* 61.9, pp. 2473–2483.

Makni, S. et al. (Mar. 2021). "Robust fault estimation and fault-tolerant tracking control for uncertain Takagi–Sugeno fuzzy systems: Application to single link manipulator". In: *Int J Adapt* 35, pp. 846–876.

Mamdani, E. and S. Assilian (1975). "An experiment in linguistic synthesis with a fuzzy logic controller". In: *Int. J. Man-Machine Studies* 7.1, pp. 1–13.

Mohammadi, A. et al. (2013). "Nonlinear disturbance observer design for robotic manipulators". In: *Control Eng. Pract* 21, pp. 253–267.

Mohammadpour, J. and C. Scherer (2012). *Control of Linear Parameter Varying Systems with Applications*. Springer Science & Business Media.

Mohammed, S. et al. (2016). "Nonlinear disturbance observer based sliding mode control of a human-driven knee joint orthosis". In: *Robotics Auton. Syst.* 75, pp. 41–49.

Mouhacine, B. (Oct. 2004). "Control of flexible manipulators: A survey". In: *Robotica* 22, pp. 533 –545.

Mozelli, L., R. Palhares, and G. Avellar (2009). "A systematic approach to improve multiple Lyapunov function stability and stabilization conditions for fuzzy systems". In: *Inf. Sci.* 179.8, pp. 1149–1162.

Márquez, R. et al. (2016). "A non-quadratic Lyapunov functional for $\mathscr{H}_\infty$ control of nonlinear systems via Takagi–Sugeno models". In: *J. Franklin Inst.* 53.4, pp. 81–96.

Nguyen, A.-T., P. Chevrel, and F. Claveau (2018). "Gain-scheduled static output feedback control for saturated LPV systems with bounded parameter variations". In: *Automatica (Oxf)* 89, pp. 420–424.

Nguyen, A.-T., T. Guerra, and V. Campos (2019). "Simultaneous estimation of state and unknown input with l_∞ guarantee on error-bounds for fuzzy descriptor systems". In: *IEEE Control Syst. Lett.* 3.4, pp. 1020–1025. ISSN: 2475-1456.

Nguyen, A.-T. et al. (2019). "Fuzzy Control Systems: Past, Present and Future". In: *IEEE Comput. Intell. Mag.* 14.1, pp. 56–68.

Nguyen, A.-T. et al. (2021a). "Avoiding unmeasured premise variables in designing unknown input observers for Takagi–Sugeno fuzzy systems". In: *IEEE Control Syst. Lett.* 5.1, pp. 79–84.

Nguyen, A.-T. et al. (2021b). "Takagi–Sugeno fuzzy observer design for nonlinear descriptor systems with unmeasured premise variables and unknown inputs". In: *Int. J. Robust Nonlinear Control* 31.17, pp. 8353–8372.

Nguyen, V.-A. et al. (2018). "A robust descriptor approach for nonlinear tracking control of serial robots". In: *IEEE Conf. Decision Control (CDC)*. Miami Beach, FL, USA, pp. 6906–6911.

— (2019). "Nonlinear Tracking Control with Reduced Complexity of Serial Robots: A Robust Fuzzy Descriptor Approach". In: *Int. J. Fuzzy Syst.* 21.4, 1038–1050.

Nubert, Julian et al. (2020). "Safe and fast tracking on a robot manipulator: robust MPC and neural network control". In: *IIEEE Robot. Autom. Lett.* 5.2, pp. 3050–3057.

Nugroho, Sebastian Adi, Ahmad Taha, and Vu Hoang (2021). "nonlinear dynamic systems parameterization using interval-based global optimization: Computing Lipschitz constants and beyond". In: *IEEE Trans. Automat. Contr.*, pp. 1–1.

Ohtake, H., K. Tanaka, and H.O. Wang (2003). "Fuzzy modeling via sector nonlinearity concept". In: *Integr Comput Aided Eng* 10.4, pp. 333–341.

Paccot, F., N. Andreff, and P. Martinet (2009). "A review on the dynamic control of parallel kinematic machines: Theory and experiments". In: *Int. J. Robot. Res.* 28.3, pp. 395–416.

Pan, J. et al. (2021). "A unified framework for asymptotic observer design of fuzzy systems with unmeasurable premise variables". In: *IEEE Trans. Fuzzy Syst.* 29.10, pp. 2938–2948.

Peaucelle, D. et al. (2000). "A new robust D–stability condition for real convex polytopic uncertainty". In: *Syst. Control Lett.* 40.1, pp. 21–30. ISSN: 0167-6911.

Peng, H. et al. (2020). "A symplectic instantaneous optimal control for robot trajectory tracking with differential-algebraic equation models". In: *IEEE Trans. Ind. Electron.* 67.5, pp. 3819–3829.

Piltan, F. et al. (2012). "Design baseline computed torque controller". In: *Int. J. Eng.* 6.3, p. 129.

Piperakis, S., M. Koskinopoulou, and P. Trahanias (2018). "Nonlinear state estimation for humanoid robot walking". In: *IEEE Robot. Autom. Lett.* 3.4, pp. 3347–3354.

Regaieg, M.A. et al. (2019). "$\mathcal{D}$U-Admissibility with static output feedback for uncertain descriptor T–S systems". In: *Int. J. Syst. Sci.* 50.10, pp. 2030–2041.

Ren, B. et al. (2018). "An Adaptive Robust Control for Trajectory Tracking Of a Robotic Manipulator System". In: *Int. J. Res. Eng. Technol.* 4.6, pp. 77–81.

Rizvi, S. et al. (2016). "A kernel-based PCA approach to model reduction of linear parameter-varying systems". In: *IEEE Trans. Control Syst. Technol.* 24, pp. 1–9.

Sala, A. and C. Ariño (2007). "Asymptotically necessary and sufficient conditions for stability and performance in fuzzy control: Applications of Polya's theorem". In: *Fuzzy Sets Syst.* 158.24, pp. 2671–2686.

— (2009). "Polynomial fuzzy models for nonlinear control: A Taylor series approach". In: *IEEE Trans. Fuzzy Syst.* 17.6, pp. 1284–1295.

Sala, A., T.-M. Guerra, and R. Babuška (2005). "Perspectives of fuzzy systems and control". In: *Fuzzy Sets and Systems* 156.3, pp. 432–444.

Sariyildiz, E., R. Oboe, and K. Ohnishi (2020). "Disturbance observer-based robust control and its applications: 35th anniversary overview". In: *IEEE Trans. Indus. Electron.* 67.3, pp. 2042–2053.

Sato, M. (2011). "Gain-scheduled output-feedback controllers depending solely on scheduling parameters via parameter-dependent Lyapunov functions". In: *Automatica (Oxf)* 47.12, pp. 2786–2790.

Scherer, C. and S. Weiland (2000). "Linear matrix inequalities in control". In: *Lecture Notes, Dutch Institute for Systems and Control, Delft, The Netherlands* 3, p. 2.

She, J., X. Xin, and Y. Pan (2011). "Equivalent-input-disturbance approach–analysis and application to disturbance rejection in dual-stage feed drive control system". In: *IEEE/ASME Trans. Mechatron.* 16.2, pp. 330–340.

She, J.-H., X. Xin, and Y. Pan (2010). "Equivalent-input-disturbance approach–Analysis and application to disturbance rejection in dual-stage feed drive control system". In: *IEEE/ASME Trans. Mechatron.* 16.2, pp. 330–340.

Shi, B. et al. (Feb. 2021). "A symplectic indirect approach for a class of nonlinear optimal control problems of differential-algebraic systems". In: *Int. J. Robust Nonlinear Control.* 31, pp. 2712–2736.

Sira-Ramírez, H. et al. (2017). *Active Disturbance Rejection Control of Dynamic Systems*. Ed. by H. Sira-Ramírez et al. Butterworth-Heinemann, pp. 1–11.

Song, Z. et al. (Sept. 2005). "A computed torque controller for uncertain robotic manipulator systems: Fuzzy approach". In: *Fuzzy Sets Syst.* 154, pp. 208–226.

Spong, M. and M. Vidyasagar (2008). *Robot Dynamics and Control*. John Wiley & Sons.

Takagi, T. and M. Sugeno (1985). "Fuzzy identification of systems and its applications to modeling and control". In: *IIEEE Trans. Syst. Man Cybern.: Syst.* SMC-15.1, pp. 116–132.

Tanaka, K., T. Ikeda, and H.O. Wang (1998). "Fuzzy regulators and fuzzy observers: relaxed stability conditions and LMI-based designs". In: *IEEE Trans. Fuzzy Syst.* 6.2, pp. 250–265.

Tanaka, K., H. Ohtake, and H.O. Wang (2007). "A descriptor system approach to fuzzy control system design via fuzzy Lyapunov functions". In: *IEEE Trans. Fuzzy Syst.* 15.3, pp. 333–341.

Tanaka, K. and M. Sugeno (1992). "Stability analysis and design of fuzzy control systems". In: *Fuzzy Sets and Systems* 45.2, pp. 135–156.

Tanaka, K. and H.O. Wang (2004). *Fuzzy Control Systems Design and Analysis: A Linear Matrix Inequality Approach*. John Wiley & Sons.

Taniguchi, T., K. Tanaka, and H.O. Wang (2000). "Fuzzy descriptor systems and nonlinear model following control". In: *IEEE Trans. Fuzzy Syst.* 8.4, pp. 442–452.

Taniguchi, T. et al. (2001). "Model construction, rule reduction, and robust compensation for generalized form of Takagi-Sugeno fuzzy systems". In: *IEEE Trans. Fuzzy Syst.* 9.4, pp. 525–538.

Thakar, S. et al. (2022). "Manipulator motion planning for part pickup and transport operations from a moving base". In: *IEEE Trans. Autom. Sci. Eng.* 19.1, pp. 191–206.

Tognetti, E., R. Oliveira, and P. Peres (2011). "Selective $\mathscr{H}_2$ and $\mathscr{H}_\infty$ Stabilization of Takagi-Sugeno Fuzzy Systems". In: *IEEE Trans. Fuzzy Syst.* 19.5, pp. 890–900.

Tuan, H.D. et al. (2001). "Parameterized linear matrix inequality techniques in fuzzy control system design". In: *IEEE Trans. Fuzzy Syst.* 9.2, pp. 324–332.

Vandenberghe, L. and S.P. Boyd (1996). "Semidefinite Programming". In: *SIAM Rev.* 38, pp. 49–95.

Voglewede, P., A. H. C. Smith, and A. Monti (2009). "Dynamic performance of a SCARA robot manipulator with uncertainty using polynomial chaos theory". In: *IEEE Trans. Robot.* 25.1, pp. 206–210.

Wang, H.O., K. Tanaka, and M.F. Griffin (1996). "An approach to fuzzy control of nonlinear systems: stability and design issues". In: *IEEE Trans. Fuzzy Syst.* 4.1, pp. 14–23.

Wang, X. et al. (2010). "A distributed control approach to a robust output regulation problem for multi-agent linear systems". In: *IEEE Trans. Automat. Contr.* 55.12, pp. 2891–2895.

Wang, Z. and F.H. Ghorbel (2004). "Control of closed kinematic chains using a singularly perturbed dynamic model". In: *CDC*. Vol. 1. 43, pp. 317–322.

Wu, F. et al. (1996). "Induced $\mathscr{L}_2-$norm control for LPV systems with bounded parameter variation rates". In: *Int. J. Robust Nonlinear Control* 6.9-10, pp. 983–998.

Xie, L. and E. de Souza Carlos (1992). "Robust $\mathcal{H}_\infty$ control for linear systems with norm-bounded time-varying uncertainty". In: *IEEE Trans. Automat. Contr.* 37.8, pp. 1188–1191.

Xie, W.-B. et al. (2018). "N ovel separation principle based H_∞ observer–controller design for a class of T–S fuzzy systems". In: *IEEE Trans. Fuzzy Syst.* 26.6, pp. 3206–3221.

Xie, W.-B. et al. (2020). "Membership function-dependent local controller design for T-S fuzzy systems". In: *IEEE Trans. Syst., Man, Cybern.: Syst.*, pp. 1–8.

Yang, C. et al. (2013). "Lyapunov stability and strong passivity analysis for nonlinear descriptor systems". In: *IEEE Trans. Circuits Syst. I: Regul. Pap.* 60.4, pp. 1003–1012.

Yedavalli, R.K. (Jan. 2014). *Robust Control of Uncertain Dynamic Systems: A Linear State Space Approach*.

Yuan, M. et al. (2020). "A review of industrial tracking control algorithms". In: *Control Eng. Pract.* 102, p. 104536. ISSN: 0967-0661.

Zadeh, L.A. (1965). "Information and control". In: *Fuzzy Sets Syst* 8.3, pp. 338–353.

Zhang, Q. et al. (2017). "Dissipativity analysis and synthesis for a class of T–S fuzzy descriptor systems". In: *IEEE Trans. Syst., Man, Cybern.: Syst.* 47.8, pp. 1774–1784.

Zhao, X et al. (2014). "Novel stability criteria for TS fuzzy systems". In: *IEEE Trans. Fuzzy Syst.* 22.2, pp. 13–23.

Zhao, Z., C.K. Ahn, and H.-X. Li (2020). "Boundary antidisturbance control of a spatially nonlinear flexible string system". In: *IEEE Trans. Ind. Electron.* 67.6, pp. 4846–4856.

Zhao-Hui, J. and I. Taiki (2008). "A neural network controller for trajectory control of industrial robot manipulators". In: *J. Comput.* 3.8, pp. 1–8.